

**Functional characterization of Ubiquitin-Proteasome
Pathway gene(s) for providing tolerance against
Tomato leaf curl New Delhi virus in tomato**

Thesis submitted to

Jawaharlal Nehru University, New Delhi

For the award of the degree of

DOCTOR OF PHILOSOPHY



Pranav Pankaj Sahu

**School of Life Sciences
Jawaharlal Nehru University
New Delhi - 110067**

2016



SCHOOL OF LIFE SCIENCES
JAWAHARLAL NEHRU UNIVERSITY
NEW DELHI -110067

Date: 22nd June, 2016

CERTIFICATE

This is to certify that the work embodied in this thesis entitled "**Functional characterization of Ubiquitin-Proteasome Pathway gene(s) for providing tolerance against Tomato leaf curl New Delhi virus in tomato**" has been carried out at School of Life Sciences, Jawaharlal Nehru University, New Delhi, India. This work is original and has not been submitted so far in part or in full, for the award of any degree or diploma by any university.

Pranav Pankaj Sahu
Student

Dr. Manoj Prasad
(Co-supervisor)
Staff Scientist V, NIPGR



Dr. MANOJ PRASAD

AvH, FNASc, FNAAS
Staff Scientist V
National Institute of Plant Genome Research
Aruna Asaf Ali Marg, New Delhi-110067

Prof. Supriya Chakraborty
(Supervisor)

School of Life Sciences, JNU
SUPRIYA CHAKRABORTY, Ph.D.
Professor
School of Life Sciences
Jawaharlal Nehru University
New Delhi - 110067

Dean 22.6.16
School of Life Sciences, JNU

Dedicated to
My Parents

ACKNOWLEDGEMENTS

The success of this research depends largely on the encouragement of many others apart from the efforts from my side. I take this opportunity to appreciate those who have been instrumental in the successful completion of my doctoral program.

First and foremost, with a deep sense of gratitude and immense respect, I thank my guide Prof. Supriya Chakraborty (School of Life sciences, Jawaharlal Nehru University, New Delhi). I am indebted to him for his deft touch to inculcate a sense of discipline while assigning me the given project. In spite of his busy schedule and paucity of time, he guided me with a humane touch during the entire course of my study. His benevolent attitude, scholarly guidance, constructive criticism and encouragement at every step helped me a lot while on work, and enabled me to perform fruitfully. The upliftment that he has given to my academic, professional, financial and moral well being cannot be described in words.

I am deeply obliged to my co-supervisor Dr. Manoj Prasad (National Institute of Plant Genome Research, New Delhi), for spending many hours in guiding and helping me, to tie down a loose end by providing broad base of knowledge for the concerned project. He left no stone unturned for making the facilities easily accessible. His caliber, cool nature and cordial behavior made me more confident to tackle the hardships in the preparedness for research work. The joy and enthusiasm he has for research was contagious and motivational, especially during tough times in the Ph.D. pursuit. In every sense, none of this work would have been possible without him.

I feel highly obliged in expressing my deep sense of gratitude to the Dean, School of Life Sciences, Prof. B.C. Tripathy, conceding me to avail the best of facilities at the elite school of the University.

I want to thank University grant commission (UGC) for providing me Non-NET research fellowship during my Ph. D and take away my financial concerns throughout this period.

I would like to record my gratitude to Dr. Debasis Chattopadhyay, NIPGR for his right preparatory guidance and cooperation. He was most instrumental in evoking my research interests by exposing me to several forefront research issues and for his timely advices to make my research more productive.

I would like to thank people from both the places, Jawaharlal Nehru University and NIPGR. They all created a wonderful working environment making my running around worthwhile. The liberality and assistance of all my lab mates at JNU, Dr. Saumik Basu, Dr. Veerendra Sharma, Dr. Biju George, Dr. Dhriti Bhattacharya, Vinoth, Ashish, Rajrani, Prabu, Divya, Kishore, Raghunathan, Prashantji, Nivedita, Ved, Manish and K. Prabhu has made my goal achievable. My heartfelt gratitude and thanks go out to especially to Dr. Nirbhay Kushawaha, Ashish, and Mansi for cooperating me in experimental and innumerable other ways.

Besides, I would also like to convey my gratitude all the respected teachers and administrative staff of SLS for their kind help and support throughout my research period in SLS. I would like to thank all the CIF members for helping me in my experiments.

I would like to extend my thanks to my NIPGR family. Particularly, I attach importance to the patient gestures Dr. Rakesh Shukla, Dr. Vineeta Tripathi, Dr. Rajeev Yadav, Dr. Neeraj Kumar, Dr. Chandrabhan Yadav, Dr. Priyanka Sood, Dr. Shweta, Kajal, Sarita, Anandji, Bharti, Tambi,

Yusuf, Aranavo, Roshan, Anju, Saurabh, Jananee, Rohit, Upma and Ritika. My time at NIPGR was made enjoyable in large part due to my ever zealous and loving colleagues and friends Dr. Aditi Gupta, Dr. Bhanu Prakash Petala, Dr. Santosh Gupta, Dr. Mukesh Meena, Dr. Kamlesh Sahu, Hitaishi, Vikas, Gulab, Siddhi, Prakash, Neeraj, Neelesh, Lalita, Megha, Sonal and Krishna.

Credits are also due to Amita, Garima and Annvi for their informal milieu, friendly and lively atmosphere. This is an appropriate time to convey my appreciation to the special bond I share with Namisha. Her tireless help in the lab-work and all her efforts in the kitchen over the last few months ensured that I reached this stage successfully. I am may be among the few lucky people who are fortunate to find such an understanding and loving junior. A special thanks to Karunesh, Awadhesh, Manjul and Raghu, for giving a lot of memorable stories to share amongst us, with some sensational and divine speeches in English, during monthly gathering.

Word of thanks goes to all the staff members of NIPGR, Arunji, Ashok ji, Shobharam ji, Anand ji, and Surender ji for making my work easy in CIF. I am thankful to Chandraprakash, Bikash and Robi da for helping me in lab as well as maintaining the plants in green house and fields.

I thank all my relatives for their cheering words, especially my loving brothers Nishant, Saurabh, Vaibhav and sister-in-law Neha for standing by me through moments of joy and despair. Without the support of my friends it was not possible to bring this work to its logical end. Those who were always a pillar of strength to me include Gaurav, Pratibha, Amit, Arpita, Sushil, Rashmi, Anju, Richa and Parul didi.

My parents have played the most pivotal role to boost my aspiration and have given moral support by patting on my back to see that my confidence is not dented at the time of stress. If we ever had a family motto that would have been – Time is the most Potent and Powerful – a philosophy of life I have been carrying with me every day. The successful completion of my doctoral program is an answer to their prayers and a fruit of their blessings. No words can be enough to thank them, for that, I dedicate my thesis to their feet. However, this is just a small step towards unveiling their dreams.

I am indebted to my other set of parents, my parents-in-law, for their continual support, encouragement and several uncountable things they have done for me. Their concern helped me deeply appreciate that how much I am cared for. A weekly visit to them (although it has not been possible for last few months) was very relaxing and inspiring. I don't say it enough, but thank you aai-baba for sharing my triumphs and tears. You mean a lot to me!

I am not left with enough and appropriate words to thank my wife. We both have shared love over long-distance for years that seemed like forever. During the period of my trial and tribulation and moments of self-doubt she acted as harbor in the tempest. She has always provided optimistic company, encouragement, sound advice, and lots of excellent initiatives throughout my research period especially during the thesis-writing. I would have been lost without her.

Finally, unfailingly I pray and thank to the Almighty for his shower of blessings and giving me the strength to do my duty to the pinnacle satisfaction of my superiors. God, it is under your compassion that I stride to live, learn and flourish.

- Pranav

TABLE OF CONTENTS

Title	Page No.
Certificate	
Acknowledgements	
Table of content	
List of Tables	
List of Figures	
Abbreviations	
Chapter 1: INTRODUCTION	1-5
Chapter 2: REVIEW OF LITERATURE	6-31
2.1 Tomato (<i>Solanum lycopersicum</i>)	6-9
2.1.1 History, origin and domestication	6
2.1.2 Description of Plant	6
2.1.3 Botanical classification	7
2.1.4 Taxonomic hierarchy	7
2.1.5 Climatic requirements for cultivation of tomato	8
2.1.6 Nutritional importance	8
2.1.7 Genome architect of Tomato	8
2.1.8 Tomato production in India	9
2.1.9 Diseases of tomato	9
2.2 Family: <i>Geminiviridae</i>	10-17
2.2.1. Genome organization of <i>Begomovirus</i>	12
2.2.2 Function of <i>Begomovirus</i> ORFs	13
2.2.3 Mechanism of replication and transcription of geminiviruses	15
2.2.4 Tomato Leaf Curl Disease (ToLCD)	17
2.3 Involvement of host factors during geminivirus-plant interactions	18-31
2.3.1 The ubiquitin-proteasome system	19
2.3.2 Ubiquitin proteasomal pathway: a trigger to destroy pathogen	21
2.3.3 Functions of 26S proteasome subunits in plant stress response	24
2.3.4 Novel function of 26S proteasome subunits in biotic stress response	24-28
2.3.4.1 Programmed cell death and activation of ROS	25
2.3.4.2 Hormone based regulation of defense	26
2.3.4.3 Establishment of plant-pathogen interaction	27
2.3.4.4 Proteasome-dependent RNase activity	27
2.3.4.5 Role in RNA recombination	28

2.3.5	Involvement of 26S proteasome subunits in abiotic stress response	28
2.3.6	26SP subunits and abiotic stress tolerance	29
2.3.7	Genetic and epigenetic control of abiotic stress through 26SP component	30
Chapter 3:	MATERIALS AND METHODS	31-66
3.1.	Material	31-44
3.1.1	Plant material	32
3.1.2	Bacterial strains	32
3.1.3	Plasmid vectors	32
3.1.4	Enzymes	33
3.1.5	Kits	33
3.1.6	Chemicals used	34
3.1.7.	Concentrations of various antibiotics	35
3.1.8.	Composition of media	36
3.1.9.	Composition of buffers	36
3.1.10.	Composition of reagents and other solutions	38
3.1.11.	Composition of SDS-PAGE	40
3.1.12.	Primer sequences	42
3.1.13	List of 168 tomato genes encoding AAA+ATPase domain protein used for phylogenetic analyses.	44
3.2	Methods	45-66
3.2.1.	Plant growth conditions and treatments	45
3.2.2.	Sterilization protocols	45
3.2.3.	General recombinant DNA techniques	46-52
3.2.3.1.	Nucleic acid extraction from plant	46
3.2.3.2.	DNase treatment and reverse transcription	47
3.2.3.3.	DNA amplification and amplicon purification	48
3.2.3.4.	Cloning of amplified fragments/genes	49-52
3.2.3.4.1.	Competent cell preparation	49
3.2.3.4.2.	Ligation	50
3.2.3.4.3.	Restriction digestion of DNA	50
3.2.3.4.4.	Transformation	51
3.2.3.4.5.	Confirmation for the presence of insert	52
3.2.4.	Agroinfection of tomato plants with ToLCNDV	53
3.2.5.	<i>In silico</i> analysis	54
3.2.6.	Phylogenetic analysis	55

3.2.7. Gene expression analysis by northern hybridization	55
3.2.8. Bacterial expression and purification of SIRPT4 protein	56-57
3.2.8.1. Cloning in protein expression vector, pGEX4T-2	56
3.2.8.2. Induction and purification of GST-SIRPT4 from <i>E. coli</i>	56
3.2.8.3. Polyacrylamide gel electrophoresis of proteins	57
3.2.9. ATPase assay	57
3.2.10. Pulldown assay for protein-protein interaction	58
3.2.11. BiFC Assay for confirmation of interacting partners	59
3.2.12. Electrophoretic mobility shift assay (EMSA)	59
3.2.13. Chromatin immunoprecipitation assay (ChIP)	60
3.2.14. TRV-mediated virus induced gene silencing (VIGS)	62
3.2.15. Analysis of ToLCNDV infectivity index on SIRPT4 silencing	63
3.2.16. <i>Agrobacterium</i> -mediated transient overexpression of <i>SIRPT4</i>	64
3.2.17. Statistical data analysis	66
Chapter 4: RESULTS	67-100
4.1. Molecular cloning and characterization of tomato RPT4a gene	67-83
4.1.1. Retrieval of full length SIRPT4a gene	67
4.1.2. Sequence analysis of SIRPT4 ORF encoding protein	67
4.1.3. Genomic organization of <i>SIRPT4</i>	68
4.1.4. Structure of the SIRPT4 protein	68
4.1.5. Phylogenetic studies of SIRPT4 protein	71
4.1.6. <i>Cis</i> -acting regulatory elements identified in <i>SIRPT4</i> promoter region	72
4.1.7. Tissue specific expression of <i>SIRPT4</i>	74
4.1.8. Expression analysis of <i>SIRPT4</i> after various hormone treatments	74
4.1.9. Bacterial protein expression of SIRPT4	75
4.1.10. SIRPT4 has ATPase activity	76
4.1.11. Novel interacting partners identified by pull-down assay	77
4.1.12. SIRPT4 protein interacts with SIBCL31 and SIDDI1	83
4.2. Elucidating the function of SIRPT4 gene in providing defense against ToLCNDV infection	84-100
4.2.1. SIRPT4 protein has viral DNA binding activity	84
4.2.2. SIRPT4 affects binding of RNA PolIII complex to viral DNA	87
4.2.3. SIRPT4 protein regulates bi-directional transcription	88
4.2.4. Efficiency of TRV-based VIGS in tomato	89
4.2.5. Silencing reduced <i>SIRPT4</i> accumulation upon virus infection	91
4.2.6. Silencing of <i>SIRPT4</i> increases ToLCNDV induced symptom	92

severity	
4.2.7. Silencing of <i>SIRPT4</i> enhances ToLCNDV-specific viral DNA accumulation	94
4.2.8. Transient overexpression of <i>SIRPT4</i> leads to the activation of HR and programmed cell death in tomato	96
4.2.9. Transient overexpression of <i>SIRPT4</i> modulates Caspase like protease activity	97
4.2.10. Silencing of <i>SIRPT4</i> decreases ToLCNDV-specific viral DNA accumulation	97
4.2.11. Involvement of reactive oxygen species (ROS) in hypersensitive response	98
Chapter 5: DISCUSSION	101-110
Chapter 6: SUMMARY	111-113
Chapter 7: REFERENCES	114-130
List of publications	131

List of Tables

Table No.	Title	Page No.
2.1.	Total area harvested and the average production of 10 major tomato growing states in India.	9
3.1.12.	Primer sequences	42-43
4.1.	List of <i>cis</i> -acting regulatory elements identified in SIRPT4 promoter.	73
4.2.	Details of identified target proteins of SIRPT4.	79-80
4.3.	Infectivity scoring of <i>Tomato leaf curl New Delhi virus</i> -inoculated control, mock and SIRPT4-silenced plant.	92

List of Figures

Figure No.	Title	Page No.
Fig. 2.1.	Morphological description of tomato plant	7
Fig. 2.2.	Organization of geminivirus genome	11
Fig. 2.3.	Interaction between Replication associated protein (Rep) and host DNA replication machinery	14
Fig. 2.4.	Schematic representation of geminivirus replication and transcription process in the nucleus.	16
Fig. 2.5.	Symptom of ToLCNDV infection in tomato	18
Fig. 2.6.	The ubiquitin-proteasome system	20
Fig. 2.7.	Structural components of 26S proteasome complex	21
Fig. 2.8.	Involvement of host factors in modulating diverse cellular process during geminivirus infection	23
Fig. 4.1.	Characterization of tomato SIRPT4a gene (SGN-U566414)	68
Fig. 4.2.	Secondary structure of SIRPT4a protein	69
Fig 4.3.	The 3D tertiary structure models of SIRPT4 protein as generated by I-TASSER software	70
Fig. 4.4.	Representation of the domain architecture of SIRPT4 protein	71
Fig. 4.5.	Phylogeny of tomato AAA domains	72
Fig. 4.6.	Tissue-specific expression of SIRPT4 gene	74
Fig. 4.7.	Hormone induced expression of <i>SIRPT4</i> transcript at 12 h post hormone treatments	75
Fig. 4.8.	Bacterial expression and purification of SIRPT4 protein	76
Fig. 4.9.	Thin-layer chromatography to evaluate ATPase activity of SIRPT4	77

Fig. 4.10.	Sliver stained 12 % SDS-PAGE showing resolved bands of probable SIRPT4 interacting partners	78
Fig. 4.11.	Gene Ontology annotation of SIRPT4 interacting proteins	81
Fig. 4.12.	Analysis of protein domains in SIRPT4 interacting proteins	82
Fig. 4.13.	BiFC analysis of SIRPT4:SIBCL31 and SIRPT4:SIDDI1 interaction	83
Fig. 4.14.	DNA binding activity of GST-tagged SIRPT4 protein	84
Fig. 4.15.	Schematic representation of Chromatin immunoprecipitation assay	86
Fig. 4.16.	Schematic representation of Chromatin immunoprecipitation assay after co-infiltration	87
Fig. 4.17.	Accumulation of <i>Rep</i> - and <i>Coat protein (CP)</i> -specific transcripts in the leaves infiltrated with empty vector (EV), SIRPT4-cmyc and RNA Pol II-3-gfp construct alone, or co-infiltration in various combinations	88
Fig. 4.18.	TRV-based VIGS in tomato and <i>Nicotiana benthamiana</i>	90
Fig. 4.19.	Accumulation of <i>SIRPT4</i> in ToLCNDV-infected cv. H-88-78-1 (H ^T) and <i>SIRPT4</i> -silenced cv. H-88-78-1-infected with ToLCNDV (H ^{SIRPT4+T})	91
Fig. 4.20.	Phenotypes of cv. H-88-78-1	93
Fig. 4.21.	Phenotypes of mock and <i>SIRPT4</i> -silenced cv. H-88-78-1 at 21 days post ToLCNDV infection	94
Fig. 4.22.	Detection of ToLCNDV genomic components	95
Fig. 4.23.	Agrobacterium-mediated transient overexpression of <i>SIRPT4</i>	96
Fig. 4.24.	Level of caspase like activity upon transient overexpression of <i>SIRPT4</i>	97
Fig. 4.25.	Accumulation of viral DNA in <i>SIRPT4</i> -overexpressed tomato cv. Punjab Chhuhara	98
Fig. 4.26.	Measurement of antioxidant enzyme activity	99
Fig. 4.27.	Assessment of antioxidant enzyme activity in cv. H-88-78-1	100

Abbreviations

%	Percent
°C	Degree Celsius
26SP	26S Proteasome
APS	Ammonium per sulfate
BiFC	Bimolecular fluorescent complementation
BLAST	Basic Local Alignment Search Tool
bp	Base pair
BSA	Bovine serum albumin
cDNA	Complementary DNA
CR	Common region
CTAB	Cetyl trimethyl ammonium bromide
cv.	Cultivar
DDI1	DNA damage inducible protein 1
DEPC	Diethyl pyrocarbonate
DMSO	Dimethyl sulfoxide
DNA	Deoxyribonucleic acid
DNase	Deoxyribonuclease
dNTPs	Deoxy nucleotide triphosphates
dpi	Days post inoculation
dsDNA	Double stranded DNA
DTT	Dithiothreitol
EDTA	Ethylene diaminetetra acetic acid
EMSA	Electrophoretic mobility shift assay
ET	Ethephon
EtBr	Ethidium bromide
g	Gram
GFP	Green fluorescent protein
GO	Gene ontology
GST	Glutathione S-transferases
HEPES	4-(2-hydroxyethyl)-1-piperazineethanesulfonic acid
IPTG	Isopropyl β -D-1-thiogalactopyranoside

IR	Intergenic region
I-TASSER	Iterative Threading ASSEmby Refinement
ITB	Inoue transformation buffer
kb	Kilo base pairs
kDa	Kilodalton
Kg	Kilogram
LB	Luria-Bertani medium
M	Molar
MDA	Malondialdehyde
MeJA	Methyl jasmonate
min	Minutes
ml	Millilitre
mm	Millimeter
mM	Millimolar
MS	Murashige and Skoog medium
ng	Nano gram
NJ	Neighbor joining
OD	Optical density
ORF	Open reading frame
PAGE	Polyacrylamide gel electrophoresis
PCR	Polymerase chain reaction
PEG	Polyethylene glycol
PMSF	Phenylmethanesulfonyl fluoride
RNA	Ribonucleic acid
RNAi	RNA interference
RNase	Ribonuclease
rpm	Revolutions per minute
RPT	Regulatory particle triple-A ATPase subunit
SA	Salicylic acid
SDS	Sodium dodecyl sulphate
sec	Second
SMART	Simple modular architecture research tool
ssDNA	Single stranded DNA
TEMED	N,N,N',N'-Tetramethylethylenediamine

ToLCNDV	<i>Tomato leaf curl New Delhi Virus</i>
v/v	Volume by volume
w/v	Weight by volume
X-gal	5-bromo-4-chloro-3-indolyl- β -D-galactopyranoside
X-Gluc	5-Bromo-4-chloro-3-indoxyl-beta-D-glucuronide cyclohexylammonium salt
μ g	Microgram
μ l	Microliter
μ M	Micromolar

Chapter 1: Introduction

Plants are under continuous challenge against a wide spectrum of pathogens. Since the origin and growth of agriculture, diseases affecting crop production is a major constrain posing threat to global food security. The first attempt to understand plant diseases was documented in the writings of Theophrastus (372-287 BC), who hypothesized their nature. Later on, through domestication of crops from their wild progenitors, farmers tended to select superior crops, thus incidentally breeding plants resistant to disease. In the modern world, application of genetics is one of the commonly practiced resistance strategies for disease control. Recent advancements in plant biology have revealed that plants are equipped with numerous defense strategies which assist them to survive the pathogen infection. Upon pathogen attack, host cell activates a series of responses, such as activation of plant disease resistant gene (R-gene mediated resistance) and hormone mediated signaling pathways. Identification and transfer of naturally occurring resistance genes through breeding (mutation, polyploidy and haploids generation) of wild plants into cultivated lines is still under progression.

Since two decades, viruses have held extensive scientific attention due to their recurrent evolution and recombination of new strains. Their extensive global distribution results in crop yield losses worldwide. Among the plant viruses, ‘Geminiviruses’ have the most devastating effect on diverse horticultural crops, particularly in tropical and subtropical regions (Moffat, 1999). Family *Geminiviridae* includes small, circular, icosahedral, single-stranded DNA (ssDNA) viruses (Stanley and Townsend, 1985). Based on genome structure, host range and insect vector transmission, *Geminiviridae* is classified into seven genera: *Becurtovirus*, *Begomovirus*, *Mastrevirus*, *Curtovirus*, *Eragrovirus*, *Topocuvirus* and *Turncurtovirus* (ICTV virus taxonomy, 2014). Among them, *Begomovirus* is the largest genus (288 species) which infects dicotyledonous plants, with whitefly (*Bemisia tabaci*) acting as a transmitter. *Begomoviruses* either have bipartite (DNA-A and DNA-B genome) originating in the New World, or monopartite (DNA-A genome) from the Old. Bipartite begomoviruses genomes are each ~2.7 kb in size, comprising of a highly conserved 200 nucleotide common region (CR) containing *cis*-acting elements for the origin of replication (*ori*). DNA-A genome has 5 open reading frames (ORFs) capable of encoding various proteins essential for viral replication and encapsidation (capsid protein; CP/AV1). The replication associated protein (Rep), encoded by the AC1

Introduction

ORF, instigate the viral DNA replication process (Laufs et al., 1995b) by interacting with *cis*-acting elements of the *ori* (Arguello-Astorga et al., 1994; Fontes et al., 1994a; Lazarowitz et al., 1992a). On the other hand, ORFs of DNA-B encodes two proteins, i.e., movement protein (MP/BC1) and nuclear shuttle protein (NSP/BV1) which act as essential factors for cell-to-cell movement as well as systemic spread of the begomovirus (Hanley-Bowdoin et al., 2000).

Resistance/tolerance of a plant against geminiviruses has been linked with hypersensitive reaction (Mubin et al., 2010; Hussain et al., 2005), quantitative trait loci (Tomas et al., 2011; Anbinder et al., 2009) and epigenetic regulation leading to RNA silencing (Raja et al., 2010; Sahu et al., 2014a). This naturally occurring RNA interference process generates small interfering RNAs (siRNAs) or microRNAs (miRNAs), which in turn identify the corresponding sequence specific RNA targets and subsequently degrade or suppress its translation (Chapman and Carrington, 2007; Sharma et al., 2013). This phenomenon of RNA silencing is exploited by both the host and the pathogen, as a counter defense strategy. For host, this provides innate immunity against virus infection (Sharma et al., 2013), while the virus utilizes it to interrupt host cellular functions, modulate gene expression associated with defense pathways (Ratcliff et al., 1997; Sahu et al., 2010, 2014b). Plant viruses elicit RNA silencing machinery by the generation of double-stranded (ds) RNA, which gets processed into siRNAs of 21-24 nucleotides. These small molecules are sequentially integrated into an effector complex known as the RNA induced silencing complex (RISC), leading to the endonucleolytic cleavage of the specific RNA target or transcriptional repression (Shimura and Pantaleo, 2011). However, viruses are equipped with the suppressor proteins to counter host RNA silencing mechanism (Bivalkar-Mehla et al., 2011).

Tomato (*Solanum lycopersicum*) belongs to the nightshade family Solanaceae. Tomato species are known to be originated in the western parts of Central and South America (Kimura and Sinha, 2008). Tomato ($2n = 24$), is a very important vegetable crop; known for high level of natural antioxidants carotene 'lycopene' (351 mg/100 g). It is commonly consumed as a fresh vegetable or processed into ketchup or soup. Tomatoes are naturally enriched (>100 mg/100 g) in minerals such as Potassium and Sodium (129 mg/100 g). They have anti-cancerous properties and can provide protection to skin against harmful UV rays (Story et al., 2010). Tomatoes are also

very good source of Vitamin C (27 mg/100 g) and Folic acid (30 mg/100 g). It has emerged as an outstanding model plant to study plant-pathogen interactions (Arie et al., 2007). An international consortium named International Solanaceae Genomics Project (SOL) has successfully sequenced the genome of cultivated tomato (The Tomato Genome Consortium, 2012). Availability of its genome data will assist to make promising development for disease resistance strategies against fungal, bacterial, and viral pathogens.

Fifty five distinct and 26 probable begomovirus species have been identified to potentially infect tomato under field conditions, out of which, 49 species were linked with Tomato Leaf Curl Disease (ToLCD) and 17 with Tomato Yellow Leaf Curl Disease (TYLCD). ToLCD has been shown to limit the tomato production in South and Southeast Asia (Chakraborty, 2008). The characteristic symptom of ToLCD infection are upward curling of leaflet margins, decreased leaflet area, in some cases yellowing of young leaves, along with arrested growth and flower abortion (Moriones and Navas-Castillo, 2000). *Tomato leaf curl New Delhi virus* (ToLCNDV) infection causes devastating effects in terms of yield loss in tomato (Saikia and Muniyappa, 1989). Source for conventional tolerance against ToLCNDV is limited in tomato. Moreover, appropriate sources of resistance are still unknown amongst the wild relatives. Therefore, there is an immediate need for understanding natural resistance, which may assist in the development of novel crop protection strategies.

In last decade, Ubiquitin proteasome system (UPS) have appeared as a new theme in plant-virus interactions and their corresponding roles have been extensively reviewed (Citovsky et al., 2009; Dielen et al., 2010; Sahu et al., 2014b). UPS mediated protein degradation involves two distinct process; polyubiquitination of target protein through the action of three enzymes and subsequent degradation of the polyubiquitinated protein via the catalytic activity of 26S proteasome complex (Smalle and Vierstra, 2004). For example, silencing of ubiquitin activating enzyme (UBA1) altered the interaction of UBA1 and transcriptional activator protein (TrAP), which assisted in the enhancement of geminivirus infection in transgenic *Nicotiana benthamiana* (Lozano-Durán et al., 2011). Similarly, upon *Cabbage leaf curl virus* infection, inhibition of RING-type E3 ubiquitin ligase expression modulated the process of infection (Ascencio-Ibáñez et al., 2008). Such studies highlight the role of UPS in inter-connecting geminivirus replication and host counter defense strategies.

Introduction

Majority of the studies on 26SP are focused on their ubiquitination dependent proteasome functions (Vierstra, 2009). However, increasing evidences have transformed the conventional opinion of combined role of 26SP in the regulation of cellular function, into the individual function of each subunit of this multimeric complex. Hence, inhibition of the UPS specific process and abundance are not the solitary contributors of plant stress response. All the subunits may play an explicit role during the perception, signaling and activation of stress adaptive pathways. Interestingly, 26SPs have also been found to be associated with genetic regulations. Genetic control of thermo-tolerance associated traits has been linked with the proteasome subunit (Li et al., 2015). Vigorous examination of such genetic loci, containing 26SP, may be utilized as a marker for the screening of the resistance sources and might be extensively exploited in crop-breeding programs. Moreover, 26SPs have emerged as a key factor in the epigenetic mechanisms governed by DNA methylation, histone modifications and chromatin remodeling to modulate the expression of stress-responsive genes (Lee et al., 2011; Sako et al., 2012). Environmentally-induced subunit functions are important for plant development and survival under adverse conditions. Novel function and molecular role of various subunits have been identified such as, RNase activity against the plant viruses (Pouch et al., 1995; Dielen et al., 2011), interaction with pathogen effectors (Üstün et al., 2014, 2015) and viral RNA recombination (Prasanth et al., 2015). The fact that there are significant impacts of 26SPs on plant growth under stress environments will be helpful to draw attention towards dissecting the roles of particular 26SP subunits but our current understanding in this area is limited. Thus, there is an immediate need to identify interacting partners of 26SP to find out their novel functions in plant stress response. Extensive studies on 26SPs will serve as an excellent foundation to develop a novel transformative approach for generating stress tolerance and disease resistance in plants.

In our previous study, we identified a cultivar, namely H-88-78-1, which was found to be tolerant towards ToLCNDV infection (Sahu et al., 2010). It was further identified that the lower level of viral DNA accumulation in this cultivar had a strong correlation with higher production of siRNAs derived from the viral genome at 21 days post-inoculation (dpi) of ToLCNDV (Sahu et al., 2010, 2012). An attempt was made to identify the host genes involved in conferring tolerance by suppression subtractive

library preparation between ToLCNDV-inoculated and mock-inoculated plants of cv. H-88-78-1 at 21 dpi. A total of 106 non-redundant transcripts were identified and categorized according to their putative functions. Out of these 106 transcripts, 34 showed > 2.5 fold expression upon ToLCNDV infection. Interestingly, higher expression (> 4 fold) was observed for components associated with Ubiquitin proteasome pathway i.e., *26S proteasome subunit RPT4a* (GR979393), *Ubiquitin conjugating enzyme* (GR979415) and *Armadillo repeat motif-containing protein* (GR979475) (Sahu et al., 2010). Thus functional characterization of these UPS-related gene(s), which were differentially expressed during ToLCNDV infection, may help a better understanding of the defense mechanisms of tomato against ToLCNDV infection. Keeping the above in view, the objectives of present study were designed as follows:

1. Cloning and molecular characterization of the Ubiquitin proteasomal pathway gene(s)
2. Elucidating the function(s) of these candidate gene(s) against ToLCNDV infection.

Chapter 2: Review of Literature

2.1 Tomato (*Solanum lycopersicum*)

2.1.1 History, origin and domestication

The name 'tomato' originates from the Spanish word '*tomate*' which is actually derived from the Mexican Nahuatl name '*tomatl*', meaning tomatillo (Rick, 1978). Tomato is generally considered to be the native of western South America and Central America (Smith, 1994). Although, the precise time and location of domestication are still unknown, Mexico is assumed to be the most possible region of domestication, along with Peru as the centre of diversity for wild relatives (Larry and Joanne, 2007). The wild cherry (*Lycopersicon esculentum* var. *cerasiforme*) is the immediate progenitor of the cultivated tomato based on its wide occurrence in central America and the existence of a shortened style length in the flower (Cox, 2000). In the 16th century, tomato further spread throughout the world and has become extremely popular in India within the last 60 years.

2.1.2 Description of Plant

Solanaceae is economically the most important family and are highly divergent in regard to habitat and morphology (Knapp et al., 2004). Tomato plants are vines and grow upto 180 cm (6 ft) with a series of branching stems (Fig. 2.1A). According to the leaf morphology, tomato plants are either classified as regular leaf (RL) plants, which have compound leaf (Fig. 2.1B), or potato leaf (PL) which have simple leaves (<http://www.gardenweb.com/>). Compound leaves of tomato can be grouped into rugose leaves (deeply grooved), and variegated, angora leaves (caused by the genetic mutation resulting in the altered chlorophyll production) (<http://faq.gardenweb.com/>). In general, leaves are 10-25 cm long, odd pinnate (5-9 leaflets per petioles), serrated margin along with the densely glandular-hairy structure (Acquaah, 2002). Flowers originate from the apical meristem and are borne in a cyme of 3 to 12. Flowers are self-fertilizing with fused anthers, 1-2 cm in length, yellow in color, along with the five pointed lobes on the corolla (Fig. 2.1C). Fruits develop from the ovary after fertilization and are classified as berry (Fig. 2.1B). The locular cavities comprise of hollow spaces rich in seeds and moisture and the flesh is composed of the pericarp walls.

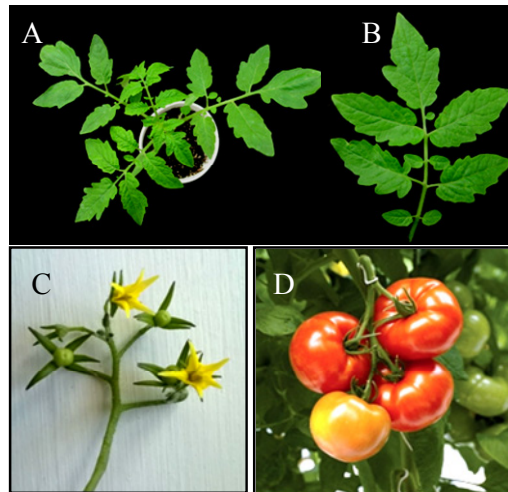


Fig. 2.1. Morphological description of tomato plant. Phenotype of tomato plant, **A**; Leaf, **B**; Flower, **C** and fruit morphology, **D**.

2.1.3 Botanical classification

The cultivated tomato was initially named *Solanum lycopersicum* by Linnaeus (1753). However, later on cultivated tomato was designated as the genus *Lycopersicon* and the species *esculentum* (Miller, 1754). Further, according to molecular and morphological information, taxonomic classification of the cultivated tomato was reaccepted as *S. lycopersicum* (Terrell et al., 1983; Spooner et al., 1993; Peralta and Spooner, 2001; Knapp et al., 2004). Other species of the genus *Lycopersicon* have also been designated or reassigned to the genus *Solanum* (Marshall et al., 2001; Peralta and Spooner, 2005).

2.1.4 Taxonomic hierarchy

Kingdom:	Plantae
Subkingdom:	Tracheobionta
Super-division:	Spermatophyta
Division:	Magnoliophyta
Class:	Magnoliopsida
Subclass:	Asteridae
Order:	Solanales
Family:	Solanaceae
Genus:	<i>Solanum</i> L.
Species:	<i>Solanum lycopersicum</i> L.

2.1.5 Climatic requirements for cultivation of tomato

Tomato is grown as a warm season crop and is unable to resist frost and high humidity climatic factor. It requires specific temperature for seed germination, growth of seedling, setting of flower as well as fruit. Optimum range of temperature is in between 21-24°C. It needs low to medium rainfall for growth, however, water stress and long drought may cause cracking of fruits. Soil requirement for the tomato cultivation is deep, well drained sandy.

2.1.6 Nutritional importance

Tomato is consumed either in the form of fresh vegetable included raw in salads, or processed into ketchup or soup. It is rich in minerals such as Potassium (146 mg/100 g), Sodium (129 mg/100 g), and Calcium (48 mg/100 g). They have high level of natural antioxidant carotene namely 'lycopene' (351 mg/100 g), which has been shown to protect the skin against harmful UV rays and keeping the skin looking youthful (Story et al., 2010). Tomatoes are also naturally enriched in Vitamin C (27 mg/100 g) and Folic acid (30 mg/100 g).

2.1.7 Genome architect of Tomato

The genome of the inbred tomato cultivar 'Heinz 1706' has recently sequenced and assembled using the 'next generation' technologies (The Tomato Genome Consortium, 2012). The genome size is about 900 megabases (Mb), out of which 760 Mb aligned onto the 12 tomato chromosomes. The tomato chromosomes comprise of pericentric heterochromatin as well as distal euchromatin, enriched within centromeres, chromomeres and telomeres. Considerably higher abundance of recombination, genes and transcripts was reported at euchromatin. However, chloroplast insertions and conserved microRNA (miRNA) genes were found to be mostly distributed in entire genome. The genome of tomato is highly syntenic among economically significant Solanaceae plants (The Tomato Genome Consortium, 2012). It has approximately 34,727 predicted protein-coding genes. Millions of SNPs present in the tomato genome sequences will permit plant breeders to re-examine the trait reservoir for biodiversity-based breeding.

2.1.8 Tomato production in India

Tomato is one of the major economically important vegetable crops of India. According to FAOstat data, India is the second largest producer of tomato after China (FAO, 2013; <http://faostat.fao.org/>). The average production of tomato is 18.22 million tonnes (MT) with average productivity of 207 hectogram/ hectare. The major tomato producing states (year 2014-2015) are Madhya Pradesh and Karnataka (Table-1; Indian Horticulture Database, 2015; <http://nhb.gov.in>).

Table 2.1. Total area harvested and the average production of 10 major tomato growing states in India.

States	Area (in '000 Ha)	Production (in '000 MT)
Madhya Pradesh	70.225	2177
Karnataka	64.25	2034.371
Andhra Pradesh	54.223	1473.542
Odisha	96.56	1374.94
Gujarat	44.57	1259.01
West Bengal	56.9	1149.585
Telangana	53.185	1080.611
Bihar	47.732	1046.435
Chhattisgarh	52.892	868.602
Maharashtra	35.452	762.161
Total (all India)	767.317	16384.98

2.1.9 Diseases of tomato

More than 200 diseases have been reported to infect tomato worldwide (Watterson, 1986). Among them, Damping off (*Pythium aphanidermatum*), Early Blight (*Alternaria solani*), Buck Eye Rot (*Phytophthora parasitica*), Late Blight (*P. infestans*), Fusarium Wilt (*Fusarium oxysporum f. sp. lycopersici*), Bacterial Wilt (*Pseudomonas solanacearum*), Bacterial Leaf Spot (*Xanthomonas campestris pv. vesicatoria*) are the major diseases of tomato. There are few diseases which have been shown to be caused by viroids, i.e., MLOs (Aster Yellows and Tomato Big Bud) (Bowyer et al., 1969).

Viruses are casual agents of more than 45 % of all emerging diseases of plant (Anderson et al., 2004). Around 140 viral species have been reported to infect the tomato (Green, 1991). A number of viruses, along with *Tomato yellow leaf curl virus*

(TYLCV; *Begomovirus*), *Pepino mosaic virus* (PepMV; *Potexvirus*), and *Tomato torrado virus* (ToTV) have been shown to severely infect and significantly affect the tomato production, globally (Hanssen et al., 2010). Presently, tomato is facing severe yield losses and survival challenge due to geminivirus infection. In the subsequent section we have provided a comprehensive overview of the family *Geminiviridae* and associated genus.

2.2 Family: *Geminiviridae*

Since early 1970s, International Committee on Taxonomy of Viruses (ICTV) began to formulate and implement guidelines for the naming and classification of viruses and the effort is carried on till date. In 2014, seven orders, 104 families, 23 subfamilies, 505 genera, and 3186 species of viruses have been distinguished (ICTV Virus Taxonomy 2014; <http://www.ictvonline.org/virusTaxonomy.asp>). Still, most of the virus families remain unordered or unplaced. Among 104 families, there are 78 families which are not yet assigned to any order. One among them is the *Geminiviridae* family having seven genera, namely, *Becurtovirus*, *Begomovirus*, *Mastrevirus*, *Curtovirus*, *Eragrovirus*, *Topocuvirus* and *Turncurtovirus*, which are characterized by single stranded circular DNA (ssDNA), circular genomes (Sahu et al., 2014b; Fig. 2.2).

Geminiviruses are geminate shaped and have ssDNA which replicates through double-stranded DNA (dsDNA) intermediate in the nucleus of the infected plant cells (Hanley-Bowdoin et al., 2000; Jeske, 2009). Electron microscopy examination discovered that the size of virus particles may range from 18-20 nm in diameter, with a length of 30 nm (Lazarowitz, 1992b; Böttcher et al., 2004). The twinned geminate shaped capsids with two incomplete T=1 icosahedral symmetry is made of pentameric capsomeres (Böttcher et al., 2004). Geminivirus has a small genome (2.5-3.0 kb), comprised of either one (monopartite) or two circular ssDNA molecules (bipartite) (Stanley and Townsend, 1985; Hanley-Bowdoin et al., 2000). Monopartite viruses contain single virus genome, i.e., DNA-A, while bipartite viruses have two genomic components, i.e., DNA-A and DNA B. Geminiviruses have bi-directional promoter for the transcription of either the virion (V) or complementary (C) sense DNA strand-specific transcripts. It contains a conserved 5' common region (IR) which is configured as a stem-loop structure harboring a nonanucleotide (TAATATTAC)

sequence. IR is the key genomic structure regulating replication of the virus. Apart from mono- or bi-partite genome, presence of an additional molecule i.e., satellite DNA has also been reported (Dry et al., 1997; Fiallo-Olivé et al., 2012). Satellite DNA (DNA β or DNA α) of monopartite viruses are smaller in size (approx 1.3 kb), single functional protein encoding, and are required for characteristic symptom development of the disease.

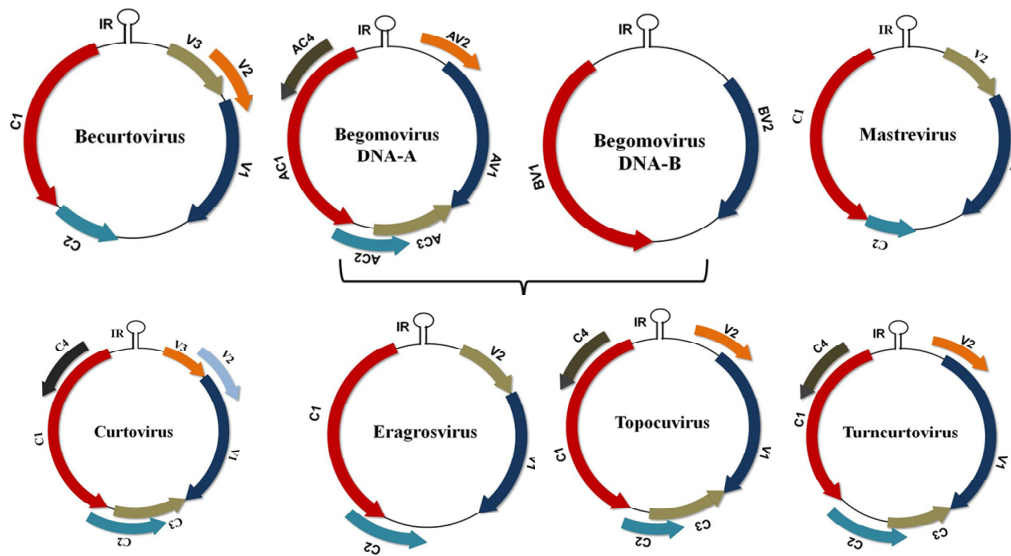


Fig. 2.2. Organization of geminivirus genome. Orientations of corresponding open reading frames (ORFs) are depicted with arrows. Genomic maps of *Becurtovirus* (*Beet curly top Iran viruses*), *Begomovirus* (*Bean golden mosaic virus*), *Mastrevirus* (*Maize streak virus*), *Curtovirus* (*Beet curly top virus*), *Eragrovirus* (*Eragrostis curvula streak virus*); *Topocuvirus* (*Tomato pseudo-curly top virus*) and *Turncurtovirus* (*Turnip curly top virus*) are shown. DNA-A encoded proteins i.e., AC1/C1 (replication initiation protein); AC2/C2 (transcription activator); AC3/C3 (replication enhancer) are depicted in arrows according to their orientation in the genome. DNA-B specific ORFs encoding AV1/V1 (coat protein) BV1/NSP-Nuclear shuttle protein and BC1/MP-Movement protein are shown. (Figure modified from Sahu et al., 2014b)

The genus *Curtovirus* of the *Geminiviridae* family has a monopartite genome which encodes for 7 proteins. Leafhoppers or treehoppers are the main vector for transmission of the viruses belonging to this group. Genus *Becurtoviruses* have two major species, i.e., *Beet curly top Iran virus* and *Spinach curly top Arizona virus*. They are biologically similar to genus *Curtovirus*, however genome organization (monopartite genome encoding 5 proteins) resembles the genus *Mastrevirus*. Viruses

of this genus are transmitted through leafhoppers and cause curly top disease in various dicot species. *Eragroviruses* (*Eragrostis curvula streak virus*) are genomically monopartite in nature, encoding 4 proteins, but their mode of spreading is still unknown. The 2nd largest species containing genus *Mastrevirus*, has monopartite genome (encoding two positive sense and two negative sense ORFs). The members of this genus infect monocotyledonous plants and are transmitted by leaf hoppers. *Topocuvirus* (*Tomato pseudo-curly top virus*) have monopartite genome enclosed of six ORFs. *Topocuvirus* mainly infect dicotyledons and are known to be transmitted by tree hoppers insect. *Turncurtovirus* comprise of a single member (*Turnip curly top virus*). It has monopartite genome which comprise of six ORFs encoding various proteins which are necessary for virus replication and systemic movement upon infection. Similar to *Eragroviruses*, mode of *Turncurtovirus* spread is still unidentified.

2.2.1 Genome organization of *Begomovirus*

Begomovirus is the largest Geminiviridae genus comprising of 288 species (ICTV Virus Taxonomy, 2014; <http://www.ictvonline.org/>) which infect a wide range of dicotyledonous plant. The mode of transmission of this genus is whiteflies (*Bemisia sp.*). In general, species of this genus are bipartite genome (DNA-A and DNA-B) (Rojas et al., 2005), however, some strains from Old World *Begomoviruses* along with few strains of Indian and China have monopartite genome (DNA-A) and a β -satellite DNA (Scholthof et al., 2011; Zhang and Ling, 2011). Existence of other satellite such as nanovirus-like satellite has also been revealed, however precise role of this molecule is still unknown (Patil and Fauquet, 2010). Among bi-partite genome, DNA-A is consist of six ORFs i.e., coat protein (AV1; CP), pre-coat protein (AV2), replication initiation protein (AC1/Rep), transcription activator protein (AC2/TrAP), replication enhancer (AC3/REn), and AC4. AV1 and AV2 are virion strand-specific, while AC1, AC2, AC3 and pathogenesis related protein AC4 are complementary sense-strand specific ORFs. On the other hand, DNA-B has two ORFs which encodes for virion strand-specific nuclear shuttle protein (BV1/NSP) and complementary sense strand-specific movement protein (BC1/MP) (Fauquet et al., 2008). Furthermore, monopartite *begomovirus* genome is analogous to DNA-A molecule of bipartite begomoviruses and encodes for six viral proteins. AV2 of monopartite

viruses also assists in the movement of the virus. Additionally, betasatellite (DNA β) couples with monopartite viruses, which contain complementary-sense strand encoding β C1 and is required as a helper DNA for the multiplication (Briddon et al., 2003).

2.2.2 Function of *Begomovirus* ORFs

Coat protein (AV1) is about ~28 kDa protein, which is implicated in the encapsidation of new viral genome (Briddon et al., 1990; Boulton et al., 1993). It has the ability to interact with both ssDNA and dsDNA molecule (Liu et al., 1997; Kunik et al., 1998; Palanichelvam et al., 1998). CP has been found to be nuclear localized and its interaction with α importin is essential for cytoplasmic trafficking of the host during virus infection (Liu et al., 1999). In monopartite viruses, it facilitates cell to cell and long distance movement of viral genome (Boulton et al., 1989; Liu et al., 1997; Kotlizky et al., 2000). It is also recognized as a determinant of vector specificity (Noris et al., 1998; Hohnle et al., 2001).

In the virus infected cells, pre-coat protein (AV2) is found to be localized in the cytoplasm as well as cell periphery (Chowda-Reddy et al., 2008). AV2 acts as a suppressor of plant RNA interference (RNAi) machinery (Chowda-Reddy et al., 2008). Mutation in pre-coat protein of bipartite *begomovirus* ToLCNDV (*Tomato leaf curl New Delhi virus*) exhibited reduction in the viral DNA accumulation in infected plants (Padidam et al., 1996). It also facilitates the intracellular, intercellular and systemic movement of the monopartite begomoviruses (Stanley et al., 1992; Hormuzdi and Bisaro, 1993).

AC1 (Rep) encodes for ~40 kDa multifunctional protein which is most essential factor for initiation and termination of viral genome replication (Fontes et al., 1994a; Hanley-Bowdoin et al., 2000). It can exclusively bind to a repeated consensus sequence present in the 5' IR of the dsDNA viral genome. It cleaves and ligates DNA at conserved nonanucleotide TAATATT↓AC within a hairpin loop of the plus-strand origin (Lazarowitz et al., 1992a; Orozco et al., 1997). Rep is a key component in the interaction with plant cell cycle regulatory elements (Kong et al., 2000; Kong and Hanley-Bowdoin, 2002), cellular proteins (Morilla et al., 2006) along with the viral REn protein (Settlage et al., 2005). Recent information suggests the role of Rep in

transcriptional gene silencing (Rodríguez-Negrete et al., 2013). During replication of plus-strand, it acts as a DNA helicase to unwind viral DNA (Bisaro, 1996). Apart from its role in viral genome replication, Rep interacts with several host factors involved in DNA replication. It also plays an essential role in activating the replication of viral as well as plant DNA. It binds to subunits of host DNA polymerase complexes (Castillo et al., 2003; Bagewadi et al., 2004; Settlage et al., 2005; Bruce et al., 2011), ssDNA binding proteins (Singh et al., 2007; Lozano-Duran et al., 2011), and recombination/repair process associated proteins to impede host DNA replication event (Fig. 2.3). These critical roles in the genome replication and interactions with multiple proteins make Rep an exceptional target for antiviral resistance strategy by the expression of mutant proteins.

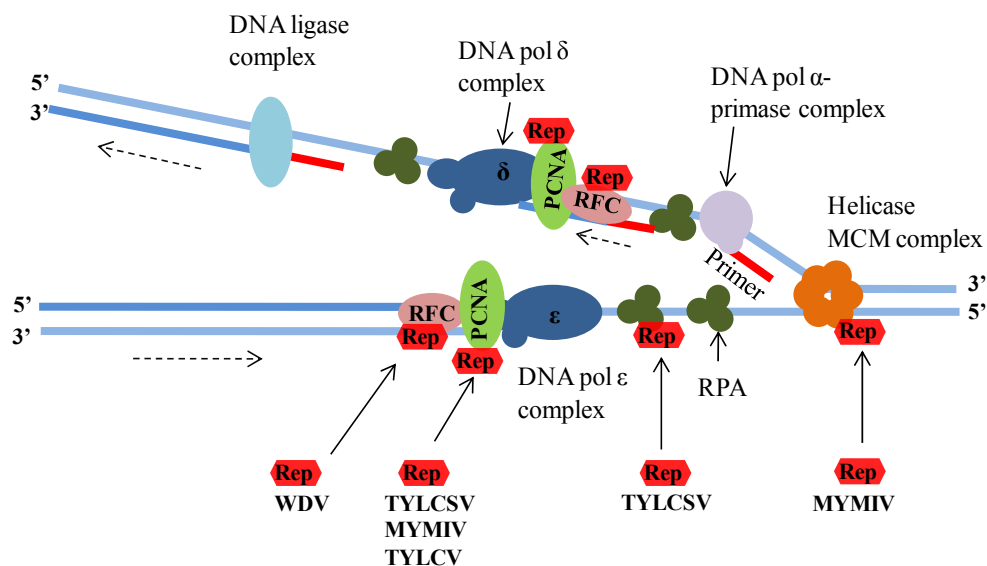


Fig. 2.3. Interaction between Replication associated protein (Rep) and host DNA replication machinery. Rep proteins of various geminiviruses interacts with proliferating cell nuclear antigen (PCNA), replication protein A (RPA), replication factor C (RFC) and minichromosome maintenance complex component 3 (MCM3) and alters the host DNA replication process.

Host genes play an important role during virus infection and act as a counter defense mechanism. On other hand, viruses are also armed with suppressors of host gene activation and gene silencing. In this regard, AC2 from bipartite and monopartite begomoviruses serves as a factor for virus pathogenicity and suppression of gene silencing (Voinnet et al., 1999; Trinks et al., 2005; Vanitharani et al., 2005; Chowda-Reddy et al., 2008). It was observed that expression of TrAP proteins from

Review of Literature

geminiviruses decreased the resistance in *N. benthamiana* and tobacco plants (Sunter et al., 2001; Hao et al., 2003).

Expression of AC3 encoding the replication enhancer protein is determined by the unidirectional left promoter (Shivaprasad et al., 2005). Interaction of this protein with Rep and PCNA is one of the prerequisites of viral DNA replication process (Castillo et al., 2003; Settlage et al., 2005). REn of *Tomato leaf curl Kerala virus* has been identified to interact with Rep, which assists the enhancement of ATPase activity of Rep (Pasumarthy et al., 2011). Disruption of AC4 resulted in reduced viral DNA accumulation and symptom development (Jupin et al., 1994; Rigden et al., 1994; Teng et al., 2010). It has also been evidenced that AC4 may suppress the posttranscriptional gene silencing (PTGS) mechanism of host plant (Vanitharani et al., 2004, 2005; Fondong et al., 2007).

Nuclear shuttle protein (BV1/NSP) has been implicated in nuclear shuttling of the viral genome while MP actively participates in cell-to-cell movement of the virus through plasmodesmata (Gafni and Epel, 2002). The MPs are also pathogenicity determinant of bipartite begomoviruses and the mutation at 3' region has been linked with symptom development (Gafni and Epel, 2002).

2.2.3 Mechanism of replication and transcription of geminiviruses

Geminivirus DNA multiplies by a specific mechanism known as rolling circle replication (Jeske et al., 2001; Fig. 2.4). It involves utilization of the host proteins such as primase and polymerase, through which minus strand genome is synthesized to produce a dsDNA replicative form (RF) of viral genome (Saunders et al., 1991; Gutierrez, 2000; Hanley-Bowdoin et al., 2000). The negative strand synthesis is started via priming of oligoribonucleotide at IR (Fig. 2.4). This RF of DNA is either subjected to generate single stranded viral genome or transcribed into the viral proteins (Hanley-Bowdoin et al., 2000; Jeske et al., 2001; Fig. 2.4).

Replication of geminivirus genome starts with the nicking at 'TAATATTAC' located in stem-loop structure of IR region. Subsequent to cleavage of phosphodiester bond, Rep covalently binds to the 5'-terminus of the fragment via a phosphotyrosine linkage (Laufs et al., 1995a; Jeske et al., 2001). On the other hand, free 3' OH terminus is used as a base for the generation of new viral plus-strand, which finally relocates the

parental plus-strand from the intact minus-strand template. Nevertheless, polymerization of viral DNA is performed by synchronized action of host polymerase (Laufs et al., 1995b,c; Gutierrez, 2000). After completion of the nascent plus strand synthesis, origin of replication is restored for the subsequent nicking by the terminase activity of Rep to discharge a nascent unit-length viral plus strand (Fontes et al., 1994a; Fontes et al., 1994b; Fig. 2.4). In the due course, this plus strand is again ligated to form new viral DNA unit (Jeske et al., 2001). Afterwards, Rep is relocated to the newly created 5' terminus (Jeske et al., 2001). Initially, circular ssDNA act as a template for the generation of minus strand viral DNA. The final stage replication cycle is required for the abundance of newly synthesized viral genomes, followed by encapsidation and transport.

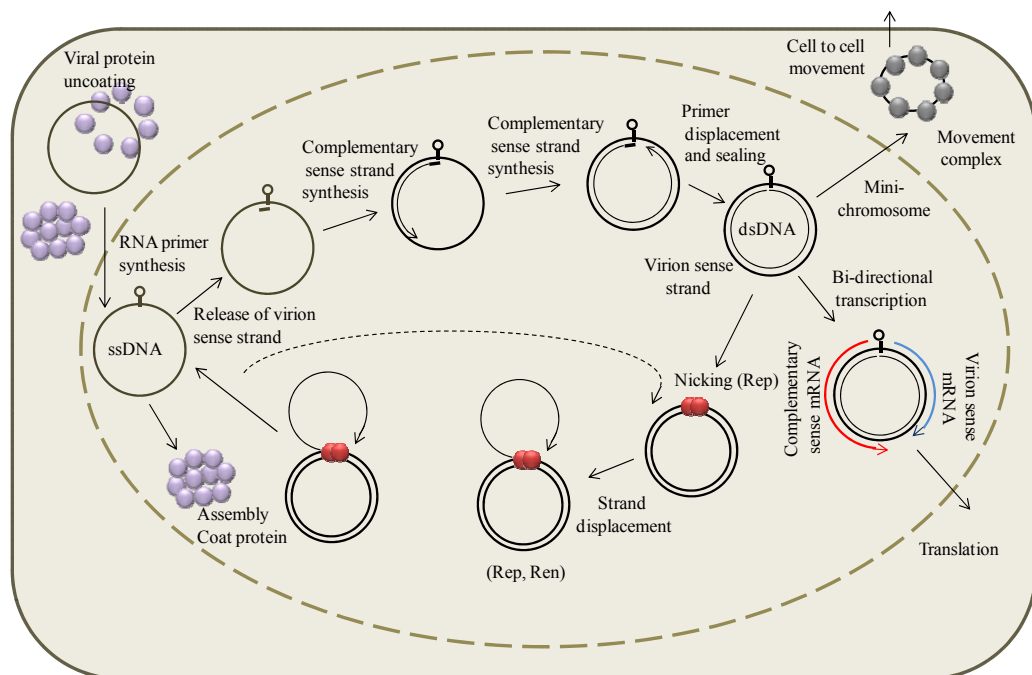


Fig. 2.4. Schematic representation of geminivirus replication and transcription process in the nucleus. Vector based transmission of uncoated circular ssDNA which is shuttled to nucleus. For complementary strand synthesis a RNA primer is implicated, which subsequently displaced and gap is filled to generate dsDNA synthesis. This dsDNA act as template for rolling circle or recombination based replication. Bi-directional transcription of mRNA occurs from ssDNA followed by translation at cytoplasm to generate the viral proteins. dsDNA is coated with CP, which moves further cell to cell via the assistance of NSP and MP proteins. (Reconstructed from Vanitharani et al., 2005).

Geminivirus genomes are transcribed in a bi-directional mode resulting in the production of mRNAs corresponding to both the virion and complementary sense ORFs (Stanley and Townsend, 1985; Hanley-Bowdoin et al., 1989; Frischmuth et al., 1991; Fig. 2.4). These reports also suggest that the viral transcripts are polyadenylated at 3' end and are transcribed by host RNA PolIII (Fig. 2.4). The transcription of geminivirus generates manifold overlapping RNA fragments, which are polycistronic in nature.

2.2.4 Tomato Leaf Curl Disease (ToLCD)

A new disease phenotype characterized by interveinal yellowing, vein clearing, inward rolling of leaves, severe stunting and bushy growth was first reported in tomato (Vasudaeva and Samraj, 1948). The disease was later named as Tomato Leaf Curl disease and the causal agent was designated as *Tomato Leaf Curl Virus* (Verma et al., 1975; Reddy and Yaraguntaiah, 1981). In 1993, this virus was cloned and partially sequenced by Chatchawankanphanich et al. (1993). Geographical distribution of tomato-infecting begomoviruses in India revealed that ToLCV isolates from south India were composed of a diverse group of monopartite viruses which were different from the bipartite tomato begomoviruses of the north India (Chatchawankanphanich et al., 1993, 1995; Padidam et al., 1995b; Muniyappa et al., 2000; Chakraborty et al., 2003).

Afterwards, bipartite ToLCVs were assumed to be present only in north India and monopartite viruses only in south India. Recently, however, a monopartite Tomato leaf curl virus from tomato in Gujarat, north India has been cloned and sequenced (Chakraborty et al., 2003; Shih et al., 2003). Till now, 7 distinct tomato-infecting begomoviruses have been documented in India by ICTV, i.e., *Tomato leaf curl Karnatka virus* (ToLCKV), *Tomato leaf curl Bangalore virus* (ToLCBV), *Tomato leaf curl Gujarat virus* (ToLCGV), *Tomato leaf curl Joydebpur virus* (ToLCJoV), *Tomato leaf curl Kerala virus* (ToLCKeV), *Tomato leaf curl New Delhi virus* (ToLCNDV) and *Tomato leaf curl Pune virus* (ToLCPuV).

ToLCNDV infection in tomato was identified nearly twenty years ago (Padidam et al., 1995a). It is naturally transmitted via whitefly species (*Bemisia tabaci*). It is widely distributed in several countries of Asia (Hussain et al., 2000; Mizutani et al., 2001; Padidam et al., 1995b), however its spread in southern Italy (Panno et al., 2016),

Tunisia (Mnari-Hattab et al., 2015) and Spain (Juárez et al., 2014) has been recently reported. In India, ToLCNDV is distributed majorly in Andhra Pradesh, Delhi, Gujarat, Haryana, Maharashtra, Punjab, Uttar Pradesh, and West Bengal.

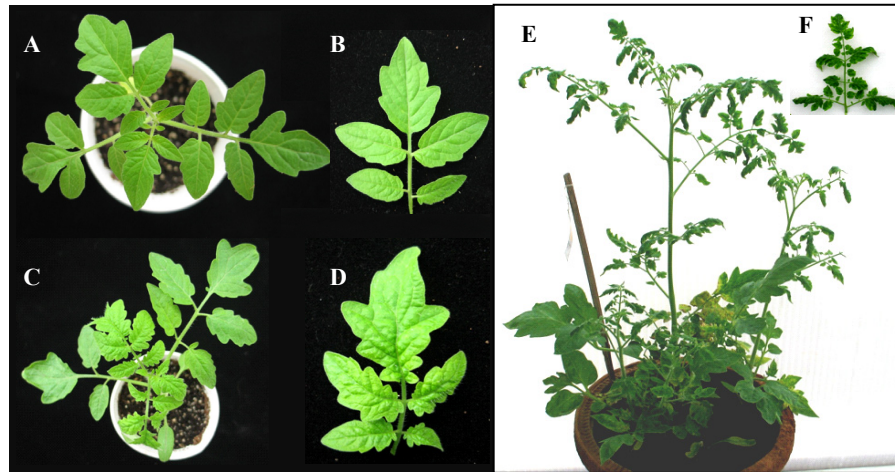


Fig. 2.5. Symptom of ToLCNDV infection in tomato. **A-B**, Morphology of control, ten-day old tomato plant. **C-D**, Phenotype of ToLCNDV agro-inoculated tomato plants showing initiation of leaf curl symptom at 10 dpi. **E-F**, Leaf curl symptom appeared after ToLCNDV infection at 40 dpi.

Infection of ToLCNDV cause phenotypic abnormality in tomato, such as stunted or dwarfed growth, upwards and inwards rolling of leaflets, often bent downwards and are stiff, thicker than normal (Fig.2.5A-F). Young leaves are slightly chlorotic and yellowish in texture (Fig.2.5C-D). ToLCNDV infection has been primarily reported on members of Solanaceae such as potato, eggplant, pepper and tobacco (Amari et al., 2008), however reports are also available suggesting their infestation on cucurbit crops (Sohrab et al., 2003; Tahir et al., 2005; Tiwari et al., 2010; Sohrab et al., 2013; Panno et al., 2016).

2.3 Involvement of host factors during geminivirus-plant interactions

Our restricted information of host gene response during geminivirus infection in plant is the major constrain for future studies. Various approaches have been exploited to establish the host gene-expression modulation during geminivirus infection (Trinks et al., 2005, Collazo et al., 2006, Ascencio- Ibáñez et al., 2008, Sahu et al., 2010; Naqvi et al., 2011; Kushwaha et al., 2015). However, our effort in finding the appropriate genes/or pathways is reduced due to the inadequate well-characterized, compatible host model suitable for transcriptome profiling studies.

Differentially expressed genes such as those encoding ubiquitin-conjugating enzyme, receptor-like protein kinase and various antioxidants were identified during the interaction of *Nicotiana megalosiphon* with *Tomato mottle Taino virus* (TMoTV) by construction of suppression subtractive library (Collazo et al., 2006). A global analysis of gene expression in *Arabidopsis-Cabbage leaf curl virus* interaction depicted the importance of host genes associated with cell cycle, hormone and regulation, genotoxic stress and DNA repair (Ascencio-Ibáñez et al., 2008). Alteration in expression of genes related to defense, signaling and components of ubiquitin-proteasomal systems were highlighted during ToLCNDV infection in a tomato host plant in a recent study (Naqvi et al., 2011). Thus, well established resistant/tolerant hosts and comprehensive analysis of differentially expressed host genes may contribute in the discovery of resistance response against geminiviruses. In this regard, functional characterization of accessible or reported datasets of proteome and transcriptome of various plant-geminivirus interaction may assist in the revealing the key regulatory component of resistance.

Application of high-throughput technologies and reverse genetic approaches, like virus-induced gene silencing (VIGS; Sahu et al., 2012a), CRISPR/Cas9 technology in combination with modern bioinformatics tools can be a feasible alternative. Recently, CRISPR/Cas9 technology has emerged as a novel tool to engineer resistance against geminiviruses (Baltes et al., 2015). Various researchers have utilized VIGS for elucidating gene function, for example resistance of tomato against *Tomato leaf curl virus* reduced by silencing of genes encoding Permease1-like protein and hexose transporter (Eybishtz et al., 2009, 2010). It suggests that during infection, viruses activate the transcription of host genes (like those involved in cell-cycle and signaling), which are required for viral DNA replication.

2.3.1 The ubiquitin-proteasome system

In the ubiquitination process, series of various enzymes catalyzes the attachment of mono- or polyubiquitin to the targeted substrates (Fig. 2.6). Initially, Ubiquitin (Ub) is activated in an ATP-dependent reaction governed by ubiquitin activating enzyme (E1). This reaction forms a high-energy thiolester bond, between Ub and E1. This activated Ub is translocated to the ubiquitin-conjugating enzyme (E2) at Cys residue, followed by subsequent transfer to the substrate protein facilitated by ubiquitin ligase

enzyme (E3). Enzyme E3 has characteristic domain, i.e., either HECT or the RING-finger. In the HECT domain containing E3 enzymes, Ub is relocated initially to an active Cys residue of HECT domain, prior to its final attachment with the substrate protein (Fig. 2.6). In the case of RING-finger domain E3 enzymes, it associates with both E2 and the substrate and directly promotes the transfer of Ub from E2 to the substrate protein. Polyubiquitin chain attached specifically by Lys 48 residue acts as an indicator for the proteasome mediated degradation of the targeted substrate.

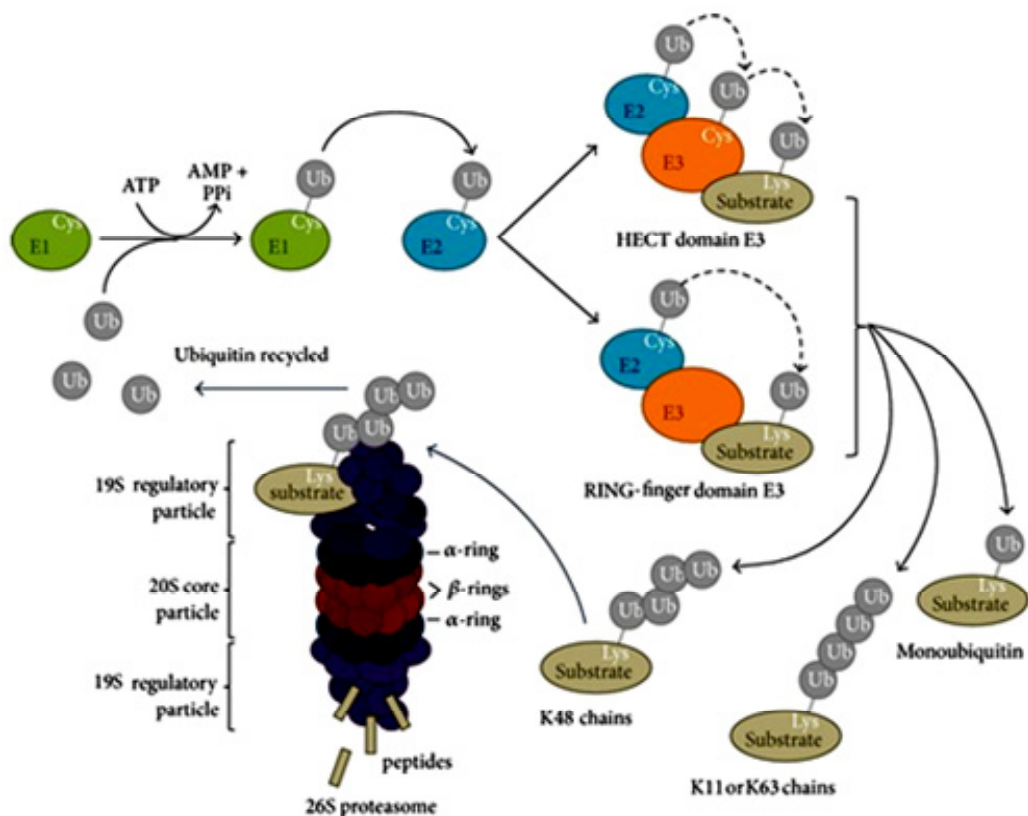


Fig. 2.6. The ubiquitin-proteasome system. This pathway has two processes, Ubiquitination and 26S proteasome mediated degradation. In ubiquitination, targeted protein (substrate) is ubiquitinated (Ub) by the action of E1, E2 and E3 enzymes. This ubiquitinated substrate is cleaved/hydrolyzed by the enzymatic activity of β -subunits of core complex. (Adapted from Lippai and Löw, 2014).

Structural constituents of 26S proteasome (26SP) in plants are: core particle (CP; or 20S proteasome) and a regulatory particle (RP or 19S proteasome) (Fig. 2.7). In these multimeric protein complexes, CP plays a pivotal role in the process of protein degradation while the RP is responsible for ATP- and Ub-dependent proteolysis of targeted protein (Wolf and Hilt, 2004; Kurepa and Smalle, 2008). CP contains four stacked rings i.e., two inner and two outer. Each of the inner rings are composed of

seven β subunits (β_1 to β_7 or PB A to G) whereas the outer rings have seven α subunits (α_1 to α_7 or PA A to G) (Fig. 2.7). These rings form an entrance for the ubiquitinated target proteins into the proteolytic chamber. Similar to the CP, RP is composed of two subcomplexes, the Lid and the Base. The Base contains six different RP Triple-A ATPases (RPT 1-6) in conjunction with three RP non-ATPase (RPN 1, 2, 10) subunit. The RP Lid contains eight RPNs (3, 5 to 9, 11 and 12).

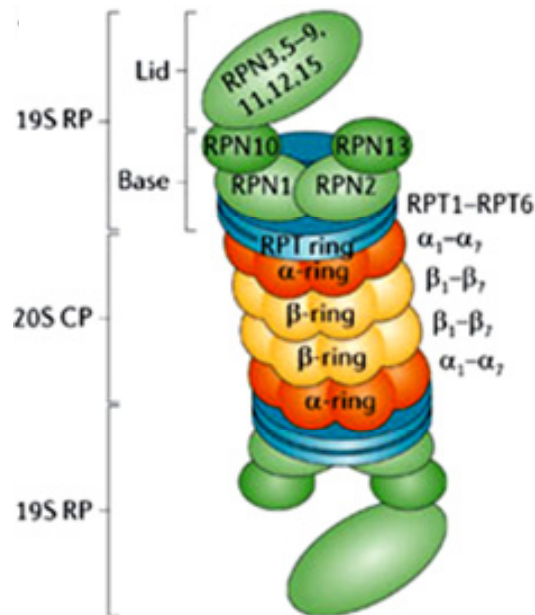


Fig. 2.7. Structural components of 26S proteasome complex. (Figure adapted from Weissman et al., 2011).

The polyubiquitin chain is identified by the RP, which helps in the binding, unfolding, and translocating the substrate into the CP (Wolf and Hilt, 2004). Within RP, The RPTs assist in the unfolding of the target proteins and subsequent access to the 20SP chamber (Smalle and Vierstra, 2004; Wolf and Hilt, 2004) on other hand, RPN subunits 1, 2 and 10 have specific function in providing the docking sites for different proteins (Wolf and Hilt, 2004). Finally, substrate is hydrolyzed enzymatically by the active β -subunits inside CP resulting into short peptides. Ubiquitin is recycled in the process.

2.3.2 Ubiquitin proteasomal pathway: a trigger to destroy pathogen

Ubiquitin proteasome systems (UPS) have appeared as a new subject in plant-microbe interactions (Zeng et al., 2006; Vierstra, 2009; Goristschnig, 2007, Craig et al., 2009). Role of ubiquitin and proteasome during plant-pathogen interaction were extensively

reviewed (Dreher and Callis, 2007; Citovsky et al., 2009; Dielen et al., 2010; Sahu et al., 2014b). UPS is involved in almost every step of the defense mechanism in plants, while the pathogens also attempt to utilize it as a protective shield for counter defense. However, very few information's have reported the role of these networks in geminivirus-plant interaction. Transcript profiling in tolerant tomato plant upon ToLCNDV infection has shown shown induction of various UPS gene (Sahu et al., 2010). Some of them are *26S proteasomal subunit RPT4*, *Ubiquitin conjugating enzyme*, *ARM repeat containing protein*, *uba/ubx domain-containing protein* and *RUB1* (Sahu et al., 2010). It suggests operation of a possible virus resistance pathway mediated or controlled by ubiquitin proteasomal degradation.

Plants' response to pathogen often relies on the network of R-proteins (Jones and Dangle, 2006). Until now, *N* gene of *Nicotiana*, a class 3 R gene, has been implicated in defense mechanism against TMV (Liu et al., 2002). *RARI* which acts as a downstream component of *N* gene mediated defense is an integral part of ubiquitin mediated degradation. This protein along with the SGT1 interacts with SCF/COP9 signalosome to activate the ubiquitin/26 proteasome pathway, thus providing the *N* gene mediated resistance (Liu et al., 2002). Silencing of *NbSGT1* resulted in depletion of *R* gene mediated resistance against *Potato virus X* (Peart et al., 2009). Other E3 ubiquitin ligase like *Avr9 induced F-Box 1* (ACIF1; van den Burg et al., 2008) and *ACRE276* (Yang et al., 2006) have been identified to be involved in *N* gene mediated resistance.

Similarly, a recent report has elucidated that geminiviral C2 protein interacts with catalytic subunit of the CSN complex (CSN5), and its expression in transgenic plants altered the CSN activity on cullin 1 (Lozano-Dura'n et al., 2011). Drastic changes in hormonal responses were observed because these activities were in control of CUL1-based SCF ubiquitin E3 ligases (Lozano-Dura'n et al., 2011). The silencing of CSN3, that redirects the activity of CULLIN RING ligases, also hinders the viral infection (Lozano-Dura'n et al., 2011). Fascinatingly, C2 from various geminiviruses like TYLCSV, TYLCV and BCTV have the ability to interact with CSN5. This suggests a common phenomenon arising for removal of the ubiquitin-like RUB moiety from cullins and subsequent alternation of hormonal activity during geminivirus infection (Lozano-Dura'n et al., 2011).

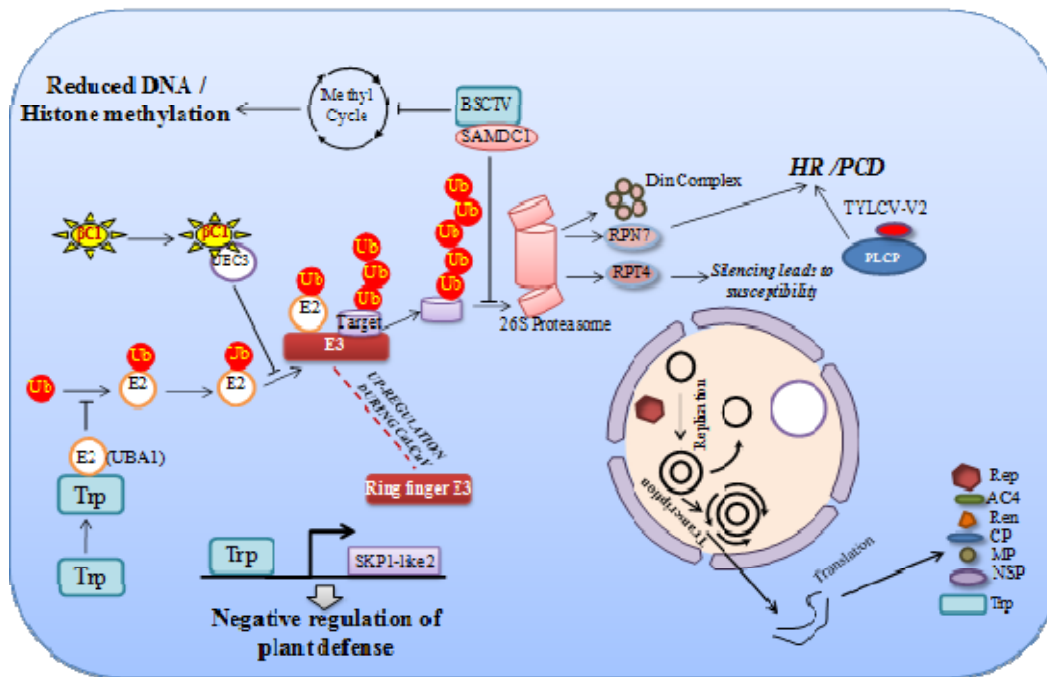


Fig. 2.8. Involvement of host factors in modulating diverse cellular process during geminivirus infection. Ubiquitin proteasomal pathway is altered by the viral protein through direct and indirect process, such as programmed cell death, suppression of plant defense and remodeling histone dynamics and DNA methylation. (Figure modified from Sahu et al., 2014b).

The interaction of β C1 with UBC3 down-regulates the host ubiquitin proteasome pathway and hence is essential for DNA- β associated symptom development (Eimi et al., 2009) (Fig. 2.8). Silencing of the *UBA1* inhibited the interaction of UBA1 and TrAP protein of geminivirus which resulted in the enhanced early infection in *N. benthamiana* (Lozano-Dura'n et al., 2011; Fig. 2.8). Similarly, upon inhibiting the expression of RING type E3 ubiquitin ligase the plant defense was unpaired (Lozano-Dura'n et al., 2011), which was found to be differentially expressed following *Cabbage leaf curl virus* (CaLCuV) infection (Ascencio-Ibáñez et al., 2008). These studies show that geminiviruses are proficient to interfere with the UPS (Fig. 2.8). Targeting these genes can help us to disclose the possible mechanisms of plant disease response and will help to generate a resistant plant in near future.

Various studies have shown that through its proteolytic activity, subunits of 26SP regulate numerous intracellular components associated with hormone signaling, transcription and translation, physiology and morphogenesis, along with the biotic abiotic response (Kim et al., 2003a; Wolf et al., 2004; Dreher and Callis, 2007; Citovsky et al., 2009; Pajeroska-Mukhtar and Dong, 2009). The individual subunit

of this multimeric complex is implicated in the diverse function. Hence, in the next section we have highlighted the complex role of 26SP subunits in diverse aspects of plant life cycle under biotic and abiotic stresses.

2.3.3 Functions of 26S proteasome subunits in plant stress response

The 26SP is an essential factor of ubiquitin-dependent proteolytic pathway. It acts as a central regulator of regulatory proteins participating in a numerous cellular signaling and metabolic pathways. Moreover, 26SP subunits are implicated in the protein quality control and help to degrade any mis-folded, defective and atypical proteins generated either during inaccurate protein translation or post-translation modification. This process requires the collective function of each subunit of 26SP along with other components of the ubiquitin pathway. Data congregated over the decades have suggested that 26SP subunit may independently target several inter- and intra-cellular regulators. They have been associated with defense pathways, hormone signaling, DNA methylation and stability of chromatin structure along with the tailoring morphogenesis in responses to adverse climatic constraint and pathogens encounter. Recent reports reinforce our view that most of the phenotypes of 26SP subunit mutants in plants illustrated to date not only reveal a general defect in 26SP subunit function but also a specific defect associated with a single subunit. This urges the need for the role of each subunit during stress imposition to be re-evaluated. In the next section, we have provided an exclusive overview of 26SP subunit's non-proteolytic function and their participation in plant stress response.

UPS contributes extensively in a wide range of plant development processes (Zeng et al., 2006; Dreher and Callis, 2007; Citovsky et al., 2009; Craig et al., 2009; Dielen et al, 2010). Ubiquitination machinery recognizes the specific ubiquitinated substrates and 26SP subsequently eliminates atypical peptides and transitory cellular regulators. This permits the cells to respond in time through the signaling network under changing environmental conditions. Maintenance and termination of this signal enables plants to recover from such adverse conditions.

2.3.4 Novel function of 26S proteasome subunits in biotic stress response

Plants are exposed to a wide range of pathogens in the natural environments. Pathogen invasion into host plant tissue activates a cascade of defense responses.

The innate immune system initiated by the host plants with the initial recognition of microbes includes specific pattern recognition receptors (PRRs) that detect the pathogen-associated molecular patterns (PAMPs) (Janeway, 1989). Subsequently, PAMP-triggered immunity (PTI) stimulates various cellular defense associated molecules and pathways such signaling kinase cascades, generation of reactive oxygen species (ROS), hormone signaling, and defense related gene expression (Schwessinger and Zipfel, 2008). Moreover, pathogens have specialized virulence effector proteins to suppress the PTI. On the other hand, host intracellular plant receptors (such as *R* genes) can recognize specific effector proteins which are mainly established for providing effector-triggered immunity (ETI) and ultimately lead to programmed cell death (PCD) (Jones and Dangl, 2006). In the subsequent sections, we have highlighted the explicit role of 26SP subunits in the establishment of plant's defense as well as counter defense strategy of microbes for growth and multiplication.

2.3.4.1 Programmed cell death and activation of ROS

Various modes of organized cellular demolitions have evolved in eukaryotes and this mechanism, known as PCD, controls several physiological and development specific processes in plants (Hatsugai et al., 2009). For example, during xylem development, programmed cell death plays an essential role in xylem cell terminal differentiation and cell expansion. Caspase-like activity is the characteristic feature of PCD which has been shown to be regulated through 20SPs (Han et al., 2012). Apart from these normal physiological processes, 26SP subunits are also linked with the disease resistance in plants (Pajerowska-Mukhtar and Dong, 2009). Several findings show that inhibition of proteasome activity leads to PCD in plants (Kim et al., 2003a; Jin et al., 2006). Contrastingly, a wide range of studies have divulged that activation of proteasome may also lead to PCD in plants (Lee et al., 2006; Vacca et al., 2007). A report by Vacca et al. (2007) states that proteasome function is a requisite for establishment of PCD in heat shocked *Nicotiana tabacum* Bright-Yellow 2 cells. This result was also supported by another study on hot pepper 26SP subunit *RPN7* induced by *Tobacco mosaic virus* (TMV) revealing involvement of this subunit in PCD (Lee et al., 2006). Such evidences clearly suggest that the subunits of 26SP have diverse function in both normal physiological and stress condition. These subunits are also necessary for broad-spectrum viral systemic movement. For example, silencing

of RPN9 in *N. benthamiana* has been shown to restrict the systemic spread of viruses, such as *Tobacco mosaic virus* and *Turnip mosaic virus* (Jin et al., 2006). More recently, interaction of RPN9b with cytochrome f has been shown to modulate the caspase-3-like activity and hence the PCD during the process of leaf senescence (Wang et al., 2014). Formation of ROS is an important event of plant defense responses which is essential for instant suppression of pathogen viability (Kurepa and Smalle, 2008). Subunits of 26SP have been revealed to be implicated in conferring plant defense responses (Becker et al., 2000; Takizawa et al., 2005). Expression of three defense-induced 20S subunits ($\beta 1$, $\alpha 3$ and $\alpha 6$ subunits) was correlated with the induction of SAR and production of ROS (Suty et al., 2003). Hence, 26SP subunits directly or indirectly regulate stress response through activation of PCD and ROS.

2.3.4.2 Hormone based regulation of defense

Both PTI and ETI activate specific set of hormone biosynthesis and signaling pathways. ETI system gets activated against biotrophic pathogens, which triggers the salicylic acid (SA) biosynthesis and signaling and leading to local and systemic acquired resistance (Mettraux et al., 1990; Delaney et al., 1994). On the contrary, PTI synergistically activates jasmonic acid (JA), and ethylene (ET) biosynthesis against necrotrophic pathogens infection (Thomma et al., 1998; Felix et al., 1999). Proteasome subunits play an important role in hormone-based defense during biotic stresses. The application of hormones also influences 26S proteasome subunit expression. For example, accumulation of $\alpha 6$ subunit of the 20S proteasome transcript was enhanced by methyl jasmonate (MeJA), NaCl and SA treatments, but not by Abscisic acid (ABA) and cold stress (Kim et al., 2003b). Recent observation suggested that *RPN1a* of Arabidopsis, which has an important role in the trichome development, was significantly repressed by gibberellin and cytokinin (CK) treatment (Yu et al., 2015). It has been shown that the RPN12 subunit of the Arabidopsis possibly regulates cytokinin-based responses as cytokinin-inducible genes; *CYCD3* and *NIA1* were up-regulated in the *rpn12a-1* mutant (Smalle et al., 2002). The UPS system specifically controls phytohormone signaling by affecting protein activity (Yu et al., 2016). An attempt to investigate the role of 26SP subunits in plant immunity against powdery mildew pathogen *Golovinomyces cichoracearum* was done in Arabidopsis (Yao et al., 2012). It was observed that mutation in *RPN1a* suppressed the *edr2*-associated disease resistance phenotypes in Arabidopsis. This mutant was

also defective in SA accumulation during the course of bacterial infection, suggesting their possible involvement in basal and R protein-mediated defense. Moreover, *RPT2a* and *RPN8a* were also involved in *edr2*-mediated disease resistance (Yao et al., 2012). Arabidopsis semi-dominant uni-1D, which is responsible for the defense responses, modulates the activation of defense responses (Chung et al., 2011). It has been reported that 26SP-RPT 2a and 2b interaction is critical for the activation of PR1-mediated defense signal, which is regulated by SA (Chung et al., 2011). Therefore, the subunits of 26SP can modulate the hormone signaling network, consequently affecting the disease resistance pathways in plants.

2.3.4.3 Establishment of plant-pathogen interaction

Pathogen effector protein and 26SP subunit interaction is crucial to establish biotic infection. In this regard, pathogen effectors are the frequent modulators of 20SP subunits. Subunits, β 1-tcI 7, α 3 and α 6 have been found to be up-regulated by the treatment of elicitor cryptogin, assisting in the hypersensitive response and SAR (Dahan et al., 2001). Furthermore, interaction of bacterial effector proteins with proteasome components was also evidenced in various studies. For example, *HopZ4*, a member of the YopJ family of T3E from *Pseudomonas syringae* pv. *lachrymans* has been shown to interact with 26SP-RPT6 *in planta*. This interaction inhibits the proteasome activity and subsequently promotes bacterial infection (Üstün et al., 2014).

Phytopathogenic bacterium, *Xanthomonas campestris*pv. *vesicatoria* (Xcv) also alters the SA-dependent defense response through the interaction of effector XopJ with the proteasomal subunit RPT6. This interaction subsequently inhibits the proteasome activity and interferes with SA-mediated defense pathway to diminish necrosis development along with gene transcription (Üstün et al., 2013). Further, proteolytic function of XopJ specifically assisted in the degradation of RPT6, which in turn inhibits the turnover of nonexpressor of pathogenesis-related1 (NPR1) (Üstün et al., 2015).

2.3.4.4 Proteasome-dependent RNase activity

Apart from functioning in protein degradation and turnover, plant proteasomes have RNase activity which appears to be a part of plant defense. First evidence of 26SP-mediated RNase activity was highlighted against plant viral RNAs *in vitro* in

cauliflower (Pouch et al., 1995) and sunflower (Ballut et al., 2003). In another study, *Arabidopsis thaliana* proteasomal $\alpha 5$ subunit was identified as a factor to degrade *Tobacco mosaic virus* (TMV) and *Lettuce mosaic virus* (LMV)-derived RNAs *in vitro* (Dielen et al., 2011). Moreover, viral proteins may also interact and alter 20SP component's catalytic activities. For example, proteinase (HcPro) of LMV was associated with the RNase activity of 26SP which further contributed in plant defense response against RNA viruses. Similarly, HcPro of *Potato virus Y* interacted with the $\alpha 1$, $\beta 2$ and $\beta 5$ subunits of the *A. thaliana* 20SP and modulated the RNase activity leading to compromised defense response against RNA viruses (Jin et al., 2007). Further observation suggested that the RNase activity of 26SP subunits is differentially regulated through diverse extra-cellular signals (Kulichkova et al., 2010). Thus, proteasome-dependent RNase activity may represent an example of battle between the plant and pathogens.

2.3.4.5 Role in RNA recombination

RNA recombination assists RNA viruses in combating the host's antiviral responses. It also helps in the rapid evolution of RNA viruses attributable to mutations and genetic modification. It has been speculated that plant proteins may have influence on viral RNA recombination, though the exact role of host components altering virus evolution not yet reported. However, a recent study on tombus viruses revealed that knocked down or a mutated proteasome-independent 26SP-Rpn11 helped in viral replication, recombination and evolution (Prasanth et al., 2015).

2.3.5 Involvement of 26S proteasome subunits in abiotic stress response

Plants respond to various environmental stresses through activating an explicit series of gene expression mediated by transcription factors or signaling cascades components (Rejeb et al., 2014). This also involves hormone signaling pathways that may induce or deactivate specific stress responses (Tuteja and Sopory, 2008; Rejeb et al., 2014). 26SP subunits play an important role in orchestrating these stress associated factors and pathways (Kurepa et al., 2008; Sakamoto et al., 2011; Yanagawa and Komatsu, 2012). In this section we have highlighted the novel function of 26SP subunits associated with the abiotic stress response of a plant.

2.3.6 26SP subunits and abiotic stress tolerance

Various abiotic stresses have been recognized to hinder 26SP activity either by escalating the substrate load and hence reducing the turnover rates of proteins or through inhibiting the non-proteolytic function of 26SP subunits. For instance, flooding stress has been associated with the altered efficiency of protein degradation of 26SP in soybean (Yanagawa and Komatsu, 2012). Moreover, total proteasome activity was increased in *Arabidopsis* RP subunits *RPT2a*, *RPN10* and *RPN12a* mutants, which led to improved tolerance to oxidative stress treatments (Kurepa et al., 2008).

In contrast, oxidative stress, can cause 26SP inhibition and subsequently affect the 26SP subunit-specific functions (Reinheckel et al., 1998). However, plant cells have established intricate molecular mechanisms to modulate 26SP activity in response to deviation in environmental circumstances. Precise function of each subunits of 26SP in abiotic stress response remains ambiguous, although recent studies have improved our standing of 26SP subunits role on abiotic stress response of plant. Proteasomal involvement in salinity tolerance has been reported in green algae by Sun et al. (2010). In this study, expression of *RPN10* subunit was shown to increase significantly in *Dunaliella viridis*, which suggested their plausible involvement in specific response to the salinity (Sun et al., 2010). Mutant of *RPN1a* not only assisted in the optimal plant growth but also improved oxidative stress tolerance (Wang et al., 2009). Contrastingly, *Arabidopsis* 26S proteasome subunit mutant *rpn10-1* was susceptible to abscisic acid (ABA), salt, and sucrose stress (Smalle et al., 2003).

In the ecosystem, around seventeen heavy metals are found to be essential for living cells (Weast, 1984). Among them, Zinc (Zn), Nickel (Ni), and Copper are nutritionally important, however may have the detrimental effect either at high or low available concentration. Furthermore, metals like Mercury, Silver, Cadmium (Cd), Arsenic and Lead are non-nutritional and have toxic effect on the plant even at lower concentration (Breckle, 1991; Nies, 1999). Plants growing on these toxic soils may have abnormal physiological and morphological effect leading to restricted crop yield. However, plants have specific defense system to adapt in these adverse soil conditions. This process generally involves variation between (ROS) and antioxidants enzyme system during metal toxicity. Recent observations have revealed that 26SP subunit play a pivotal role in the regulation of metal-stress response in plants.

For example, *Arabidopsis* 26SP subunits, i.e., *RPT2a* and *RPT5a* have been correlated with the Zn deficiency-tolerance (Sakamoto et al., 2011). Mutation in *RPT2a* and *RPT5a* leads to the susceptibility towards Zn deficiency with characteristic enriched level of Zn deficiency-inducible genes transcripts along with the increased lipid peroxidation levels in comparison to the wild-type. This study provides a strong evidence of association of *RPT2a* and *RPT5a* with Zn deficiency-tolerance, probably by enhanced oxidative stresses in *Arabidopsis* (Sakamoto et al., 2011).

Similarly, mutant analysis has assisted in the identification of an arsenic tolerant mutant, *ars5* in *Arabidopsis*. Through microarray-based expression mapping, *ars5* mutation in the alpha subunit F (PFA) of 26SP subunit was reported (Sung et al., 2009). Simultaneously, characterization of *pafl* mutation resulted in the improved understanding of thiol accumulation and arsenic tolerance phenotypes of *Arabidopsis*. However, arsenic tolerance was specifically associated with the *PAF1* and another homologous PAF gene, *PAF2*, had no observable effect in the metal tolerance (Sung et al., 2009). Another metal Cd may adversely affect the normal cellular proteolytic responses in the roots and leaves of tomato (Dong et al., 2005). Upon Cd stress, difference between roots and leaves was revealed in terms of antioxidant responses and metabolic sensitivity. Moreover, enhanced expression of 20SP related genes also suggested their possible involvement in the Cd stress tolerance (Djebali et al., 2008). Functional complementation of maize *ZmPAA* gene encoding a 20SP α -subunit in yeast have been linked in conferring resistance to Ni, Cd and cobalt. The relative level of the *ZmPAA* transcript was increased in maize shoots upon nickel stress, which imply that proteasome subunit is an important component in providing nickel resistance through scavenging metal oxidized proteins *in planta* (Forzani et al., 2002).

2.3.7 Genetic and epigenetic control of abiotic stress through 26SP component

Plants are equipped with the complex genetic and epigenetic regulatory systems to adapt rapidly to adverse environments such as heat, cold, drought, and pathogen infections. The genetic aspect of plant responses to abiotic stresses have been well studied (Atkinson and Urwin, 2012). However, genetic basis of abiotic stress tolerance is mainly quantitative (Richards, 1996) and identification of loci associated with the specific traits is essential for successfully achieving the breeding objectives. Genetic control of stress tolerance traits has also been linked with the proteasome subunit (Li et al., 2015). For instance recent study on thermo-tolerance in rice

Review of Literature

(*Oryza glaberrima*) revealed that major quantitative trait locus (QTL) for thermotolerance i.e., *Thermo-tolerance 1* (TT1), encodes for $\alpha 2$ subunit of 26SP. Molecular analysis also suggested that OgTT1 guards the cells from heat stress by the removing cytotoxic proteins. Further characterization of OgTT1 showed that its overexpression enhanced thermo-tolerance in various plants such as rice and Arabidopsis (Li et al., 2015). The study suggests that subunits of proteasome are linked with the thermo-tolerance traits in plants. Similarly, recent advancement has suggested that the components of 26SP are the key elements in the epigenetic regulation of abiotic stress in plants.

In brief, epigenetic regulation occurs thorough the DNA methylation, histone modifications, ATP-dependent chromatin remodelling, along with RNA-directed DNA methylation mechanisms (Lee et al., 2011; Sako et al., 2012). It assists in regulating the expression of stress-responsive genes and further prevents from stress induced damage (Muratani and Tansey, 2003). Binding of Rpt6 and Rpt4 to chromatin were shown to be associated with the regulation of histone H3 lysine 4 (H3K4) and histone H3 lysine 79 (H3K79) methylation (Ezhkova and Tansey, 2004). Hence, the recruitment of 19S ATPases to chromatin may assist the activation of chromatin structure, through histone modifications. Similar reports in plant system have also been reported. For example, 26SP subunit RPT2 subunit was found to assist in the modulating histone dynamics in Arabidopsis (Lee et al., 2011). Moreover, few reports have suggested that Arabidopsis 19SP subunit RPT2a play an important role in regulating gene expression via DNA methylation (Sako et al., 2012). In this study it was observed that knockout mutation of RPT2a gene altered transcriptional activities of a transgene reporter. Although direct link of these 26SP subunit mediated epigenetic regulation of plant stress responses are not yet well understood, but their importance cannot be neglected.

Chapter 3: Materials and Methods

3.1 MATERIALS

3.1.1 Plant material

Material	Source	Purpose
<i>Solanum lycopersicum</i> cultivars i.e., H-88-78-1 and Punjab Chhuhara	Indian Institute of Vegetable Research, Varanasi, Uttar Pradesh, India	Throughout the experiment as a model
<i>Nicotiana benthamiana</i>	School of Life Sciences (SLS), Jawaharlal Nehru University (JNU), New Delhi, India	Virus induced gene silencing (VIGS)

3.1.2 Bacterial strains

Material	Strain	Source	Purpose
<i>Escherichia coli</i>	DH5 α	Stratagene, CA	Gene cloning
	BL21 (DE3 codon plus)	Stratagene, CA	Protein expression in bacteria
<i>Agrobacterium tumefaciens</i>	EHA105	Novagen, Germany	Transient expression in plants by agro-infiltration
	GV3101	Novagen, Germany	Transient expression in plants

3.1.3 Plasmid vectors

Vector	Source	Purpose
pGEM-T Easy	Promega Life Sciences, USA	Cloning vector
pGEX4T-2	Novagen, Germany	Bacterial expression vector
GATEWAY series vectors, pGWB17 and pGWB6	National Institute of Plant Genome Research (NIPGR), New Delhi, India	Chromatin immunoprecipitation assay (ChIP) analysis

Materials and Methods

<i>Tobacco rattle virus</i> -based VIGS vectors	Kindly provided by Dinesh-Kumar, Plant Biology Department, University of California, USA	VIGS
pCAMBIA 1302	Clontech laboratories, USA	Binary vector with GFP for transient expression
pENTR	Invitrogen, Life Technologies, USA	For GATEWAY cloning
P19 helper	NIPGR, New Delhi	BiFC analysis
pSPYNE 173	NIPGR, New Delhi	BiFC analysis
pSPYCE (M)	NIPGR, New Delhi	BiFC analysis

3.1.4 Enzymes

Material	Source
General restriction enzymes	New England Biolabs (NEB), USA
T4 DNA Ligase	NEB, USA
DNA polymerase I; Klenow fragment	NEB, USA
DNA Polymerase; <i>Taq/Pfu</i>	Sigma Aldrich, USA
Turbo DNase	Thermo Fisher Scientific, USA
RNaseA	Sigma Aldrich, USA
RNaseH	Invitrogen, Life Technologies, USA

3.1.5 Kits

Material	Source
Wizard® Plus SV Minipreps DNA Purification System	Promega, USA
Advantage® 2 Polymerase Mix	Clontech, USA
QIAEX II Gel Extraction Kits	Qiagen, Germany
NEBlot Kit	NEB, USA
Protoscript M-MuLV RT kit	NEB, USA
Clonase Gateway LR Clonase-II Kit	Invitrogen, Life Technologies, USA
CasPASE™ Apoptosis Fluorometric Assays	G-biosciences, USA

3.1.6 Chemicals used

Category	Material	Source
General use	Acetic acid, Ammonium persulfate, Boric acid, EDTA, CaCl ₂ , Chloroform, Ethanol, Formaldehyde, Glucose, Glycerol, Glycine, Glycogen, H ₂ SO ₄ , HCl, HNO ₃ , Hydrogen peroxide, Iso-amyl alcohol, Isopropanol, K ₂ HPO ₄ , KCl, KH ₂ PO ₄ , KOH, Lactic acid, Methanol, MgCl ₂ , MgSO ₄ , Na ₂ HPO ₄ , Sodium azide, NaCl, Sodium dioxycholate, NaH ₂ PO ₄ , NaOH, NP-40, Potassium acetate, Potassium dichromate, Sodium acetate, Sucrose, Tris base, Tris equilibrated phenol, Tri-Sodium citrate	Qualigens, India SRL, India Ameresco, USA Himedia, India
Fine chemicals	2-Thiobarbituric acid (TBA), 3-(N-morpholino) propanesulfonic acid (MOPS), 4-(2-hydroxyethyl)-1-piperazineethanesulfonic acid (HEPES), Acetonitrile, Acetosyringone, Acrylamide, Agarose, MES buffer, Ammonium bicarbonate, Ascorbate, Bis-Acrylamide, Cetyl-trimethylammonium bromide (CTAB), Chloral hydrate, DEPC, Dithiothretol (DTT), Formamide, Formic acid, Poly (di-dC), Glutathione, Bovine Serum Albumin (BSA), Glutathione-Sepharose 4B, Glycine, Iodoacetamide, Isopropyl β-D-thiogalactopyranoside (IPTG), Lithium chloride, Phenylmethylsulfonyl fluoride (PMSF), Potassium ferricyanide, Protease inhibitor (Bacterial and Plant), IBS buffer, RNaseOut, Sodium dodecyl sulfate (SDS), Sodium thiosulfate,	Amersham, USA USB, USA Sigma Aldrich, USA G-biosciences

Materials and Methods

	Tetramethylethylenediamine (TEMED), TRI reagent, Triton-X-100, Trizma base, X-gal, β -mercaptoethanol,	
Culture media components	Agar, Bacto-agar, Beef extract, Luria-Bertani broth, MgSO ₄ , MgCl ₂ , KCl, NaCl, Sucrose, Tryptone, Yeast Extract, Peptone	Difco, USA Qualigens, India Sigma Aldrich, USA Amersham, USA
Markers and dNTPs	DNA ladder (1 kb and 100 bp), λ DNA size marker, Protein markers (Pre-stained marker)	NEB, USA Biochem Life Sciences, India
Staining Dyes	Bromophenol blue, Xylene cyanol, Coomassie Brilliant Blue, Trypan blue, Ethidium bromide (EtBr)	Amersham, USA Sigma Aldrich, USA
Blotting membrane, X-ray films and cassettes	Hybond N ⁺ , Phosphoimager screen/cassettes, Polyethyleneimine TLC plate	Kodak, India Amersham, USA
Radioisotopes	α P ³² deoxycytidine triphosphate, (α P ³² dCTP); γ P ³² deoxyadenosine triphosphate (γ P ³² dATP)	Perkin Elmer, USA
Antibiotics	Ampicillin, Kanamycin, Rifampicin, Hygromycin,	Sigma Aldrich, USA Amersham, USA
Hormones	Salicylic acid, Methyl Jasmonate and Ethephon	Sigma Aldrich, USA

3.1.7 Concentrations of various antibiotics

Antibiotic	Abbreviation	Final Concentration
Ampicillin	Amp	100 μ g/ml
Kanamycin	Kan	50 μ g/ml
Rifampicin	Rif	25 μ g/ml
Hygromycin	Hyg	20 μ g/ml

3.1.8 Composition of media

Luria Bertani (LB) medium: Liquid medium prepared according to manufacturer's recommendations. For solid media

Constituents	Concentration (g/L)
LB broth	25.0
Agar	8.0

YEB medium

Constituents	Amount (g/L)
Peptone	5.0
Yeast extract	1.0
Sucrose	5.0
Beef extract	5.0
Adjust pH to 7.0 with 2 N KOH	
MgSO ₄	0.491

SOB medium

Constituents	Amount (g/L)
Tryptone	20.0
Yeast extract	5.0
NaCl	0.5
KCl	0.19
Adjust pH to 7.0 with 2 N KOH	
MgCl ₂	2.4

3.1.9 Composition of buffers

Tris-HCl buffer

Constituents	Amount (for 1 L)
Tris base	121.1 g
Adjust pH as required by adding conc. HCl	

Materials and Methods

10X Tris-Borate-EDTA (TBE) buffer for electrophoresis

Constituents	Amount (for 1 L)
Tris Base	108.0 g
Boric Acid	55.0 g
EDTA (0.5 M; pH 8.0)	20.0 ml

10X TAE buffer for electrophoresis

Constituents	Amount (for 1 L)
Tris Base	48.4 g
Glacial acetic acid	11.44 ml
EDTA (0.5 M; pH 8.0)	20.0 ml

Sodium Phosphate buffer, pH 7.0

Constituents	Amount (for 1 L)
Na ₂ HPO ₄ (1 M)	57.7 ml
NaH ₂ PO ₄ (1 M)	42.3 ml

Phosphate Buffer saline (PBS, pH 7.0)

Constituents	Final concentration (mM)
Sodium Phosphate buffer (pH 7.0)	10.0
NaCl	140.0
KCl	2.7

10X MOPS buffer

Constituents	Amount (g/L)
MOPS	41.2
Sodium acetate	10.9
EDTA (pH 8.0)	3.7
Adjust pH to 7.0 with 1N NaOH	

ITB buffer

Constituents	Amount (g/100 ml)
MnCl ₂	1.088
CaCl ₂	0.22
KCl	1,865

3.1.10 Composition of reagents and other solutions

CTAB DNA extraction buffer

Chemical	Final Concentration
CTAB	2.0 %
NaCl	1.4 M
EDTA	20.0 mM
Tris-HCl (pH 8.0)	100.0 mM
Add 0.2 % β -merceptoethanol (v/v) just before use	

Solutions for Plasmid DNA isolation

Chemical	Final Concentration
Solution I	
Glucose	50.0 mM
EDTA (pH 8.0)	10.0 mM
Tris-HCl (pH 8.0)	25.0 mM
Solution II	
NaOH	0.2 N
SDS	1.0 % (w/v)
Solution III	
Potassium Acetate	5.0 M

20X SSC

Chemical	Amount (g/L)
Tri Sodium citrate	88.23
NaCl	175.32
Adjust pH to 7.0-8.0 with conc. HCl	

Materials and Methods

Southern Blotting reagents

Constituents	Final Concentration
Depurination solution	
HCl	0.2 N
Denaturation solution	
NaCl	1.5 M
NaOH	0.5 N
Neutralization solution	
Tris-HCl (pH 7.4)	1.0 M
NaCl	1.5 M

20X SSC

Chemical	Amount (g/L)
Tri Sodium citrate	88.23
NaCl	175.32
Adjust pH to 7.0-8.0 with conc. HCl	

Radioactivity washing buffer

Chemical	Final Concentration
20X SSC	2X
10% SDS	0.1 % (v/v)

Prehybridization/Hybridization buffer for radioactivity

Chemical	Final Concentration
Sodium phosphate buffer (pH 7.2)	1.0 M
SDS	7.0 % (w/v)
EDTA (pH 8.0)	1.0 mM

10X Formaldehyde gel loading buffer for RNA

Chemical	Final Concentration
Formamide	50 % (v/v)
Formaldehyde	20 % (v/v)
10X MOPS	1X
EtBr (10 mg/ml)	10 µg/ml
10X RNA loading dye	2 µl

6X gel loading dye for RNA

Chemical	Final Concentration
Bromophenol blue	0.25 % (w/v)
Xylene cyanol FF	0.25 % (w/v)
Glycerol in DEPC water	30.0 % (v/v)

Agarose gel 6X loading dye for DNA

Chemical	Concentration
Bromophenol blue	0.25 % (w/v)
Xylene cyanol FF	0.25 % (w/v)
Glycerol in water	30.0 % (v/v)

3.1.11 Composition of sodium dodecyl sulphate-polyacrylamide gel electrophoresis (SDS-PAGE)

Separating gel (12 %)

Component	Volume for 5 ml
Acrylamide (30 %)	2.0 ml
Tris-HCl, pH 8.8 (1.5 M)	1.25 ml
SDS (10 %)	50.0 µl
APS (10 %)	50.0 µl
TEMED	2.0 µl
Make up volume to 5 ml with water	

Separating gel (10 %)

Component	Volume for 5 ml
Acrylamide (30 %)	1.7 ml
Tris-HCl, pH 8.8 (1.5 M)	1.3 ml
SDS (10 %)	50.0 µl
APS (10 %)	50.0 µl
TEMED	2.0 µl
Make up volume with water	

Materials and Methods

Stacking gel (5 %)

Component	Volume for 2 ml
Acrylamide (30 %)	330.0 μ l
Tris-HCl, pH 6.8 (1.0 M)	250.0 μ l
SDS (10 %)	20.0 μ l
APS (10 %)	20.0 μ l
TEMED	2.0 μ l
Make up volume with water	

Tris-glycine buffer (5X)

Component	Amount (for 1 L)
Tris base	15.1 g
Glycine	94.0 g
SDS (10 %)	50.0 ml
Make up volume with water	
pH adjusted to 8.3	

SDS loading dye (5X)

Component	Concentration
Tris-HCl (pH 6.8)	225.0 mM
Glycerol	50.0 % (v/v)
SDS	5.0 % (w/v)
Bromophenol Blue	0.05 % (w/v)
DTT	250.0 mM

3.1.12 Primer sequences

Bacterial expression		
Primer name	Forward Primer Sequence (5'-3')	Reverse Primer Sequence (5'-3')
pGEX4:SIRPT4	CGGGATCCATGGCGACCGAAGAAGACG	CGGAATTCTTATTCTTGCCAAAATCAG
Virus Induced Gene Silencing (VIGS)		
pTRV-Slpds	CCGCTCGAGCTGACGAGCTTTCGATGCAGTGC	CGGGATCCATATATGGGACATTTATCACAGGA
pTRV-SIRPT4	CCGCTCGAGGTAATGCAGCCAACTCTTTCTCT	CGGGATCCCCTCTACTATATTACACCCCGTCCT
Southern blot analysis		
Coat protein	ACAGAAAACCCAGAATGTACAGAA	CAACATTAAGGCATTTTCAGTATG
BC1	GTTTTGTGTCCCCCTCCGTCA	ATGTCAATAGGAAATGATGGTATG
Transient expression analysis		
pCAMBIA1302: SIRPT4	CATGCCATGACATGATGGCGACCGAAGAAGACG	GGACTAGTTTATTCTTGCCAAAATCAGCA
pENTR-RPT4	CACCATGGCGACCGAAGAAGACGCCG	TTCCTTGCCAAAATCAGCACTGTAG
pENTR-RNA Pol-II-3	CACCATGGAGGGCGTTTCGTACCAG	TTAACCTCCACGCATATGAGCGCCCA
Northern blot analysis		
<i>Rep</i>	TTTAAAGTGCTTTAGATAGTG	CACAATTACTTGTGTGGACAT
<i>Coat Protein</i>	ATGAAATTCACGCTACATGGCCTA	CGTTGAAATGATGATATCTGCTGG
<i>SIRPT4</i>	CCGCTCGAGGTAATGCAGCCAACTCTTTCTCT	CGGGATCCCCTCTACTATATTACACCCCGTCCT

Contd...

Materials and Methods

<i>Slpds</i>	CCGCTCGAGCTGACGAGCTTTCGATGCAGTGC	CGGGATCCATATATGGGACATTTATCACAGGA
<i>NbpdS</i>	TAAACCCTGACGAGCTTTCGATGC	TTTATCACAGGAACTCCCCTACTAGC
<i>αTubulin</i>	TCAAACCTCAAAGAAGCTGTCA	ACAATTTATCCCTCACCACAGG
Electrophoretic Mobility Shift Assay (EMSA) and Chromatin Immuno-Precipitation (ChIP)		
DNA-A-IR_EMSA (2592-47)	AAAACCTTGTCGTTTTGATT	TGGTTGAGGGCCCACCTAAA
DNA-B-IR_EMSA (2617-67)	ACACCATATGGCATTATTGTAAT	AACGGCGTGCAATGATTACGC
DNA-A-Rep_EMSA (1939-2046)	GACTATGCTTATGGGCCTAAA	CCATTTTCAATTTTCATCCT
IR_ChIP (2592-47)	AAAACCTTGTCGTTTTGATT	TGGTTGAGGGCCCACCTAAA
pENTR-RPT4	CACCATGGCGACCGAAGAAGACGCCG	TTCCTTGCCAAAATCAGCACTGTAG
pENTR-RNA Pol-II-3	CACCATGGAGGGCGTTTCGTACCAG	TTAACCTCCACGCATATGAGCGCCCA
<i>Actin 7</i>	CTGGTGTGTGATAATGGAACG	GCTTCATCACCAACATACGC
Bimolecular fluorescence complementation (BiFC)		
SIBCL-31	CGGGATCCATGATTCAGTTGTTGTTTAT	GGACTAGTACTCCGATAACCATGAGC
SIDDI1	CGGGATCCATGAAGATCACTGTAATGAC	GGACTAGTACCCCAAATAGATATCCGGC
SIRPT4	CGGGATCCATGGCGACCGAAGAAGAC	GGACTAGTTTCCTTGCCAAAATCAGCACTG

3.1.13. List of 168 tomato genes encoding AAA+ATPase domain protein used for phylogenetic analyses.

Solyc06g082560.1	Solyc03g031910.2	Solyc06g008730.2	Solyc09g005100.2
Solyc00g029080.1	Solyc03g033790.2	Solyc06g010110.1	Solyc09g008070.2
Solyc01g007640.2	Solyc03g033820.1	Solyc06g011370.2	Solyc09g010950.2
Solyc01g068330.2	Solyc03g033840.2	Solyc06g011400.2	Solyc09g014380.2
Solyc01g068480.2	Solyc03g046340.2	Solyc06g019170.2	Solyc09g055230.2
Solyc01g073700.2	Solyc03g063760.2	Solyc06g034180.1	Solyc09g074950.2
Solyc01g079250.2	Solyc03g082630.2	Solyc06g051460.2	Solyc09g091650.2
Solyc01g088380.1	Solyc03g082640.1	Solyc06g053150.1	Solyc10g007280.2
Solyc01g094150.2	Solyc03g083250.2	Solyc06g053160.2	Solyc10g019190.1
Solyc01g094760.2	Solyc03g093300.2	Solyc06g054020.2	Solyc10g024320.1
Solyc01g096230.2	Solyc03g097370.2	Solyc06g054050.1	Solyc10g054040.1
Solyc01g099760.2	Solyc03g110900.2	Solyc06g060150.2	Solyc10g055260.1
Solyc01g102990.2	Solyc03g112590.2	Solyc06g060350.2	Solyc10g076790.1
Solyc01g104640.2	Solyc03g115230.2	Solyc06g063140.2	Solyc10g078320.1
Solyc01g104920.2	Solyc03g117350.1	Solyc06g063410.2	Solyc10g079630.1
Solyc01g109940.2	Solyc03g117850.2	Solyc06g064550.2	Solyc10g084050.1
Solyc01g111310.2	Solyc03g117950.2	Solyc06g066810.2	Solyc10g086540.1
Solyc01g111980.2	Solyc03g118320.1	Solyc06g071980.2	Solyc10g086550.1
Solyc02g014350.2	Solyc03g118340.2	Solyc06g072000.1	Solyc11g005070.1
Solyc02g021620.2	Solyc03g121120.2	Solyc06g074980.2	Solyc11g007170.1
Solyc02g032960.2	Solyc03g123730.2	Solyc06g076860.2	Solyc11g008250.1
Solyc02g062550.2	Solyc03g124010.2	Solyc06g082630.2	Solyc11g012820.1
Solyc02g062700.2	Solyc04g005520.2	Solyc06g082660.2	Solyc11g013310.1
Solyc02g070440.2	Solyc04g005830.2	Solyc06g083620.2	Solyc11g013570.1
Solyc02g079000.2	Solyc04g050840.1	Solyc06g084530.2	Solyc11g013650.1
Solyc02g079140.1	Solyc04g057960.2	Solyc07g005880.2	Solyc11g013700.1
Solyc02g081420.2	Solyc04g063360.2	Solyc07g006540.2	Solyc11g040390.1
Solyc02g081550.2	Solyc04g072260.1	Solyc07g006810.2	Solyc11g050800.1
Solyc02g082520.1	Solyc04g072270.1	Solyc07g023990.1	Solyc11g050880.1
Solyc02g084090.1	Solyc04g072830.2	Solyc07g044970.1	Solyc11g067230.1
Solyc02g084120.1	Solyc04g076180.2	Solyc07g055320.2	Solyc11g067240.1
Solyc02g084900.2	Solyc04g077460.2	Solyc07g062760.1	Solyc11g069720.1
Solyc02g084910.2	Solyc04g080680.2	Solyc08g007110.2	Solyc11g069780.1
Solyc02g087530.1	Solyc04g082250.2	Solyc08g043170.2	Solyc11g069950.1
Solyc02g087540.1	Solyc05g007470.2	Solyc08g063050.2	Solyc11g071430.1
Solyc02g088610.2	Solyc05g008540.2	Solyc08g077420.2	Solyc12g007100.1
Solyc02g094100.2	Solyc05g012190.2	Solyc08g077440.2	Solyc12g013590.1
Solyc03g006420.2	Solyc05g015060.2	Solyc08g080510.2	Solyc12g014150.1
Solyc03g006480.1	Solyc05g018570.2	Solyc08g081740.2	Solyc12g040520.1
Solyc03g007330.2	Solyc05g018590.2	Solyc08g082080.2	Solyc12g042060.1
Solyc03g007760.2	Solyc05g053800.2	Solyc08g082530.2	Solyc12g055810.1
Solyc03g031900.1	Solyc06g005950.2	Solyc08g083020.2	Solyc12g076340.1

3.2 METHODS

3.2.1 Plant growth conditions and treatments

Seeds were sown in soil composed of a mixture of peat compost and vermiculite in the ratio 3:1 (w/w), germinated and maintained in a two chambered PGC-6L growth cabinet (Percival Scientific Inc., USA). The growth chamber was set at 22°C with 70 % relative humidity, and a 14 h photoperiod with 250 $\mu\text{mol photons m}^{-2} \text{s}^{-1}$ light intensity. Twenty one-day-old seedlings were used in all the experiments except for analysis of transcript in reproductive tissues. Untreated plants were maintained as controls. The above experiments were repeated in triplicate to ensure precision and reproducibility. For silencing and ToLCNDV inoculation experiment, the temperature was maintained at 22°C throughout as higher temperature inhibits the T-DNA transfer. Immediately after harvesting, the samples were frozen in liquid nitrogen and stored -80°C until use. *N. benthamiana* plants were grown under similar conditions with the temperature maintained at 22°C under light intensity of 200 $\mu\text{moles photons m}^{-2}\text{s}^{-1}$. Upon ToLCNDV treatment, plants were kept in a glasshouse at 25°C for symptom development until 21 days post inoculation.

Hormone treatments

For hormonal treatments, 21-day-old tomato seedlings were treated with 10 μM methyl jasmonate (MeJA), 100 μM salicylic acid (SA) or 100 μM ethephon following Li et al. (2014). For control, sterile water was used as a treatment. Samples were collected after 12 h of foliar spray.

3.2.2 Sterilization protocols

Standard sterilization protocols were followed by autoclaving glasswares, culture media and tissue culture tools for 15 min at 121.6°C under 15 lb psi pressure. Heat labile reagents were filter sterilized using 0.22 μm pore size polyvinylidene difluoride filters (MillexTM, Millipore, USA) driven with a dispensable syringe.

For work involving RNA, all required materials like glassware and mortar-pestle were incubated at 180°C for 5-6 h. Precaution was taken to prevent RNase contamination of gel running unit and other plasticwares by treating them with 3 % H_2O_2 overnight. DEPC-treated sterile Milli-Q (MQ) water was used to make all solutions. Working space and regular use items were cleaned with RNase-OUT reagent (G-Biosciences).

For all bacterial and tissue culture work, the steps were performed under an aseptic laminar air flow hood. The working space was sterilized with 70 % ethanol (v/v) before the work.

3.2.3 General recombinant DNA techniques

3.2.3.1 Nucleic acid extraction from plant

RNA isolation by Trizol method

Approximately 100 mg of tissue was pulverized to a fine powder with mortar and pestle using liquid nitrogen and 2 ml of TRI reagent (Sigma-Aldrich, USA) was added immediately. The homogenate was incubated for 10-15 min followed by addition of chloroform (0.2 ml/ml TRI reagent used) and again kept for 15 min. After spinning at 13,000 rpm for 15 min at 4°C in a table top centrifuge (Eppendorf 5415, Germany), the aqueous RNA-containing phase was transferred to a new microcentrifuge tube. RNA was precipitated by adding 0.5 ml isopropanol and incubating for 30 min on ice followed by a 15 min centrifugation at 13,000 rpm. Resultant RNA pellet was washed twice with 80 % ethanol (v/v) at 8,000 rpm, air dried and dissolved in 20-30 µl sterile DEPC-treated MQ water. For RNA isolation from tomato fruits, subsequent to Trizol treatment LiCl precipitation was performed, as described by Wang et al. (2009).

Genomic DNA isolation by CTAB method

Genomic DNA was isolated from leaf tissue the CTAB method as described by Porebski et al. (1997). About 1 g of sample was ground to a fine power using liquid Nitrogen and 10 ml of preheated (at 65°C) CTAB extraction buffer was added. After incubation at 65°C for 1 h, the suspension was cooled to room temperature and centrifuged at 8000 rpm for 20 min. To the supernatant, equal volume of chloroform: isoamyl alcohol (24:1; v/v) solution of was added, thoroughly mixed and centrifugation at 8,000 rpm for 10 min. The extraction was repeated once more and subsequently DNA was precipitated with isopropanol (600 µl/ml of aqueous layer). After incubating overnight at 4°C, DNA was pelleted by spinning at 8,000 rpm 4°C for 15 min followed by two washes with 70 % ethanol (v/v) by centrifuging at 8,000 rpm for 10 min. The pellet suspended in 500 µl sterile MQ after it was air dried. To remove downstream contamination with RNA, the dissolved DNA was mixed with 5 µl RNaseA (100 µg/ml) and incubated at 37°C for 45 min. RNase-treated DNA was extracted twice with 0.5 vol chloroform: isoamyl alcohol (24:1; v/v) followed by

Materials and Methods

precipitation with equal volume of ice cold ethanol and centrifugation for 20 min, 8,000 rpm at 4°C. Pellet obtained was washed with cold 70 % ethanol (v/v), air dried and dissolved in appropriate amount of sterile MQ water.

Electrophoresis for analysis of nucleic acids

Horizontal agarose (Ameresco, India) gel electrophoresis for used to separate RNA, DNA and PCR amplified products. For RNA, a denaturing 1.2 % (w/v) formaldehyde gel was made by adding 10 ml 10X MOPS and 18 ml formaldehyde to 72ml molten agar and cast in pre-set trays with fitted combs. About 10 µg of total RNA was mixed with formaldehyde gel loading buffer and incubated at 65°C for 10 min followed by quick chilling on ice. Denatured RNA samples were loaded after added 2 µl of 10X RNA gel loading dye and run in 1X MOPS buffer at low voltage until dyes were well separated. For DNA/PCR samples appropriate percentage of gel was chosen based on product size (0.8-2.0 %; w/v), molten in 1X TBE/TAE buffer and poured onto gel trays after adding 0.5 µg/ml EtBr. Two µl of 6X DNA gel loading dye was added to samples which were then run in 1X TBE/TAE along with appropriate size standards on an electric current of 3 V/cm and ended depending on the distance between the migrated bands of the dyes present in the DNA loading buffer. The nucleic acids were detected in a gel-documentation system on a UV-transilluminator.

Spectrophotometric estimation

Nucleic acid quality and quantity were checked by measuring absorbance at 230, 260 nm and 280 nm with NanoDrop 1000 Spectrophotometer (Thermo Scientific, USA). The RNA samples with A_{260}/A_{280} ratio of 1.8-2.0 were considered pure. For DNA, good extraction was considered when the A_{260}/A_{280} ratio was 1.7-1.8.

3.2.3.2 DNase treatment and reverse transcription

RNA was reverse transcribed to synthesize the first strand cDNA using Protoscript M-MuLV RT kit (NEB, USA) following manufacturer's instructions. Initially, 10 µg of total RNA was subjected to DNase treatment through 2 U/µL TURBO DNase enzymes (Thermo Fisher Scientific, USA). DNase treated RNA (1-5 µg) was combined with 5 µM of oligo (dT)₁₈ primer and mixture was incubated at 70°C for 5 min then briefly chilled on ice and centrifuged. To this, 4 µl of 5 X M-MuLV reaction mixtures, 2 µl of 10mM dNTP mix, 1 µl ribonuclease inhibitor were added, mixed gently and incubated at 37°C for 5 min followed by addition of 1 µl M-MuLV

Reverse Transcriptase enzyme (0.5 U/μl). The reaction was kept at 42°C for 60 min followed termination at 85°C for 10 min. The synthesized cDNA was used for downstream PCR application reaction using respective gene specific primers.

3.2.3.3 DNA amplification and amplicon purification

Polymerase Chain Reaction (PCR)

Specific DNA/cDNA fragments were PCR amplified using the *Taq* DNA polymerase (5 U/μl; Sigma Aldrich, USA) or / *Pfu* polymerase (5 U/μl; Sigma Aldrich, USA) and a set of convergent primers (Mullis and Faloona, 1987). For cloning purposes, sometimes synthetic restriction enzyme recognition sequences were added at the 5' end of the primer. A basic reaction mix was made of 1X PCR buffer, 200 μM individual dNTP, 0.2 μM each forward and reverse primer, 50-100 ng template, 0.05 U/μl of polymerase. The amplification reaction was done in a thermocycler generally using the following program:

Step	Temperature (°C)	Time (min)	Cycle repeat
Initial denaturation	94	3	× 1
Denaturation	94	0.5	× 25-35
Annealing	55-68	0.5-1	
Elongation	72	1	
Final elongation	72	10-15	× 1
Hold	4	∞	× 1

Elution of DNA from agarose gel

The PCR amplified fragments resolved on agarose/EtBr gel were cut with a sharp sterile scalpel blade and collected. The DNA elution from the gel slice was performed using QIAEX II gel extraction kit (Qiagen, USA) according to the manufacturer's instructions with minor modifications. To the tube, 600 μl of the QX1 buffer and 10 μl of silica beads provided in the kit were added and incubated at 60°C for 10 min to dissolve the agarose. After the complete dissolution of agarose, a spin of 13,000 rpm for 1 min was given to pellet down the beads. These beads were then washed with 500 μl of QX1 buffer and twice with 500 μl of PE buffer. The beads were dried at 37°C and finally DNA was eluted by adding 15-20 μl of sterile water.

Materials and Methods

Purification of PCR products

For some applications, PCR products were instead purified with QIAquick PCR purification kit (Qiagen, USA) following kit's protocol. To one volume of PCR amplified product 5 volumes PB buffer was added and warmed to 60°C dissolve the gel slice. The suspension was loaded onto a QIAquick column and centrifuged at 13,000 rpm for 1 min and flow-through was discarded. On the column PE buffer (750 µl) was added and it was again spin at 13,000 rpm for 1 min. Re-discarded the flow through and dried the column by centrifuging for 1 min. DNA was eluted in a fresh tube with 20 µl nuclease-free water/or 50 µl elution buffer (10 mM Tris-HCl, pH 8.5) after centrifuged for 1 min at 13,000 rpm.

3.2.3.4 Cloning of amplified fragments/genes

3.2.3.4.1 Competent cell preparation

Ultracompetent E. coli cells

As a primary step for general gene cloning, *E. coli* DH5α strain was made ultracompetent as described by Inoue et al. (1990) with few modifications. A single colony from freshly activated DH5α was primary cultured at 37°C in 10 ml SOB medium and grown overnight. Of this, 1% was used to as inoculum for a secondary culture which was then grown in an incubator shaker at 22°C, 200-250 rpm till the OD₆₀₀ reached 0.55. The culture was chilled on ice for 10 min, transferred to sterile centrifuge tubes and spun at 3,000 rpm for 10 min at 4°C. The pellet was suspended in ice-cold Inoue transformation buffer (ITB), incubated on ice for 10 min and again centrifuged at 3,000 rpm for 10 min at 4°C. The pellet obtained was allowed to dissolve in 8 ml of ITB buffer along with 600 µl of DMSO and incubated on ice for 10 min. The competent cells were distributed in small aliquots of 50-100 µl and snap-frozen in liquid nitrogen and stored at -80°C until use.

A. tumefaciens competent cells

A single active colony of *A. tumefaciens* was grown in as primary inoculum in 50 ml LB medium with vigorous shaking at 28°C until OD₆₀₀ reached 0.5. Further growth was terminated by chilling the cells on ice and cells were collected by centrifugation at 3,900 rpm for 5 min at 4°C. The pellet obtained was gently suspended in 1 ml ice

cold calcium chloride (20 mM). From this, 100 µl was aliquoted into fresh tubes and stored at -80°C for future use.

3.2.3.4.2 Ligation

T/A cloning of PCR products

The amplified and purified DNA fragment contains a few deoxyadenosine nucleotides (dA) at its 3' end due to the terminal deoxynucleotidyl transferase activity of *Taq* polymerase, which can be utilized for cloning in a vector having a 5' deoxythymidine (dT). For this purpose the pGEMT[®]-Easy (Promega, USA) cloning vector was used. The insert fragment was incubated with 3 times molar excess of pGEMT[®]-Easy vector, 2 µl of 5X ligation buffer and 1 µl of T4 DNA ligase (3 U/µl) at 16°C for >12 h.

Directional cloning of DNA fragments

The conventional cloning of a DNA fragment based on phosphodiester bond between 3' hydroxyl and free 5' phosphate groups of DNA and selected plasmid vectors was performed using *T4* DNA ligase enzyme (NEB, USA). About 3 times molar excess of insert DNA was added to the vector DNA along with 1 µl of 10X ligation buffer and 1 µl of *T4* DNA ligase (400 U/µl). The ligation was allowed to proceed at 16°C for at least 16 h.

For some cloning procedures, Gateway cloning system was used. Forward primer was designed by adding an adaptor sequence 'CACC' at the 5' end for directional cloning. The desired genes were amplified by PCR using a polymerase with proofreading activity like *Pfu* polymerase (Promega, USA) to produce blunt end PCR product. The purified product was directionally cloned into TOPO pENTR vector (pENTR/D-TOPO; Invitrogen). PCR product was mixed with 1 µl salt solution, mixed gently and incubated at room temperature for 5 min to make the ligated recombinant clone.

3.2.3.4.3 Restriction digestion of DNA

Endonuclease type II restriction enzymes were used for DNA digestion for cloning and analytical purposes. Enzymes were selected from respective plasmid's multiple cloning sites (MCS). Generally two enzymes were selected from 5' end and 3' end. The reactions were incubated in appropriate buffers under optimized and recommended conditions. Double digestion reactions were used with a universal

Materials and Methods

buffer system. Plasmid DNA (2-3 µg) was digested by using 1 U of enzyme and 10X buffer in 20 µl reaction volume. The reaction mix was incubated at 37°C for 3 h and identities of the digested fragments were checked by loading onto 1% agarose/EtBr gel along with DNA ladder.

3.2.3.4.4 Transformation

Transformation of E. coli

For most general cloning, ultracompetent *E. coli* cells were transformed by the Hanahan (1983) method. Vial containing 100 µl competent cells was thawed on ice and recombinant or pure plasmid was added. The suspension was tapped gently and incubated for 30 min on ice followed by a heat shock at 42°C for 1.30 min and ice incubation again for 5 min. Finally, 900 µl of LB broth was added and cells were incubated at 37°C for 45 min with shaking. The transformed cells were spread on LB agar plate supplemented with antibiotic and kept in 37°C incubator overnight (Sambrook and Russell, 2001). As per requirement, blue-white selection of the colonies containing the recombinant plasmid was carried out on plates containing X-gal (40 µl of 2 %), IPTG (7 µl of 20 %) besides antibiotic.

For specialized Gateway cloning, transformation of chemically competent *E. coli* was done according to manufacturer's recommendations (Invitrogen, USA). Two µl of ligation mix was added to OneShot chemically competent *E. coli* and mixed gently. Heat shock was given at 42°C for 30 sec and immediately transferred to ice. About 50-200 µl of bacterial suspension was spread on LB selection plates containing appropriate antibiotics which were then incubated overnight at 37°C.

Transformation of A. tumefaciens

Agrobacterium transformation was performed by freeze thaw method with 1-3 µg of recombinant/ pure plasmid added to competent cells and incubated for 10 min on ice. The cells were frozen with liquid nitrogen and thawed at 37°C in water bath for 5 min and immediately transferred to ice. After 10 min, 1 ml YEB was added cells were incubated at 28°C for >2 hr with gentle shaking. Transformed cells were plated selection plates and kept at 28°C incubator for 2-3 days.

3.2.3.4.5 Confirmation for the presence of insert

PCR, restriction digestion and sequencing methods were used to confirm the transformed cells containing the recombinant plasmid. Restriction digestion method has been explained previously.

Colony PCR

Colony PCR with either gene-specific primers or primers compatible with cloning vector was used for preliminary screening of positive transformants. Individual colonies were tooth-picked in 10 µl sterile water and lysed by boiling for 10 min. Of this, 2 µl was used as the PCR template. The reaction mixture was prepared as discussed previously. PCR conditions were set according to the T_m of primers. Amplified products were resolved on agarose/EtBr gel and appropriate size markers were simultaneously run to confirm the presence and correct size of inserts.

Plasmid DNA isolation by alkaline lysis method and PEG purification

Plasmid DNA isolation was performed by alkaline lysis method as described in Sambrook and Russel (2001). A single colony of bacterial cell containing the desired clone (pure or recombinant plasmid) was inoculated in 5 ml (100 ml for midiprep) LB medium with appropriate antibiotic(s) and grown overnight at 37°C with vigorous shaking. The cells were harvested by centrifuging at 13,000 rpm for 1 min at room temperature. The pellet was resuspended in 200 µl (200 ml for midiprep) of ice cold solution I. Three hundred µl (5 ml for midiprep) of freshly prepared solution II was added; tubes were inverted a few times gently and incubated for 5 min at room temperature. After addition of 300 µl (5 ml for midiprep) of ice cold solution III, it was incubated for 5 min on ice. Supernatant collected by centrifuging the suspension at 14,000 rpm for 30 min at 4°C was treated with RNaseA (20 µg/ml) at 45°C for 1 h. To avoid protein contamination, it was extracted twice with chloroform and each time the upper aqueous DNA containing layer was collected in a fresh tube. DNA was precipitate with equal volume of isopropanol by centrifuging at 13,000 rpm for 20 min followed by two washes of 70 % ethanol (v/v). The pellet was air dried and dissolved in 20-100 µl of sterile MQ water.

Before confirmation of insert identity by sequencing, the plasmid DNA was precipitated by adding 4 M NaCl (8 µl) and 13 % (w/v) polyethylene glycol (40 µl) and volume made up to 100 µl with water. The plasmid was mixed well by tapping

Materials and Methods

the tube, incubated on ice for 30 min and centrifuged at 13,000 rpm for 20 min at 4°C. The pellet was washed with 70 % ethanol (v/v) twice, air dried and dissolved in 20 µl sterile water. After gel and spectrophotometric quantification of DNA, it was stored at -20°C until use.

Sequencing

Automated Sanger sequencing using dideoxynucleotide chain termination method (Sanger et al., 1977) was performed using Big Dye Terminator kit version 3.0 (Applied Biosystems, USA) and evaluated with capillary based DNA analyzer (ABI Sequencer, Version No. 3700/3770, Applied Biosystems, USA). Nucleotide sequences for both the strands were determined using specific primer pairs. Screening out of vector and synthetic adaptors from primer sequences was done by VECSCREEN program (<http://www.ncbi.nlm.nih.gov/VecScreen/VecScreen.html>). Sequence homology search was performed using BLASTN and BLASTX (Altschul et al., 1990) programs in NCBI database to finally confirm positive recombinant clones.

3.2.4 Agroinfection of tomato plants with ToLCNDV

ToLCNDV infectious clone construction

Tandem repeat constructs of ToLCNDV genomic components (DNA-A and DNA-B) have been previously prepared in the laboratory (Chakraborty et al., 2008). Briefly, pCAMBIA2301 was used to reclone these constructs at *Sma*I site and confirmed by restriction digestion. Freeze-thaw method described previously was used to introduce these ToLCNDV genomic components into *A. tumefaciens* strain EHA105.

ToLCNDV agroinfection

Tomato seeds were germinated in agropeat:vermiculite (3:1) to the two-leaf stage. Meanwhile, the above transformed *A. tumefaciens* cells were grown overnight at 28°C in YEB medium (pH 7.0). After centrifuging at 3000 rpm for 10 min, the pellet was suspended in YEB (pH 5.6) containing 100 µM acetosyringone (Sigma Aldrich, USA). Agroinoculation of tomato was performed by first making wounds by pricking three to four times with a 30-gauge needle around the growing nodal area of stem (stem inoculation method). About 20 ml equimolar mixture of *A. tumefaciens* harbouring DNA-A and *A. tumefaciens* harbouring DNA-B was applied to fresh

wounds. For mock inoculation, *Agrobacterium* harbouring the pCAMBIA2301 vector backbone alone, without the ToLCNDV genomic components, was used.

3.2.5 *In silico* analysis

Tomato *26S proteasomal subunit RPT4a*, a differentially expressed transcript against ToLCNDV infection H-88-78-1 (ToLCNDV tolerant cultivar) was selected for this study (Sahu et al., 2010).

Sequence retrieval

Partial clone (GenBank accession GR979393) was subjected to BLAST analysis at Sol Genomics Network (<https://solgenomics.net/tools/blast/>). The full-length gene sequence of *SIRPT4* was retrieved SOL genomics website (<https://solgenomics.net/>) using the identifier SGN-U566414 as keyword. The server SMART (<http://smart.embl-heidelberg.de/>) and (<http://www.ncbi.nlm.nih.gov/Structure/cdd/wrpsb.cgi>) were used to analyse domains present in the translated protein. The pI and molecular weight of the protein were calculated using the pI/Mw tool (http://web.expasy.org/compute_pi/).

Protein modelling

The secondary structure of *SIRPT4* was predicted using the web-based GORIV secondary structure prediction tool (https://npsa-prabi.ibcp.fr/NPSA/npsa_gor4.html). The 3D structural models with good quality and resolution were generated through I-TASSER server (Zhang, 2008). TM-align structural alignment program of first I-TASSER model was performed to identify the available structures in the PDB library (<http://zhanglab.ccmb.med.umich.edu/TM-align/>). To examine the biological annotations of *SIRPT4* protein, a meta-server approach namely COACH (<http://zhanglab.ccmb.med.umich.edu/COACH/>) was applied.

Promotor identification

The 5' sequence upstream to *SIRPT4* start codon of coding sequence (locus SL2.50ch01:96772912-96771913) was extracted from the SOL genomics website (<https://solgenomics.net/>). In order to find out putative *cis*-regulatory elements this sequence was used as an input file for PlantPAN2 (Chaw et al., 2016) and PlantCare databases (Lescot et al., 2002).

3.2.6. Phylogenetic analysis

AAA domain profile was made from the available AAA domain containing proteins of Arabidopsis (486) and rice (698) genome through InterProScan (<https://www.ebi.ac.uk/interpro/interproscan.html>). Tomato protein sequences were obtained from Phytozome v10.2 (Goodstein et al., 2012) and HMMER search was performed using the PFAM domain (PF09820) (Finn et al., 2011). In total, 684 AAA-domain containing protein from tomato were retrieved. After aligning these sequences by CLUSTALW (Thompson et al., 1994; www.genome.jp/tools/clustalw/), phylogeny was analyzed using MEGA v6.06 (Tamura et al., 2013) with the distance matrix using neighbour-joining (NJ) method with 1000 iterations bootstrap model of poisson correction, to calculate protein distance.

3.2.7 Gene expression analysis by northern hybridization

For checking the gene-specific transcript accumulation in various tissues, RNA was extracted from various vegetative and reproductive tissues of tomato. RNA was also extracted from hormone-treated and untreated leaf samples. For Northern analysis, 10 µg total RNA was used for electrophoresis as previously described and transferred by capillary method to positively charged nylon membrane (Hybond-N⁺, Amersham Bioscience, USA). Target transcript was PCR amplified using gene-specific primer pairs for probe preparation (Section 3.1.12). Probes were labeled with α P³² dCTP using NEBlot Kit according to the manufacturer's protocol (NEB, USA). For this, 25 ng of DNA was boiled for 5 min and quickly chilled on ice. To this, 5 µl octadeoxyribonucleotides in 10X labeling buffer, 1 µl of 10 mM each dNTP without dCTP and 2 µl of α P³² dCTP (20 µCi/µl) were added and incubated at 37°C for 10 min. Radiolabeled probes were purified by sephadex G-50 and heat denatured (boiling for 5 min and quick chill on ice for 5 min). Probe was suspended in the bottles containing prehybridized membranes (for 3 h at 65°C) and allowed to hybridize with the probe for 24 h. After washing the membranes at 65°C three times for 10 min each, the hybridized membranes were put in a cassette with phosphor-screen. Signal intensity was recorded as images were by scanning the blots with a phosphor-imager (Typhoon 9210, GE Healthcare, USA). Further densitometry of the signal was done through available software (Quantity One; Bio-Rad, USA). The local

background value was subtracted and the normalized data was subjected to fold difference calculation. The amount of transcript of control tissues was designated 1.0.

3.2.8 Bacterial expression and purification of SIRPT4 protein

3.2.8.1 Cloning in protein expression vector, pGEX4T-2

SIRPT4 transcript without the stop codon was PCR amplified with the gene specific primers harbouring *Bam*HI adaptor in the forward and *Eco*RI in reverse primer (Section 3.1.12). The purified amplicon was digested with *Bam*HI and *Eco*RI along with pGEX4T-2 vector (GST-tag). The digested pGEX4T-2 vector and SIRPT4 PCR fragments were ligated to get pGEX4T-2-SIRPT4 constructs which were transformed into *E. coli* BL21 (DE3)-codon plus cells. Clones were selected on ampicillin containing LB-agar plates.

3.2.8.2 Induction and purification of GST-SIRPT4 from *E. coli*

The transformed bacteria harbouring pGEX4T-2 and pGEX4T-2-SIRPT4 were first inoculated in 5 ml of LB supplemented with 100 µg/ml ampicillin and incubated overnight with shaking at 37°C. They were transferred to 1 L fresh medium and the secondary culture was re-incubated at 37°C till OD₆₀₀ reached 0.6. The cultures were induced by 1 mM IPTG and incubated for additional 6 h at 37°C. The induced cells were harvested by centrifugation (5000 rpm, 20 min, 4°C) followed by a wash with ice cold 10 mM PBS (pH 7.0). The pellet was re-suspended in lysis buffer (10 mM PBS; pH 7.0, 1 mM PMSF and 1X bacterial protease inhibitors) for 1 h and lysed by gentle sonication (6 cycles, 20 s) on ice. After centrifugation for at 12,000 rpm for 10 min, the supernatant was separately collected. The obtained pellet was dissolved in IBS buffer (G-biosciences, USA) at 4°C for 1 h. Abundance of protein in supernatant and pellet were checked by resolving them on 12 % SDS-PAGE.

By affinity chromatography, SIRPT4-GST fusion protein was purified from the IBS treated supernatant using Glutathione-Sepharose 4B beads (GE Healthcare, USA). The beads slurry was taken for desired 50 % beads and centrifuged at 3,000 rpm for 3 min. The resin was washed thoroughly with chilled 10 mM PBS, pH 7.0. After washing, the resin was centrifuged again and supernatant was decanted. For protein binding, the washed beads were mixed with cell mixtures at 4°C for 1 h. Supernatant

Materials and Methods

were poured off after completion of binding and the beads were washed extensively with 250 mM Tris-HCl (pH 8.0) to avoid binding of non-specific proteins.

An elution buffer composed of 50 mM Tris-HCl (pH 8.8), 20 mM reduced glutathione, 300mM NaCl and 0.1 % Triton X-100 was prepared to elute the bound fusion proteins which were then collected in ten fractions of 100 μ l each. The purity and apparent molecular mass of eluted proteins were analysed by resolving them on 12 % SDS-PAGE. The protein concentration was estimated by Bradford assay using BSA as standard. The eluted protein was stored at -80°C. The selected fractions with highest concentration of GST-SIRPT4 were pooled and dialyzed in a dialysis buffer containing 50 mM HEPES (pH 7.5), 40 mM KCl, 12.5 mM MgCl₂, 2 mM DTT, 1 mM PMSF 0.2 mM EDTA, 20 % (v/v) glycerol.

3.2.8.3 Polyacrylamide gel electrophoresis of proteins

Gels for SDS-PAGE were prepared as outlined in section 3.1.11. Protein samples were prepared for gel loading by adding 1/4 vol of 5X sample buffer [225 mM Tris-HCl, pH 6.8, 5 % SDS (w/v), 50 % glycerol (v/v), 250 Mm DTT and 0.05 % bromophenol blue (w/v)] and boiling for 5 min. Gels were run in a vertical apparatus, Mini PROTEAN Tetra System (Bio-RAD) at a constant voltage of 100 V. Gels were carefully removed from the glass plates and stained with staining solution [0.25 % coomassie brilliant blue R-250 (w/v), 50 % methanol (v/v) and 10 % acetic acid (v/v)] as described by Laemmli (1970). Detaining was done with methanol: acetic acid: water; 4:1:5 (v/v/v).

3.2.9 ATPase assay

Thin-layer chromatography (TLC) method was used for ATPase assay as demonstrated by Choudhury et al. (2006). Briefly, different amounts of purified GST-SIRPT4 fusion protein were incubated in ATPase assay buffer [10 mM Tris-HCl (pH 8.0), 5 mM MgCl₂, 50 mM KCl, 10 mM DTT, and 100 μ g/ml BSA] containing 0.2 μ Ci of γ P³² labelled-ATP (Perkin Elmer Life Sciences, USA), at 37°C for 30 min. TLC was performed after spotting 2 μ l reaction sample on a polyethyleneimine TLC plate. Air dried reaction mix was resolved on a solvent consisting of 500 mM lithium chloride and 1 M formic acid. TLC paper was air dried and subsequently exposed to phosphor-screen and subjected to image scanned using phosphor-imager (Typhoon 9210, GE Healthcare, USA).

3.2.10 Pulldown assay for protein-protein interaction*Plant protein extraction*

Twenty one day old ToLCNDV infected cultivar H88-78-1 seedlings were harvested (100 g) and ground in 50 ml of homogenization buffer [50 mM HEPES-KOH (pH 7.5), 1 mM DTT, 1 mM PMSF, 1 % (v/v) plant phosphatase inhibitor cocktail 3 (Sigma Aldrich, USA), 1 tablet protease inhibitor cocktail (Roche Applied Science, Germany), 1 % polyvinylpolypyrrolidone]. The supernatant collected after centrifuging the suspension at 11,000 rpm for 20 min was filtered through several layers of Miracloth (Millipore, USA). Magnesium-ATP was added to a final concentration of 0.5 mM and Amicon ultra-15 tubes (cutoff 3 kDa) were used to concentrate the filtrate to the final volume of 10 ml according to the manufacturer's instructions (Millipore, USA). The concentrated protein extract was finally cleared by spinning again at 13,000 rpm for 20 min. Estimation of protein concentration was done with Bradford assay using BSA as standard.

GST-pulldown of SIRPT4 fusion protein

The plant protein was diluted with buffer containing 50 mM HEPES-KOH (pH 7.5) and 1 mM cantharidin to a 5 mg/ml final concentration. A 20 ml fraction of this sample was mixed with 2 mM ATP, 1X plant protease inhibitor, and 0.5 mM PMSF and incubated for 10 min at 30°C. Total plant proteins were pre-cleared with GST protein to avoid any nonspecific binding. Finally, pre-cleared protein sample and 5 mg of GST-tagged recombinant SIRPT4 proteins were mixed with 150 mM NaCl at 4°C for 1 h. The solution was then passed through GST GraviTrap disposable columns (GE Healthcare, UK). The prepared column was washed thoroughly with 50 mM HEPES-KOH (pH 7.5), 0.5 M NaCl and 20 mM reduced glutathione. The eluates were collected in small fractions (500 µl) which were then concentrated using Amicon ultra-4 tubes (Millipore, USA) to a final volume of 200 µl.

Identification of interacting protein by MALDI-TOF/MS

To identify the SIRPT4 interacting proteins, the eluates were resolved on the 12 % SDS-PAGE gel. The gel was silver stained and visible bands were excised (1×1 mm pieces). These gel pieces were washed with water and incubated with destaining solution (0.1 M sodium thiosulfate and 30 mM potassium ferricyanide) for 15 min at 4°C. Destaining solution was decanted and wash solution (50 mM ammonium

Materials and Methods

bicarbonate in 50 % acetonitrile) was added to the gel piece followed by 100 % Acetonitrile. Translucent gel piece was further subjected to reduction and alkylation process through incubating the gel piece with reduction buffer (10 mM DTT in 50 mM ammonium bicarbonate) and alkylating buffer (55 mM iodoacetamide in ammonium bicarbonate), respectively. Resultant sample was washed with wash solution, twice. Acetonitrile (50-100 μ l) was used to shrink the gel and air dried.

For trypsin digestion, air dried sample was incubated in the 10 μ l of trypsin solution (0.2 μ g/ μ l trypsin in digestion buffer) to allow gel piece to swell. Around 25 μ l of digestion buffer (50 mM ammonium bicarbonate in water) was added and incubated at 37°C for 4h. Digestion mixes containing the peptides were analyzed by LC/MS/TOF (electrospray ionization time-of-flight mass spectrometry) which is joined online with MALDI-TOF-TOF (Applied Biosystems, USA). MASCOT (<http://www.matrixscience.com>) search engine was used for identifying peptides by searching the peak list with GPS Explorer v3.5 (Applied Biosystems, USA). SMART (<http://smart.embl-heidelberg.de/>) was used to predict the domain structure of these interacting proteins. The target proteins were annotated using Blast2GO.

3.2.11 BiFC Assay for confirmation of interacting partners

Cloning into the BiFC Vectors and Transformation

Gene inserts containing adaptor sequence were digested with *Bam*HI and *Spe*I and ligated into pre-digested pSPYCE173 with a nYFP (N-terminus fragment of YFP) tag and pSPYNE (M) with cYFP (C-terminus fragment of YFP) BiFC vectors at the C-terminus. These chimeric plasmids were transformed into onion epidermal peel by the Biolistic PDS 1000-helium particle delivery system (Bio-Rad, USA) and peels were incubated for 2 days at 22°C. Laser confocal scanning microscope (Leica Microsystems) was used to visualize the fluorescence keeping the laser and pinhole settings of the microscope identical throughout the study.

3.2.12 Electrophoretic mobility shift assay (EMSA)

Probe preparation for DNA-binding

Firstly for performing gel shift, ToLCNDV fragments corresponding to DNA-A-IR, DNA-B-IR and Replication associated gene fragments were PCR amplified using primers listed in section 3.1.12. PCR amplified products were radiolabeled with

α P³² dCTP at 5' end using Klenow fragment of DNA polymerase I, as discussed in section 3.2.7.

Gel shift assay

EMSA was performed according to the protocol described by Hellman and Fried (2007). The DNA-binding assay was done by incubating 5 μ g protein and radiolabelled viral DNA fragments in 30 μ l of binding buffer [75 mM HEPES (pH 7.5); 150 mM KCl, 0.1 mM DTT, 1 mM EDTA (pH 8), 5 mM MgCl₂, 30 % (w/v) glycerol and 0.1 mg/ml BSA] containing poly (di-dC) and incubated for 30 min at 25°C. After incubation samples were resolved in 10% native PAGE containing 2% glycerol in 1X TAE buffer at 10 mA. After electrophoresis, the dried gel were exposed to phosphor-screen and subjected to image scanning using phosphor-imager (Typhoon 9210, GE Healthcare, USA).

Composition for 10% native PAGE

Solutions	Amount
MQ	5.960 ml
Acrylamide Stock Solution (30 %)	3.33 ml
50X TAE	200 μ l
Glycerol (50 %)	400 μ l
Ammonium persulphate (10 %)	100 μ l
TEMED	10 μ l

3.2.13 Chromatin immunoprecipitation assay (ChIP)

Cloning SIRPT4 in pGWB17 vector

The SIRPT4 cloned in pENTR (using forward and reverse pENTR-RPT4 primers) was recombined with the destination vector pGWB17 harbouring a C-terminal MYC tag using the LR clonase enzyme mix (Invitrogen, USA). Reaction mix was prepared by adding LR reaction buffer (5X), 300 ng destination vector and 100-300 ng entry clone. LR clonase enzyme mix was added to this mixture, vortexed briefly and incubated at 25°C for 1 h. One μ l Proteinase K solution was added to the cocktail and further incubated for 10 min at 37°C for reaction termination. Bacterial transformants were selected on LB-agar plate containing Hygromycin (50 μ g/ml) and confirmed by sequence analysis.

Materials and Methods

Cloning siRNA PolII subunit 3 in pGWB6

The *RNA polymerase II subunit 3 (Solyc05g010300.2.1)* cloned in pENTR (using forward and reverse pENTER-RNA Pol-II-3 primers) was cloned into destination vector pGWB6 harbouring a C-terminal GFP tag using the reaction described above. Bacterial transformants were selected as above and confirmed by sequence analysis.

DNA binding affinity assay with ChIP

ChIP assay was performed following the protocol described by Saleh et al. (2008). This procedure involved immune-precipitation, reverse cross-linking, digestion of protein followed by DNA precipitation. Leaves of cv. Punjab Chhuhara were agro-infiltrated either individually with pGWB17:SIRPT4-cmyc, pGWB6:SIRNAPol-II_3-gfp or co-inoculation with both the constructs (1:1). Approximately, 4 g agroinfiltrated sample was subjected to cross-linking with the buffer containing 400 mM sucrose, 10 mM Tris-HCl (pH 8.0), 1 mM PMSF; 1 mM EDTA and 1 % formaldehyde. Submerged leaves were vacuum-infiltrated for 20 min followed by 10 min vacuum infiltration of 2 M Glycine to stop cross-linking. Immunoprecipitation, reverse cross-linking, digestion of protein followed by DNA precipitation was performed as described by Grimm and Osborne (1999). Tissues (4 g) were ground to a fine powder using liquid Nitrogen and re-suspended into nuclei isolation buffer (250 mM sucrose; 10 mM Tris-HCl pH 8.0; 10 mM MgCl₂; 1 % triton X-100; 5 mM β-mercaptoethanol, 1 mM PMSF; protease inhibitor). Homogenized mix was filtered through muslin cloth and centrifuged at 11,000 rpm for 20 min at 4°C. Resultant pellet was dissolved in nuclei lysis buffer (50 mM HEPES, pH 7.5; 150 mM NaCl; 1 mM EDTA, 1 mM PMSF; 1 % SDS; 0.1 % Na deoxycholate; 1 % tritonX-100; Protease inhibitor). This mix was sonicated (8 cycles, 15 sec) followed by centrifugation at 11,600 rpm for 10 min at 4°C. Sonicated chromatin was subjected to immunoprecipitation via anti-cmyc and anti-gfp antibodies (Abcam, UK) to obtain the desired genomic DNA fragments of ToLCNDV-DNA-A-IR. For experimental control *Actin7* gene specific fragment were PCR amplified with anti-H₃K₄Me₃ antibody immunoprecipitated DNA. As a negative control, anti-IgG antibody was used for immunoprecipitation, while input control was non-immunoprecipitated sample. Obtained DNA was used for PCR amplification of targeted region of IR and *Actin7* by region specific primers (Section 3.1.12). Amplified products were resolved on 1 % agarose gel.

Expression analysis of viral transcripts

For checking the viral replication specific transcript accumulation, RNA was extracted from leaves agro-infiltrated with pGWB17:SIRPT4-cmyc, pGWB6:SIRNAPol-II_3-gfp, pGWB17:SIRPT4-cmyc + pGWB6:SIRNAPol-II_3-gfp or empty vector. Then, 10 µg total RNA was electrophoresed and transferred onto nylon membrane as previously described. ToLCNDV Rep and CP genes were PCR amplified using primer mentioned in section 3.1.12 for probe preparation. Probe preparation, purification, hybridization and washing were done as described earlier in section 3.2.7.

3.2.14 TRV-mediated virus induced gene silencing (VIGS)

Gene cloning in TRV vectors

TRV mediated gene silencing was performed using the pTRV1 and pTRV2 vector. The target gene silencing construct were prepared using pTRV1 and pTRV2 vectors according to the established protocol (Liu et al., 2002). To minimize the effect of off-target silencing, a 231 bp fragment from 3' UTR of *SIRPT4* was PCR amplified from cDNA using primers listed in section 3.1.12 and cloned into pTRV2 between *XhoI/BamHI* sites to form pTRV2:RPT4 construct. Further, to test the efficiency of TRV-based VIGS system in cultivar H-88-78-1, an endogenous control *Phytoene desaturase (Slpds; SGN-U593894)* was also similarly cloned in TRV2 vector. As a positive control, phytoene desaturase from *N. benthamiana (NbPDS; Niben101Scf01283g02002.1)* from was also cloned (to assess degree of silencing).

Agroinfiltration of pTRV constructs

The constructs were introduced into *A. tumefaciens* strain EHA105. Cells harbouring pTRV1 and pTRV2 or pTRV derivatives were incubated overnight at 28°C in LB supplemented with 100 µm MES buffer (pH 5.5), 50 µg/ml kanamycin and 50 µg/ml rifampicin. The cultures were centrifuged at 3,200 rpm for 10 min and re-suspended in the same volume of re-suspension buffer (10 mM MgCl₂, 100 µM acetosyringone and 1 mM MES buffer; pH 5.5). After adjusting OD₆₀₀ to 1, transformed cells were incubated for 3 h at room temperature. These cultures were mixed according to the experimental set up (i.e. control, mock and gene silencing constructs) in 1:1 ratio and infiltrated at two leaf stage into tomato and *N. benthamiana* leaves as discussed in section 3.2.4. Efficiency of VIGS was evaluated 21 days post-silencing by phenotypic

Materials and Methods

evaluation of leaves showing leaf decolouration in both tomato and *Nicotiana*. Effect of VIGS on transcript levels was checked by northern blot analysis using radiolabelled probes specific to *Slpds*, *Nbpds* and *SIRPT4* by methods described in previous sections.

3.2.15 Analysis of ToLCNDV infectivity index on *SIRPT4* silencing

Infectivity scoring

Subsequent to silencing experiment, ToLCNDV agroinfection was done as described in section 3.2.4. Tomato cultivar H-88-78-1 was termed on the basis of various treatments, namely $H^{TRV:00}$ (TRV:00 vector infiltrated H-88-78-1 as Mock), $H^{TRV:SIRPT4}$ (*SIRPT4* silenced cultivar H-88-78-1), $H^{TRV:SIRPT4+T}$ (*SIRPT4*-silenced cultivar H-88-78-1 and ToLCNDV-infected), $H^{TRV:00+T}$ (Mock plants inoculated with ToLCNDV) and H^T (only ToLCNDV-inoculated H-88-78-1). A set of 75 plants from three independent experiments (25 plants/experiment) were scored based on symptom appearance at 21 dpi.

	TRV VIGS VECTOR	SIRPT4	ToLCNDV
H^T	-	-	+
$H^{TRV:00}$	+	-	-
$H^{TRV:00+T}$	+	-	+
$H^{TRV:SIRPT4}$	+	+	-
$H^{TRV:SIRPT4+T}$	+	+	+

Detection of virus-specific DNA by Southern hybridization

The leaf samples from control and above mentioned series of plants were collected from five plants per treatment and total DNA was isolated by CTAB method as described in section 3.2.3.1. Equal amount of total DNA (5 μ g) from each experimental samples were electrophoresed on 1 % agarose gel in 1X TBE. Before transfer, the gel was kept for 20 min in depurination solution, then 30 min in denaturation solution and finally treated with neutralization solution for 30 min. DNA was transferred onto to positively charged nylon membrane (HYBOND-N⁺, Amersham Bioscience, USA) by capillary transfer method (Southern, 1975). After overnight transfer in 20X SSC, the DNA was immobilized by UV crosslinking (Sambrook et al., 1989). The blot was pre-hybridized for 3-4 h at 60°C in pre-hybridization buffer. Meanwhile, ToLCNDV-specific CP gene (DNA-A) and

BC1 (DNA-B) probes were prepared through labelling the DNA fragments with αP^{32} dCTP using NEBlot Kit according to the manufacturer's protocol (NEB, USA). Probe preparation, purification, hybridization and washing were done as described earlier in section 3.2.7.

3.2.16 *Agrobacterium*-mediated transient overexpression of *SIRPT4*

Gene cloning in TRV vectors

Full length *SIRPT4* CDS was amplified with gene specific primers harbouring *NcoI* and *SpeI* adaptors in forward and reverse primers, respectively (Section 3.1.12). The amplified fragment was cloned into pCAMBIA1302 vector between *NcoI/SpeI* restriction sites. Recombinant plasmid was transformed into strain GV3101 of *A. tumefaciens*. Transformed cells harbouring pCAMBIA1302:*SIRPT4* along with the empty vector were cultured and re-suspended as described above. The re-suspended culture's absorbance (OD₆₀₀) was adjusted to 0.8 and infiltrated into tomato leaves at two leaf stage. Tomato cultivar Punjab Chhuhara infiltrated with different constructs were named as PC^V (pCAMBIA1302 vector infiltrated cultivar Punjab Chhuhara), PC^{SIRPT4} (*SIRPT4* overexpressed cultivar Punjab Chhuhara), PC^{SIRPT4+T} (*SIRPT4* overexpressed and ToLCNDV infected cultivar Punjab Chhuhara) and PC^T (only ToLCNDV infiltrated cultivar Punjab Chhuhara). After 2 to 3 days, the infiltrated leaves were used for molecular analysis.

Name	pCAMBIA1302 VECTOR	SIRPT4	ToLCNDV
PC ^T	-	-	+
PC ^V	+	-	-
PC ^{SIRPT4}	+	+	
PC ^{SIRPT4+T}	+	+	+

Trypan blue staining

Trypan blue staining was performed in *SIRPT4* overexpressed tomato according to Hwang and Hwang (2010). In brief, cell death in the tomato leaves was examined by staining with trypan blue reagent which was composed of 10 ml lactic acid, 10 ml glycerol, 10 g phenol, and 10 mg trypan blue dye (Sigma Aldrich, USA). The treated leaves were boiled for 1 min in capped Falcon tube and kept overnight in Chloral hydrate for destaining. Photographs were taken using a stereomicroscope (SMZ 1500, Nikon, USA).

Materials and Methods

Measurement of Caspase-like activity

Caspase kit from G-biosciences (USA) was used for this experiment. Leaves (1 g) from different treatments were ground in caspase lysis buffer. Homogenates were kept for 15 min on ice, centrifuged and supernatants were separately collected. Resultant supernatants (50 μ l) were mixed with equal volume (50 μ l) of 2X caspase assay buffer with two different peptide substrates: 150 μ M LEHD-AFC for caspase 9-like activity and 150 μ M DEVD-AFC for caspase 3-like activity, as peptide substrates. After incubation at 37°C for 60 min, the AFC hydrolysis generated fluorescence was quantified by spectrofluorophotometer (Varian, Victoria, Australia) at 400 nm excitation and 505 nm emission wavelengths. To evaluate the protein concentration, enzymatic activity was normalized with the fold activity of control extracts. Three independent experiments were conducted for measurement of fold activity.

Measurement of catalase (CAT) and ascorbate peroxidase (APX) activity

CAT activity was assayed according to protocol of Aebi et al. (1983). For this, 100 mg of leaves from each set of treatments were ground in liquid Nitrogen and suspended in 100 mM potassium phosphate buffer (pH 7.0) with 1 mM EDTA (pH 8.0). After centrifugation at 4°C, supernatants were taken and measured for CAT activity with 60 mM H₂O₂ at 240 nm wavelength using a UV-visible spectrophotometer (UV2550, Shimadzu, Japan). For APX, leaves were homogenized in the homogenization buffer (50 mM HEPES; pH 7.0, 0.1 mM EDTA; pH 8.0). After centrifugation at 4°C, supernatants were measured for the APX activity with 0.03 mM Ascorbate and 0.1 mM H₂O₂ at 290 nm wavelength. Total protein was estimated using BSA as standard with Bradford reagent (Bradford, 1976).

Measurement of Lipid peroxidase (LP) activity and electrolytic leakage (EL)

The lipid peroxidation levels in the experimental samples were evaluated with 2-Thiobarbituric acid (TBA) reaction by determining malondialdehyde content (Hodgson and Raison, 1991). For this, 100 mg tissues were homogenized in 10 mM sodium phosphate buffer (pH 7.4) followed by centrifugation at 6,400 rpm for 5 min at room temperature. In a reaction mixture containing 8.1 % SDS (w/v), 20 % Acetic acid (w/v; pH 3.5), and 0.8% aqueous TBA (w/v); 100 μ l of the supernatant was added. These reaction was allowed to proceed at 98°C for 1 h, cooled to room temperature and centrifuged at 6,400 rpm for 5 min. Incubated samples were

subjected to the measurement of absorbance and non-specific absorbance at 535 nm and at 600 nm wavelength, respectively.

Electrolytic leakage (EL) was measured as described by Dionisio-Sese and Tobita (1998). After *Agrobacterium* infiltration, the infiltrated leaf from the different treatments were collected and analyzed. Fifteen leaf discs (5-10 mm diameter) were floated on the 0.4 M sorbitol. The leaf discs were incubated in the dark for 12 h. Primary conductivity (E1) was checked with a microprocessor-based conductivity meter (Model 1601, ESICO, India). After boiling for 5 min, the pre-incubated leaves were cooled to room temperature and further subjected to measure final conductivity (E2). Percentage EL was calculated using the formula i.e., $(E1/E2) \times 100$.

3.2.17 Statistical data analysis

All reported values are means of at least three independent experiments. The significance (at *, $P < 0.05$; **, $P < 0.01$; ***, $P < 0.001$) of difference between mean values of control and each treatment was performed using one way analysis of variance (ANOVA) and comparison among means was carried out using Tukey-Kramer multiple comparisons test with the help of GraphPad InStat software (version 3.10), San Diego, California, USA (<http://graphpad.com/quickcalcs/ttest1.cfm>).

Chapter 4: Results

In our previous study, we identified a naturally tolerant cv. of tomato, namely H-88-78-1, which has reduced infectivity and viral titre at 21 days post inoculation (dpi) in comparison to a susceptible cv. Punjab Chhuhara (Sahu et al., 2010). Further to identify host factors involved in the tolerant attribute of cv. H-88-78-1, we constructed a suppression subtractive library between ToLCNDV-inoculated and mock-inoculated cv. H-88-78-1 samples at 21 dpi. Through this approach, a set of 106 transcripts were identified to be differentially accumulated between these samples. Interestingly, 3 genes associated with the ubiquitin proteasome pathway showed relatively higher (> 4 fold) expression in the tolerant cultivar, in comparison to the susceptible cultivar. These genes were *26S proteasome subunit RPT4a* (GR979393), *Ubiquitin conjugating enzyme* (GR979415) and *Armadillo repeat motif-containing protein* (GR979475) (Sahu et al., 2010).

For the purpose of this study *26S proteasome subunit RPT4a* (GR979393) was selected as a candidate gene for molecular and functional characterization. The results of the current proceeding are as follows:

4.1. Molecular cloning and characterization of tomato RPT4a gene

4.1.1. Retrieval of full length SIRPT4a gene

Among several ESTs generated from subtracted cDNA library in ToLCNDV tolerant cultivar H-88-78-1, a partial cDNA clone (GenBank accession GR979393) having sequence homology to 26S proteasome AAA-ATPase subunit RPT4a was chosen as a candidate for further studies. This partial clone was subjected to BLAST analysis at Sol Genomics Network (<https://solgenomics.net/tools/blast/>). Hit obtained was most significant (e value=0e+00) to 26S proteasome subunit RPT4a (Unigene ID: SGN-U566414) and the transcript was named as *SIRPT4*.

4.1.2. Sequence analysis of SIRPT4 ORF encoding protein

The SIRPT4 ORF sequence was 1,197 bp in length which was flanked by 5' and 3' untranslated regions (UTRs) of 95 and 216 bp, respectively, including a 12 bp poly A tail (Fig. 4.1). It encoded a protein of 399 amino acids with 44.7 kDa molecular mass and a theoretical isoelectric point of 7.488. Deduced amino acid sequence revealed the presence of a conserved AAA domain from 141 to 308 amino acids. A Coiled-coil (CC) domain was also found in the N-terminal of the protein.

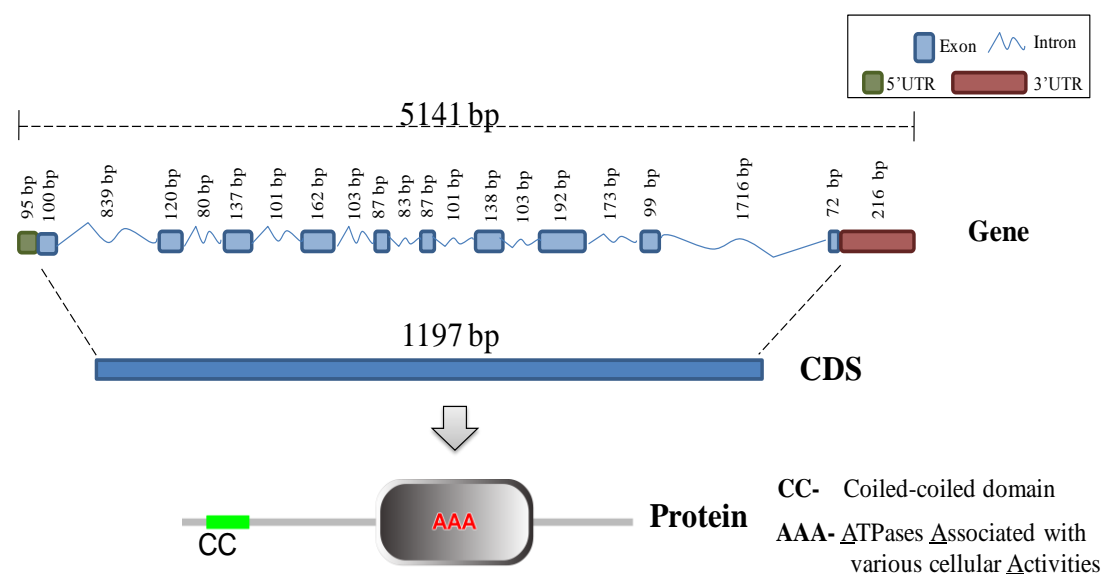


Fig. 4.1. Characterization of tomato SIRPT4a gene (SGN-U566414). Genomic structures such as exons, introns, along with 3' and 5' untranslated regions (UTRs) have been depicted. Coding sequences is translated into a protein which has characteristic CC and AAA domains.

4.1.3. Genomic organization of *SIRPT4*

Initial examination to understand the genome organization (intron number and size) was done. The genomic structure suggested that the full length SIRPT4 gene spans about 5,141 bp in size with ten exons and nine introns (Fig. 4.1). Two of the nine introns were 839 and 1,716 nucleotides long; however others were between the ranges of 80-173 bp.

4.1.4. Structure of the SIRPT4 protein

Secondary structure prediction

The secondary structure calculation was performed using GORIV secondary structure prediction method. The results showed that the primary amino acid structure is organised mostly as alpha helix (57.54 %) followed by random coil arrangement of (33.67 %) and extended strand of 8.9 % (Fig. 4.2).

The three dimensional (3D) structure models

The 3D protein structural models with good quality and resolution were generated through I-TASSER server. Out of the two models generated, the model 1 was selected

as the best predicted tertiary structure model of SIRPT4 protein based on its correlation quality score (C-score=0.24).

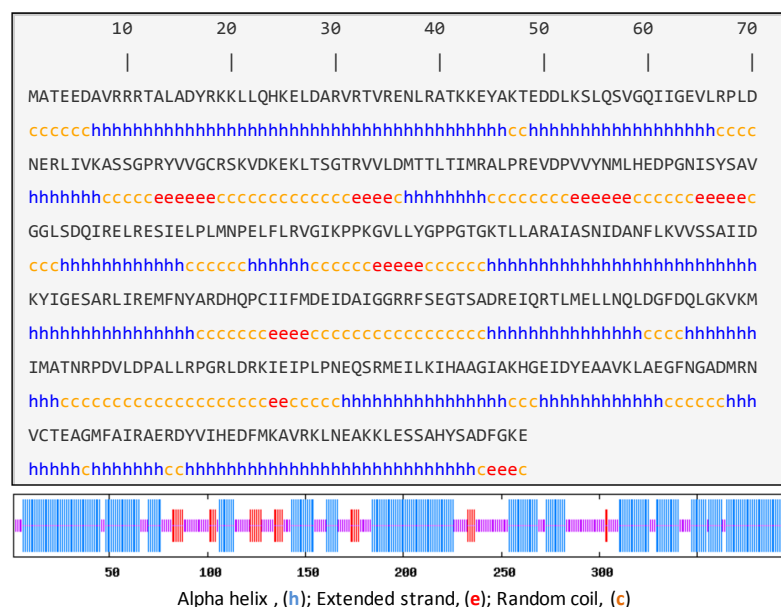


Fig. 4.2. Secondary structure of SIRPT4a protein. Random coil (c), extended strand (e) and alpha helix (h) have been represented. Corresponding location of these structures are depicted as blue (h), red (e) and orange (c) bars.

This selection was further substantiated by other criteria for model predictions, such as RMSD and TM score. The TM score and RMSD values of SIRPT4 model 1 were 0.75 ± 0.11 and $6.3 \pm 3.8 \text{ \AA}$, respectively (Fig. 4.3A). Model 2, which had low C-score (0.05), was not considered further (Fig. 4.3B).

TM-align, which is a structural alignment program of I-TASSER, was employed to identify available proteins in the Protein Data Bank (PDB), which had similar structure like the first SIRPT4 model. This analysis revealed that there were 6 proteins from the PDB which had the closest structural similarity to model 1. Among these, the proteasome component PRE3 (a putative hydrolase, PDB code 4cr2J) protein from *S. cerevisiae* showed the maximum TM score (0.915) with RMSD value of 1.17 and was thus closest structural homologue of SIRPT4 protein (Fig. 4.3C).

To examine the biological annotations of SIRPT4 protein, a meta-server approach namely COACH (utilizing the I-TASSER structure prediction results) was applied.

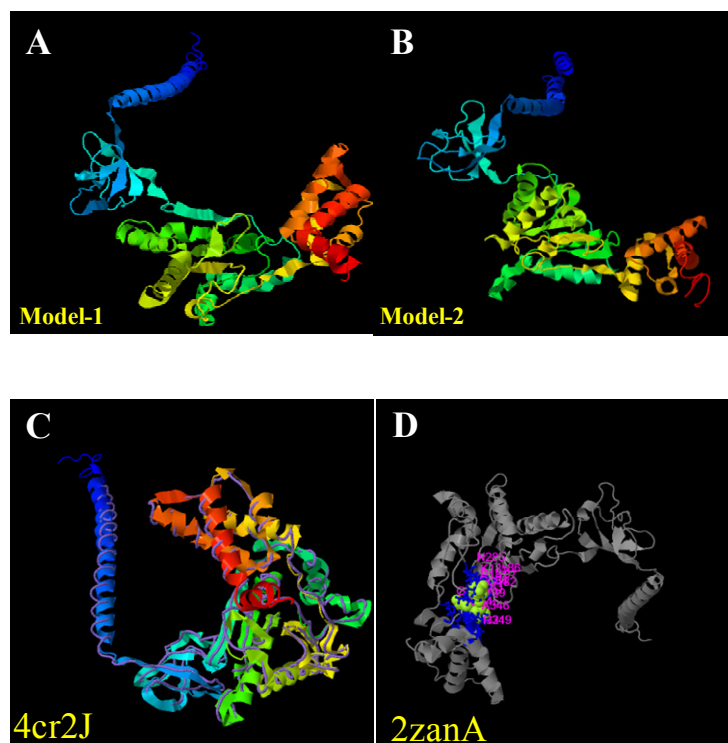


Fig 4.3. The 3D tertiary structure models of SIRPT4 protein as generated by I-TASSER software. Model 1, **A**; and Model 2, **B**, were generated through SPICKER program to cluster all the decoys depending on the pair-wise structure similarity. **C**, The closest structural similarity of SIRPT4 protein was with 4cr2J which is the proteasome component PRE3 from *Saccharomyces cerevisiae*. **D**, Biological annotations and ligand binding sites prediction of SIRPT4 protein. The closest similarity of SIRPT4 protein was with 2zanA which is the Vacuolar protein sorting-associated protein 4B from *S. cerevisiae*.

Analysis suggested that the SIRPT4 protein closely resembled PDB-ID 2zan (C-score = 0.90), which is functionally annotated as vacuolar protein sorting-associated protein 4B (UniProt ID, P46467) (Fig. 4.3D). Ligand-protein binding search suggested that this protein had 16 ATP binding sites, as predicted through BioLiP software.

Conserved domains within the SIRPT4 protein

Full length SIRPT4 protein (399aa) was searched in the NCBI-Conserved Domains Database (<http://www.ncbi.nlm.nih.gov/Structure/cdd/wrpsb.cgi>). SIRPT4 showed maximum similarity with RPT1 protein (Accession No: COG1222; Bit Score: 561.89; e-value: 0e+00). It was observed that this protein also had AAA domain. A characteristic triple AAA-ATPase domain, belonging to the P-loop NTPase family

proteins, was present at the region corresponding to 141aa to 308aa of the protein. SMART domain search showed that this protein had a predicted CC domain (28aa to 53aa) at N-terminal of the protein (Fig. 4.4). SIRPT4 protein had specific Walker-A and Walker-B motifs which are required for the hydrolysis of ATP, along with a C-terminal helicase motif found in many RNA/DNA helicases proteins (Fig. 4.4).



Fig. 4.4. Representation of the domain architecture of SIRPT4 protein. Regions of the proteins indicating the domains conserved within the AAA superfamily of proteins, AAA-ATPase (AAA) and Coiled-coil domain (CC). Motifs corresponding to Walker-A, Walker-B and Helicase are depicted in the protein sequence of SIRPT4.

4.1.5. Phylogenetic studies of SIRPT4 protein

The typical 'AAA' domain was searched by HMM search from Hidden Markov Model (HMM) profile (PF09820). All the methods predicted a total of 684 unique AAA domain containing protein sequences (after removal of alternate transcripts) in tomato. This set of 684 sequences was subjected to cluster analysis which resulted in a compact cluster for AAA proteins. Among them, a set of 168 proteins was well separated from neighbouring clusters and was further analysed to present an approximate picture of important sequence families (Fig. 4.5). In-depth analysis of these 168 proteins revealed two major sub-clusters belonging to either P-loop NTPase or to AAA+ATPase. Sub cluster P-loop NTPase was strongly interconnected by pairwise relationships and included AAA-ATPases, 26SP (including SIRPT4),

Results

metalloproteases, meiotic group, D2 domain (two AAA domains). The AAA+ sub cluster included proteins belonging to Clp/Hsp100 (Clp family in *E. coli*), Lon (protease La), AAA, RuvB (resistance to the effects of UV B), Mg²⁺ chelatase.

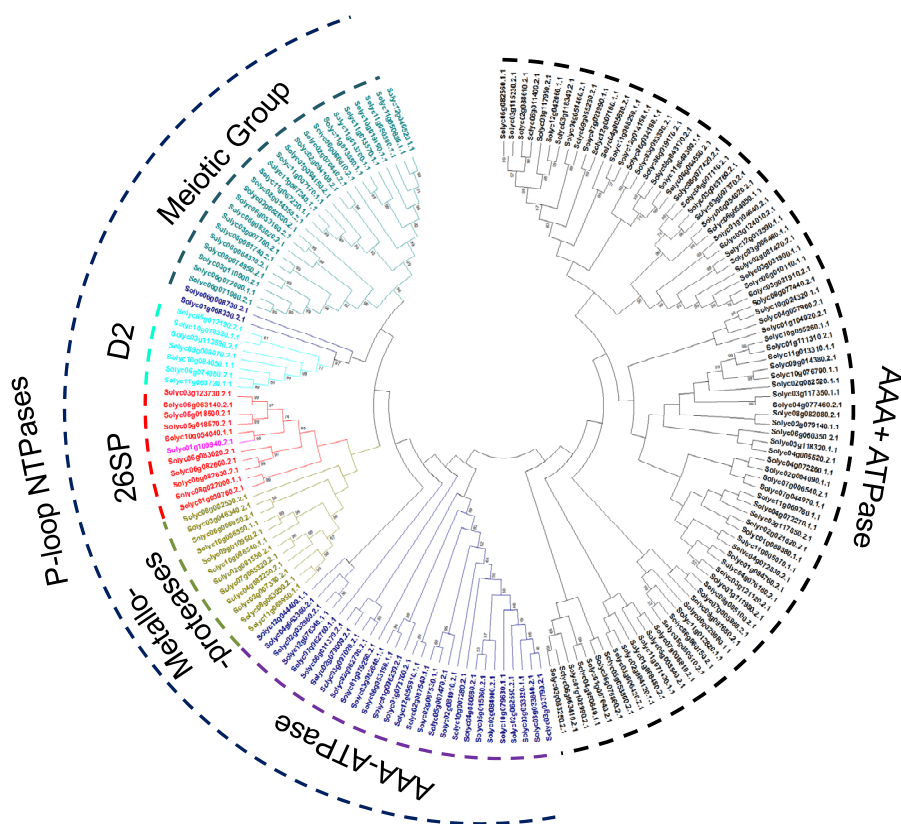


Fig. 4.5. Phylogeny of tomato AAA domains. The depicted phylogeny is a composite tree, formed of subtrees calculated under various saturation correction scenarios. Gene ID in pink font within 26SP clade represents SIRPT4 protein.

4.1.6. *Cis*-acting regulatory elements identified in *SIRPT4* promoter region

Cis-acting regulatory elements are essential molecular switches implicated in the transcription regulation of gene functions controlling various biological processes and response to environmental stresses. Hence, to identify the *cis*-regulatory elements present upstream of the *SIRPT4* gene, a 1000bp upstream sequence (locus SL2.50ch01:96772912-96771913) was retrieved from the tomato genome (available at SGN; <https://solgenomics.net/>). In this sequence, several putative transcription factor binding sites and conserved *cis*-acting regulatory elements were identified using PlantCARE and PlantPAN 2.0 databases (Table 4.1). These included binding sites for Myb (Myeloblastosis)-related, bHLH (basic/helix-loop-helix), NAM (no apical meristem), HD-ZIP (Homeodomain-leucine zipper), C2H2 and WRKY

transcription factors. Interestingly, *SIRPT4* promoter was rich in the stress responsive *cis*-elements such as ethylene-responsive transcription factor (ERF), dehydrin, heat shock factors (HSF) and ethylene insensitive 3 (EIN3).

Table 4.1. List of *cis*-acting regulatory elements identified in *SIRPT4* promoter.

Element	Sequence	Position	Function
3-AF1 binding site	AAGAGATATTT	-583	Light responsive element
bHLH	CCAAGTAGG	-666	Helix-loop-helix DNA-binding domain
Box-W1	TTGACC	+350	Fungal elicitor responsive element
C ₂ H ₂	TACACTT	+466	C ₂ H ₂ -type zinc finger
chs-CMA2a	TCACTTGA	+346	Part of a light responsive element
Circadian	CAANNNNATC	+787	<i>Cis</i> -acting regulatory element involved in circadian control
Dehydrin	CCGAC	+923	Cold- or drought- induced gene expression
EIN3	AATGTATTTA	-443	Positive regulator in the ethylene response pathway
ERF	TCCGAC/ TAGAT	+922, -618	Ethylene-responsive element
HD-ZIP	GCAATAATA/ TCAATAATT	-331, -838	Homeobox domain
HSF	AGAATATTAT	+45, +978	Heat stress related
MYB-related	AAAATATCGC	+823, -71	NAC transcription factor
NAM	GTTTGACTT/ ACTTGACCA	-120, -349	NAC transcription factor
TC-rich repeats	ATTTTCTTCA	-904	TC-rich repeats
TCT-motif	TCTTAC	+163	Light responsive element
WRKY	TTTGACTT	-121, -350	WRKY71 like
CG-1	GCGCGG	+/- 28	Regulates transcriptional activity in response to calcium signals

Additionally, few elements like the ERF and EIN3-motif, which are involved in ethylene and MeJA responsiveness respectively, were identified. In addition to the above, several light responsive elements such as 3-AF1 binding site, chs-CMA2a and TCT-motif and circadian elements were also found.

Results

4.1.7. Tissue specific expression of *SIRPT4*

The tissue-specific expression of *SIRPT4* was estimated by northern blot analysis of upper leaves, lower leaves, stem, root, flower, green fruit and red fruit of tomato cv. H-88-78-1 (Fig. 4.6A, B). It was found that under control conditions, upper leaf, flower and red fruit tissues had significantly ($P<0.001$) >4 fold higher level of *SIRPT4* expression than the green fruit. The transcript accumulation was also significantly ($P<0.01$) higher in root tissues. Interestingly, level of *SIRPT4* was higher in upper leaves in comparison to the lower leaves of tomato cv. H-88-78-1 (Fig. 4.6A, B).

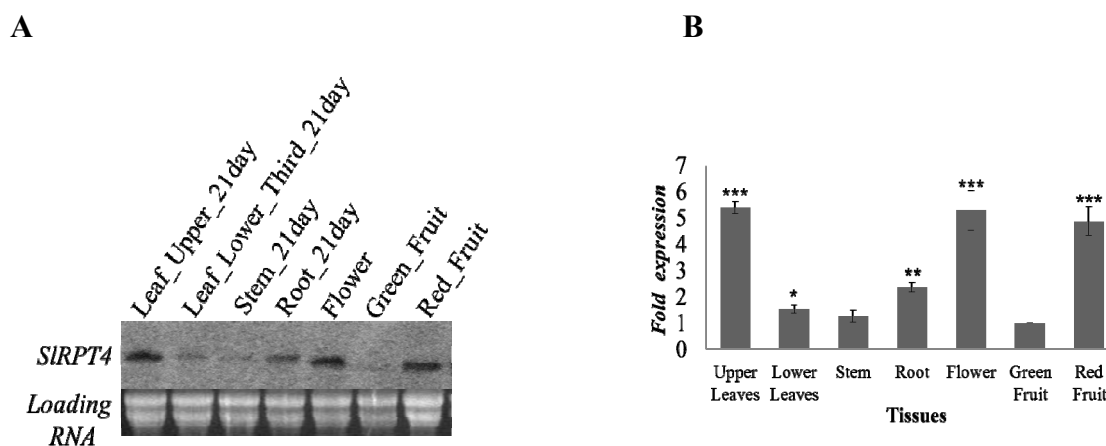


Fig. 4.6. Tissue-specific expression of *SIRPT4* gene. **A**, Northern blot analysis showing the level of *SIRPT4* transcript accumulated on upper leaves, lower leaves, stem, root, flower, green fruit and red fruit of tomato cv. H-88-78-1. **B**, Relative fold change in the corresponding tissues of cv. H-88-78-1. Accumulation of *SIRPT4* in green fruits was selected as control. Data depicts means \pm SD of three independent experiments ($n=3$); *, $P<0.05$; **, $P<0.01$; ***, $P<0.001$.

4.1.8. Expression analysis of *SIRPT4* after various hormone treatments

Northern blot analysis revealed that *SIRPT4* expression was significantly altered after external foliar spray of hormones salicylic acid (SA), methyl jasmonate (MeJA), and ethephone (ET). It was found that the *SIRPT4* expression was significantly ($P<0.001$) higher in the leaf tissues treated with ET in comparison to the control sample (sterile water treatment) (Fig. 4.7A, B). Level of *SIRPT4* was also significantly ($P<0.01$) higher in the SA and MeJA treated leaves after 12h of treatment (Fig. 4.7A, B).

This suggests that SIRPT4 gene expression is modulated in response to hormones like SA, MeJA and ET in leaf.

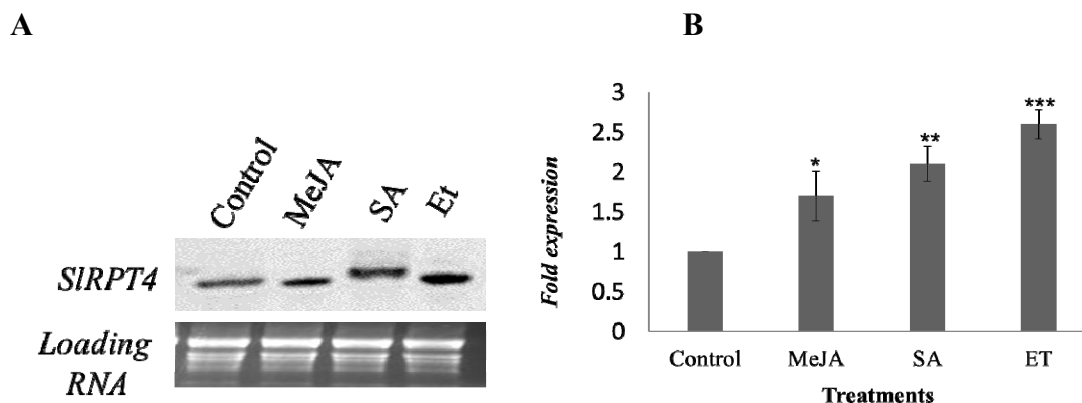


Fig. 4.7. Hormone induced expression of SIRPT4 transcript at 12 h post hormone treatments. **A**, Northern blot analysis to evaluate the level of *SIRPT4* expression after salicylic acid (SA), methyl jasmonate (MeJA), and ethephone (ET) treatments on cv. H-88-78-1. **B**, Relative fold change for the corresponding treatments in cv. H-88-78-1. Expression of *SIRPT4* in leaves treated with sterile water was taken as control. Data depicts means \pm SD of three independent experiments (n=3); *, $P < 0.05$; **, $P < 0.01$; ***, $P < 0.001$.

4.1.9. Bacterial protein expression of SIRPT4

To study functionality of the protein, the SIRPT4 coding sequence (1,197 bp) was cloned into pGEX-4T-2 vector and further confirmed by digesting with *Bam*HI-*Eco*RI enzymes followed by sequencing (Fig. 4.8A, B). SIRPT4 protein was expressed as an N-terminal fusion with GST, under the control of IPTG inducible *lac* promoter in *E. coli* BL21 (Fig. 4.8A, B). Bacterial culture harbouring GST-tagged SIRPT4 (SIRPT-GST) and empty vector were induced with IPTG, denatured and separated on 12 % SDS-PAGE (w/v) to evaluate the protein composition of each preparation. SDS-PAGE showed a highly expressed ~69 kDa (GST 25kDa + SIRPT4 44kDa) desired polypeptide for SIRPT4-GST fusion protein in the IPTG induced fraction as compared to un-induced fraction (Fig. 4.8C). As the protein was found in the induced pellet, hence IBS buffer was used to extract the fusion protein into a supernatant. Further this protein was purified by using 20 mM reduced glutathione and resolved on the 12 % SDS-PAGE (Fig. 4.8D).

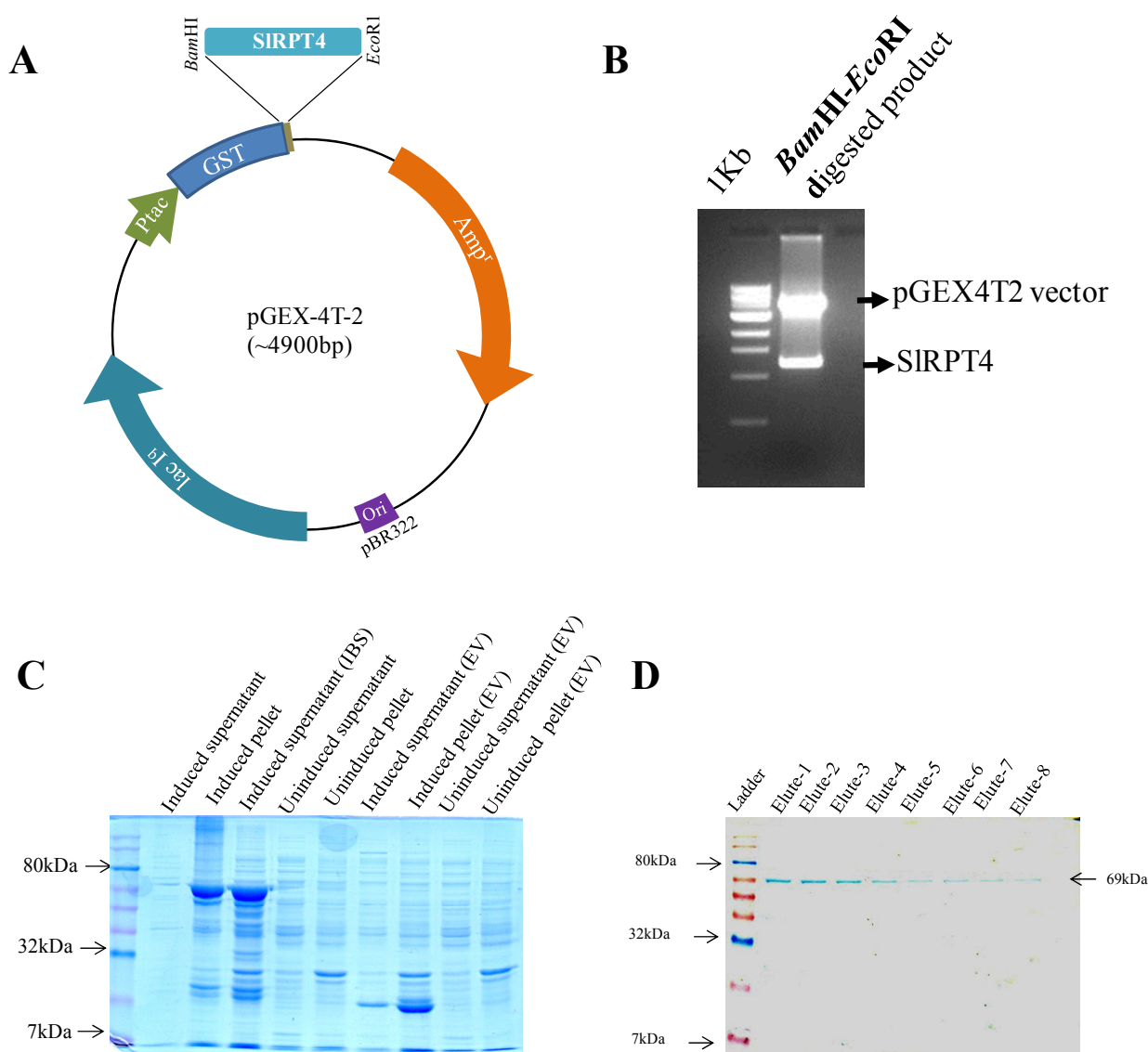


Fig. 4.8. Bacterial expression and purification of SIRPT4 protein. **A**, Vector map of pGEX-4T-2. Coding sequence of *SIRPT4* was cloned into *Bam*H1 and *Eco*R1 restriction sites of pGEX-4T-2 vector. **B**, Confirmation of cloning through digestion with *Bam*H1 and *Eco*R1 enzyme. **C**, Coomassie brilliant blue stained 12 % SDS-PAGE showing induction of GST fused SIRPT4 protein (~69 kDa) in comparison to 25 kDa GST in empty vector (EV) control. **D**, Purified bacterially expressed SIRPT4 protein. Band represents GST-affinity purification fractions of SIRPT4-GST fusion protein.

4.1.10. SIRPT4 has ATPase activity

SIRPT4 is a member of AAA family of proteins. Since it possess ATPase domain, it was essential to check for its ATPase activity. For this, different amounts of

SIRPT4-GST fusion protein were incubated with $\gamma\text{P}^{32}\text{ATP}$. It was evident from the thin layer chromatography that SIRPT4 protein had the ability to hydrolyze $\gamma\text{P}^{32}\text{ATP}$ in a concentration dependent manner (Fig. 4.9).

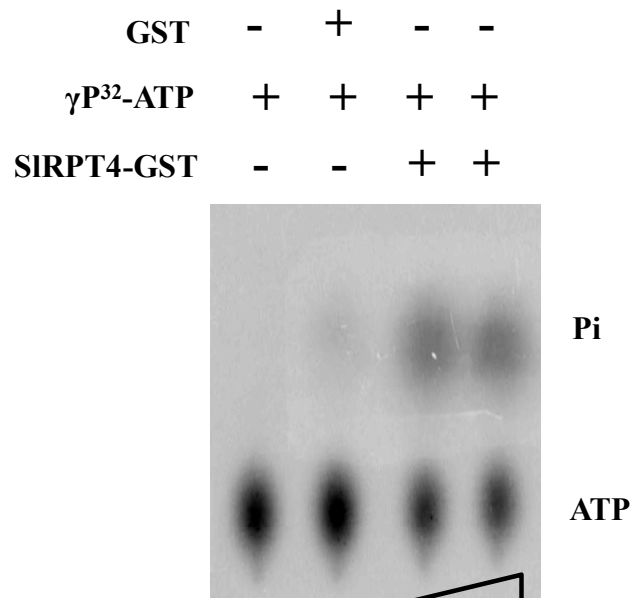


Fig. 4.9. Thin-layer chromatography to evaluate ATPase activity of SIRPT4. Figure shows dissociation of Pi from γP^{32} -labelled ATP. Level of Pi was enriched upon increasing the amount of protein. GST protein was used as a negative control of the experiment.

4.1.11. Novel interacting partners identified by pull-down assay

To identify the putative interacting targets of SIRPT4, pull down assay was performed. For this, total plant proteins were isolated from the ToLCNDV-infected cv. H-88-78-1 at 21 dpi and further pre-cleared with GST proteins to avoid its non-specific binding with the target proteins. GST pre-cleared total plant proteins and SIRPT4-GST fusion proteins were mixed together and filtered through GST affinity column. Affinity bound proteins were eluted and resolved on 12 % SDS-PAGE gel. This resolved gel was subjected to silver staining. All the visible bands (Fig. 4.10) were excised and subjected to trypsin digestion for LC-MS/MS analysis. LC-MS/MS result showed that SIRPT4 can interact with sixteen probable plant proteins (Table 4.2).

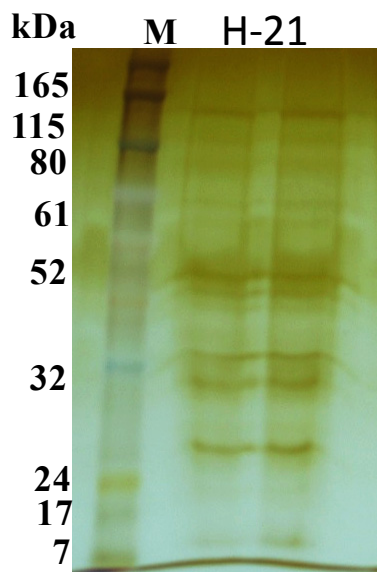


Fig. 4.10. Silver stained 12 % SDS-PAGE showing resolved bands of probable SIRPT4 interacting partners. M, Protein marker; H-21, eluted plant proteins from 21 day post ToLCNDV-infected cv. H-88-78-1.

Blast2Go analysis of the predicted SIRPT4 interacting partners showed their participation in diverse biological processes and molecular functions in different cellular locations (Fig. 4.11). Majority of proteins have cell and membrane associated functions (Fig. 4.11). Conserved domain analysis of the identified 16 proteins showed them to possess variety of domains, which suggests the plausible involvement of SIRPT4 in diverse cellular processes (Fig. 4.12). Interestingly, CC and trans-membrane (TM) domains were common in most of the interacting proteins.

Interestingly, manual annotation of these protein suggested that the identified target proteins are related to disease resistance protein (NBS-LRR, resistance protein), signaling molecules (B-cell receptor-associated protein, Signal transducer and activator of transcription B and Serine threonine protein kinase), along with metabolic process related proteins (Aldehyde dehydrogenase-dependent, Glucan synthase like 3 and Serine acetyltransferase). Overall, these analyses suggest that SIRPT4 is a functionally diverse protein.

Table 4.2. Details of identified target proteins of SIRPT4.

S.No.	Peptide name	Accession No.	Score (hit)	Similarity with tomato protein	Tomato gene ID	Peptide*
1.	Hypothetical protein [<i>Arabis alpina</i>]	gi 674249569	57 (1)	Tpr protein (Fragment)	Solyc06g053570.2.1	R.AESENLENLLKQK.Q
2.	B-cell receptor-associated protein [<i>Phoenix dactylifera</i>]	gi 672164759	51 (1)	B-cell receptor-associated protein	Solyc09g059570.2.1	R.LHHCLQKVINLR.K
3.	Probable disease resistance protein [<i>Vitis vinifera</i>]	gi 731403513	50 (4)	NBS-LRR, resistance protein	Solyc08g013970.1.1	R.AEAMELEVVDQLIR.D
4.	Sodium transporter [<i>Nicotiana tomentosiformis</i>]	gi 697117041	48 (2)	Bile acid sodium symporter	Solyc07g014740.2.1	K.ISSNINRSQLLIR.A
5.	Nuclear pore complex protein [<i>Sesamum indicum</i>]	gi 747052404	72 (3)	RAN binding protein 3	Solyc03g120280.1.1	M.GDAENNFQPSK.K
6.	Uncharacterized protein [<i>Glycine max</i>]	gi 571520381	50 (1)	Signal transducer and activator of transcription B	Solyc07g062050.2.1	K.SPLNSMASR.R
7.	Uncharacterized protein [<i>Cicer arietinum</i>]	gi 502086825	50 (1)	Ubiquitin	Solyc05g032790.1.1	K.YEQLQAEIGK.T
8.	Hypothetical protein [<i>Populus trichocarpa</i>]	gi 566148382	50	Serine threonine protein kinase	Solyc08g083040.2.1	K.YEQLQQQLK.A

Contd...

Results

9.	Pectinesterase inhibitor [<i>Gossypium arboreum</i>]	gi 728808567	50 (1)	HGWP repeat containing protein	Solyc06g043370.1.1	K.YEELQQCLK.A
10.	Hypothetical protein [<i>Ricinus communis</i>]	gi 255544858	49 (1)	Aldehyde dehydrogenase-dependent	Solyc01g011510.2.1	R.VKNLISDLAVQK.S
11.	Uncharacterized protein [<i>Zea mays</i>]	gi 670369301	49 (1)	Glucan synthase like 3	Solyc01g006370.2.1	K.LSNNQLQPIIDK.V
12.	BnaA08g00140D [<i>Brassica napus</i>]	gi 674890344	48 (1)	Serine acetyltransferase	Solyc07g065340.1.1	R.SLSSALANILSVK.L
13.	PHD finger protein [<i>Glycine max</i>]	gi 356499807	47 (1)	PHD finger family protein	Solyc04g008420.1.1	R.NATINDLKLEVER.N
14.	MADS-box protein [<i>Beta vulgaris</i>]	gi 731321614	47 (1)	MADS-box transcription factor 29	Solyc11g005120.1.1	K.NQLMQQLENLR.R
15.	Os02g0198600 [<i>Oryza sativa</i>]	gi 115444859	61 (2)	DNA-damage inducible protein	Solyc10g005890.2.1	K.VTSNERPSQDIIR.L
16.	Legumin A2 [<i>Vicia faba</i>]	gi 22008	58 (1)	Legumin 11S-globulin	Solyc03g005580.2.1	R.DFLEDALNVNR.H

*Dot sign in the peptide refers to the deamination of amino acid.

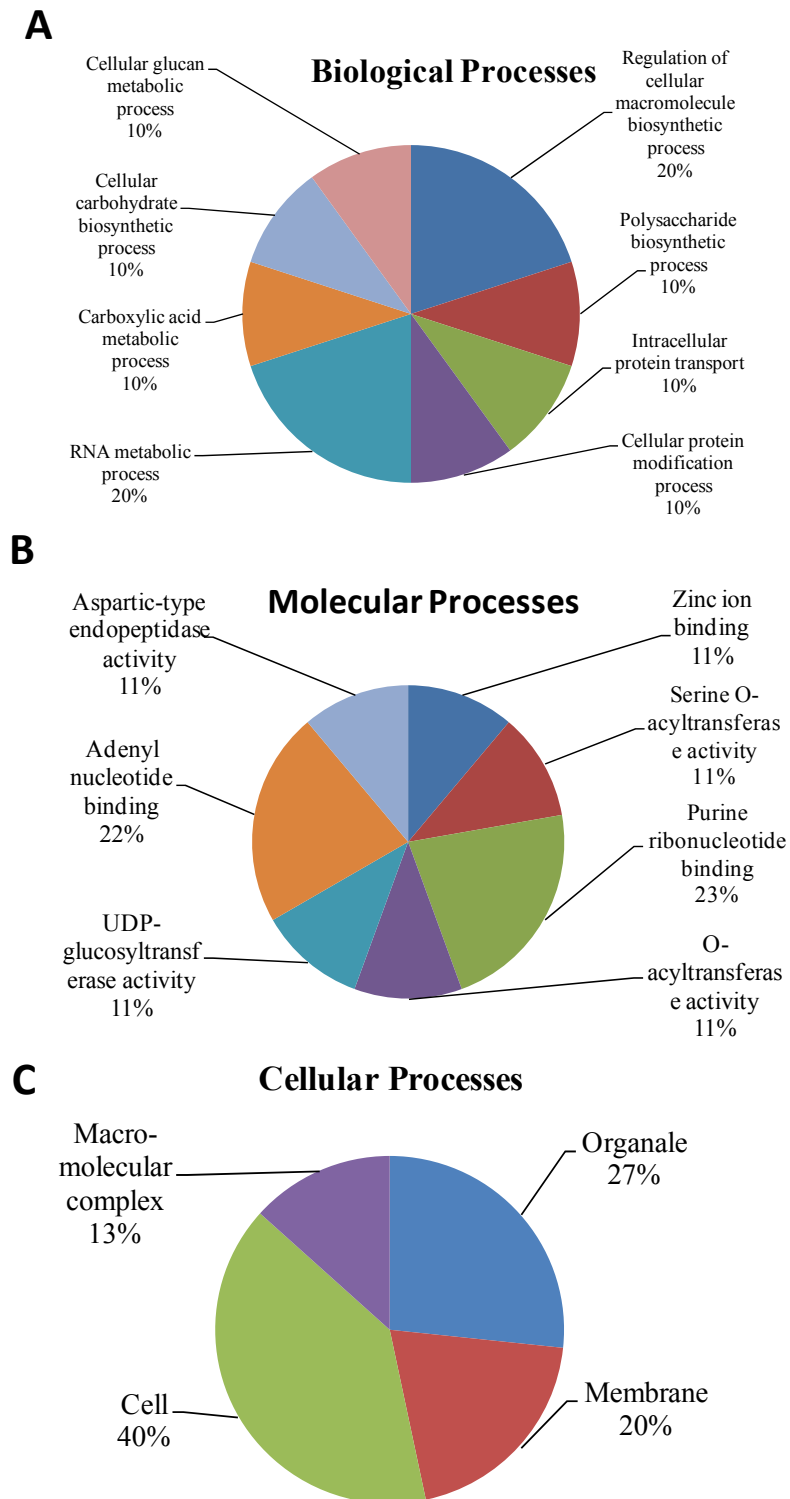


Fig. 4.11. Gene Ontology annotation of SIRPT4 interacting proteins. The Blast2GO output defining; **A**, Biological processes; **B**, Molecular functions and **C**, Cellular components.

Results

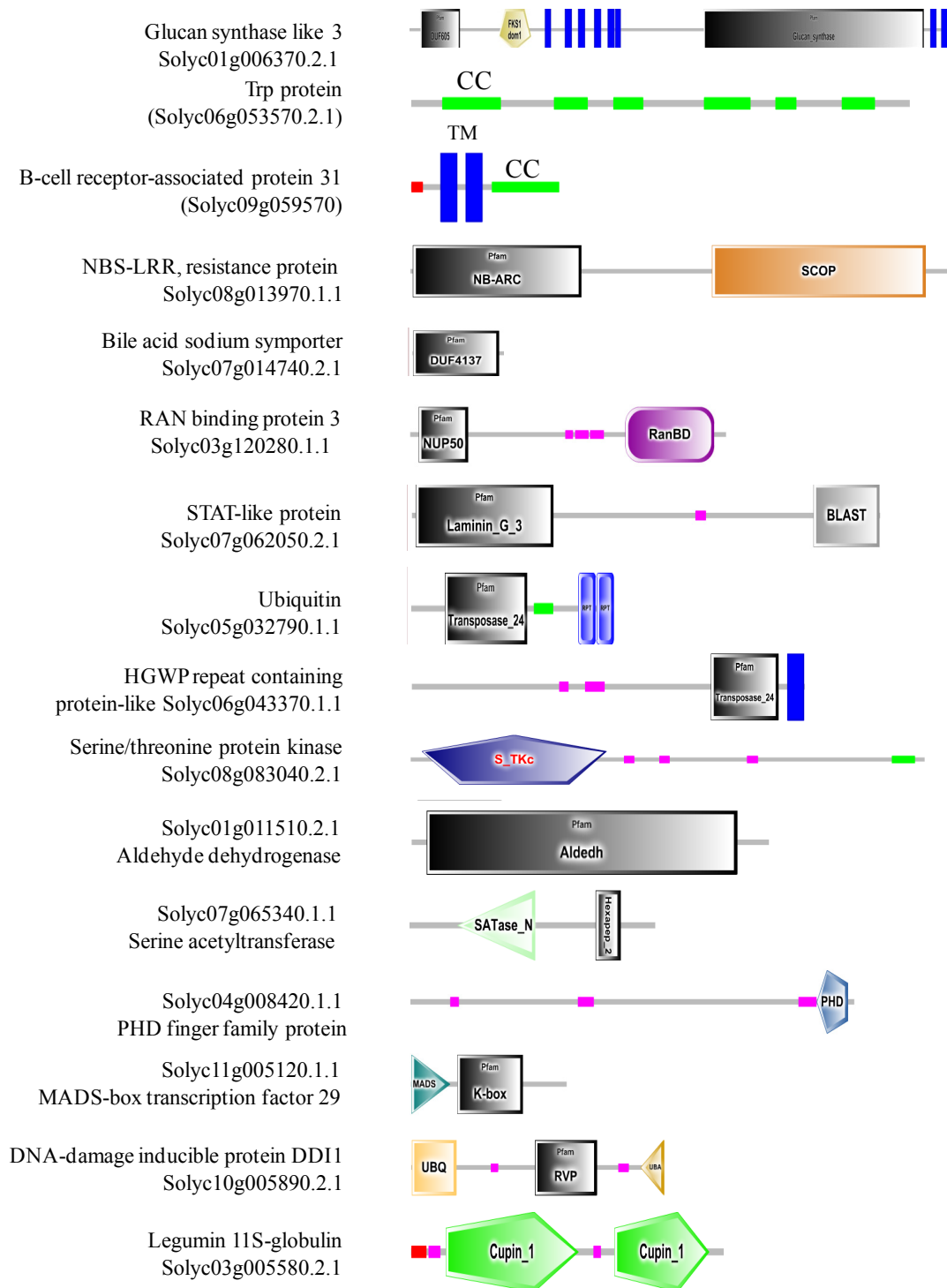
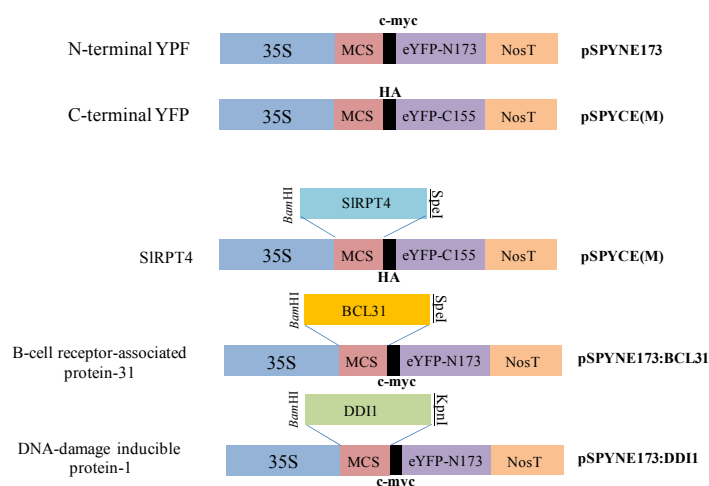


Fig. 4.12. Analysis of protein domains in SIRPT4 interacting proteins. Simple Modular Architecture Research Tool (SMART) was used to identify the domain within the proteins.

4.1.12. SIRPT4 protein interacts with SIBCL31 and SIDDI1

To confirm some of these putative interactions *in vivo*, BiFC analysis was conducted, in which the active YFP is reconstituted only when the non-fluorescent N-terminal (pSPYNE-173) and C-terminal (pSPYCE-M) YFP fragments interact (Fig. 4.13).

A



B

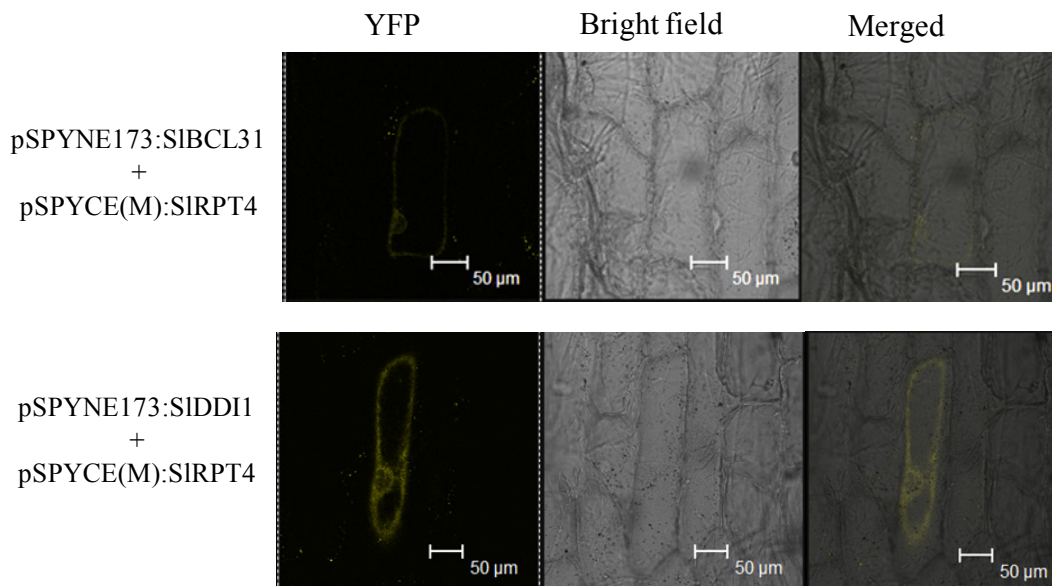


Fig. 4.13. BiFC analysis of SIRPT4:SIBCL31 and SIRPT4:SIDDI1 interaction. A, Cloning and construct preparation. SIRPT4 protein was cloned in pSPYCE(M) containing C-terminal of YFP. SIBCL31 and SIDDI1 were cloned into the pSPYNE173 harbouring N-terminal of YFP. B, *In vivo* analysis of interaction of the SIRPT4 protein with SIBCL31 and SIDDI1 through BiFC assay. Figure showing the YFP fluorescent in the cytoplasm of onion epidermal cell.

Results

Therefore, *SIRPT4* was cloned in the pSPYCE(M) vector and two randomly selected genes *SIBCL31* (*B-cell receptor-associated protein-31*) and *SIDD11* (*DNA-damage inducible protein 1*) in the pBIFP3 (pSPYNE-173) vectors (Fig. 4.13). For this, full length gene was amplified through cDNA using gene-specific primers listed in section 3.1.12. After conformation of cloning, recombinant vectors with appropriate combination of inserts were particle-bombarded to be co-expressed in the onion epidermal cell. It was found that both the proteins co-localized with SIRPT4 and this interaction occurred in the cytoplasm (Fig. 4.13).

4.2 Elucidating the function of SIRPT4 gene in providing defense against ToLCNDV infection

4.2.1 SIRPT4 protein has viral DNA binding activity

DNA binding activity of SIRPT4 protein was evaluated through electrophoretic mobility shift assay (EMSA). The GST-tagged SIRPT4 protein (SIRPT4-GST) was incubated with radiolabelled fragments of intergenic regions (IRs) of DNA-A and DNA-B along with viral replication (Rep) regions.

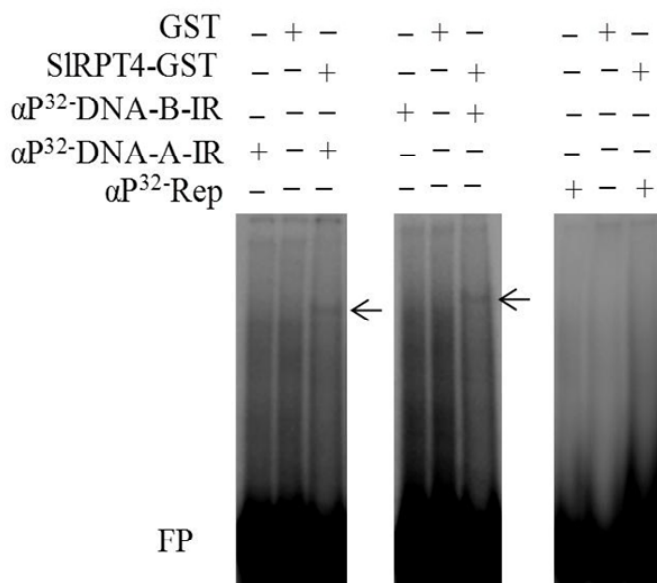


Fig. 4.14. DNA binding activity of GST-tagged SIRPT4 protein. Binding of SIRPT4 protein with αP^{32} dCTP-labeled fragments of DNA-A-IR, DNA-B-IR and Rep fragment of ToLCNDV are shown as retarded DNA-protein complex. Signs, +/- represent the presence/absence of components. GST protein was selected as a control substrate.

It was observed that the SIRPT4-GST protein formed complex only with DNA-A-IR and DNA-B-IR specific probes (Fig. 4.14). However, this DNA-protein complex was absent in the reaction mix of SIRPT4-GST and Rep-specific fragment. As a control for the experiment, purified GST protein was incubated with these radiolabelled fragments, which did not show binding affinity with the viral DNA fragments (Fig. 4.14).

Examination of characteristic domain/structure corresponding to the IR and Rep fragments showed that IRs of both DNA-A and DNA-B have the presence of a secondary stem loop structure, however, Rep region had no such structures. Hence, this suggested that SIRPT4 protein may have a binding affinity towards stem-loop structure of IR. Overall, the results suggested that SIRPT4 is a secondary structure specific DNA binding protein.

The interaction between SIRPT4 and viral DNA fragments corresponding to the DNA-A-IR was further validated by chromatin immunoprecipitation assay. Chromatin complexes were isolated from cross-linked ToLCNDV-infected leaves of susceptible cv. Punjab Chuhara which had been agro-infiltrated SIRPT4-myc overexpression construct (i.e., pGWB17:SIRPT4-myc) (Fig. 4.15A). Sonicated chromatin was immunoprecipitated through monoclonal anti-myc antibodies and immune-purified DNA was amplified with DNA-IR specific primers (Section 3.1.12). Amplification of the DNA-A-IR specific product was detected in the chromatin samples immunoprecipitated with anti-myc antibody (Fig. 4.15A). However samples immunoprecipitated with anti-IgG antibody failed to amplify the DNA-A-IR specific region. These results suggested that SIRPT4-myc had affinity to the DNA-A-IR of ToLCNDV (Fig. 4.15A). The binding of SIRPT4 protein to the IR suggests that it might be involved in the viral genome transcription. Hence, possible role of SIRPT4-IR complex in ToLCNDV genome transcription was examined.

RNA PolIII plays a major role in the geminivirus transcription; therefore gfp-tagged subunit-3 of *RNA PolIII* was transiently expressed in the ToLCNDV-infected leaves of cv. Punjab Chuhara (Fig. 4.15B). Immunoprecipitation with the monoclonal anti-gfp antibody revealed that DNA-A-IR specific primers were able to amplify the ToLCNDV-DNA-A-IR region from the immunoprecipitated samples, suggesting the IR-specific binding activity of SIRNA PolIII subunit-3 (Fig. 4.15B).

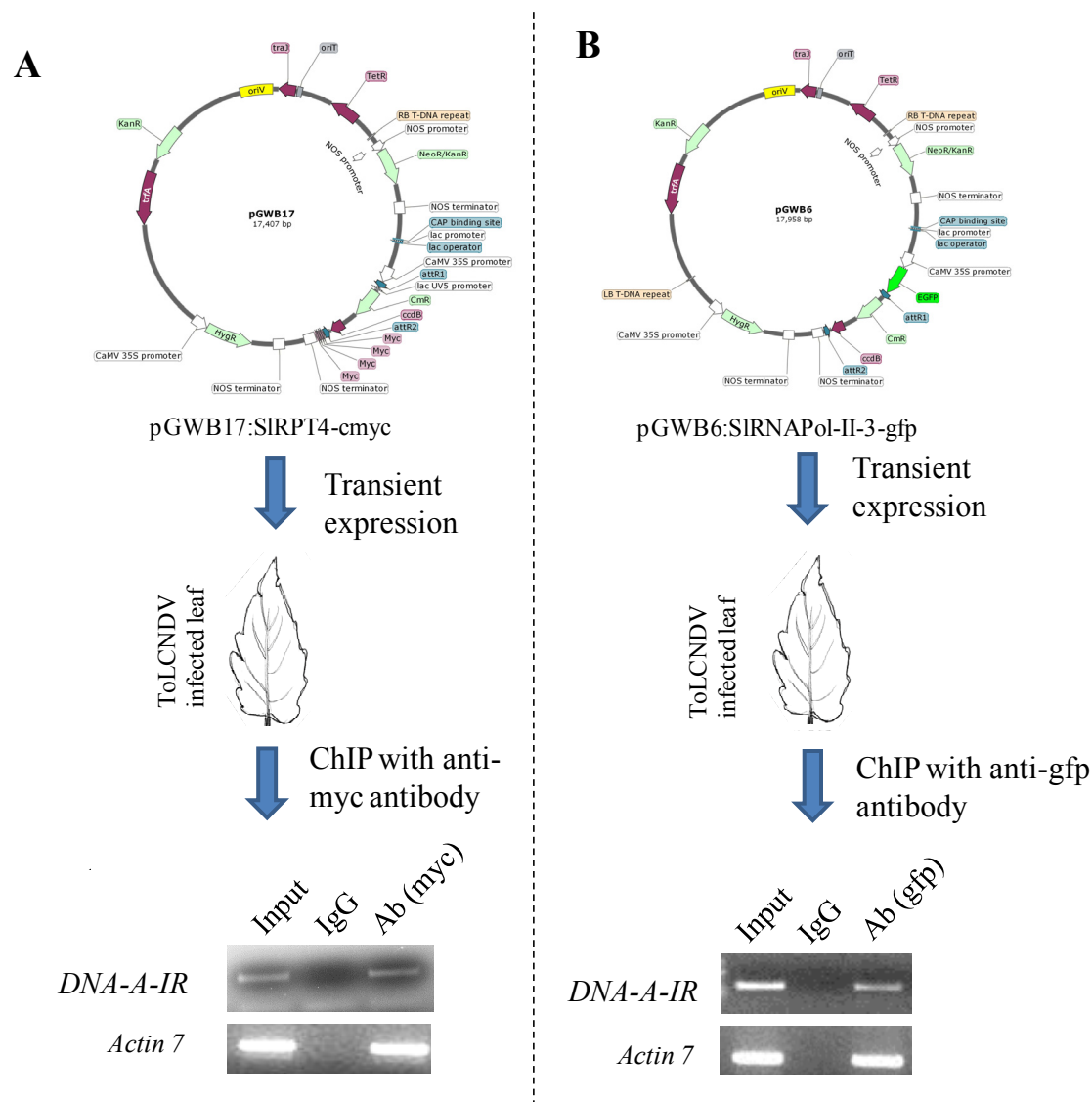


Fig. 4.15. Schematic representation of chromatin immunoprecipitation assay. *SIRPT4* and *SIRNA PolIII subunit-3* coding sequences were cloned in GATEWAY cloning vector pGWB17 and pGWB6, respectively. ChIP assay was performed by transiently overexpressing *SIRPT4*, **A**; and *SIRNA PolIII subunit-3*, **B**. Figure depicts the amplification of DNA-A-IR from the immuno-precipitated DNA from the ToLCNDV-infected cv. Punjab Chuhara using *c*-myc-tag, gfp-tag and immunoglobulin G (IgG-negative control) specific monoclonal antibodies. Total input chromatin (input control) was used for the linear amplification of DNA-A-IR fragment. Actin7 gene was amplified using H3K4Me3-specific monoclonal antibody, as a positive control.

4.2.2 SIRPT4 affects binding of RNA PolII complex to viral DNA

ToLCNDV genome DNA-A and DNA-B have an intergenic region (IR) through which viral genes diverge in both the viral and complementary sense. The region acts as the characteristic RNA polymerase II-type promoter, which is essential for the bidirectional expression of viral genes. Hence, the effect of SIRPT4-IR interaction on the bi-directional transcription of ToLCNDV, was checked. The consequences of SIRPT4 binding on DNA-A-IR was evaluated by transiently co-expressing myc-tagged *SIRPT4* and gfp-tagged *SIRNA PolII subunit-3* in tomato leaves infected with ToLCNDV. PCR amplification of anti-gfp antibody immunoprecipitated DNA of tomato leaves co-infiltrated with pGWB6:RNAPII-3 + pGWB17:SIRPT4 resulted in a significant ($P < 0.001$) reduction (~ 60 %) of the IR-specific fragment in comparison to the input control (Fig. 4.16A, B). Leaves co-infiltrated with RNA PolII-3-gfp and vector control (pGWB17:00) showed insignificant reduction (~ 15 %) in the level of IR-specific fragments in comparison to the input control (Fig. 4.16A, B).



Fig. 4.16. Schematic representation of chromatin immunoprecipitation assay after co-infiltration. ChIP assay was performed by transiently co-expressing *SIRNA PolII subunit-3* with either *SIRPT4* (pGWB6:RNAPII-3 + pGWB17:SIRPT4) or without *SIRPT4* (pGWB6:RNAPII-3 + pGWB17:00). **A**, Figure depicts the amplification of DNA-A-IR from the immuno-precipitated ToLCNDV-infected cv. Punjab Chuhara leaf samples using gfp-tag and immunoglobulin G (IgG-negative control) specific monoclonal antibodies. Total input chromatin (input control) was used for the amplification of DNA-A-IR fragment. **B**, Bar graph showing relative accumulation of DNA-A-IR-specific fragments. Data depicts means \pm SD of three independent experiments ($n=3$); *, $P < 0.05$; **, $P < 0.01$; ***, $P < 0.001$.

Comparison of the DNA-A-IR specific accumulation between the samples co-infiltrated with either *RNA PolII-3* + EV or *RNA PolII-3* + *SIRPT4*, showed a

Results

significant ($P < 0.001$) decrease in the IR-specific fragment amplification in the *RNA PolIII-3* + *SIRPT4*-infiltrated leaves. These results suggested that *SIRPT4* may bind to the IR, which may subsequently hinder the binding of RNA PolIII complex.

4.2.3 *SIRPT4* protein regulates bi-directional transcription

Alteration of ToLCNDV-specific transcript accumulation due to binding of *SIRPT4* at DNA-A-IR was confirmed by northern blot analysis of tissues overexpressing *SIRPT4*, *SIRNA PolIII-3* (denoted as *SIRNA PolIII*), and with *SIRPT4* and *SIRNA PolIII-3* co-overexpression.

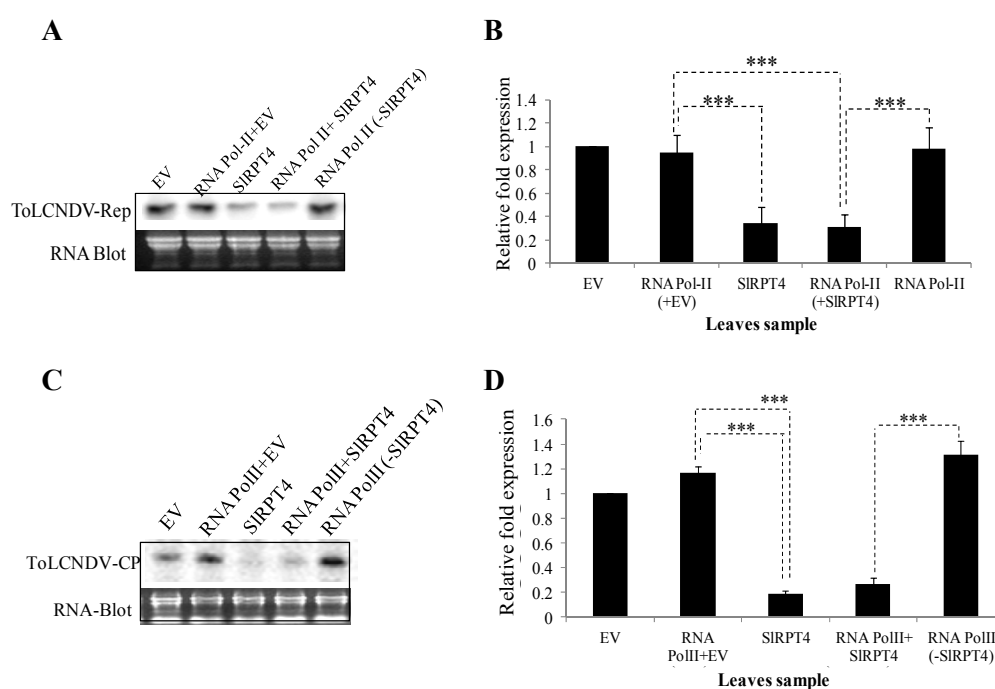


Fig. 4.17. Accumulation of *Rep*- and *Coat protein (CP)*-specific transcripts in the leaves infiltrated with empty vector (EV), *SIRPT4*-myc and RNA Pol II-3-gfp construct alone, or co-infiltration in various combinations. Fragments corresponding to *Rep* or *CP* were used as probe. **A**, Northern blot analysis showing the accumulation of *Rep*. **B**, Relative fold expression of *Rep* in the experimental leaves sample. **C**, Northern blot analysis showing the accumulation of *CP*. **D**, Relative fold expression of *CP* in the experimental leaves sample. Total RNA used for RNA blotting is depicted as equivalent loading in the experiment. EV, pGWB17:00 infiltration; RNAPolIII + EV, pGWB6RNPII-3 + pGWB17:00; SIRPT4, pGWB17:SIRPT4; RNAPolIII + SIRPT4, pGWB6RNPII-3 + pGWB17:SIRPT4; RNAPolIII (-SIRPT4), pGWB6RNPII-3 infiltration. Data depicts means \pm SD of three independent experiments. *, $P < 0.05$; **, $P < 0.01$; ***, $P < 0.001$.

It was observed that upon *SIRPT4* overexpression, level of both complementary (Rep) as well as virus sense (CP) strand-specific genes were significantly ($P<0.001$) down-regulated in comparison to leaves inoculated with either EV (pGWB17:00) or co-inoculated *SIRNA PolIII* with EV (Fig. 4.17A-D). Co-expression of *SIRNA Pol-II* and *SIRPT4* also resulted in the significant ($P<0.001$) reduction in the relative abundance of both Rep and CP gene specific transcripts, in comparison either EV or *SIRNA PolIII*+ EV co-expressed tissues (Fig. 4.17A-D). In contrast to tissues overexpressing *SIRNA PolIII* (without-*SIRPT4*), Rep gene-specific transcript accumulation in tissues co-expressing *SIRNA PolIII* and *SIRPT4* was found to be significantly ($P<0.001$) declined (~ 70 %), (Fig. 4.17A, B). Transient expression of either *SIRNA PolIII* or *SIRNA PolIII* with mock (EV) did not affected the relative level of *Rep*-specific transcript, in comparison to only mock (EV)-infiltrated leaves (Fig. 4.17A, B). Similarly, CP gene-specific transcript accumulation was significantly ($P<0.001$) reduced (~ 80 % reduction) in the tissues transiently co-expressing *SIRNA PolIII* and *SIRPT4* in comparison to only RNA Pol-II (without-*SIRPT4*)-infiltrated leaves (Fig. 4.17C, D). These results suggested that *SIRPT4* may hinder the ToLCNDV bi-directional transcription.

4.2.4 Efficiency of TRV-based VIGS in tomato

Tobacco rattle virus-based VIGS vector was employed to identify the possible function of *SIRPT4* in regulation of ToLCNDV infection in tomato using the strategy depicted in Fig. 4.18A, B. A 231 bp fragment from 3' UTR of *SIRPT4* was cloned into pTRV2 vector (Fig. 4.18B, C). Effectiveness of TRV-based VIGS system was initially tested in cv. H-88-78-1, which is previously identified as a source of natural tolerance (Sahu et al., 2010). For visual characterization of silencing, tomato *Phytoene desaturase* (*Slpds*) was used, which demonstrates typical photo-bleaching effect upon silencing. As the natural host of TRV is *Nicotiana*, hence this system was selected as a reference to assess the extent of silencing (Fig. 4.18D). Upon silencing of *Slpds*, the characteristic photo-bleaching symptoms appeared at upper-most leaves around 10 days post-silencing, and enriched maximum at 21 days post-silencing (Fig. 4.18D). Photo-bleaching effect also correlated with the relative transcript abundance of *Slpds* silencing showing >70 % reduction in accumulation, in comparison to mock-inoculated H-88-78-1 plant (Fig. 4.18E). Relative level of *NbpdS* transcript was also reduced in the *NbpdS*-silenced plants (Fig. 4.18E). This result

Results

suggests that TRV-based VIGS system is an efficient tool to study effect of transient gene downregulation in tomato.

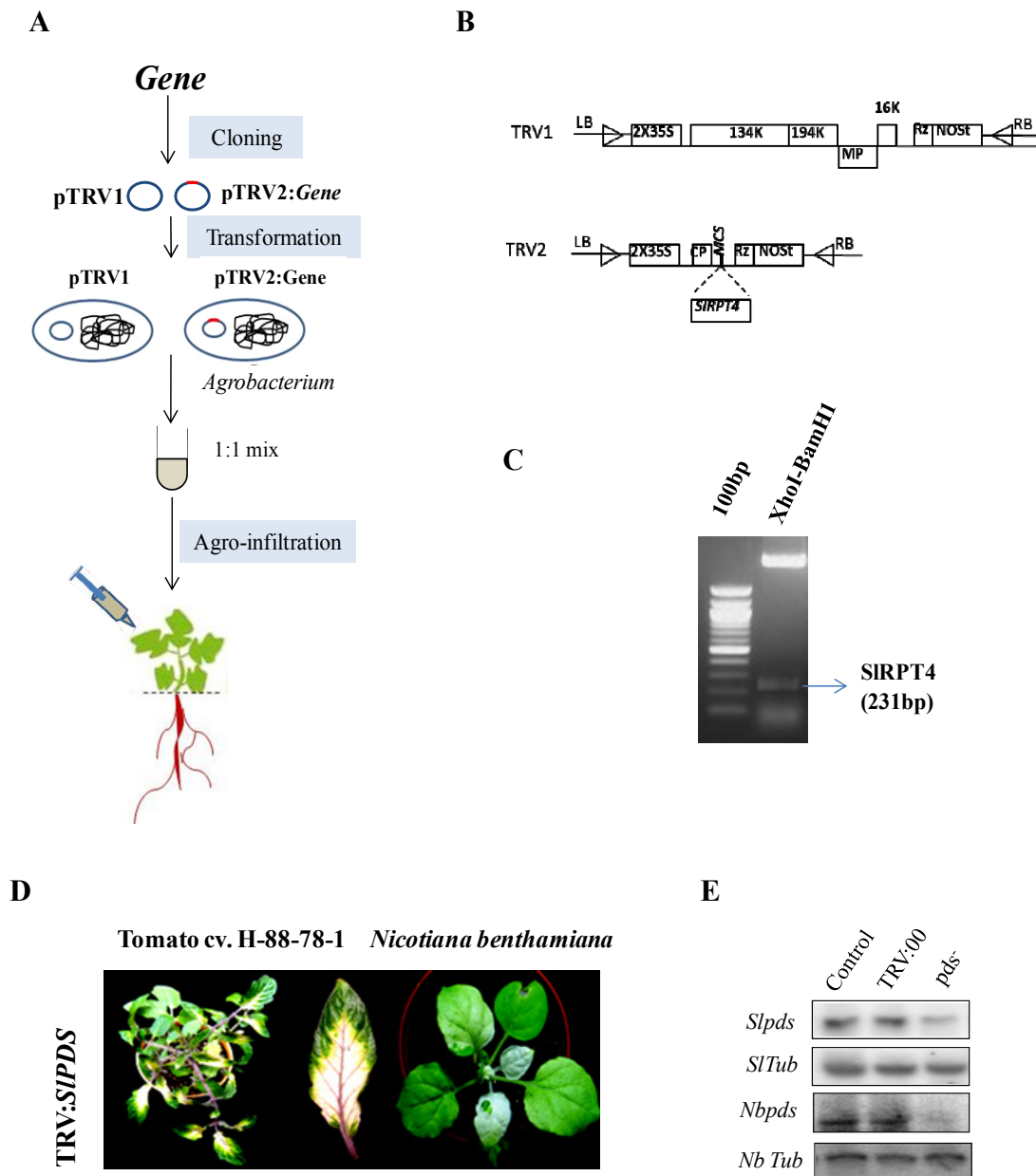


Fig. 4.18. TRV-based VIGS in tomato and *Nicotiana benthamiana*. **A**, Strategy for VIGS in tomato. **B**, Vector map of TRV-VIGS. **C**, Picture of agarose gel showing restriction digested product of pTRV2:SIRPT4 construct. **D**, Phenotypes of *SIPDS*-silenced tomato and *N. benthamiana* plants at 21 day post-silencing. **E**, RNA blot analysis to evaluate the relative level of *pds* gene in control, vector-infiltrated (TRV:00) and *pds*⁻ plants. *Tubulin* from tomato and *Nicotiana* was used as an internal control.

4.2.5 Silencing reduced *SIRPT4* accumulation upon virus infection

Silencing of *SIRPT4* was performed through the agro-infiltration of constructs at two-leaf stage in tomato cv. H-88-78-1. To assess the infectivity of virus in the silenced plant, ToLCNDV stem-node inoculation was performed subsequent to the silencing experiment. Non-silenced tolerant cv. H-88-78-1 infiltrated with ToLCNDV (H^T) at two-leaf stage was used as an experimental control. Upon ToLCNDV infection, level of *SIRPT4* was found to be up-regulated by >4 folds in H^T plants at 21 days (Fig. 4.19A, B). This result was in agreement with our previous observation where enhanced expression of *SIRPT4* was identified upon ToLCNDV inoculation in cv. H-88-78-1 at 21 dpi (Sahu et al., 2010). In this study, RNA blot analysis showed that >4 folds reduction in the level of *SIRPT4* transcript accumulation in silenced cv. H-88-78-1 ($H^{SIRPT4+T}$) at 21 dpi (Fig. 4.19A, B).

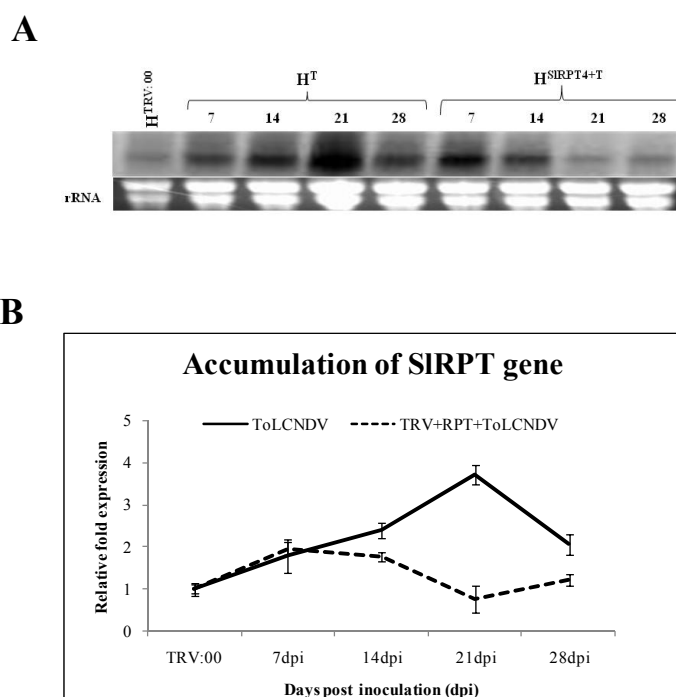


Fig. 4.19. Accumulation of *SIRPT4* in ToLCNDV-infected cv. H-88-78-1 (H^T) and *SIRPT4*-silenced cv. H-88-78-1-infected with ToLCNDV ($H^{SIRPT4+T}$). **A**, Northern blot analysis to examine the expression of *SIRPT4* transcript. **B**, Relative accumulation of *SIRPT4* in the experimental samples. Cultivar H-88-78-1 infiltrated with TRV:00 vector was used as negative control. Bars show standard deviations (\pm SD). EtBr-stained rRNA is shown as the equivalent loading control for the experiment.

Results

4.2.6 Silencing of *SIRPT4* increases ToLCNDV induced symptom severity

A detailed study was performed to evaluate how *SIRPT4* silencing affects the plant upon ToLCNDV infection in cv. H-88-78-1. Samples were named as H^{TRV:00} (vector-infiltrated cv. H-88-78-1; Mock), H^{TRV:SIRPT4} (*SIRPT4*-silenced), H^{TRV:00+T} (mock-inoculated with ToLCNDV), H^{TRV:SIRPT4+T} (*SIRPT4*-silenced and ToLCNDV-infected cv. H-88-78-1) and H^T (ToLCNDV-infected cv. H-88-78-1). Infectivity scoring was performed at 21 dpi (Table 4.3; Fig. 4.20A-M; Fig. 4.21).

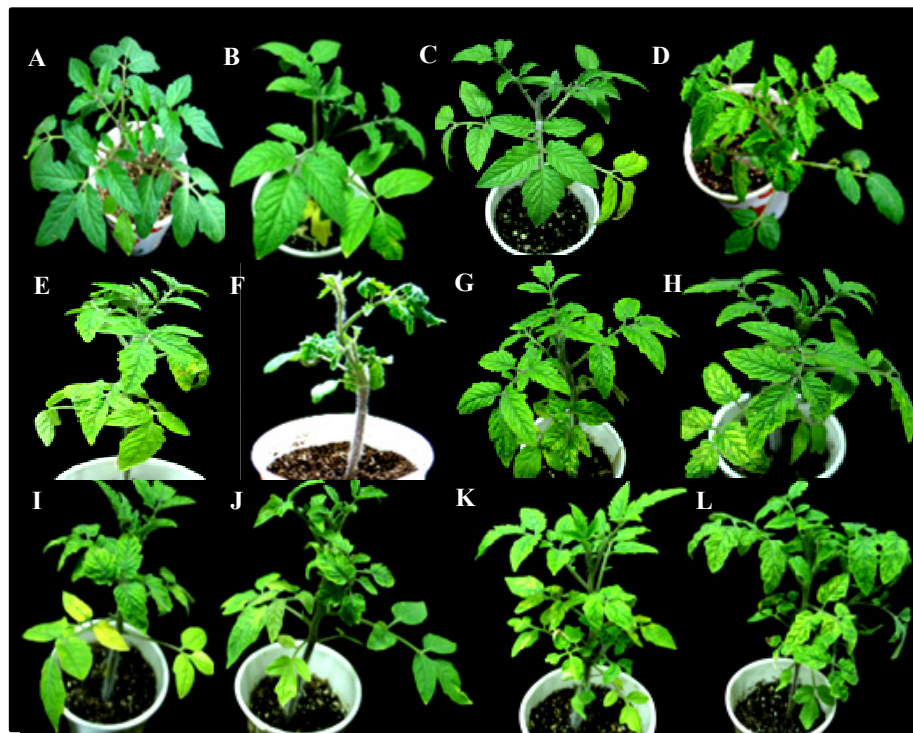
Table 4.3. Infectivity scoring of *Tomato leaf curl New Delhi virus*-inoculated control, mock and *SIRPT4*-silenced plant.

Plant	Plant infected/ inoculated	Severe symptom appearance	Symptom severity ^a	Overall grade ^b
H-88-78-1 (H ^T)	5/75	14	+	T
Mock (H ^{TRV:00+T})	7/75	13	+	T
SIRPT4-silenced (H ^{TRV:SIRPT4+T})	51/75	7	++++	HS
Mock (H ^{TRV:00})	-	-	-	-
SIRPT4-silenced (H ^{TRV:SIRPT4})	-	-	-	-

Infectivity indexing was done on systemic leaves of experimental plants at 21 dpi, following the protocol described by Sahu et al. (2010). Briefly, a) +, Least severe; ++, moderately severe; +++, severe; +++++, highly severe. b) T, Tolerant (1-20%); MT, Moderate tolerant (20.1-40%); S, Susceptible (40.1-60%); HS, Highly susceptible (60.1-100%). ‘-’ represents non-ToLCNDV-infected samples.

In the non-ToLCNDV infection, no phenotypic difference was evidenced upon silencing of *SIRPT4* (H^{TRV:SIRPT4}) and plants appeared similar to H^{TRV:00} (mock)-infiltrated plants (Fig. 4.20B, C). Severe symptom of infection (leaf curling) started to appear in H^T at 14 dpi (Fig. 4.20F, Fig. 4.21) whereas the symptom initiated within 7 dpi in H^{TRV:SIRPT4+T} (Fig. 4.20I, Fig. 4.21). Recovery from the ToLCNDV symptom started in systemic leaves 14 dpi onwards and at 21 dpi leaf-curling symptom was diminished in upper systemic leaves of ToLCNDV-infected mock (H^{TRV:00+T}) plants (Fig. 4.20D, Fig. 4.21). However, in H^{TRV:SIRPT4+T} plants, no evidence of symptom remission was detected at 21 dpi (Fig. 4.20K, M and Fig. 4.21). Symptom severity in terms of stunted growth, leaf curling and yellowing was highest in the H^{TRV:SIRPT4+T}

(Fig. 4.21). Interestingly, ~ 70% of *SIRPT4*-silenced plants showed the severe leaf curling symptom at 21 dpi (Table 4.3).



M

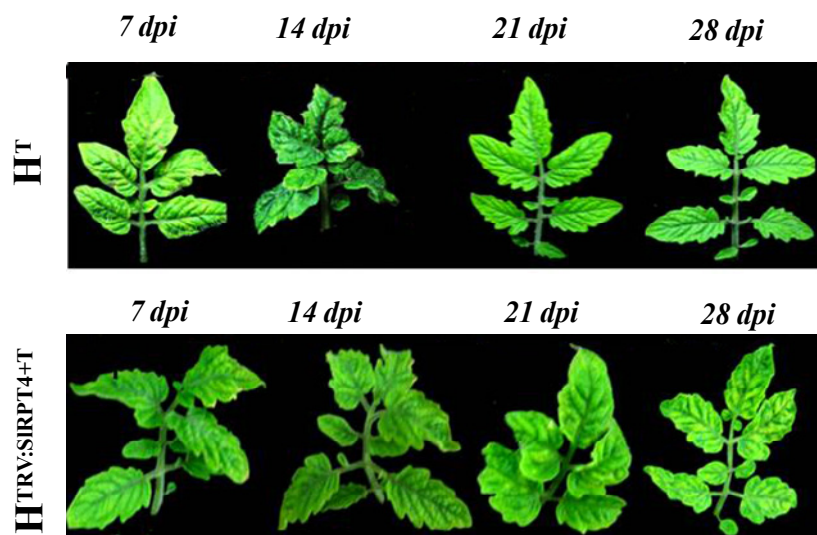


Fig. 4.20. Phenotypes of cv. H-88-78-1. **A**, Control; **B**, Mock ($H^{TRV:00}$); **C**, *SIRPT4*-silenced ($H^{TRV:SIRPT4}$); **D**, Mock-infected ($H^{TRV:00+T}$). ToLCNDV-infected cv. H-88-78-1 (H^T) at 7 dpi, **E**; 14 dpi, **F**; 21dpi, **G** and 28 dpi, **H**. Symptom progression in $H^{TRV:SIRPT4+T}$ (ToLCNDV-infected *SIRPT4*-silenced cv. H-88-78-1) at 7 dpi, **I**; 14 dpi, **J**; 21 dpi, **K** and 28 dpi, **L**. **M**, Comparison of leaf curl symptom progression between H^T and *SIRPT*-silenced cv. H-88-78-1 ($H^{TRV:SIRPT4+T}$).



Fig. 4.21. Phenotypes of mock and *SIRPT4*-silenced cv. H-88-78-1 at 21 days post ToLCNDV infection. Symptom remission was detected in $H^{TRV:00+T}$ at 21 dpi. $H^{TRV:00+T}$, mock plant infected with ToLCNDV; $H^{TRV:SIRPT4+T}$, *SIRPT4*-silenced plant infected with ToLCNDV, UL, upper leaf; LL, lower leaf.

4.2.7 Silencing of *SIRPT4* enhances ToLCNDV-specific viral DNA accumulation

Assessment of viral DNA accumulation in all the experimental plants was done through Southern blot analysis, to correlate the symptom phenotype with the level of viral titre in the respective samples. It was observed that viral DNA-A-specific accumulation at 21 and 28 dpi was significantly higher ($P < 0.01$ and < 0.001 , respectively) in the *SIRPT4*-silenced plant ($H^{TRV:SIRPT4+T}$), in contrast to the H^T plant which showed significantly ($P < 0.001$) lower accumulation (~20%) at 21 dpi and 28 dpi (Fig. 4.22A, B). Vector inoculation ($H^{TRV:00+T}$) did not affect the accumulation of viral DNA-A, as no visible difference in DNA-A accumulation was evident between H^T and $H^{TRV:00+T}$ at 21 dpi. This suggests that the TRV-VIGS vector inoculation does not alter the tolerant attribute of cv. H-88-78-1.

Level of DNA-B component was also examined in the ToLCNDV-infected samples at 21 dpi, which suggested that upon *SIRPT4* silencing, level of DNA-B accumulation was significantly ($P < 0.001$) enhanced in $H^{TRV:SIRPT4+T}$ during ToLCNDV infection (Fig. 4.22C, D). Hence, silencing of *SIRPT4* resulted in enhanced accumulation of both DNA-A and DNA-B, which suggests the plausible contribution of *SIRPT4* in providing defense against ToLCNDV.

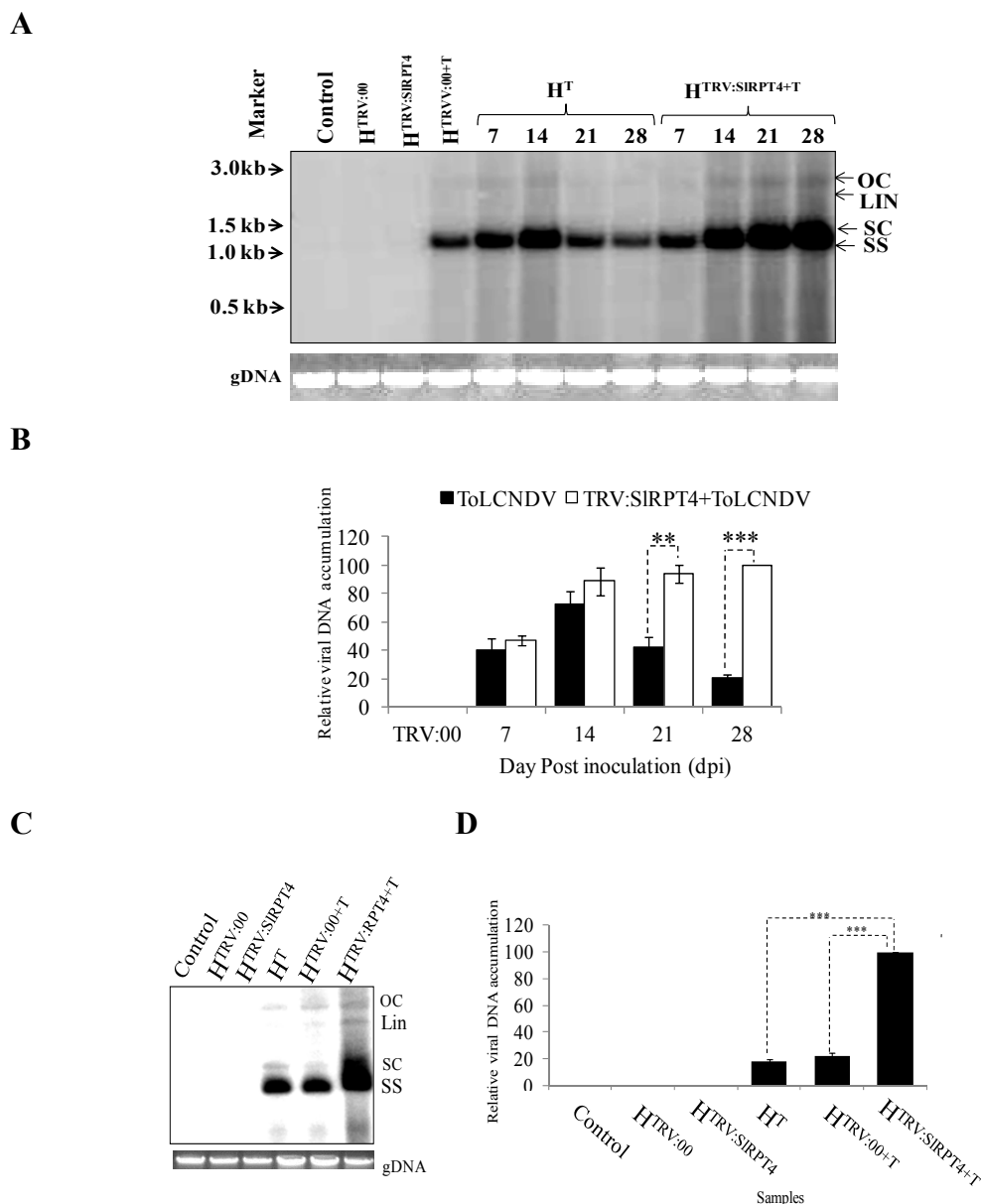


Fig. 4.22. Detection of ToLCNDV genomic components. **A**, Level of DNA-A accumulation in samples of control (non-ToLCNDV-infected cv. H-88-78-1), H^T (ToLCNDV- infected cv. H-88-78-1) and H^{TRV:SIRPT4+T} (*SIRPT4*-silenced H-88-78-1 infected with ToLCNDV) at 7-28 dpi. Total genomic DNA isolated from the respective experimental plants was hybridized with CP gene specific probe. Replicative forms of virus are illustrated as open circular (OC), linear (Lin), supercoiled (SC) and single strand (SS). TRV:00-infiltrated H-88-78-1 was taken as a mock control. **B**, Relative accumulation of DNA-A in H^T and H^{SIRPT4+T} at different time points. **C**, Level of DNA-B accumulation in control, mock, *SIRPT4*-silenced, H^T, H^{TRV:00+T} and H^{TRV:SIRPT4+T} samples at 21 dpi. DNA was hybridized with BC1 gene-specific probe. **D**, Relative accumulation of DNA-B in the experimental plant samples. EtBr stained DNA is provided as equivalent loading control. Data represents means \pm SD of three independent experiments; **, $P < 0.01$; ***, $P < 0.001$.

4.2.8 Transient overexpression of *SIRPT4* leads to the activation of HR and programmed cell death in tomato

In planta transient overexpression of *SIRPT4* was performed to examine the involvement of this gene in the activation of HR. Fully expanded leaves of cv. Punjab Chuahhara were agro-infiltrated either with overexpression construct of *SIRPT4* (PC^{SIRPT4}), and ToLCNDV (PC^T), or mixed culture of ToLCNDV and overexpression construct *SIRPT4* ($PC^{SIRPT4+T}$). *Agrobacterium* harbouring pCAMBIA1302 vector was infiltrated as a vector control (PC^V). It was observed that upon overexpression of *SIRPT4* (PC^{SIRPT4}), corresponding leaves had relatively more HR-specific symptom appearance in comparison to PC^V (Fig. 4.23A). However, these symptoms were also noticeable in PC^T and $PC^{SIRPT4+T}$ leaves (Fig. 4.23A).

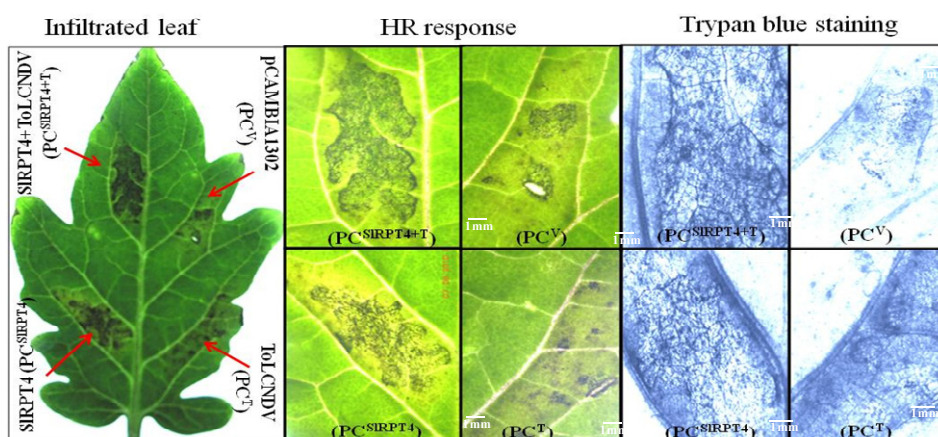


Fig. 4.23. *Agrobacterium*-mediated transient overexpression of *SIRPT4*. Punjab Chuhara leaves were agro-infiltrated with *SIRPT4* overexpression construct (PC^{SIRPT4}), pCAMBIA1302 vector (PC^V), mixed culture of *SIRPT4* overexpression construct and ToLCNDV construct ($PC^{SIRPT4+T}$), and ToLCNDV construct alone (PC^T). Leaves were stained with trypan blue to confirm the cell death.

Further, trypan blue staining showed typical cell death appearance in PC^{SIRPT4} and $PC^{SIRPT4+T}$ samples (Fig. 4.23). Nevertheless, PC^V also indicated some cell death which may be a consequence of the infiltration-associated compatible interaction with *Agrobacterium* harbouring virulent construct. This suggests that the cell death appearing in PC^{SIRPT4} and $PC^{SIRPT4+T}$ -infiltrated leaves is specific to *SIRPT4* gene causing cell death.

4.2.9 Transient overexpression of *SIRPT4* modulates caspase-like protease activity

Participation of certain caspase-like proteases in regulating the cell death process in plants have been documented in diverse pathogenic as well as non-pathogenic responses (Mlejnek and Prochazka, 2002; Xu and Zhang, 2009). Therefore, synthetic fluorogenic substrates LEHD-AFC and DEVD-AFC were used, which can be specifically cleaved by caspase-9-like and caspase-3-like proteases, respectively. As compared to the control samples (PC^V), there was >5 folds induction in relative activities of caspase-9 and caspase-3 proteases in PC^{SIRPT4} (Fig. 4.24A, B). On the other hand, $PC^{SIRPT4+T}$ showed relatively lower accumulation of caspase 9- and caspase 3-like activity in comparison to the PC^{SIRPT4} (Fig. 4.24A, B). Over all, these results suggest that overexpression of *SIRPT4* may lead to PCD in plant cell.

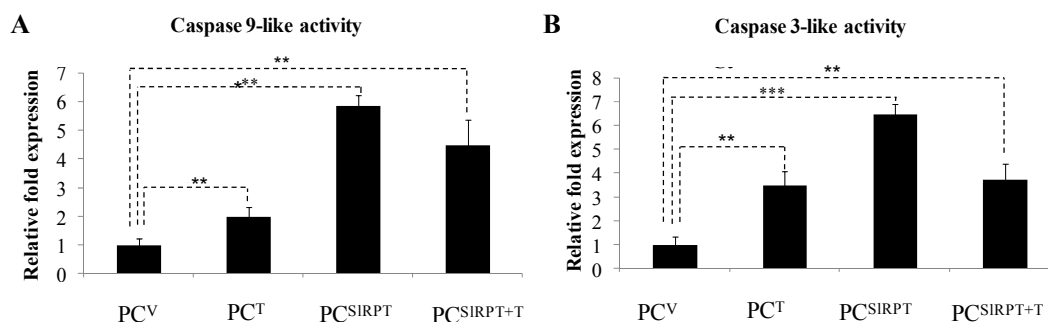


Fig. 4.24. Level of caspase like activity upon transient overexpression of *SIRPT4*. Estimation of caspase 9-like activity **A**; and caspase 3-like activity, **B**, in the extracts of leaves samples agro-infiltrated with (Control, PC^V ; ToLCNDV, PC^T ; *SIRPT4*, PC^{SIRPT4} and *SIRPT4*+ToLCNDV, $PC^{SIRPT4+T}$). Samples were incubated with peptide substrates corresponding to caspase-9- and caspase-3-like proteases i.e., LEHD-AFC and DEVD-AFC, respectively. Relative fluorescence was calculated and enzymatic activities were normalized for protein concentration.

4.2.10 Silencing of *SIRPT4* decreases ToLCNDV-specific viral DNA accumulation

Viral DNA accumulation was also studied, in the corresponding tissues of cv. Punjab Chhuhara through Southern blot analysis. Leaf samples from PC^V , PC^{SIRPT4} , PC^T , $PC^{SIRPT4+T}$ and PC^{V+T} were harvested after 3 dpi and subjected to DNA isolation. It was observed that relative level of viral DNA-A accumulation was significantly ($P < 0.001$) higher in the samples corresponding to PC^T than in $PC^{SIRPT4+T}$ (Fig. 4.25A,

Results

B). This suggests that upon *SIRPT4* overexpression, multiplication of ToLCNDV and its relative accumulation may get reduced probably due to the activation of HR/PCD.

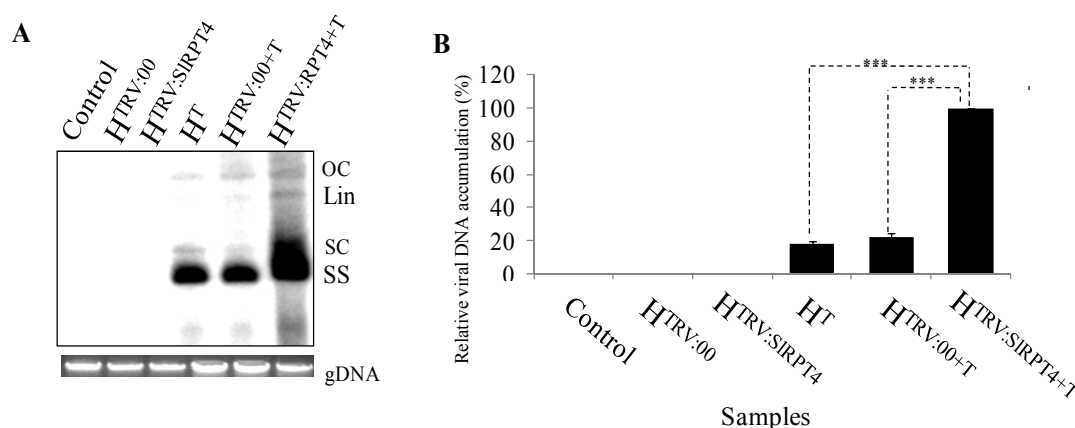


Fig. 4.25. Accumulation of viral DNA in *SIRPT4*-overexpressed tomato cv. Punjab Chhuhara. **A**, Southern blot of total genomic DNA isolated from Control (PC^V), ToLCNDV-infiltrated Punjab Chhuhara (PC^T), *SIRPT4*-infiltrated Punjab Chhuhara (PC^{SIRPT4}), *SIRPT4*+ToLCNDV co-infiltrated ($PC^{SIRPT4+T}$) and vector+ToLCNDV co-infiltrated samples (PC^{V+T}). Blots were hybridized with ToLCNDV coat protein gene specific probe. **B**, Relative accumulation of viral DNA in different treatments. Each experiment was repeated thrice and means \pm SD of these independent experiments, are illustrated in the figure. Sign *** denotes level of significance $P < 0.001$.

4.2.11 Involvement of reactive oxygen species (ROS) in hypersensitive response

The activity of antioxidant enzymes such as ascorbate peroxidase (APX) and catalase (CAT) were calculated to examine the generation of ROS in all the experimental tissues. It was observed that *SIRPT4* overexpression with (PC^{SIRPT4}) or without ($PC^{SIRPT4+T}$) ToLCNDV-infection caused a significant ($P < 0.01$) reduction in the APX specific activity in comparison to control sample (PC^V) (Fig. 4.26A). On the other hand, level of CAT was found to be the significantly ($P < 0.01$) higher in both ToLCNDV- infiltrated leaves (PC^T) and $PC^{SIRPT4+T}$ in comparison to control sample infiltrated with only vector (Fig. 4.26B). Interestingly, tissues from PC^{SIRPT4} have no significant change in the specific activity of CAT, in respect of PC^V tissues (Fig. 4.26B).

Membrane damage and HR was evaluated through Lipid peroxidation (LP) assay to test the membrane integrity. It was found that the level of Malondialdehyde (MDA) increased significantly ($P < 0.001$) in PC^{SIRPT4} than the control PC^V (Fig. 4.26C). It was also significantly ($P < 0.01$) higher in ToLCNDV-infiltrated leaves as compared to PC^V . Interestingly, MDA level reduced significantly ($P < 0.01$) in $PC^{SIRPT4+T}$ sample in comparison to $SIRPT4$ overexpressed tissues (PC^{SIRPT4}) (Fig. 4.26C).

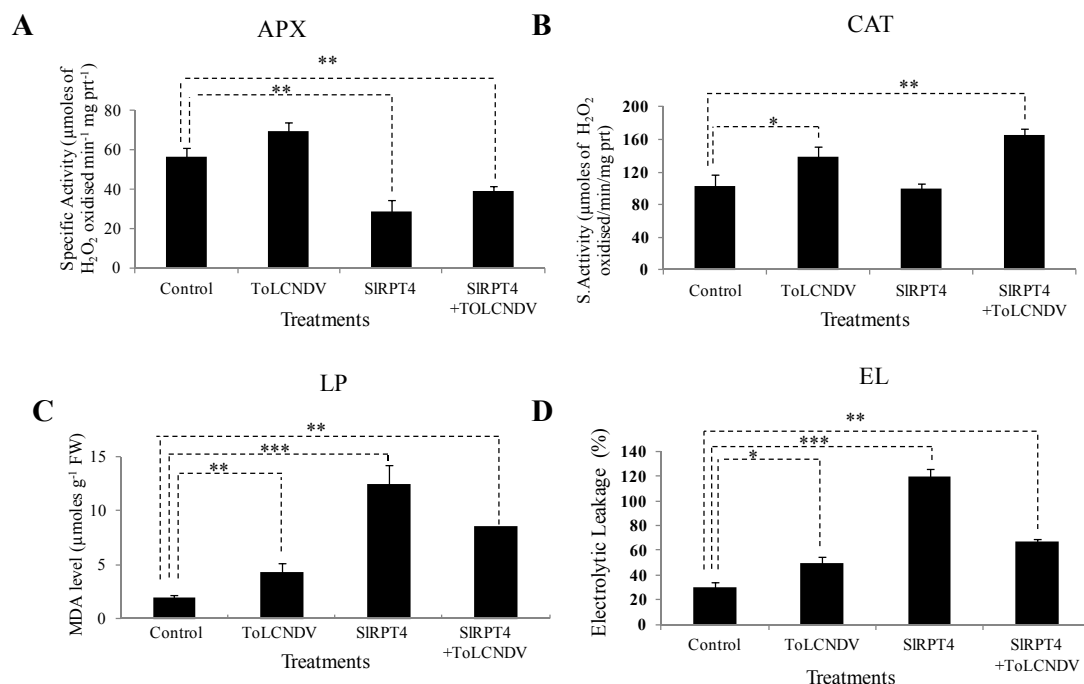


Fig. 4.26. Measurement of antioxidant enzyme activity. **A**, Specific activity of APX was calculated as 1 μmol of ascorbate oxidized per min. **B**, Specific activity of CAT was calculated as 1 μmol H₂O₂ oxidized per min. **C**, Levels of lipid peroxidation expressed in terms of MDA concentration. **D**, Percentage electrolytic leakage. Data showing the means ± SD of three independent experiments. Sign denotes *, $P < 0.05$; **, $P < 0.01$; ***, $P < 0.001$. Control, PC^V ; ToLCNDV, PC^T ; SIRPT4, PC^{SIRPT4} and SIRPT4+ToLCNDV, $PC^{SIRPT4+T}$.

For further validation, electrolytic leakage (EL) was measured. It was observed that PC^{SIRPT4} showed significantly ($P < 0.01$) higher level of ion-leakage than the PC^V (Fig. 4.26D). Moreover, ToLCNDV-infiltration (PC^T) slightly increased the rate of EL, which may apparently be due to cultivar-specific response against the ToLCNDV. Hence, these results suggest that there is a correlation between *SIRPT4* overexpression and alteration of antioxidant enzyme mechanism, leading to the cell death.

Results

Antioxidant enzyme activities in *SIRPT4*-silenced cv. H-88-78-1 ($H^{TRV: SIRPT4}$), was also measured. There was a significant increase ($P < 0.05$) in the specific activity of APX in $H^{TRV: SIRPT4}$ in comparison to $H^{TRV:00}$ (Fig. 4.27A). Interestingly, non-significant alteration in the specific activity of CAT, level of MDA (LP) and relative ion leakage (EL) was observed in between these samples (Fig. 4.27B-D).

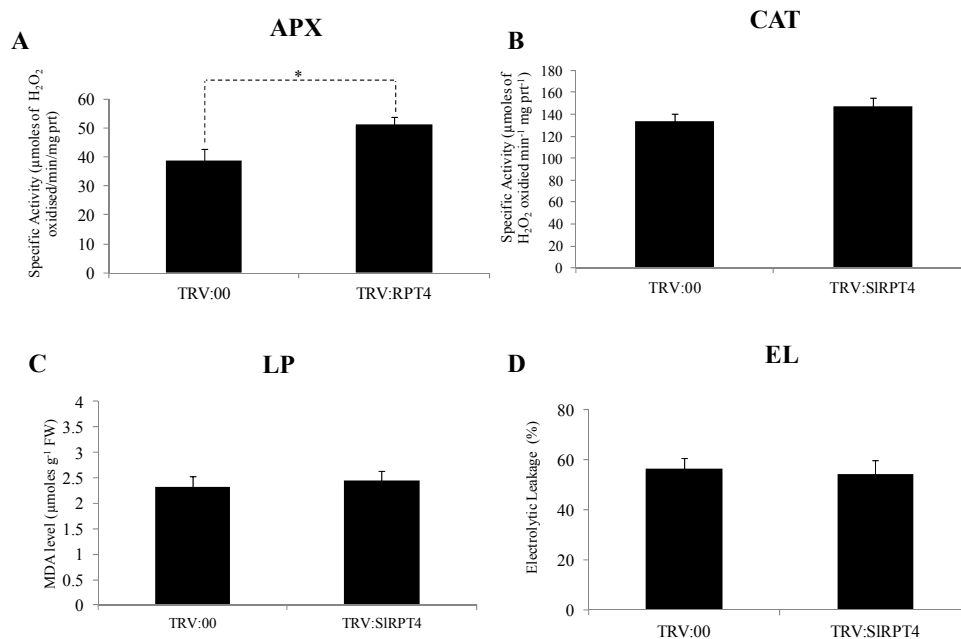


Fig. 4.27. Assessment of antioxidant enzyme activity in cv. H-88-78-1. **A**, Specific activity of APX was calculated as 1 μmol of ascorbate oxidized per min. **B**, Specific activity of CAT was evaluated as 1 μmol H_2O_2 oxidized per min. **C**, Level of LP accumulated in terms of MDA concentration. **D**, Electrolytic leakage (%). Data illustrates means \pm SD of 3 independent experiments. Sign denotes, *, $P < 0.05$; **, $P < 0.01$; ***, $P < 0.001$. Mock, TRV:00-infiltrated cv. H-88-78-1; TRV:SIRPT4; *SIRPT4*-silenced cv. H-88-78-1.

Chapter 5: Discussion

All organisms have extremely selective proteolytic systems for removal and degradation of atypical and unnecessary intracellular proteins (Vierstra, 1996; Hershko and Ciechanover, 1998). The 26SP, a multi-subunit complex, has the ATP-dependent proteolytic function, which is required for the degradation of ubiquitinated intracellular proteins. Information on the significance of 26SP subunits in autonomously targeting various physiological and morphological pathway components are increasingly evident (Sadanandom et al., 2012; Yu et al., 2015; Yu et al., 2016). Studies on mutants corresponding to 26SP subunit revealed that proteolytic defect lead to physiological abnormalities in Arabidopsis. This study further advocated the necessity for reassessing the role of each 26SP subunit.

The complex is composed of two relatively stable sub-particles, the 20S proteasome, a hollow cylindrical structure which contains the proteolytic active sites in its lumen, and the 19S regulatory particle (RP) which binds to either end of the cylinder and provides ATP-dependence and specificity for ubiquitinated proteins. RP is comprised of six subunits (RPT 1-6; RPT for RP Triple A-ATPases) which are members of ATPases belonging to the AAA superfamily (ATPases Associated with various cellular Activities) (Dubiel et al., 1992; Glickman et al., 1998).

Although, the exact function(s) of RPTs in protein degradation are still unestablished, their implication in several apparently unrelated biological processes such as control of cell cycle, modulation of gene expression, regulation of viral infection and interaction with receptor proteins have been highlighted in previous studies (Nelbock et al., 1990; Swafield et al., 1992; Ghislain et al., 1993; Gordon et al., 1993, vom Bauer et al., 1996). Most reports on functions of RPT4 are recognized in yeast cells, such as, in the dislocation of endoplasmic reticulum-associated degradation substrates (Lipson et al., 2008). However, only a handful of information is presented in plants, suggesting either the proteolytic or non-proteolytic functions of RPT4 proteins (Han et al., 2008). Involvement of rice RPT4 protein in facilitating the root morphology through its interaction with a rice root architecture associated1 (RAA1) was reported by Han et al, (2008). However, neither the proteolytic nor the non-proteolytic functions of SIRPT4 have been documented in regulating the defense response against geminivirus. Keeping above in view, along with previous observation of differential expression of SIRPT4 gene in a naturally tolerant cultivar of tomato namely H-88-78-

Discussion

1, (Sahu et al., 2010), functional characterization of SIRPT4 was undertaken to identify its role in ToLCNDV tolerance.

In silico analysis showed that *SIRPT4* encodes a 399 amino-acid protein which conserved in regards to the domain/motifs present within the protein. These highly conserved domains are structurally similar to the members of P-loop NTPase domain superfamily. This superfamily has two major structural categories: the KG (kinase-GTPase) class which includes Ras-like GTPases and additional strand catalytic E (ASCE). RPT4s belong to the ASCE class which also includes proteins belonging to ATPase Binding Cassette (ABC), DExD/H-like helicases, 4Fe-4S iron sulphur, RecA-like F1-ATPases proteins (Frickey and Lupas, 2004). SIRPT4 has a typical 168-amino-acid AAA cassette which is necessary among Walker-type ATPases (Beyer, 1997). The Walker A and B motifs have been shown to bind the beta-gamma phosphate moiety of ATP or GTP and Mg^{2+} ions, respectively (Hanson and Whiteheart, 2005). SIRPT4 contains the consensus Walker P loop/motif A (GXXXXGKS/T) and motif B (4 hydrophobic hhhhD/E) which are involved in ATP hydrolysis. SIRPT4 also possesses a predicted coiled coil motif of 28-53 residues along with the C-terminal RNA/DNA helicases, similar to the other RPTs of Arabidopsis (Fu et al., 1999). Knowledge of the 3D structure of a protein is a necessary prerequisite for understanding its molecular function. Overall, 3D structure of SIRPT4 revealed that it is structurally similar to a putative hydrolase, namely proteasome component PRE3 (PDB code 4cr2J) protein from *Saccharomyces cerevisiae*. This PRE3 protein is essential for the peptidyl-glutamyl-peptide-hydrolyzing activity of proteasome (Enenkel et al., 1994). Hence, it may be predicted that the active involvement of SIRPT4 in 26SP mediated degradation pathways.

Biological annotation of SIRPT4 protein revealed its resemblance to Vacuolar protein sorting-associated protein 4B (PDB-ID, 2zan) which has 16 predicted ATP binding sites. This protein has been shown to regulate biosynthetic membrane proteins transport from endosomal compartment to the vacuole (Babst et al., 1997, 1998). Hence, based on the domain architecture and its 3D structure, it might be predicted that the SIRPT4 may have the ability to bind with ATP, along with its involvement in the endosomal transport related functions.

AAA proteins are one of the largest families of proteins and various attempts have been made to phylogenetically analyse the members of this family (Beyer, 1997; Frohlich, 2001). Due to the large number of members, various approaches have been applied, based on the number of protein sequences analyzed and the presence of one or more AAA domains. From these, a plausibly steady representation has emerged comprising five main clades of AAA domains, which are D1 (AAA), D2 (two AAA domains), proteasome subunits, metalloproteases, and a meiotic group comprising katanins, spastins, and MSP1 (Frickey and Lupas, 2004). This group of proteins participate in diverse functions including membrane fusion, proteolysis, DNA replication and alteration of the state of DNA-protein complexes in a eukaryotic cell (Ogura and Wilkinson, 2001). Present analysis was also in agreement with these cluster analyses in previous studies, which revealed the close relation of SIRPT4 protein with proteasome subunits, metalloproteases, domains D1 and D2 of ATPases with two AAA domains, and the meiotic group. This suggests the possible role of SIRPT4 in the cellular functions associated with membrane fusion, proteolysis and DNA replication.

The *cis*-regulatory element analysis revealed the presence of several putative transcription binding sites and conserved *cis*-acting regulatory elements. Presence of various stress-responsive elements such as, dehydrin and heat shock factors (HSF) as well as few hormone linked elements like the ethylene-responsive transcription factor (ERF) and ethylene insensitive 3 (EIN3) were found in the promoter sequence. Presence of these elements implies that SIRPT4 may be involved in various stress response pathways involving a hormone signaling cross-talk. In addition to the above, promotor of SIRPT4 was also rich in the light responsive elements which suggest possible involvement of this protein in the physiological processes of tomato. Moreover, presence of Myb-related, bHLH, NAC/NAM, HD-ZIP, C₂H₂ and WRKY specific elements in its promoter provides an overview that SIRPT4 may be a frequent target of such transcription factors. NAC1 transcription factor has previously been reported to be involved in enhancing the *Tomato leaf curl virus* (TLCV) DNA accumulation (Selth et al., 2005). Overall, it showed that the SIRPT4 expression is controlled by various factors which either regulate normal physiological response or a stress-specific reaction.

Discussion

Tissue-specific and hormone-induced expression of *SIRPT4* gene was examined. It was found that the upper leaves, flower and red fruit have highest expression of this gene, which indicates that it may have specific functions in the development of corresponding tissues. Plant hormones are the controller of almost every physiological process including development, stress adaptation and defense signaling. Among them, ethylene (ET), jasmonates (JA) and salicylic acid (SA) play pivotal roles in plant disease and pest resistance (Munné-Bosch and Müller, 2013). Although involvement of *RPT4* in regulation of these pathways is not yet clear, other subunits of 26S proteasome have been found to be regulated or involved in the regulation of physiological and developmental response. For example, *26SP-RPN1a* was found to be differentially expressed by GA (gibberellin) and CK (cytokinin) application and plays an essential role in trichome development (Yu et al., 2015). Hence, the hormone induced expression of *SIRPT4* was analysed. Highest expression of *SIRPT4* in ET-treated leaves may be due to the availability of ET specific *cis* elements i.e., ERF and EIN3. An ET-inducible signaling network employs transcription factors such as EIN and ERF (Guo and Ecker, 2004). In broad-spectrum, ethylene directs diverse cellular and physiological processes, during plant-pathogen interaction (Broekaert et al., 2006). Moreover, its involvement in the PCD regulation is also highlighted during in plant-pathogen interactions (Bouchez et al., 2007). Hence, presence of ET responsive elements and observed enhancement of *SIRPT4* transcript upon ET treatment signify that activation of *SIRPT4* during ToLCNDV infection may be regulated by ET and associated factors.

Structural and phylogenetic analysis of *SIRPT4* protein established that it has a conserved AAA domain which may have the ability to bind and hydrolyze ATP. Hence, evaluation of ATP hydrolyzing activity of *SIRPT4* protein was conducted. AAA proteins accomplish diverse functions in the cell such as disassembling complexes, unfolding or unwinding macromolecules, and transportation of cellular proteins (Maurizi et al., 2010). This process needs a chemo-mechanical modulator which obtains its energy through ATP hydrolysis. Majority of AAA domain proteins can hydrolyze ATP in order to generate a conserved conformational change in their structure (Santos et al., 2006). In this process, an activated water molecule attacks the γ -phosphate of ATP, shifting the molecule into a transition state that is stabilized by positively charged ion such as Mg^{2+} . Consequently the γ -phosphate is eliminated from

the ATP. This analysis also revealed that the SIRPT4 protein has the ability to hydrolyze $\gamma\text{P}^{32}\text{ATP}$ in a concentration dependent manner.

In order to investigate the cellular functions of SIRPT4, probable interacting proteins of SIRPT4 was identified by pull-down assay. It was revealed that this protein has 16 probable interacting partners acting in diverse biological, cellular and molecular functions. These proteins have diverse structural domains, suggesting their involvement in multifaceted function. For example, SIRPT4 could interact with proteins associated with disease resistance (NBS-LRR, resistance protein) and signaling molecules (B-cell receptor-associated protein, signal transducer, activator of transcription B, serine-threonine protein kinase). These results suggest that SIRPT4 may be an important component of the disease signaling mechanism. Interestingly, majority of proteins identified in this study were novel in terms of their binding with SIRPT4 protein, thus providing the first report suggesting the possible participation of SIRPT4 in disease resistance. Although, probable interaction between SIRPT4 and NBS-LRR protein is not yet reported, direct involvement of another RPT i.e., *atRPT2* in Arabidopsis, with CC-NBS-LRR protein induced signaling pathways, has been highlighted (Chung and Tasaka, 2011). Results obtained in this study also revealed the interaction of SIRPT4 with various proteins functioning in metabolic pathways. For example, aldehyde dehydrogenase-dependent, glucan synthase like 3 and serine acetyltransferase which may be the target proteins for degradation process mediated by 26SP.

SIRPT4 interaction with the two proteins, i.e., signal transducer and activator of transcription B (STAT-B) and B-cell receptor associated protein 31 (BAP31) was particularly fascinating. This was because functions of these proteins are well established in animal system but their specific functions are yet to be identified in plants. For example, STAT-B is a member of STAT protein family which are intracellular mobile transcription factors, regulating cellular immunity, proliferation, apoptosis and differentiation in animal cells (Jiang et al., 2009; Seo et al., 2016). Hence, interaction between SIRPT4 and STAT-B protein might exert similar function in plant cells infected with ToLCNDV. However, detailed studies on the plausible role of this interaction need to be performed. B-cell receptor associated protein 31 (BAP31) is predicted to be involved in the export of secreted proteins from the endoplasmic reticulum to the plasma membrane. Further, *BAP31* expression was

Discussion

found to alter during oxidative stress in Arabidopsis (Baxter et al., 2007). RPT4 has been shown to help in the dislocation of endoplasmic reticulum-associated degradation (ERAD) substrates in yeast cell (Lipson et al., 2008), however interaction between SIRPT4 and BAP31 is not yet reported. Characterization of the protein-protein interaction through BiFC assay also confirms that these proteins interact in the cytoplasm. This provides a novel insight into proteasome mediated export of cellular proteins from ER to the plasma membrane, which might be linked with cellular transport of the geminivirus protein.

DDI1 links the 19SP and polyubiquitinated proteins through UBA domain interaction with ubiquitin for the successive degradation and required for S-phase checkpoint control of cell cycle (Kaplun et al., 2005; Diaz-Martinez et al., 2006). Upon geminivirus infection cells exhibit reprogramming of cell cycle (Hanley-Bowdoin et al., 2013). During this process, UBA domain containing proteins such as Rad23 and DDI1 play an important role in regulating cell cycle which in turn allows commencement of anaphase and chromosome maintenance in yeast (Bertolaet et al., 2002). The hydrophobic surface on the UBA domain has been predicted to be a protein-protein interaction site, apart from its characteristic ubiquitin binding action (Bertolaet et al., 2002). By demonstrating that DDI1 and SIRRT4 interact within the cytoplasm through BiFC assay, it may be hypothesized that UBA domains helps in this, which may in turn regulate the cell division process during geminivirus interaction.

Till date, none of the subunits of 26SP have been characterized for their role in defense against geminivirus. However, various non-proteolytic functions of 26SPs, such as RNase activity, were highlighted previously during plant-RNA virus interaction (Pouch et al., 1995; Petit et al., 1997; Ballut et al., 2003). For example, $\alpha 5$ subunit of Arabidopsis has the capacity to degrade TMV and *Lettuce mosaic virus* (LMV)-derived RNAs *in vitro* (Dielen et al., 2011). Although this represents the plant-specific defense response, viruses do exert specialized proteins which can interact and modulate the 20SP components catalytic activities. In this regard, HcPro of *Potato virus Y* (PVY) has been shown to inhibit Arabidopsis $\alpha 1$, $\beta 2$ and $\beta 5$ subunits function and alter the RNase activity causing susceptibility against RNA viruses (Sahana et al., 2012). Hence, these represent an excellent example of the battle between the plant and virus.

Till date, contribution of SIRPT4 in regulating tomato-geminivirus interaction has not been documented. Present study provides a first report of possible mechanism of SIRPT4-mediated regulation of defense against geminivirus. For initial examination, the DNA binding ability of SIRPT4 was evaluated through EMSA assay. For this, three region corresponding to DNA-A-IR, DNA-B-IR and Rep gene regions were selected as probes. Protein-DNA complexes were only observed in SIRPT4-DNA-A-IR and SIRPT4-DNA-B-IR but absent when Rep fragment was used as a probe. This suggests that SIRPT4 may have the DNA-binding ability specifically to IR which contains characteristic stem-loop structure. Previous reports suggest that N-terminal AAA+ ATPase domain of some proteins have DNA binding ability (He et al., 2008; Rizvi et al., 2016). For example, the N-terminal AAA+ ATPase domain of archaeal Orc1/Cdc6 protein has the DNA binding activity which is involved in origin recognition during DNA replication initiation (He et al., 2008). In another study, MCM4 a subunit of Minichromosome maintenance (MCM) complex was found to possess single-stranded DNA binding property of the MCM4/6/7 complex (You et al. 1999, 2002). This signifies the importance of N-terminal-AAA-ATPase domain in the SIRPT4 in binding to DNA.

The IR, present in both genomes of ToLCNDV, acts as a promoter from which viral genes are derived in both the viral and complementary sense. This RNA polymerase II-type promoter is essential for the bidirectional expression of viral genes. It was revealed that binding of SIRPT4 on IR may inhibit the binding of SIRNA PolIII, which in turn regulates the ToLCNDV genome transcription. A strong association between reduction in the expression of *Rep*- and *CP*-specific transcripts and binding of SIRPT4 onto IR of ToLCNDV was established. Therefore, it can be hypothesized that SIRPT4 has a DNA binding activity which subsequently inhibits the transcription of viral ORFs. It is more interesting that SIRPT4 does not have nuclear localization signal (NLS), and both the transcription and replication of viral genome are nucleus associated events. The possible explanation could be that 26SP complex is found within the nucleus as well as cytoplasm, although precise mechanism of their transport is still unclear (Fu et al., 1999; Enenkel, 2014a). Out of six RPTs, only RPT2a has a NLS (Fu et al., 1999; Enenkel, 2014b), suggesting an NLS independent mechanism of SIRPT4 transport into the nucleus. More interestingly, pull-down analysis revealed that the SIRPT4 could bind to RAN binding protein 3 (RanBP3) in

Discussion

the cytoplasm. This protein has been shown to play an important role in nuclear export during influenza A virus infection (Predicala and Zhou, 2013). Hence, it might be possible that during ToLCNDV infection, binding of SIRPT4 with RanBP3 may assist in SIRPT4 transport into the nucleus.

VIGS study reveals direct evidence that inhibition of *SIRPT4* may transform the tolerant attributes of cultivar H-88-78-1 into susceptibility. It was found that *SIRPT4* silencing increases symptom severity and diminishes the symptom remission phenotype of cultivar H-88-78-1 during ToLCNDV inoculation. Increased viral titre corresponding to DNA-A and DNA-B upon SIRPT4 silencing may be due to consequential effect of *SIRPT4* silencing, which may have restricted the binding of this protein onto IR and affected the transcription and ensuing reduction in the viral DNA accumulation. Therefore, loss of *SIRPT4* function assists in viral genome replication, thereby enhancing the viral infection and multiplication.

Numerous reports are available revealing the importance of 26S proteasome subunits in providing defense against pathogens (Becker et al., 2000; Suty et al., 2003; Takizawa et al., 2005). Both repression as well as activation of proteasome function has been directly or indirectly correlated with the PCD in plants (Jin et al., 2006; Lee et al., 2006; Vacca et al., 2007). Differential expression of 26SP subunit RPN7 during TMV infection in hot pepper was linked with the activation of PCD (Lee et al., 2006). Apart from the plants, reports congregated from animal systems also suggest that the proteasome mediated initiation or inhibition of PCD depends on the cell type and cellular environment (Grimm and Osborne, 1999). Such facts undoubtedly endorse that the subunits of 26SP have a complex role in PCD and specific role of all subunits needs to be investigated further. Transient overexpression of *SIRPT4* in ToLCNDV sensitive tomato cultivar revealed that affected cells exhibited characteristic features of HR and cell death, thereby restricting the ToLCNDV spread and infection. Proteasome-mediated cell death pathway was associated with caspase-9- and caspase-3-like activity. The elevated activity of caspase-like enzymes possibly correlates with PCD. This may be the localized response at the site of pathogen attack exhibiting PCD in specific manner for preventing the spread of pathogens (Mur et al., 2008). Thus, *SIRPT4* mediated activation of HR leads to PCD which consecutively hampers the virus multiplication and sequential transmission from the infected cells. Hence, SIRPT4a may have a generic response in directing ROS-mediated PCD

(as ToLCNDV is established as a non-necrotic virus). Other observations also support that SIRPT4 is crucial for PCD, for example, presence of ethylene responsive *cis*-elements suggest possible regulation of SIRPT4 through ethylene, which act as a major factor of hormone induced PCD during in plant-pathogen interactions (Bouchez et al., 2007). Moreover, interaction of SIRPT4 protein with the apoptosis regulating protein STAT-B protein provides a further line of evidence.

Reactive oxygen species (ROS) act as positive regulators of HR and activate plant defences (Bindschedler et al., 2006; Choi et al., 2007). Reduced ROS scavenging system activities may contribute to higher ROS congregation leading to enhanced HR and defense against pathogens (Dat et al., 2003; Mittler et al., 2004; Sahu et al., 2012b). CAT and APX participate in encountering excess ROS, hence their down-regulation enriches ROS levels leading to cell death (Klessig et al., 2000; Yang et al., 2004). Examination of APX/CAT activity showed a significant decrease in *SIRPT4*-overexpressing susceptible cultivar, PC^{SIRPT4}. ROS can also generate cellular membrane lipid derivatives, for example malondialdehyde, affecting cell viability (Montillet et al., 2005). Reduced cellular viability could limit the pathogens spread and assist in the establishment of defense against pathogen (Torres, 2010). Enhanced levels of relative ion leakage and MDA upon *SIRPT4* transient expression indicated the possible function of this gene in regulating cell viability. Hence, it suggests that the altered response of these biochemical markers may lead to the activation of defense signaling during ToLCNDV infection in tomato.

Overall present study provides substantial evidence for the novel non-proteolytic function of a tomato 26S proteasome subunit, SIRPT4. Presence of AAA domain and active ATPase domain revealed its multifunctional properties; however, functional validation of ATP hydrolysis during the course of ToLCNDV infection in tomato requires more effort to unravel the precise mechanism of defense. Viral DNA binding properties of SIRPT4 provided a novel feature of bi-directional transcription regulation leading to reduced level of corresponding viral genes. Moreover, involvement of SIRPT4 in restricting viral spread through the activation of HR and PCD contributed in the inhibition of ToLCNDV pathogenesis and progression. Nevertheless, exact mechanism of cell death by the SIRPT4 needs to be explored further. A detailed functional study of *SIRPT4* and its promoter will help to uncover the *cis*-acting elements to determine the pathway of *SIRPT4* expression. Protein-

Discussion

protein interaction study identified novel interacting partners, which provides an insight into the unexplored function of SIRPT4 regulating linked with cellular transport, cell cycle, signaling process and metabolic activity. Most of the interactions were novel and thus need further characterization in regard to the geminivirus defense. Furthermore, a comprehensive study is required to decipher the mechanism of SIRPT4 transport into the nucleus and interaction with nuclear pore complex protein, RanBP3 during ToLCNDV infection. Silencing of this proteasomal subunit transformed the naturally tolerant cultivar of tomato into the susceptible; hence stable transgenic lines in tomato could be expected to provide resistance against ToLCNDV. Efforts are being made to initiate the generation of stable transgenic lines overexpressing *SIRPT4* in tomato. Moreover, this study will also motivate plant biologists and virologists to explore the autonomous function of the other UPS components for improved understanding of plant-pathogen interactions.

Chapter 6: Summary

During the last decade there has been a significant accrual of information on the proteins of the ubiquitin/proteasome system and their enormous function in plant development and stress response. Functional studies have revealed that these proteins function either in a complex or autonomously to regulate the degradation of diverse proteins. The intricacy and active nature of 26S proteasome components is still unestablished and one of the foremost confront of the immediate future is to decipher how the individually each subunit function is regulated.

In this regard, for the first time, attempt was made to functionally characterize the 26S proteasome subunit SIRPT4, which was found to be differentially expressed upon ToLCNDV infection in a naturally tolerant cv. H-88-78-1. The key conclusions of the study are summarized below:

1. *SIRPT4* encoded a 399 amino-acid protein which is conserved in regard to the AAA-ATPase domain present within the protein.
2. Genome-wide identification of AAA domain of tomato revealed presence of 684 AAA domain containing proteins. SIRPT4 protein belonged to the proteasome subunits (26SP) clad and is closely related to metalloproteases, domains D1 and D2 of ATPases with two AAA domains, and the meiotic group. This shows evidence of the possible role of SIRPT4 in the cellular functions such as membrane fusion, proteolysis and DNA replication.
3. SIRPT4 contained the consensus Walker P loop/motif A (GXXXXGKS/T) and motif B (4 hydrophobic hhhhD/E) which are involved in ATP hydrolysis.
4. Tissue-specific expression of SIRPT4 genes revealed that this gene was highly expressed in upper leaves, flower and red fruit, indicating its role in developmental processes, especially leaf and fruit maturation.
5. The *cis*-regulatory element analysis revealed the presence of various stress-responsive elements such as, dehydrin and heat shock factors (HSF) as well as some hormone linked elements like the ethylene-responsive transcription factor (ERF) and ethylene insensitive 3 (EIN3).
6. Expression of SIRPT4 gene was enhanced in response to foliar spray of phytohormones such as SA, MeJA and ET.

Summary

7. SIRPT4 was successfully expressed in the *E. coli*. A SIRPT4-GST fusion protein of ~69kDa was purified. This protein was used for further downstream analysis.
8. SIRPT4 protein had the ability to hydrolyze $\gamma\text{P}^{32}\text{ATP}$ in a concentration dependent manner.
9. Pull-down assay identified 16 putative target proteins of SIRPT4 from ToLCNDV-infected tomato cv. H-88-78-1. Most of them were novel putative targets. Gene ontology analysis revealed that these putative targets participate in diverse biological processes and molecular functions.
10. Two of the novel putative targets SIBCL31 and SIDDI1 interacted with SIRPT4 the cytoplasmic region.
11. For the first time present study revealed the novel DNA binding property of SIRPT4. SIRPT4 protein had the affinity towards the stem-loop region present in the IR of both DNA-A and DNA-B genome of ToLCNDV.
12. Binding of SIRPT4 on IR inhibited the subsequent binding of SIRNA PolIII, which in turn altered the ToLCNDV genome transcription.
13. A strong correlation was demonstrated between the binding of SIRPT4 onto IR of ToLCNDV and reduction in expression of virion-sense and complementary-sense specific genes accumulation.
14. *Tobacco rattle virus*-based VIGS directly evidenced that inhibition of *SIRPT4* may transform the tolerant attribute of cultivar H-88-78-1 into susceptibility. Symptom remission phenotype of a naturally tolerant cultivar H-88-78-1 was diminished upon SIRPT4 silencing, suggesting the possible role of this gene in pathogenesis and symptom emergence.
15. Transient overexpression of *SIRPT4* in ToLCNDV sensitive tomato cultivar revealed that affected cells exhibited characteristic features of HR and cell death, thereby restricting the ToLCNDV spread and infection.
16. The elevated activity of caspase-3- and caspase-9-like enzymes was identified in the leaves transiently expressing SIRPT4 gene. This suggest that the enhanced expression of SIRPT4 gene upon ToLCNDV infection may assist in

the activation of caspase-like enzyme activity to establish the PCD in the virus infected tissues thereby preventing the spread of pathogens.

17. Reduced ROS scavenging system such as APX and CAT activities was found to be linked with higher ROS generation leading to enhanced HR, upon transient expression of *SIRPT4*.
18. Increased levels of the lipid derivatives such as MDA along with the increased relative ion leakage upon *SIRPT4* transient expression indicated the promising role of this gene in regulating cell viability.

References

- Acquaah G. (2002). Horticulture: Principles and Practices. New Jersey: Prentice Hall.
- Aebi HE. (1983). Catalase. In: Bergmeyer HU, Bergmeyer J, GraBL M, eds. Methods of enzymatic analysis. Verlag Chemie, Weinheim, pp. 273-286.
- Altschul SF, Gish W, Miller W, Myers EW and Lipman DJ. (1990). Basic local alignment search tool. *J Mol Biol.* 215:403-410.
- Amari K, Gonzalez-Ibeas D, Gómez P, Sempere RN, Sanchez-Pina MA, Aranda MA, et al. (2008). Tomato torrado virus is transmitted by *Bemisia tabaci* and infects pepper and eggplant in addition to tomato. *Plant Dis.* 92:1139.
- Anbinder I, Reuveni M, Azari R, Paran I, Nahon S, Shlomo H, et al. (2009). Molecular dissection of Tomato leaf curl virus resistance in tomato line TY172 derived from *Solanum peruvianum*. *Theor Appl Genet.* 119:519-530.
- Anderson PK, Cunningham AA, Patel NG, Morales FJ, Epstein PR and Daszak P. (2004). Emerging infectious diseases of plants: pathogen pollution, climate change and agrotechnology drivers. *Trends Ecol Evol.* 19:535-544.
- Arguello-Astorga GR, Guevara-Gonzalez RG, Herrera-Estrella LR and Rivera-Bustamante RF. (1994). Geminivirus replication origins have a group-specific organization of iterative elements: a model for replication. *Virology.* 203:90-100.
- Arie T, Takahashi H, Kodama M and Teraoka T. (2007). Tomato as a model plant for plant-pathogen interactions. *Plant Biotechnol.* 24:135-147.
- Ascencio-Ibáñez JT, Sozzani R, Lee TJ, Chu TM, Wolfinger RD, Cella R, et al. (2008). Global analysis of Arabidopsis gene expression uncovers a complex array of changes impacting pathogen response and cell cycle during geminivirus infection. *Plant Physiol.* 148:436-454.
- Atkinson NJ and Urwin PE. (2012). The interaction of plant biotic and abiotic stresses: from genes to the field. *J Exp Bot.* 63:3523-3543.
- Babst M, Sato TK, Banta LM and Emr SD. (1997). Endosomal transport function in yeast requires a novel AAA-type ATPase, Vps4p. *EMBO J.* 16:1820-1831.
- Babst M, Wendland B, Estepa EJ and Emr SD. (1998). The Vps4p AAA ATPase regulates membrane association of a Vps protein complex required for normal endosome function. *EMBO J.* 17:2982-2993.
- Bagewadi B, Chen S, Lal SK, Choudhury NR and Mukherjee SK. (2004). PCNA interacts with Indian mung bean yellow mosaic virus rep and downregulates Rep activity. *J Virol.* 78:11890-11903.
- Ballut L, Petit F, Mouzeyar S, Le Gall O, Candresse T, Schmid P, et al. (2003). Biochemical identification of proteasome-associated endonuclease activity in sunflower. *Biochimica et Biophysica Acta.* 1645:30-39.
- Baltes NJ, Hummel AW, Konecna E, Cegan R, Bruns AN, Bisaro DM, et al. (2015). Conferring resistance to geminiviruses with the CRISPR–Cas prokaryotic immune system. *Nature Plant.* 1:15145.
- Baxter CJ, Redestig H, Schauer N, Repsilber D, Patil KR, Nielsen J, et al. (2007). The metabolic response of heterotrophic Arabidopsis cells to oxidative stress. *Plant Physiol.* 143:312-325.
- Becker J, Kempf R, Jeblick W and Kauss H. (2000). Induction of competence for elicitation of defense responses in cucumber hypocotyls requires proteasome activity. *Plant J.* 21:311-316.

References

- Bertolaet BL, Clarke DJ, Wolff M, Watson MH, Henze M, Divita G, et al. (2002). UBA domains of DNA damage-inducible proteins interact with ubiquitin. *Nat Struct Biol.* 8:417-422.
- Beyer A. (1997). Abstract sequence analysis of the AAA protein family. *Protein Sci.* 6:2043-2058.
- Bindschedler LV, Dewdney J, Blee KA, Stone JM, Asai T, Plotnikov J, et al. (2006). Peroxidase-dependent apoplastic oxidative burst in Arabidopsis required for pathogen resistance. *Plant J.* 47:851-863.
- Bisaro DM. (1996). Geminivirus DNA Replication. Cold Spring Harbor Laboratory Press. 9:833-854.
- Bivalkar-Mehla S, Vakharia J, Mehla R, Abreha M, Kanwar JR, Tikoo A, et al. (2011). Viral RNA silencing suppressors (RSS): Novel strategy of viruses to ablate the host RNA interference (RNAi) defense system. *Virus Res.* 155:1-9.
- Böttcher B, Unseld S, Ceulemans H, Russell RB and Jeske H. (2004). Geminate structures of African cassava mosaic virus. *J Virol.* 78:6758-6765.
- Bouchez O, Huard C, Lorrain S, Roby D and Balagué C. (2007). Ethylene is one of the key elements for cell death and defense response control in the Arabidopsis lesion mimic mutant vad1. *Plant Physiol.* 145:465-477.
- Boulton MI, Pallaghy CK, Chatani M, MacFarlane S and Davies JW. (1993). Replication of maize streak virus mutants in maize protoplasts: evidence for a movement protein. *Virology.* 192:85-93.
- Boulton MI, Steinkellner H, Donson J, Markham PG, King DI and Davies JW. (1989). Mutational analysis of the virion-sense genes of maize streak virus. *J Gen Virol.* 70:2309-2323.
- Bowyer JW, Atherton JG, Teakle DS and Ahern GA. (1969). Mycoplasma-like bodies in plants affected by legume little leaf, tomato big bud, and lucerne witches' broom diseases. *Aus J Biol Sci.* 22:271-274.
- Bradford MM. (1976). A rapid and sensitive method for quantitation of microgram quantities of protein utilizing the principle of roteindye binding. *Anal Biochem.* 72:248-254.
- Breckle CW. (1991). Growth under heavy metals. In: Waisel Y, Eshel A, and Kafkafi U, eds. *Plant roots: the hidden half.* Marcel Dekker, New York, USA, pp. 351-373.
- Briddon RW, Bull SE, Amin I, Idris A M, Mansoor S, Bedford ID, et al. (2003). Diversity of DNA β , a satellite molecule associated with some monopartite begomoviruses. *Virology.* 312:106-121.
- Briddon RW, Pinner MS, Stanley J, and Markham PG. (1990). Geminivirus coat protein gene replacement alters insect specificity. *Virology.* 177:85-94.
- Broekaert WF, Delauré SL, De Bolle MF, Cammue BP. (2006). The role of ethylene in host-pathogen interactions. *Annu Rev Phytopathol.* 44:393-416.
- Bruce G, Gu M, Shi N, Liu Y and Hong Y. (2011). Influence of retinoblastoma-related gene silencing on the initiation of DNA replication by African cassava mosaic virus Rep in cells of mature leaves in *Nicotiana benthamiana* plants. *Virol J.* 8:561.
- Castillo AG, Collinet D, Deret S, Kashoggi A and Bejarano ER. (2003). Dual interaction of plant PCNA with geminivirus replication accessory protein (Ren) and viral replication protein (Rep). *Virology.* 312:381-394.
- Chakraborty S, Pandey PK, Banerjee MK, Kalloo G and Fauquet CM. (2003). Tomato leaf curl Gujarat virus, a new Begomovirus species causing a severe leaf curl disease of tomato in Varanasi, India. *Phytopathol.* 93:1485-1495.

- Chakraborty S. (2008). Tomato leaf curl viruses from India (*Geminiviridae*). In: Mahy BWJ and Van Regenmortel MHV, eds. Encyclopedia of Virology. Oxford, Elsevier. pp. 124-133.
- Chapman EJ and Carrington JC. (2007). Specialization and evolution of endogenous small RNA pathways. *Nat Rev Genet.* 8:884-896.
- Chatchawankanphanich O, Chiang BT, Green SK, Singh SJ and Maxwell DP. (1993). Nucleotide sequence of a geminivirus associated with tomato leaf curl from India. *Plant Dis.* 77:1168.
- Chatchawankanphanich O, Chiang BT, Green SK, Singh SJ and Maxwell DP. (1995). Tomato leaf curl virus strain Bangalore, India isolate. GenBank accession U38239.
- Choi HW, Kim YJ, Lee SC, Hong JK and Hwang BK. (2007). Hydrogen peroxide generation by the pepper extracellular peroxidase CaPO₂ activates local and systemic cell death and defense response to bacterial pathogens. *Plant Physiol.* 145:890-904.
- Choudhury NR, Malik PS, Singh DK, Islam MN, Kaliappan K and Mukherjee SK. (2006). The oligomeric Rep protein of Mungbean yellow mosaic India virus (MYMIV) is a likely replicative helicase. *Nucl Acids Res.* 34:6362-6377.
- Chow CN, Zheng HQ, Wu NY, Chien CH, Huang HD, Lee TY, et al. (2016). PlantPAN 2.0: an update of plant promoter analysis navigator for reconstructing transcriptional regulatory networks in plants. *Nucl Acids Res.* 44:D1154-D1160.
- Chowda-Reddy RV, Achenjang F, Felton C, Etarock MT, Anangfac MT, Nugent P, Fondong VN. (2008). Role of a geminivirus AV2 protein putative protein kinase C motif on subcellular localization and pathogenicity. *Virus Res.* 135:115-124.
- Chung K and Tasaka M. (2011). RPT2a, a 26S proteasome AAA-ATPase, is directly involved in Arabidopsis CC-NBS-LRR protein uni-ID-induced signaling pathways. *Plant Cell Physiol.* 52:1657-1664.
- Citovsky V, Zaltsman A, Kozlovsky SV, Gafni Y and Krichevsky A. (2009). Proteasomal degradation in plant-pathogen interactions. *Semin Cell Dev Biol.* 20:1048-1054.
- Collazo C, Ramos PL, Chacon O, Borroto CJ, Lopez Y, Pujol M, et al. (2006). Phenotypical and molecular characterization of the Tomato mottle Taino virus- Nicotiana megalosiphon interaction. *Physiol Mol Plant Pathol.* 67:231-236.
- Cox S. (2000). I Say Tomayto, You Say Tomahto (<http://lamar.colostate.edu/~samcox/Tomato.html>).
- Craig A, Ewan R, Mesmar J, Gudipati V and Sadanandom A. (2009). E3 ubiquitin ligases and plant innate immunity. *J Exp Bot.* 60:1123-1132.
- Dahan J, Etienne P, Petitot AS, Houot V, Blein JP and Suty L. (2001). Cryptogein affects expression of alpha3, alpha6 and beta1 20S proteasome subunits encoding genes in tobacco. *J Exp Bot.* 52:1947-1948.
- Dat JF, Pellinen R, Beeckman T, Van De Cotte B, Langebartels C, et al. (2003). Changes in hydrogen peroxide homeostasis trigger an active cell death process in tobacco. *Plant J.* 33:621-632.
- Delaney TP, Uknes S, Vernooij B, Friedrich L, Weymann K, Negrotto D, et al. (1994). A central role of salicylic acid in plant disease resistance. *Science.* 266:1247-1250.
- Diaz-Martinez LA, Kang Y, Walters KJ and Clarke DJ. (2006). Yeast UBL-UBA proteins have partially redundant functions in cell cycle control. *Cell Div.* 1:28.
- Dielen AS, Badaoui S, Candresse T and German-Retana S. (2010). The ubiquitin/26S proteasome system in plant-pathogen interactions: a never-ending hide-and-peek game. *Mol Plant Pathol.* 11:293-308.

References

- Dielen AS, Sasaki FT, Walter J, Michon T, Ménard G, Pagny G, et al. (2011). The 20S proteasome $\alpha 5$ subunit of *Arabidopsis thaliana* carries an RNase activity and interacts *in planta* with the lettuce mosaic potyvirus HcPro protein. *Mol Plant Pathol.* 12:137-150.
- Dionisio-Sese ML and Tobita S. (1998). Antioxidative responses of rice seedlings to salinity stress. *Plant Sci.* 135:1-9.
- Djebali W, Gallusci P, Polge C, Boulila L, Galtier N, Raymond P, et al. (2008). Modifications in endopeptidase and 20S proteasome expression and activities in cadmium treated tomato (*Solanum lycopersicum* L.) plants. *Planta.* 227:625-639.
- Dong J, Wu F-B, and Zhang GP. (2005). Effect of cadmium on growth and photosynthesis of tomato seedlings. *J Zhejiang Univ Sci B.* 6:974-980.
- Dreher K and Callis J. (2007). Ubiquitin, hormones and biotic stress in plants. *Ann Bot.* 99:787-822.
- Dry IB, Krake LR, Rigden JE and Rezaian MA. (1997). A novel subviral agent associated with a geminivirus: the first report of a DNA satellite. *Proc Natl Acad Sci USA.* 94:7088-7093.
- Dubiel W, Ferrell K, Pratt G and Rechsteiner M. (1992). Subunit 4 of the 26S protease is a member of a novel eukaryotic ATPase family. *J Biol Chem.* 267:22699-22702.
- Eini O, Dogra S, Selth LA, Dry IB, Randles JW and Rezaian MA. (2009). Interaction with a host ubiquitin-conjugating enzyme is required for the pathogenicity of a geminiviral DNA beta satellite. *Mol Plant Microbe Interact.* 22:737-746.
- Enenkel C, Lehmann H, Kipper J, Gueckel R, Hilt W and Wolf DH. (1994). PRE3, highly homologous to the human major histocompatibility complex-linked LMP2 (RING12) gene, codes for a yeast proteasome subunit necessary for the peptidylglutamyl-peptide hydrolyzing activity. *FEBS Lett.* 341:193-196.
- Enenkel C. (2014a). Proteasome dynamics. *Biochimica et Biophysica Acta.* 1843:39-46.
- Enenkel C. (2014b). Nuclear Transport of Yeast Proteasomes. *Biomolecules.* 4:940-955.
- Eybishtz A, Peretz Y, Sade D, Akad F and Czosnek H. (2009). Silencing of a single gene in tomato plants resistant to Tomato yellow leaf curl virus renders them susceptible to the virus. *Plant Mol Biol.* 71:157-171.
- Eybishtz A, Peretz Y, Sade D, Gorovits R and Czosnek H. (2010). Tomato yellow leaf curl virus infection of a resistant tomato line with a silenced sucrose transporter gene LeHT1 results in inhibition of growth, enhanced virus spread, and necrosis. *Planta.* 231:537-548.
- Ezhkova E and Tansey WP. (2004). Proteasomal ATPases link ubiquitylation of histone H2B to methylation of histone H3. *Mol Cell.* 13:435-442.
- FAO 2013. FAOSTAT database collections. Food and Agriculture Organization of the United Nations. Rome. Access date: 2016-04-23. (<http://faostat.fao.org>)
- Fauquet CM, Briddon RW, Brown JK, Moriones E, Stanley J, Zerbini M, et al. (2008). Geminivirus strain demarcation and nomenclature. *Arch Virol.* 153:783-821.
- Felix G, Duran JD, Volko S and Boller T. (1999). Plants have a sensitive perception system for the most conserved domain of bacterial flagellin. *Plant J.* 18:265-276.
- Fiallo-Olivé E, Martínez-Zubiaur Y, Moriones E and Navas-Castillo J. (2012). A novel class of DNA satellites associated with New World begomoviruses. *Virology.* 426:1-6.
- Finn RD, Clements J and Eddy SR. (2011). HMMER web server: interactive sequence similarity searching. *Nucl Acids Res.* 39:W29-W37.

- Fondong VN, Reddy RV, Lu C, Hankoua B, Felton C, Czymbek K, et al. (2007). The consensus N-myristoylation motif of a geminivirus AC4 protein is required for membrane binding and pathogenicity. *Mol Plant Microbe Interact.* 20:380-391.
- Fontes EP, Eagle PA, Sipe PS, Luckow VA and Hanley-Bowdoin L. (1994a). Interaction between a geminivirus replication protein and origin DNA is essential for viral replication. *J Biol Chem.* 269:8459-8465.
- Fontes EP, Gladfelter HJ, Schaffer RL, Petty IT and Hanley-Bowdoin L. (1994b). Geminivirus replication origins have a modular organization. *Plant Cell.* 6:405-416.
- Forzani C, Lobréaux S, Mari S, Briat JF and Lebrun M. (2002). Metal resistance in yeast mediated by the expression of a maize 20S proteasome alpha subunit. *Gene.* 293:199-204.
- Frickey T and Lupas AN. (2004). Phylogenetic analysis of AAA proteins. *J Struct Biol.* 146:2-10.
- Frischmuth T and Stanley J. (1991). African cassava mosaic virus DI DNA interferes with the replication of both genomic components. *Virology.* 183:539-544.
- Frohlich KU. (2001). An AAA family tree. *J Cell Sci.* 114:1601-1602.
- Fu H, Doelling JH, Rubin DM and Vierstra RD. (1999). Structural and functional analysis of the six regulatory particle triple-A ATPase subunits from the Arabidopsis 26S proteasome. *Plant J.* 18:529-539.
- Gafni Y and Epel BL. (2002). The role of host and viral proteins in intra- and inter-cellular trafficking of geminiviruses. *Physiol Mol Plant Pathol.* 60:231-241.
- Ghislain M, Udvardy A and Mann C. (1993). *S. cerevisiae* 26S protease mutants arrest cell division in G2/metaphase. *Nature.* 366:358-362.
- Glickman MH, Rubin DM, Fried VA and Finley D. (1998). The regulatory particle of the *Saccharomyces cerevisiae* proteasome. *Mol Cell Biol.* 18:3149-3162.
- Goodstein DM, Shu S, Howson R, Neupane R, Hayes RD, Fazo J, et al. (2012). Phytozome: a comparative platform for green plant genomics. *Nucleic Acids Res.* 40:D1178-86.
- Gordon C, McGurk G, Dillon P, Rosen C and Hastie ND. (1993). Defective mitosis due to a mutation in the gene for a fusion yeast 26S protease subunit. *Nature.* 366:355-357.
- Goritschnig S, Zhang Y and Li X. (2007). The ubiquitin pathway is required for innate immunity in Arabidopsis. *Plant J.* 49:540-551.
- Green SK. (1991). Guidelines for diagnostic work in plant Virology. *AVRDC Tech Bull.* 15:63.
- Grimm LM and Osborne BA. (1999). Apoptosis and the proteasome. *Results Probl Cell Differ.* 23:209-228.
- Guo H and Ecker JR. (2004). The ethylene signaling pathway: new insights. *Curr Opin Plant Biol.* 7:40-49.
- Gutierrez C. (2000). DNA replication and cell cycle in plants: learning from geminiviruses. *EMBO J.* 19:792-799.
- Han JJ, Lin W, Oda Y, Cui KM, Fukuda H and He XQ. (2012). The proteasome is responsible for caspase-3-like activity during xylem development. *Plant J.* 72:129-141.
- Han Y, Cao H, Jiang J, Xu Y, Du J, Wang X, et al. (2008). Rice ROOT ARCHITECTURE ASSOCIATED1 binds the proteasome subunit RPT4 and is degraded in a D-box and proteasome-dependent manner. *Plant Physiol.* 148:843-855.

References

- Hanahan D. (1983). Studies on transformation of *Escherichia coli* with plasmids. *J Mol Biol.* 166:557-580.
- Hanley-Bowdoin L, Bejarano ER, Robertson D, Mansoor S. (2013). Geminiviruses: masters at redirecting and reprogramming plant processes. *Nat Rev Microbiol.* 11:777-788.
- Hanley-Bowdoin L, Elmer JS and Rogers SG. (1989). Functional expression of the leftward open reading frames of the A component of tomato golden mosaic virus in transgenic tobacco plants. *Plant Cell.* 1:1057-1067.
- Hanley-Bowdoin L, Settlege SB, Orozco BM, Nagar S and Robertson D. (2000). Geminiviruses: models for plant DNA replication, transcription, and cell cycle regulation. *Crit Rev Biochem Mol Biol.* 35:105-140.
- Hanson PI and Whiteheart SW. (2005). AAA+ proteins: have engine, will work. *Nat Rev Mol Cell Biol.* 6:519-529.
- Hao L, Wang H, Sunter G and Bisaro DM. (2003). Geminivirus AL2 and L2 proteins interact with and inactivate SNF1 kinase. *Plant Cell.* 15:1034-1048.
- Hatsugai N, Iwasaki S, Tamura K, Kondo M, Fuji K, Ogasawara K, et al. (2009). A novel membrane fusion-mediated plant immunity against bacterial pathogens. *Genes Dev.* 23:2496-2506.
- He ZG, Feng Y, Wang J and Jiang PX. (2008). The regulatory function of N-terminal AAA+ ATPase domain of eukaryote-like archaeal Orc1/Cdc6 protein during DNA replication initiation. *Arch Biochem Biophys.* 471:176-183.
- Hellman LM and Fried MG. (2007). Electrophoretic mobility shift assay (EMSA) for detecting protein-nucleic acid interactions. *Nat Protoc.* 2:1849-1861.
- Henssen IM, Lapidot M and Thomma PHJ. (2010). Emerging viral diseases of tomato crops. *Mol Plant Microbe Interact.* 23:539-548.
- Hershko A and Ciechanover A. (1998). The ubiquitin system. *Annu Rev Biochem.* 67:425-479.
- Hodgson RAJ and Raison JK. (1991). Lipid peroxidation and superoxide dismutase activity in relation to photo inhibition induced by chilling in moderate light. *Planta.* 185:215-219.
- Höhnle M, Höfer P, Bedford ID, Briddon RW, Markham PG and Frischmuth T. (2001). Exchange of three amino acids in the coat protein results in efficient whitefly transmission of a nontransmissible Abutilon mosaic virus isolate. *Virology.* 290:164-171.
- Hormuzdi SG and Bisaro DM. (1993). Genetic analysis of beet curly top virus: Evidence for three virion sense genes involved in movement and regulation of single-and double-stranded DNA levels. *Virology.* 193:900-909.
- Hussain M, Mansoor S, Iram S, Fatima AN and Zafar Y. (2005). The nuclear shuttle protein of Tomato leaf curl New Delhi virus is a pathogenicity determinant. *J Virol.* 79:4434-4439.
- Hussain M, Mansoor S, Iram S, Zafar Y and Briddon RW. (2000). First report of Tomato leaf curl New Delhi virus affecting chilli pepper in Pakistan. *New Dis Rep.* 9:20.
- Hwang IS and Hwang BK. (2010). The Pepper 9-Lipoxygenase Gene CaLOX1 Functions in Defense and Cell Death Responses to Microbial Pathogens. *Plant Physiol.* 152:948-967.
- ICTV Virus Taxonomy. (2014). Virus Taxonomy: 2014 Release. EC 46, Montreal, Canada. (www.ictvonline.org/virustaxonomy.asp).
- Indian Horticulture Database. (2015). National Horticulture Board, India. (<http://nhb.gov.in>).

- Inoue H, Nojima H, Okayama H. (1990). High efficiency transformation of *Escherichia coli* with plasmids. *Gene*. 96::23-28.
- Janeway CA Jr. (1989). Approaching the asymptote? Evolution and revolution in immunology. *Cold Spring Harb Symp Quant Biol*. 54:1-13.
- Jeske H, Lütgemeier M and Preiss W. (2001). DNA forms indicate rolling circle and recombination-dependent replication of Abutilon mosaic virus. *EMBO J*. 20:6158-6167.
- Jeske H. (2009). Geminiviruses. *Curr Top Microbiol Immunol*. 331:185-226.
- Jiang H, Patel PH, Kohlmaier A, Grenley MO, McEwen DG, Edgar BA. (2009). Cytokine/Jak/Stat signaling mediates regeneration and homeostasis in the *Drosophila* midgut. *Cell*. 137:1343-1355.
- Jin H, Li S and Villegas Jr. A. (2006). Down-regulation of the 26S proteasome subunit RPN9 inhibits viral systemic transport and alters plant vascular development. *Plant Physiol*. 142:651-661.
- Jin Y, Ma D, Dong JJJ, Li D, Deng C and Wang T. (2007). HC-pro protein of Potato Virus Y can interact with three Arabidopsis 20S proteasome subunits in planta. *J Virol*. 81:12881-12888.
- Jones JD and Dangl JL. (2006). The plant immune system. *Nature*. 444:323-329.
- Juárez M, Tovar R, Fiallo-Olivé E, Aranda MA, Gosálvez B, Castillo P et al. (2014). First detection of Tomato leaf curl New Delhi virus infecting zucchini in Spain. *Plant Dis*. 98:857.
- Jupin I, De Kouchkovsky F, Jouanneau F, Gronenborn B. (1994). Movement of tomato yellow leaf curl geminivirus (TYLCV): involvement of the protein encoded by ORF C4. *Virology*. 204:82-90.
- Kaplun L, Tzirkin R, Bakhrat A, Shabek N, Ivantsiv Y and Raveh D. (2005). The DNA damage-inducible UbL-UbA protein Ddi1 participates in Mec1-mediated degradation of Ho endonuclease. *Mol Cell Biol*. 25:5355-5362.
- Kim M, Ahn JW, Jin UH, Choi D, Paek KH and Pai HS. (2003a). Activation of the programmed cell death pathway by inhibition of proteasome function in plants. *J Biol Chem*. 278:19406-19415.
- Kim M, Yang KS, Kim YK, Paek KH and Pai HS. (2003b). Molecular characterization of NbPAF encoding the $\alpha 6$ subunit of the 20S proteasome in *Nicotiana benthamiana*. *Mol Cells*. 15:127-132.
- Kimura S and Sinha N. (2008). Tomato (*Solanum lycopersicum*): A model fruit-bearing crop. *CSH Protoc*. 2008:pdb.emo105.
- Klessig DF, Durner J, Noad R, Navarre DA, Wendehenne D, Kumar D, et al. (2000). Nitric oxide and salicylic acid signaling in plant defense. *Proc Natl Acad Sci USA*. 97:8849-8855.
- Knapp S, Bohs L, Nee M and Spooner DM. (2004). Solanaceae - a model for linking genomics with biodiversity. *Comp Funct Genom*. 5:285-291.
- Kong LJ and Hanley-Bowdoin L. (2002). A geminivirus replication protein interacts with a protein kinase and a motor protein that display different expression patterns during plant development and infection. *Plant Cell*. 14:1817-1832.
- Kong LJ, Orozco BM, Roe JL, Nagar S, Ou S, Feiler HS, et al. (2000). A geminivirus replication protein interacts with the retinoblastoma protein through a novel domain to determine symptoms and tissue specificity of infection in plants. *EMBO J*. 19:3485-3495.

References

- Kotlizky G, Boulton MI, Pitaksutheepong C, Davies JW and Epel BL. (2000). Intracellular and intercellular movement of maize streak geminivirus V1 and V2 proteins transiently expressed as green fluorescent protein fusions. *Virology*. 274:32-38.
- Kulichkova VA, Tsimokha AS, Fedorova OA, Moiseeva TN, Bottril A, Lezina L, et al. (2010). 26S proteasome exhibits endoribonuclease activity controlled by extra-cellular stimuli, *Cell Cycle*. 9:840-849.
- Kunik T, Palanichelvam K, Czosnek H, Citovsky V and Gafni Y. (1998). Nuclear import of the capsid protein of tomato yellow leaf curl virus (TYLCV) in plant and insect cells. *Plant J*. 13:393-399.
- Kurepa J and Smalle JA. (2008). Structure, function and regulation of plant proteasomes. *Biochimie*. 90:324-335.
- Kurepa J, Toh-E A and Smalle JA. (2008). 26S proteasome regulatory particle mutants have increased oxidative stress tolerance. *Plant J*. 53:102-114.
- Kushwaha N, Sahu PP, Prasad M and Chakraborty S. (2015). Chilli leaf curl virus infection highlights the differential expression of genes involved in protein homeostasis and defense in resistant chilli plants. *Appl Microbiol Biotechnol*. 99:4757-4770.
- Laemmli UK. (1970). Cleavage of structural proteins during the assembly of the head of bacteriophage T4. *Nature*. 227:680-685.
- Larry R and Joanne L. (2007). Genetic resources of tomato. In: Razdan MK and Mattoo AK, eds. *Genetic improvement of solanaceous crops*. Science Publishers Enfield, NH, Vol. 2.
- Laufs J, Jupin I, David C, Schumacher S, Heyraud-Nitschke F and Gronenborn B. (1995c). Geminivirus replication: genetic and biochemical characterization of Rep protein function, a review. *Biochimie*. 77:765-73.
- Laufs J, Schumacher S, Geisler N, Jupin I and Gronenborn B. (1995b). Identification of the nicking tyrosine of geminivirus Rep protein. *FEBS Lett*. 377:258-262.
- Laufs J, Traut W, Heyraud F, Matzeit V, Rogers SG, Schell J, et al. (1995a). *In vitro* cleavage and joining at the viral origin of replication by the replication initiator protein of tomato yellow leaf curl virus. *Proc Natl Acad Sci USA*. 92:3879-3883.
- Lazarowitz SG, Wu LC, Rogers SG and Elmer JS. (1992a). Sequence-specific interaction with the viral AL1 protein identifies a geminivirus DNA replication origin. *Plant Cell*. 4:799-809.
- Lazarowitz SG. (1992b). Geminiviruses: Genome structure and function. *Crit Rev Plant Sci*. 11:327-349.
- Lee BJ, Kwon SJ, Kim SK, Kim KJ, Park CJ, Kim YJ, et al. (2006). Functional study of hot pepper 26S proteasome subunit RPN7 induced by Tobacco mosaic virus from nuclear proteome analysis. *Biochem Biophys Res Commun*. 351:405-411.
- Lee KH, Minami A, Marshall RS, Book AJ, Farmer LM, Walker JM, et al. (2011). The RPT2 subunit of the 26S proteasome directs complex assembly, histone dynamics, and gametophyte and sporophyte development in Arabidopsis. *Plant Cell*. 23:4298-4317.
- Lescot M, Dehais P, Thijs G, Marchal K, Moreau Y, Van de Peer Y, et al. (2002). PlantCARE, a database of plant cis-acting regulatory elements and a portal of tools for in-silico analysis of promoter sequences. *Nucl Acids Res*. 30:325-327.
- Li X, Zhang Y, Huang L, Ouyang Z, Hong Y, Zhang H, et al. (2014). Tomato SIMKK2 and SIMKK4 contribute to disease resistance against *Botrytis cinerea* *BMC Plant Biol*. 14:166.

- Li XM, Chao DY, Wu Y, Huang X, Chen K, Cui LG, et al. (2015). Natural alleles of a proteasome $\alpha 2$ subunit gene contribute to thermotolerance and adaptation of African rice. *Nat Genet.* 47:827-833.
- Linnaeus C. (1753). *Species Planatarium*, 1st ed. Holmiae, Stockholm, Sweden.
- Lippai M and L w P. (2014). The role of the selective adaptor p62 and ubiquitin-like proteins in autophagy. *Biomed Res Int.* 2014:832704.
- Lipson C, Alalouf G, Bajorek M, Rabinovich E, Atir-Lande A, Glickman M, et al. (2008). A proteasomal ATPase contributes to dislocation of endoplasmic reticulum associated degradation (ERAD) substrates. *J Biol Chem.* 283:7166-7175.
- Liu H, Boulton MI and Davies JW. (1997). Maize streak virus coat protein binds single- and double-stranded DNA *in vitro*. *J Gen Virol.* 78:1265-1270.
- Liu H, Boulton MI, Thomas CL, Prior DA, Oparka KJ and Davies JW. (1999). Maize streak virus coat protein is karyophilic and facilitates nuclear transport of viral DNA. *Mol Plant Microbe Interact.* 12:894-900.
- Liu Y, Schiff M and Dinesh-Kumar SP. (2002). Virus induced gene silencing in tomato. *Plant J.* 31:777-786.
- Liu Y, Schiff M, Serino G, Deng X-W and Dinesh-Kumar S. (2002). Role of SCF ubiquitin-ligase and the COP9 signalosome in the N gene-mediated resistance response to Tobacco mosaic virus. *Plant Cell.* 14:1483-1496.
- Lozano-Dur n R, Rosas-D az T, Luna AP and Bejarano ER. (2011). Identification of host genes involved in geminivirus infection using a reverse genetics approach. *PLoS One.* 6:e22383.
- Marshall JA, Knapp S, Davey MR, Power JB, Cocking EC, Bennett MD, et al. (2001). Molecular systematics of *Solanum* section *Lycopersicum* (*Lycopersicon*) using the nuclear ITS rDNA region. *Theor Appl Genet.* 103:1216-1222.
- Maurizi MR and Li C-CH. (2010). AAA proteins: in search of a common molecular basis International meeting on cellular functions of AAA proteins. *EMBO Rep.* 2:980-985.
- M traux JP, Signer H, Ryals J, Ward E, Wyss-Benz M, Gaudin J, et al. (1990). Increase in salicylic acid at the onset of systemic acquired resistance in cucumber. *Science.* 250:1004-1006.
- Miller P. (1754). *The gardeners dictionary*, 4th edition, London, UK.
- Mittler R, Vanderauwera S, Gollery M and Van Breusegem F. (2004). Reactive oxygen gene network of plants. *Trends Plant Sci.* 9:490-498.
- Mizutani T, Daryono BS, Ikegami M and Natsuaki KT. (2001). First report of Tomato leaf curl New Delhi virus infecting cucumber in Central Java, Indonesia. *Plant Dis.* 95:1485.
- Mlejnek, P and Prochazka S. (2002). Activation of caspase-like protease and induction of apoptosis by isopentenyladenosine tobacco BY-2 cells. *Planta.* 215:158-166.
- Mnari-Hattab M, Zammouri S, Belkadh MS, Bellon Do a D, Ben Nahia E and Hajlaoui MR. (2015). First report of Tomato leaf curl New Delhi virus infecting cucurbits in Tunisia. *New Dis Rep.* 31:21.
- Moffat A. (1999). Geminiviruses emerge as serious crop threat. *Science.* 286:1835-1835.
- Montillet JL, Chamnongpol S, Rust rucci C, Dat J, van de Cotte B, Agnel JP, et al. (2005). Fatty acid hydroperoxides and H₂O₂ in the execution of hypersensitive cell death in tobacco leaves. *Plant Physiol.* 138:1516-1526.

References

- Morilla G, Castillo AG, Preiss W, Jeske H and Bejarano ER. (2006). A versatile transreplication-based system to identify cellular proteins involved in geminivirus replication. *J Virol.* 80:3624-3633.
- Moriones E and Navas-Castillo J. (2000). Tomato yellow leaf curl virus, an emerging virus complex causing epidemics worldwide. *Virus Res.* 71:123-134.
- Mubin M, Amin I, Amrao L, Briddon RW and Mansoor S. (2010). The hypersensitive response induced by the V2 protein of a monopartite begomovirus is countered by the C2 protein. *Mol Plant Pathol.* 11:245-254.
- Mullis KB, Faloona FA. (1987). Specific synthesis of DNA in vitro via a polymerase-catalyzed reaction. *Methods Enzymol.* 155:335-350.
- Muniyappa V, Venkatesh HM, Ramappa HK, Kulkarni RS, Zeidan M, Tarba CY, et al. (2000). Tomato leaf curl virus from Bangalore (ToLCV-Ban4): sequence comparison with Indian ToLCV isolates, detection in plants and insects, and vector relationships. *Arch Virol.* 145:1583-1598.
- Munné-Bosch S and Müller M. (2013). Hormonal cross-talk in plant development and stress responses. *Front Plant Sci.* 4:529.
- Mur LAJ, Kenton P, Lloyd AJ, Ougham H and Prats E. (2008). The hypersensitive response; the centenary is upon us but how much do we know? *J Exp Bot.* 59:501-520.
- Muratani M and Tansey WP. (2003). How the ubiquitin–proteasome system controls transcription. *Nat Rev Mol Cell Biol.* 4:192-201.
- Naqvi AR, Sarwat M, Pradhan B, Choudhury NR, Haq QM and Mukherjee SK. (2011). Differential expression analyses of host genes involved in systemic infection of Tomato leaf curl New Delhi virus (ToLCNDV). *Virus Res.* 160:395-399.
- Nelbock P, Dillon PJ, Perkins A and Rosen AC. (1990). A cDNA for a protein that interacts with the human immunodeficiency virus Tat transactivator. *Science.* 248:1650-1653.
- Nies DH. (1999). Microbial heavy-metal resistance. *Appl Microbiol Biotechnol.* 51:730-750.
- Noris E, Vaira AM, Caciagli P, Masenga V, Gronenborn B and Accotto GP. (1998). Amino acids in the capsid protein of tomato yellow leaf curl virus that are crucial for systemic infection, particle formation, and insect transmission. *J Virol.* 72:10050-10057.
- Ogura T and Wilkinson AJ. (2001). AAA+ superfamily ATPases: common structure–diverse function. *Genes Cells.* 6:575-597.
- Orozco BM, Miller AB, Settlege SB and Hanley-Bowdoin L. (1997). Functional domains of a geminivirus replication protein. *J Biol Chem.* 272:9840-9846.
- Padidam M, Beachy RN and Fauquet CM, (1995b). Classification and identification of Geminiviruses using sequence comparisons. *J. Gen Virol.* 76:249-263.
- Padidam M, Beachy RN and Fauquet CM. (1995a). Tomato leaf curl geminivirus from India has a bipartite genome and coat protein is not essential for infectivity. *J Gen Virol.* 76:25-35.
- Padidam M, Beachy RN and Fauquet CM. (1996). The role of AV2 ("precoat") and coat protein in viral replication and movement in tomato leaf curl geminivirus. *Virology.* 224:390-404.
- Pajerowska-Mukhtar K and Dong X. (2009). A kiss of death-proteasome mediated membrane fusion and programmed cell death in plant defense against bacterial infection. *Genes Dev.* 23:2449-2454.

- Palanichelvam K, Kunik T, Citovsky V and Gafni Y. (1998). The capsid protein of tomato yellow leaf curl virus binds cooperatively to single-stranded DNA. *J Gen Virol.* 79:2829-2833.
- Panno S, Iacono G, Davino M, Marchione S, Zappardo V, Bella P, et al. (2016). First report of Tomato leaf curl New Delhi virus affecting zucchini squash in an important horticultural area of southern Italy. *New Dis. Rep.* 33:6.
- Pasumarthy KK, Mukherjee SK and Choudhury NR. (2011). The presence of tomato leaf curl Kerala virus AC3 protein enhances viral DNA replication and modulates virus induced gene-silencing mechanism in tomato plants. *Viol J.* 8:178.
- Patil BL and Fauquet CM. (2010). Differential interaction between cassava mosaic geminiviruses and geminivirus satellites. *J Gen Virol.* 91:1871-1882.
- Peart J, Lu R, Sadanandom A, Malcuit I, Moffett P, Brice, D, et al. (2002). Ubiquitin ligase-associated protein SGT1 is required for host and nonhost disease resistance in plants. *Proc Natl Acad Sci USA.* 99:10865-10869.
- Peralta IE and Spooner DM. (2001). GBSSI gene phylogeny of wild tomatoes (*Solanum* L. section *Lycopersicon* [Mill.] Wettst. subsection *Lycopersicon*). *Am J Bot.* 88:1888-1902.
- Peralta IE and Spooner DM. (2005). Morphological characterization and relationships of wild tomatoes (*Solanum* L. Section *Lycopersicon*). *Monogr Syst Bot, Missouri Bot Gard.* 104:227-257.
- Petit F, Jarrousse AS, Dahlmann B, Sobek A, Hendil KB, Buri J, et al. (1997). Involvement of proteasomal subunits zeta and iota in RNA degradation. *Biochem J.* 326:93-98.
- Porebski S, Bailey LG and Baurin BR. (1997). Modification of a CTAB DNA extraction protocol for plants containing high polysaccharide and polyphenol components. *Plant Mol Biol Rep.* 15:8-15.
- Pouch MN, Petit F, Buri J, Briand Y and Schmid HP. (1995). Identification and initial characterization of a specific proteasome (prosome) associated RNase activity. *J Biol Chem.* 270:22023-22028.
- Prasanth KR, Barajas D and Nagy PD. (2015). The proteasomal Rpn11 metalloprotease suppresses tombusvirus RNA recombination and promotes viral replication via facilitating assembly of the viral replicase complex. *J Virol.* 89:2750-2763.
- Predicala R and Zhou Y. (2013). The role of Ran-binding protein 3 during influenza A virus replication. *J Gen Virol.* 94:977-984.
- Raja P. (2010). Methylation of Geminivirus Genomes: Investigating its role as a host defense and evaluating its efficacy as a model to study chromatin methylation in plants. Diss.: Ohio State University.
- Ratcliff F, Harrison BD and Baulcombe DC. (1997). A similarity between viral defense and gene silencing in plants. *Science.* 276:1558-1560.
- Reddy KS and Yaraguntaiah RC. (1981). Virus-vector relationship in leafcurl disease of tomato. *Indian Phytopathol.* 34:310-313.
- Reinheckel T, Sitte N, Ullrich O, Kuckelkorn U, Davies KJ and Grune T. (1998). Comparative resistance of the 20S and 26S proteasome to oxidative stress. *Biochem J.* 335:637-642.
- Rejeb IB, Pastor V and Mauch-Mani B. (2014). Plant responses to simultaneous biotic and abiotic stress: molecular mechanisms. *Plants.* 3:458-475.
- Richards RA. (1996). Defining selection criteria to improve yield under drought. *Plant Growth Regul.* 20:157-166.

References

- Rick CM. (1978). The Tomato. *Sci Amer.* 23:76-87.
- Rigden JE, Krake LR, Rezaian MA and Dry IB. (1994). ORF C4 of tomato leaf curl geminivirus is a determinant of symptom severity. *Virology.* 204:847-850.
- Rizvi I, Choudhury NR and Tuteja N. (2016). Arabidopsis thaliana MCM3 single subunit of MCM2-7 complex functions as 3' to 5' DNA helicase. *Protoplasma.* 253:467-475.
- Rodríguez-Negrete E, Lozano-Durán R, Piedra-Aguilera A, Cruzado L, Bejarano ER and Castillo AG. (2013). Geminivirus Rep protein interferes with the plant DNA methylation machinery and suppresses transcriptional gene silencing. *New Phytol.* 199:464-475.
- Rojas MR, Hagen C, Lucas WJ and Gilbertson RL. (2005). Exploiting chinks in the plant's armor: Evolution and emergence of geminiviruses. *Annu Rev Phytopathol.* 43:361-394.
- Sadanandom A, Bailey M, Ewan R, Lee J and Nelis S. (2012). The ubiquitin-proteasome system: central modifier of plant signalling. *New Phytol.* 196:13-28.
- Sahana N, Kaur H, Basavaraj, Tena F, Jain RK, Palukaitis P, et al. (2012). Inhibition of the host proteasome facilitates Papaya ringspot virus accumulation and proteasomal catalytic activity is modulated by viral factor HcPro. *PLoS One* 7:e52546.
- Sahu PP, Puranik S, Khan M and Prasad M. (2012a). Recent advances in tomato functional genomics: utilization of VIGS. *Protoplasma.* 249:1017-1027.
- Sahu PP, Rai NK, Puranik S, Roy A, Khan M and Prasad M. (2012b). Dynamics of defense-related components in two contrasting genotypes of tomato upon infection with Tomato Leaf Curl New Delhi Virus. *Mol Biotechnol.* 52:140-150.
- Sahu PP, Rai NK, Chakraborty S, Singh M, Ramesh B, Chattopadhyay D, et al. (2010). Tomato cultivar tolerant to Tomato leaf curl New Delhi virus infection induces virus-specific short interfering RNA accumulation and defence-associated host gene expression. *Mol Plant Pathol.* 11:531-544.
- Sahu PP, Sharma N, Puranik S, Prasad M. (2014a). Post-transcriptional and epigenetic arms of RNA silencing: A defense machinery of naturally tolerant tomato plant against Tomato Leaf Curl New Delhi Virus. *Plant Mol Biol Rep.* 32:1015-1029.
- Sahu PP, Sharma N, Puranik S, Muthamilarasan M and Prasad M. (2014b). Involvement of host regulatory pathways during geminivirus infection: a novel platform for generating durable resistance. *Funct Integr Genomics.* 14:47-58.
- Saikia AK and Muniyappa V. (1989). Epidemiology and control of Tomato leaf curl virus in Southern India. *Trop Agric.* 66:350-354.
- Sakamoto T, Kamiya T, Sako K, Yamaguchi J, Yamagami M and Fujiwara T. (2011). Arabidopsis thaliana 26S proteasome subunits RPT2a and RPT5a are crucial for zinc deficiency-tolerance. *Biosci Biotechnol Biochem.* 75:561-567.
- Sako K, Maki Y, Kanai T, Kato E, Maekawa S, Yasuda S, et al. (2012). Arabidopsis RPT2a, 19S proteasome subunit, regulates gene silencing via DNA methylation. *PLoS One.* 7:e37086.
- Saleh A, Alvarez-Venegas R and Avramova Z. (2008). An efficient chromatin immunoprecipitation (ChIP) protocol for studying histone modifications in Arabidopsis plants. *Nat Protoc.* 3:1018-1025.
- Sambrook J, Fritsch EF, Maniatis T. (1989). *Molecular cloning: a laboratory manual.* Cold Spring Harbor Laboratory Press, Cold Spring Harbor, NY.
- Sambrook J, Russell DW. (2001). *Molecular Cloning: a laboratory manual, third ed.* Cold Spring Harbor Laboratory Press, Cold Spring Harbour, NY.

- Sanger F, Nicklen S, Coulson AR. (1977). DNA sequencing with chain terminating inhibitors. *Proc Natl Acad Sci USA*. 74:5463-5467.
- Santos L. (2006). Molecular mechanisms of the AAA proteins in plants. In: Guevara-González RG and Torres-Pacheco I, eds. *Advances in Agricultural and Food Biotechnology*. Research Signpost, Trivandrum, India, pp. 1-15.
- Saunders K, Lucy A and Stanley J. (1991). DNA forms of the geminivirus African cassava mosaic virus consistent with a rolling circle mechanism of replication. *Nucleic Acids Res*. 19:2325–2330.
- Scholthof KBG, Adkins S, Czosnek H, Palukaitis P, Jacquot E, Hohn T, et al. (2011). Top 10 plant viruses in molecular plant pathology. *Mol Plant Pathol*. 12:938-954.
- Schwessinger B and Zipfel C. (2008). News from the frontline: recent insights into PAMP-triggered immunity in plants. *Curr Opin Plant Biol*. 11:389-395.
- Selth LA, Dogra SC, Rasheed MS, Healy H, Randles JW and Rezaian MA. (2005). A NAC domain protein interacts with tomato leaf curl virus replication accessory protein and enhances viral replication. *Plant Cell*. 17:311-325.
- Seo HS, Ku JM, Choi HS, Choi YK, Woo JK, Kim M, et al. (2016). Quercetin induces caspase-dependent extrinsic apoptosis through inhibition of signal transducer and activator of transcription 3 signaling in HER2-overexpressing BT-474 breast cancer cells. *Oncol Rep*. doi: 10.3892/or.2016.4786.
- Settlage SB, See RG and Hanley-Bowdoin L. (2005). Geminivirus C3 protein: replication enhancement and protein interactions. *J Virol*. 79:9885-9895.
- Sharma N, Sahu PP, Puranik S, and Prasad M. (2013). Recent advances in plant-virus interaction with emphasis on small interfering RNAs (siRNAs). *Mol Biotechnol*. 55:63-77.
- Shih SL, Tsai WS, Green SK, Hanson PM, Valand GB, Kalloo G, et al. (2003). Molecular characterization of a new tomato begomovirus from India. *Plant Dis*. 87:598.
- Shimura H and Pantaleo V. (2011). Viral induction and suppression of RNA silencing in plants. *Biochimica et Biophysica Acta*. 1809:601-612.
- Shivaprasad PV, Akbergenov R, Trinks D, Rajeswaran R, Veluthambi K, Hohn, T et al. (2005). Promoters, transcripts, and regulatory proteins of Mungbean yellow mosaic geminivirus. *J Virol*. 79:8149-8163.
- Singh DK, Islam MN, Choudhury NR, Karjee S and Mukherjee SK. (2007). The 32 kDa subunit of replication protein A (RPA) participates in the DNA replication of Mung bean yellow mosaic India virus (MYMIV) by interacting with the viral Rep protein. *Nucl Acids Res*. 35:755-770.
- Smalle J and Vierstra RD. (2004). The ubiquitin 26S proteasome proteolytic pathway. *Annu Rev Plant Biol*. 55:555-590.
- Smalle J, Kurepa J, Yang P, Babiychuk E, Kushnir S, Durski A, et al. (2002). Cytokinin growth responses in Arabidopsis involve the 26S proteasome subunit RPN12. *Plant Cell*. 14:17-32.
- Smalle J, Kurepa J, Yang P, Emborg TJ, Babiychuk E, Kushnir S et al. (2003). The pleiotropic role of the 26S proteasome subunit RPN10 in Arabidopsis growth and development supports a substrate-specific function in abscisic acid signaling. *Plant Cell*. 15:965-980.
- Smith AF. (1994). *The tomato in America: early history, culture, and cookery*. University of South Carolina Press, Columbia.

References

- Sohrab SS, Mandal B, Pant RP and Varma A. (2003). First report of association of Tomato leaf curl New Delhi virus with the yellow mosaic disease of *Luffa cylindrica*. *Plant Dis.* 87:1148.
- Sohrab SS, Karim S, Varma A, Azhar EI, Mandal B, Abuzenadah AM, et al. (2013). Factors affecting sap transmission of Tomato leaf curl New Delhi begomovirus infecting sponge gourd in India. *Phytoparasitica.* 41:591-592.
- Southern E. (1975). Detection of specific sequences among DNA fragments separated by gel electrophoresis. *J Mol Biol.* 98:503-517.
- Spooner DM, Anderson GJ and Jansen RK. (1993). Chloroplast DNA evidence for the interrelationships of tomatoes, potatoes and pepinos (Solanaceae). *Am J Bot.* 80:676-688.
- Stanley J and Townsend R. (1985). Characterisation of DNA forms associated with cassava latent virus infection. *Nucl Acids Res.* 13:2189-2206.
- Stanley J, Latham J, Pinner MS, Bedford I and Markham PG. (1992). Mutational analysis of the monopartite geminivirus beet curly top virus. *Virology.* 191:396-405.
- Story EN, Kopec RE, Schwartz SJ and Harris GK. (2010). An update on the health effects of tomato lycopene. *Annu Rev Food Sci Technol.* 1:189-210.
- Sun X, Meng X, Xu Z and Song R. (2010). Expression of the 26S proteasome subunit RPN10 is upregulated by salt stress in *Dunaliella viridis*. *J Plant Physiol.* 167:1003-1008.
- Sung DY, Kim TH, Komives EA, Mendoza-Cózatl DG and Schroeder JI. (2009). ARS5 is a component of the 26S proteasome complex, and negatively regulates thiol biosynthesis and arsenic tolerance in Arabidopsis. *Plant J.* 59:802-813.
- Sunter G, Sunter J and Bisaro DM. (2001). Plants expressing tomato golden mosaic virus AL2 or beet curly top virus L2 transgenes show enhanced susceptibility to infection by DNA and RNA viruses. *Virology.* 285:59-70.
- Suty L, Lequeu J, Lançon A, Etienne P, Petitot AS, Blein JP. (2003). Preferential induction of 20S proteasome subunits during elicitation of plant defense reactions: towards the characterization of "plant defense proteasomes". *Int J Biochem Cell Biol.* 35:637-650.
- Swafield JC, Bromberg JF and Johnston SA. (1992). Alterations in a yeast protein resembling HIV Tat-binding protein relieve requirement for an acidic activation domain in GAL4. *Nature.* 357:698-700.
- Tahir M and Haider MS. (2005). First report of Tomato leaf curl New Delhi virus infecting bitter gourd in Pakistan. *New Dis Rep.* 10:50.
- Takizawa M, Goto A and Watanabe Y. (2005). The tobacco ubiquitin-activating enzymes NtE1A and NtE1B are induced by *Tobacco mosaic virus*, wounding and stress hormones. *Mol Cells.* 19:228-231.
- Tamura K, Stecher G, Peterson D, Filipinski A and Kumar S. (2013). MEGA6: molecular evolutionary genetics analysis version 6.0. *Mol Biol Evol.* 30:2725-2729.
- Teng K, Chen H, Lai J, Zhang Z, Fang Y, Xia R, et al. (2010). Involvement of C4 protein of beet severe curly top virus (family Geminiviridae) in virus movement. *PLoS One.* 5:e11280.
- Terrell EE, Broome CR and Reveal JL. (1983). Proposal to conserve the name of the tomato as *Lycopersicon esculentum* P. Miller and reject the combination *Lycopersicon lycopersicum* (L.) Karsten (Solanaceae). *Taxon.* 32:310-314.
- Thomma BP, Eggermont K, Penninckx IA, Mauch-Mani B, Vogelsang R, et al. (1998). Separate jasmonate-dependent and salicylate-dependent defense-response pathways in

- Arabidopsis are essential for resistance to distinct microbial pathogens. Proc Natl Acad Sci USA. 95:15107-15111.
- Thompson JD, Higgins DG, Gibson TJ. (1994). CLUSTAL W: improving the sensitivity of progressive multiple sequence alignment through sequence weighting, position-specific gap penalties and weight matrix choice. Nucl Acids Res. 22:4673-4680.
- Tiwari AK, Sharma PK, Khan MS, Snehi SK, Raj SK and Rao GP. (2010). Molecular detection and identification of Tomato leaf curl New Delhi virus isolate causing yellow mosaic disease in bitter melon (*Momordica charantia*), a medicinally important plant in India. Med Plants. 2:117-123.
- Tomas DM, Canizares MC, Abad J, Fernandez-Munoz R and Moriones E. (2011). Resistance to Tomato yellow leaf curl virus accumulation in the tomato wild relative *Solanum habrochaites* associated with the C4 viral protein. Mol Plant Microbe Interact. 24:849-861.
- Tomato Genome Consortium. (2012). The tomato genome sequence provides insights into fleshy fruit evolution. Nature. 485:635-641.
- Torres MA. (2010). ROS in biotic interactions. Physiol Plant. 138:414-429.
- Trinks D, Rajeswaran R, Shivaprasad PV, Akbergenov R, Oakley E, Veluthambi K et al. (2005). Suppression of RNA silencing by a geminivirus nuclear protein, AC2, correlates with transactivation of host genes. J Virol. 79:2517-2527.
- Tuteja N and Sopory SK. (2008). Chemical signaling under abiotic stress environment in plants. Plant Signal Behav. 3:525-536.
- Üstün S and Börnke F. (2015). The *Xanthomonas campestris* type III effector XopJ proteolytically degrades proteasome subunit RPT6. Plant Physiol. 168:107-119.
- Üstün S, Bartetzko V and Börnke F. (2013). The *Xanthomonas campestris* type III effector XopJ targets the host cell proteasome to suppress salicylic-acid mediated plant defence. PLoS Pathog. 9:e1003427.
- Üstün S, König P, Guttman DS and Börnke F. (2014). HopZ4 from *Pseudomonas syringae*, a member of the HopZ type III effector family from the YopJ superfamily, inhibits the proteasome in plants. Mol Plant Microbe Interact. 27:611-623.
- Vacca RA, Valenti D, Bobba A, de Pinto MC, Merafina RS and De Gara L. (2007). Proteasome function is required for activation of programmed cell death in heat shocked tobacco Bright-Yellow 2 cells. FEBS Lett. 581:917-922.
- van den Burg HA, Tsitsigiannis DI, Rowland O, Lo J, Rallapalli G, Maclean D, et al. (2008). The F-box protein ACRE189/ACIF1 regulates cell death and defense responses activated during pathogen recognition in tobacco and tomato. Plant Cell. 20:697-719.
- Vanderschuren H, Stupak M, Fütterer J, Gruissem W and Zhang P. (2007). Engineering resistance to geminiviruses--review and perspectives. Plant Biotechnol J. 5:207-220.
- Vanitharani R, Chellappan P and Fauquet CM. (2005). Geminiviruses and RNA silencing. Trends Plant Sci. 10:144-151.
- Vanitharani R, Chellappan P, Pita JS and Fauquet C. (2004). Differential roles of AC2 and AC4 of cassava geminiviruses in mediating synergism and suppression of posttranscriptional gene silencing. J Virol. 78:9487-9498.
- Vasudeva RS and Samraj J. (1948). A leaf curl disease of tomato. Phytopathol. 38:364-369.
- Verma HN, Srivastava KM and Mathur AK. (1975). A whitefly-transmitted yellow mosaic virus b disease of tomato from India. Plant Dis Rep. 59:494-498.

References


- Vierstra R. (2009). The ubiquitin-26S proteasome system at the nexus of plant biology. *Nat Rev Mol Cell Biol.* 10:385-397.
- Vierstra RD. (1996). Proteolysis in plants: mechanisms and functions. *Plant Mol Biol.* 32:275-302.
- Voinnet O, Pinto YM and Baulcombe DC. (1999). Suppression of gene silencing: a general strategy used by diverse DNA and RNA viruses of plants. *Proc Natl Acad Sci USA.* 96:14147-14152.
- vom Baur E, Zechel C, Heery D, Heine MJ, Garnier JM, Vivat V, et al. (1996). Differential ligand-dependent interactions between the AF-2 activating domain of nuclear receptors and the putative transcriptional intermediary factors mSUG1 and TIF1. *EMBO J.* 15:110-124.
- Wang H, Zhu X, Li H, Cui J, Liu C, Chen X et al. (2014). Induction of caspase-3-like activity in rice following release of cytochrome-f from the chloroplast and subsequent interaction with the ubiquitin-proteasome system. *Sci Rep.* 4:5989.
- Wang H-M, Yin WC, Wang CK and To K-Y. (2009). Isolation of functional RNA from different tissues of tomato suitable for developmental profiling by microarray analysis. *Bot Studies.* 50:115-125.
- Wang S, Kurepa J and Smalle JA. (2009). The Arabidopsis 26S proteasome subunit RPN1a is required for optimal plant growth and stress responses. *Plant Cell Physiol.* 50:1721-1725.
- Watterson JC. (1986). Diseases. The tomato crops. Atherton and Rudich ed. Chapman and Hall Ltd. NY. pp. 461-462.
- Weast RC. (1984). CRC Handbook of chemistry and physics, 64th edn. Boca Raton, CRC Press.
- Weissman AM, Shabek N and Ciechanover A. (2011). The predator becomes the prey: regulating the ubiquitin system by ubiquitylation and degradation. *Nat Rev Mol Cell Biol.* 12:605-620.
- Wolf DH and Hilt W. (2004). The proteasome: a proteolytic nanomachine of cell regulation and waste disposal. *Biochim Biophys Acta.* 1695:19-31.
- Wolf DH, Sommer T and Hilt W. (2004). Death gives birth to life: the essential role of the ubiquitin-proteasome system in biology. *Biochim Biophys Acta.* 1695:1-2.
- Xu Q and Zhang L. (2009). Plant caspase-like proteases in plant programmed cell death. *Plant Signal Behav.* 4:902-904.
- Yanagawa Y and Komatsu S. (2012). Ubiquitin/proteasome-mediated proteolysis is involved in the response to flooding stress in soybean roots, independent of oxygen limitation. *Plant Sci.* 185-186:250-258.
- Yang CW, Gonzalez-Lamothe R, Ewan R, Rowland O, Yoshioka H, Shenton M, et al. (2006). The E3 ubiquitin ligase activity of Arabidopsis PLANT U-BOX17 and its functional tobacco homolog ACRE276 are required for cell death and defense. *Plant Cell.* 18:1084-1098.
- Yang Y, Qi M and Mei C. (2004). Endogenous salicylic acid protects rice plants from oxidative damage caused by aging as well as biotic and abiotic stress. *Plant J.* 40:909-919.
- Yao C, Wu Y, Nie H and Tang D. (2012). RPN1a, a 26S proteasome subunit, is required for innate immunity in Arabidopsis. *Plant J.* 71:1015-1028.

- You Z, Ishimi Y, Masai H and Hanaoka F. (2002). Roles of Mcm7 and Mcm4 subunits in the DNA helicase activity of the mouse Mcm4/6/7 complex. *J Biol Chem.* 277:42471-42479.
- You Z, Komamura Y and Ishimi Y. (1999). Biochemical analysis of the intrinsic Mcm4-Mcm6-Mcm7 DNA helicase activity. *Mol Cell Biol.* 19:80038015
- Yu D, Yu F, Du C, Li X, Zhao X and Liu X. (2015). RPN1a, a subunit of the 26S proteasome, controls trichome development in Arabidopsis. *Plant Physiol Biochem.* 88:82-88.
- Yu F, Wu Y and Xie Q. (2016). Ubiquitin-proteasome system in ABA signaling: from perception to action. *Mol Plant.* 9:21-33.
- Zeng LR, Vega-Sanchez M, Zhu T and Wang GL. (2006). Ubiquitination-mediated protein degradation and modification: an emerging theme in plant-microbe interactions. *Cell Res.* 16:413-426.
- Zhang SC and Ling KS. (2011). Genetic diversity of sweet potato begomoviruses in the United States and identification of a natural recombinant between sweet potato leaf curl virus and sweet potato leaf curl Georgia virus. *Arch Virol.* 156:955-968.
- Zhang Y. (2008). I-TASSER server for protein 3D structure prediction. *BMC Bioinfo.* 9: 40.

Publications

1. **Sahu PP, Sharma N, Puranik S, Chakraborty S and Prasad M.** (2016). Tomato 26S Proteasome subunit RPT4a regulates ToLCNDV transcription and activates hypersensitive response in tomato. *Scientific reports*, 6, 27078.
2. **Kushwaha N, Sahu PP, Prasad M and S Chakraborty.** (2015). Chilli leaf curl virus infection highlights the differential expression of genes involved in protein homeostasis and defense in resistant chilli plants. *Applied microbiology and biotechnology*, 99:4757-4770.

SCIENTIFIC REPORTS



OPEN

Tomato 26S Proteasome subunit RPT4a regulates ToLCNDV transcription and activates hypersensitive response in tomato

Received: 09 March 2016

Accepted: 09 May 2016

Published: 01 June 2016

Pranav Pankaj Sahu^{1,2}, Namisha Sharma¹, Swati Puranik^{1,†}, Supriya Chakraborty² & Manoj Prasad¹

Involvement of 26S proteasomal subunits in plant pathogen-interactions, and the roles of each subunit in independently modulating the activity of many intra- and inter-cellular regulators controlling physiological and defense responses of a plant were well reported. In this regard, we aimed to functionally characterize a *Solanum lycopersicum* 26S proteasomal subunit RPT4a (SIRPT4) gene, which was differentially expressed after *Tomato leaf curl New Delhi virus* (ToLCNDV) infection in tolerant cultivar H-88-78-1. Molecular analysis revealed that SIRPT4 protein has an active ATPase activity. SIRPT4 could specifically bind to the stem-loop structure of intergenic region (IR), present in both DNA-A and DNA-B molecule of the bipartite viral genome. Lack of secondary structure in replication-associated gene fragment prevented formation of DNA-protein complex suggesting that binding of SIRPT4 with DNA is secondary structure specific. Interestingly, binding of SIRPT4 to IR inhibited the function of RNA Pol-II and subsequently reduced the bi-directional transcription of ToLCNDV genome. Virus-induced gene silencing of SIRPT4 gene incited conversion of tolerant attributes of cultivar H-88-78-1 into susceptibility. Furthermore, transient overexpression of SIRPT4 resulted in activation of programmed cell death and antioxidant enzymes system. Overall, present study highlights non-proteolytic function of SIRPT4 and their participation in defense pathway against virus infection in tomato.

Importance of the ubiquitin/26S proteasome (UPS) pathway in different plant-pathogen interactions is well recognized^{1–5}. UPS pathway has been implicated in diverse aspects of eukaryotic cell regulation as it rapidly removes intracellular proteins⁶. In addition to these functions, it is also associated with immune responses to pathogen invasion. UPS components are indirectly or directly involved in signaling and regulation of non-host disease resistance, resistance gene-mediated responses, basal immunity and systemic acquired resistance^{7–10}. It is used not only by the host cells in providing immunity and biotic stress responses, but also by pathogens, including viruses, for their own use^{3,11,12}. Structurally, the 26S proteasome (26SP) in plants consists of a core particle (CP)/20S proteasome (20SP) and a regulatory particle (RP)/19S proteasome. The 20SP is involved in degradation of proteins whereas the 19S confers ATP- and Ub-dependence to the protease¹³. CP is a barrel-shaped ATP- and Ub-independent protease, built out of four stacked rings i.e., two inner and two outer. The inner rings consist of seven β subunits (β 1 to β 7) while outer rings have seven α subunits (α 1 to α 7). These rings gate the access of proteins to the proteolytic chamber. The regulatory particle, on the other hand, is composed of two sub-complexes, the Lid and the Base. The Base contains six different RP Triple-A ATPases (RPTs) along with three RP Non-ATPase (RPN) subunits 1, 2 and 10. The RP Lid composed of eight RPNs (3, 5 to 9, 11 and 12). The RPTs unfold target proteins and open entrance of the 20SP chamber^{14,15}. RPN subunits 1, 2 and 10 function as docking sites for different proteins.

¹National Institute of Plant Genome Research, Aruna Asaf Ali Marg, New Delhi-110067, India. ²School of Life Sciences, Jawaharlal Nehru University, New Delhi-110067, India. [†]Present address: Institute of Biological, Environmental and Rural Sciences, Aberystwyth University, Gogerddan Campus, Aberystwyth, Ceredigion, SY23 3EB, United Kingdom. Correspondence and requests for materials should be addressed to M.P. (email: manoj_prasad@nipgr.ac.in)

Tomato leaf curl disease is caused by several strain/species of begomoviruses in India^{16,17}, of which *Tomato leaf curl New Delhi virus* (ToLCNDV) is the most predominant and severe¹⁶. Due to lack of effective control measurements against the viruses, host resistance/tolerance is the main strategy for the efficient disease control. A few tomato (*Solanum lycopersicum*) cultivars/hybrids have displayed resistance/tolerance against the strains of tomato leaf curl virus in India¹⁸. Resistant sources to *Tomato leaf curl virus* are available in various accessions of *Solanum* species but the mechanism behind the resistance/tolerance has not been examined^{19,20}. In our previous study, we identified a set of genes which were differentially expressed in ToLCNDV tolerant tomato cultivar H-88-78-1²¹. We reported higher abundance of UPS components like 26SP subunit RPT4 and Ubiquitin conjugating enzyme E2, along with many signaling and defense related genes, in tolerant tomato cultivar²¹. In the present study, we functionally characterized *Solanum lycopersicum* 26SP-RPT4a (SIRPT4) gene as a novel virus defense component of the tolerant cultivar. Here, we demonstrated that SIRPT4 protein may interfere with the ToLCNDV genome transcription and activates hypersensitive response (HR) in tomato.

Results

SIRPT4 has ATPase and DNA-binding activity. To examine the biochemical properties of SIRPT4 protein, it was firstly purified as a SIRPT4-GST fusion protein (~69 kDa) from E.coli strain BL21 (Supplementary Fig. 1). The protein showed ATP hydrolyzing activity in an ATPase assay suggesting that the protein can efficiently hydrolyze γ P³²-ATP and dissociate inorganic Phosphate (Pi) (Fig. 1A).

DNA binding activity of SIRPT4 protein was probed using amplified radiolabelled fragments of intergenic regions (IR) of DNA-A and DNA-B and with replication (Rep) regions by electrophoretic mobility shift assay (EMSA). After incubation, SIRPT4 protein formed complex only with DNA-A-IR and DNA-B-IR specific probes (Fig. 1B). However, this DNA-protein complex was not detected with the Rep-specific fragment, which lacks the secondary structure (Fig. 1B). This suggests that SIRPT4 protein may have binding affinity towards stem-loop structure of IR. Further, to check that the complex formation was not due to the binding affinity of GST protein, we incubated it with IR and Rep specific probes (Fig. 1B). Absence of any band showed that purified GST protein lacked DNA binding activity. Overall, the results suggested that SIRPT4 is an ATP-hydrolyzing and secondary structure specific DNA binding protein.

We also validated DNA-A-IR:SIRPT4 interaction through ChIP analysis (Fig. 1C,D). For this, SIRPT4-myc overexpression construct (i.e., pGWB17:SIRPT4-myc) was agro-infiltrated in ToLCNDV infected leaves of susceptible cultivar Punjab Chhuhara. After 3 day post-infiltration, cross-linked chromatin complexes were isolated. Fragmented chromatin was incubated with monoclonal anti-myc antibodies for immunoprecipitation of the complexes. DNA eluted was analyzed by PCR using primers corresponding to IR regions of ToLCNDV-DNA-A (Table 1). Result suggested that SIRPT4-myc has affinity to the DNA-A-IR of ToLCNDV (Fig. 1C).

We examined the possible interfering role of SIRPT4-IR complex with virus genome transcription. As RNA PolII plays an important role in the transcription of virus genome, gfp-tagged subunit-3 of *RNA PolIII* was transiently expressed in ToLCNDV infected leaves. Immunoprecipitation was performed with the monoclonal anti-gfp antibody and obtained complexes were subjected to the PCR analysis. It was observed that DNA-A-IR specific primers were able to amplify the region from the immunoprecipitated samples, which suggested that the RNA PolII subunit binds to the IR region (Fig. 1D). Furthermore, both *SIRPT4* and *SIRNA PolIII subunit-3* were transiently expressed into tomato leaves infected with ToLCNDV. Immunoprecipitation complex of DNA-A-IR:SIRNA PolII-3-gfp with anti-gfp antibodies were subjected to PCR analysis. It was revealed that the reproducibility of the IR-specific amplified product was significantly ($P < 0.001$) reduced ~40% in the sample co-infiltrated with RNA PolII-3-gfp and SIRPT4-myc overexpression construct (Fig. 1E,F). However, tomato leaves co-infiltrated with RNA PolII-3-gfp and vector control showed relatively low reduction (~15%) in the level of IR-specific fragments (Fig. 1E,F). These results suggested that SIRPT4 binds to the IR, which subsequently hinders the binding of RNA PolII complex, there by restricting ToLCNDV transcription in the infected cell.

To validate the ToLCNDV-specific transcript accumulation, *SIRNA PolII* over-expressed tissues with- and without-SIRPT4 co-expression were subjected to northern blot analysis. Tissues transiently expressing empty vector (EV) was used as experimental control. It was observed that upon *SIRPT4* expression, level of both complementary (Rep) and virus sense (CP) strand specific transcript were significantly ($P < 0.001$) down-regulated in comparison to co-expressed SIRNA PolII with EV tissues (Fig. 1G,H, Supplementary Fig. 2). Co-expression of *SIRNA Pol-II subunit* and *SIRPT4* also significantly ($P < 0.001$) reduces relative abundance of both Rep and CP transcript accumulation, in comparison to co-expressed *SIRNA PolIII* with EV tissues (Fig. 1G,H, Supplementary Fig. 2). Rep-specific transcript accumulation on *SIRNA PolIII* transiently expressed tissues with *SIRPT4* was significantly ($P < 0.001$) reduced, in comparison to only *SIRNA PolIII* (without-SIRPT4) expressed tissues (Fig. 1G,H). Moreover, transient expression of *SIRNA PolIII* in mock (EV) did not affect the level of Rep-specific transcript, as no significant differences between mock and *SIRNA PolIII* overexpressed mock plant was observed (Fig. 1G). Virus sense strand specific-CP transcript accumulation was significantly ($P < 0.001$) down-regulated (~80% reduction) in the tissues transiently co-expressed with *SIRNA PolIII* and *SIRPT4* in comparison to *RNA Pol-II* alone (without-SIRPT4) infiltrated leaf tissues (Supplementary Fig. 2A,B). These results suggested that SIRPT4 may alter the level of ToLCNDV transcript in both directions, there by restricting virus infection in ToLCNDV infected tissues in tomato.

Silencing of *SIRPT4* increases ToLCNDV induced symptom severity. Various studies have utilized the *Tobacco rattle virus* (TRV)-mediated VIGS system for the functional characterization of tomato genes²². Thus, we used TRV-VIGS vector to understand the role of *SIRPT4* in the alteration of ToLCNDV infection. The silencing efficiency of TRV-based VIGS system in cultivar H-88-78-1 was tested using an endogenous control *Phytoene desaturase* (*Slpds*). Tobacco was selected as reference to assess the degree of silencing (Supplementary Fig. 3). The characteristic photo-bleaching effect of PDS silencing started to appear at upper-most leaves at 10

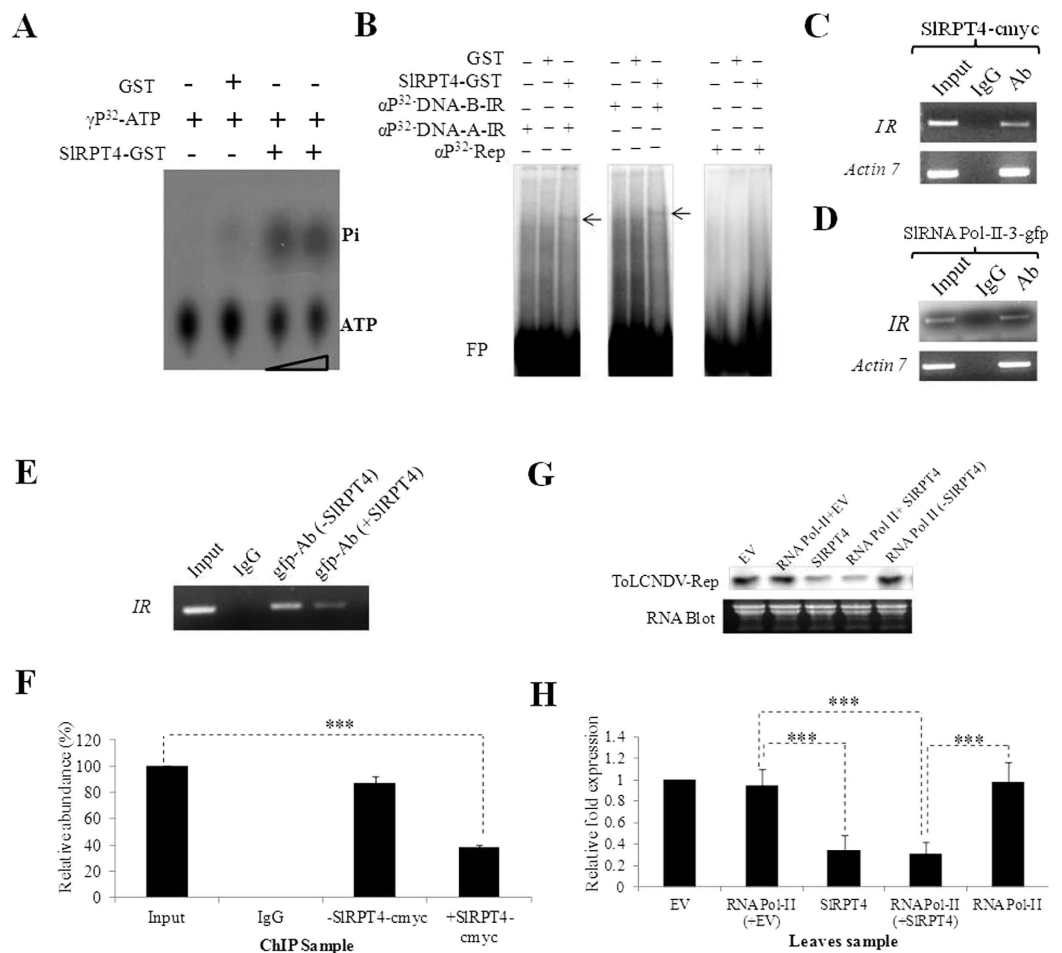


Figure 1. Molecular characterization of SIRPT4 protein. (A) Thin-layer chromatography (TLC) to evaluate ATPase activity. Figure shows dissociation of Pi from γ P³²-labelled ATP. Level of Pi was enriched upon increasing the amount of protein. GST protein was used as a negative control of the experiment. (B) DNA binding activity of SIRPT4-GST protein. Binding of SIRPT4 protein onto α P³²-dCTP-labelled corresponding fragment of DNA-A-IR, DNA-B-IR and Rep regions are shown by retarded DNA-protein complex through EMSA on 6% native polyacrylamide gel. Signs, +/- represent the presence/absence of components. GST protein was used as a control substrate. *In vivo* binding assay was performed by transiently overexpressing SIRPT4 (C); SIRNA PolII subunit-3-gfp construct (D); and SIRPT4 and SIRNA PolII subunit-3 co-infiltration (E), in ToLCNDV infected leaves. Figures depict the amplification of IR fragments from the chromatin immunoprecipitated from the sample by using tag-corresponding to *c-myc* and *gfp*. (E) Relative abundance of IR specific fragments in the experimental samples. (F) Accumulation of *Tomato leaf curl New Delhi virus* ToLCNDV specific *Rep* transcripts in H^T (ToLCNDV infected cultivar H-88-78-1) and H^{SIRPT4+T} (*SIRPT4* silenced H-88-78-1 infected with ToLCNDV), (G) Northern hybridization showing the accumulation of *Rep* transcripts, (H) Relative accumulation of *Rep* transcripts in the leaf samples infiltrated with empty vector (EV), *SIRPT4*-myc and RNA Pol II-3-gfp construct alone, and co-infiltrated with RNA Pol II-3-gfp and *SIRPT4*-myc construct. Fragment corresponding to ToLCNDV-*Rep* gene was used as probe. Total RNA is shown as equivalent loading in the experiment. Data depicts means \pm SD of three independent experiments (n = 3); **P* < 0.05; ***P* < 0.01; ****P* < 0.001.

days post-silencing and reached maximum at 21 days post-silencing (Supplementary Fig. 3). Transcript abundance of *Slpds* silenced plants were experimentally validated and showed >70% reduction in their accumulation, in comparison to mock-inoculated H-88-78-1 plant (Supplementary Fig. 3). Similar reduction in transcript level was recorded in the *Nbpd*s silenced plants (Supplementary Fig. 3).

For silencing of *SIRPT4*, a 231 bp fragment was cloned into the VIGS vector system and agro-infiltrated at two-leaf stage into cultivar H-88-78-1. ToLCNDV infection was performed subsequent to the silencing experiment. Tolerant cultivar H-88-78-1 challenged with ToLCNDV at two-leaf stage was used as an experimental control. RNA blot analysis revealed that the level of *SIRPT4* in silenced cultivar H-88-78-1 started declining 7 days post-silencing and reduced to minimum till 21 days post-silencing (Supplementary Fig. 4). A total of 75 plants from three independent experiments were tested for infectivity. Samples were denoted as H^{TRV:00} (vector infiltrated cultivar H-88-78-1 as Mock), H^{TRV:SIRPT4} (*SIRPT4* silenced cultivar H-88-78-1), mock infiltrated

Plant	Plant infected/ inoculated	Severe symptom appearance	Symptom severity ^a	Over all grade ^b
H-88-78-1 (H ^T)	5/75	14	+	T
Mock (H ^{TRV:00+T})	7/75	13	+	T
SIRPT4 silenced (H ^{TRV:SIRPT4+T})	51/75	7	++++	HS
Mock (H ^{TRV:00})	-	-	-	-
SIRPT4 silenced (H ^{TRV:SIRPT4})	-	-	-	-

Table 1. Infectivity scoring of Tomato leaf curl New Delhi virus-infiltrated control, mock and SIRPT4 silenced plant. Infectivity indexing was done on systemic leaves of experimental plants at 21 days post-inoculation, following the protocol described elsewhere²¹. Briefly, a) +, Least severe; ++, moderately severe; +++, severe; +++++, highly severe. b) T, Tolerant (1–20%); MT, Moderate tolerant (20.1–40%); S, Susceptible (40.1–60%); HS, Highly susceptible (60.1–100%). ‘-’ represent non-ToLCNDV infected samples.

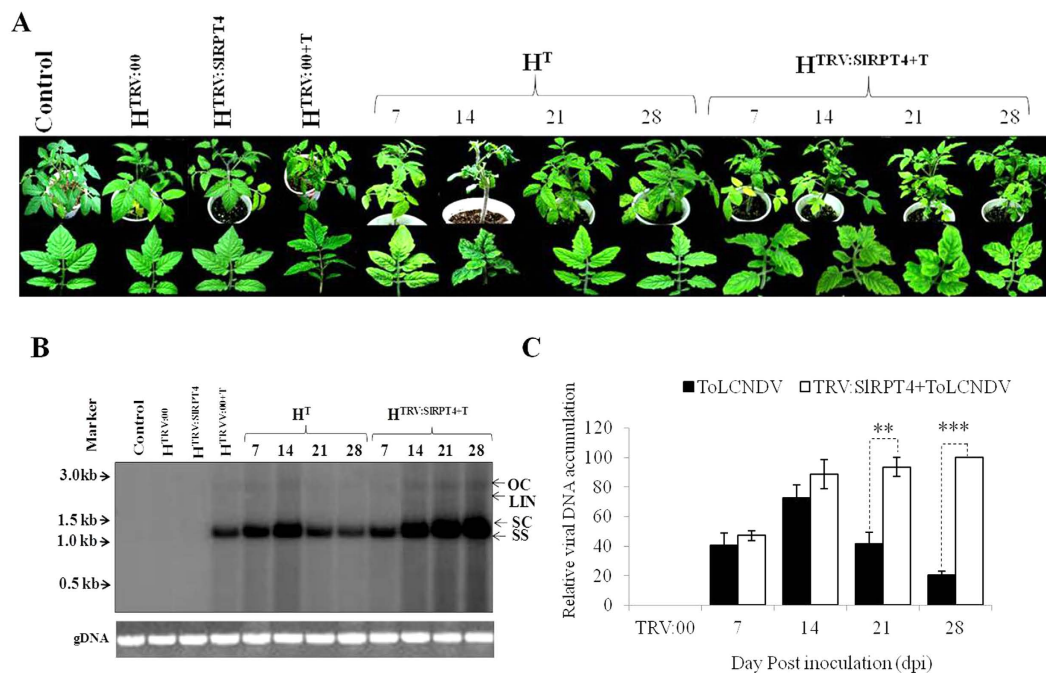


Figure 2. Plant phenotyping and molecular analysis of SIRPT4 silenced tomato plants. (A) phenotype of experimental tomato plants. ToLCNDV tolerant cultivar H-88-78-1 plants were infiltrated with *Agrobacterium* containing the TRV:SIRPT4 construct (H^{SIRPT4}). Subsequent to SIRPT4 silencing process, ToLCNDV infection was performed. The photographs of the plants were taken at 7, 14, 21 and 28 days post inoculation (dpi). H^{SIRPT4,SIRPT4} silenced H-88-78-1; H^{TRV:00}, vector infiltrated control plant; H^{TRV:00+T} vector infiltrated control plant infected with ToLCNDV; H^{SIRPT4+T}, SIRPT4 silenced H-88-78-1 infected with ToLCNDV; H^T, cultivar H-88-78-1 agroinfiltrated with ToLCNDV. Level of viral DNA in H^T (ToLCNDV infected cultivar H-88-78-1) and H^{TRV:SIRPT4+T} (SIRPT4 silenced H-88-78-1 infected with ToLCNDV) at different dpi. (B) Southern blot of tomato genomic DNA from all experimental plants were hybridized with ToLCNDV-coat protein gene specific probe. Replicative forms of ToLCNDV genome are designate as open circular (OC), linear (Lin), supercoiled (SC) and single strand (SS). TRV:00 infiltrated H-88-78-1 was taken as a mock control. Ethidium bromide stained DNA from each experiments were shown as equivalent loading. (C) Relative accumulation of viral DNA in the samples H^T and H^{SIRPT4+T} at different time points. Data depicts means \pm SD of three independent experiments (n = 3); *P < 0.05; **P < 0.01; ***P < 0.001.

with ToLCNDV (H^{TRV:00+T}), H^{TRV:SIRPT4+T} (SIRPT4 silenced and ToLCNDV infected cultivar H-88-78-1) and H^T (ToLCNDV infected H-88-78-1). Infectivity scoring was performed at 21 dpi as described²¹ (Table 1). Leaf curl symptoms started to appear in H^{TRV:SIRPT4+T} within 7 dpi, whereas in H^T, severe symptom initiation started at 14 dpi (Fig. 2A). Symptom remission started in upper systemic leaves after 14 dpi and at 21 dpi leaf-curling symptom was diminished in ToLCNDV-infected mock (H^{TRV:00+T}) plants. H^{TRV:SIRPT4+T} plants failed to start symptom remission (Supplementary Fig. 5A,B). Severity of infection was higher in the H^{TRV:SIRPT4+T} and plants showed stunted growth, leaf curling and yellowing (Fig. 2A). Upon silencing, ~70% plants showed the typical leaf curling symptom at 21 dpi. However, no contrasting phenotypic difference was observed in H^{TRV:SIRPT4} and H^{TRV:00} (mock) infiltrated plants.

Phenotypic changes in terms of viral infection and symptom development after down-regulation of *SIRPT4* subunit, were validated by examining the accumulation of viral DNA-A at 7–28 dpi in both $H^{TRV:SIRPT4+T}$ and H^T plants. Southern blot analysis revealed that viral DNA accumulation at 21 and 28 dpi was maximum (100%) in $H^{TRV:SIRPT4+T}$, while H^T showed minimum (~20%) accumulation at 28 dpi (Fig. 2B,C). Level of viral DNA accumulation was significantly higher in $H^{TRV:SIRPT4+T}$ at 21 dpi and 28 dpi ($P < 0.01$ and < 0.001 , respectively), in comparison to H^T plants. We also evaluated the accumulation of DNA-B upon *SIRPT4* silencing and found that level of corresponding molecule was significantly ($P < 0.001$) increased in *SIRPT4* silenced tomato cv. H-88-78-1 during ToLCNDV infection (Supplementary Fig. 6). Overall, the silencing of *SIRPT4* led to enhanced accumulation of both DNA-A and DNA-B, which signifies the involvement of this gene in providing tolerance against bipartite geminivirus.

Transient overexpression of *SIRPT4* induces HR and Programmed cell death. In order to investigate whether *SIRPT4* gene is involved in programmed cell death (PCD) or not, *in planta* transient overexpression of *SIRPT4* was performed in a ToLCNDV susceptible tomato cultivar Punjab Chhuhara. Fully expanded leaves of cultivar were agro-infiltrated with overexpression construct *SIRPT4* (PC^{SIRPT4}), ToLCNDV (PC^T), mixed culture of ToLCNDV and overexpression construct *SIRPT4* ($PC^{SIRPT4+T}$). *Agrobacterium* containing the pCambia1302 vector was infiltrated as a control measure and termed PC^V . We found that overexpression of *SIRPT4* (PC^{SIRPT4}) can produce HR symptoms as opposed to PC^V where less HR was observed (Fig. 3A). However, HR symptoms were also visible in infiltrated leaves of PC^T and $PC^{SIRPT4+T}$ (Fig. 3A). HR-mediated programmed cell death (PCD) was examined by staining leaves with trypan blue reagent which showed characteristic cell death symptoms in PC^{SIRPT4} and $PC^{SIRPT4+T}$ plants (Fig. 3A). However, leaf sample of PC^V also showed cell death symptom which may be due to the infiltration-associated compatible interaction with *Agrobacterium* containing the virulent vector. Interestingly, cell death symptoms were enriched upon ToLCNDV co-infiltration (Fig. 3A). In animal cells, during apoptosis cytochrome-c provokes a caspase-9 activating complex assembly, which consecutively triggers a cascade of caspases, including caspase-3²³. Although, direct homologues of caspase genes are absent in the plant genome, involvement of certain caspase-like proteases in the control of cell death activation is reported in different pathogenic and non-pathogenic responses^{24,25}. Therefore, synthetic fluorogenic substrates for caspase-9 (LEHD-AFC) and caspase-3 (DEVD-AFC) were used to detect caspase like activity in tomato cultivar Punjab Chhuhara with different treatments, mentioned previously. It was found that the caspase-9 and caspase-3 activity showed >5 fold induction in PC^{SIRPT4} in comparison to the control (Fig. 3B,C). $PC^{SIRPT4+T}$ showed relatively lower accumulation of caspase 9- and caspase 3-like activity in comparison to the PC^{SIRPT4} (Fig. 3B,C). These observations suggested that up-regulation of *SIRPT4* could be involved in the regulation of PCD in plant cell.

We also studied viral DNA accumulation in the corresponding tissues through Southern blot analysis. Leaf tissues of PC^{SIRPT4} , PC^T , $PC^{SIRPT4+T}$, PC^V and PC^{V+T} were harvested after 3 dpi, and subjected to the DNA isolation. It was observed that viral DNA accumulation was more in the case of PC^T in comparison to $PC^{SIRPT4+T}$. Approximately 75% decrease in the viral DNA accumulation was observed in the *SIRPT4* overexpressed tissues, in comparison to PC^V and PC^{V+T} samples (Fig. 3D,E). This indicates that viral multiplication decreases due to activation of PCD by *SIRPT4* overexpression.

Involvement of ROS in hypersensitive response. The activity of enzymes like ascorbate peroxidase (APX) and catalase (CAT) were measured to test the production of reactive oxygen species (ROS) in the experimental tissues. In PC^{SIRPT4} treatment, a significant ($P < 0.01$) decrease in APX activity was observed in comparison to PC^V (Fig. 4A). However, specific activity of APX in PC^V was also significantly ($P < 0.01$) higher than $PC^{SIRPT4+T}$ (Fig. 4A). Similarly, level of CAT was significantly higher in PC^T and $PC^{SIRPT4+T}$ in contrast to the PC^V (Fig. 4B). However, *SIRPT4* transiently expressed tissue PC^{SIRPT4} showed non-significant change in CAT activity in comparison to PC^V tissues (Fig. 4B). In addition to the *SIRPT4* overexpressed Punjab chhuhara, antioxidant enzyme activities were also analyzed in *SIRPT4*-VIGS lines. Although, significant reduction in only APX activities was observed in $H^{TRV:00}$ in comparison to $H^{TRV:SIRPT4}$ (Supplementary Fig. 7A,B). Further, as a measure to assess membrane integrity, we evaluated the membrane damage and HR through Lipid peroxidation (LP) assay. The level of Malondialdehyde (MDA), which is an indicator of degree of LP, increased significantly ($P < 0.001$) in PC^{SIRPT4} with respect to vector control PC^V (Fig. 4C). LP was also significantly ($P < 0.01$) higher in PC^T infected leaves than PC^V , however, MDA level decreased significantly ($P < 0.01$) in $PC^{SIRPT4+T}$ sample (Fig. 4C). With the aim to examine membrane damage as well as to validate the lipid peroxidation assay, we measured the electrolytic leakage (EL) in both *SIRPT4*-transiently expressed and -silenced samples. It was observed that PC^{SIRPT4} exhibited significantly ($P < 0.01$) higher rate of ion leakage than the PC^V (Fig. 4D). Moreover, ToLCNDV infection (PC^T) increased the rate of EL, which may be due to cultivar-specific response to the virus infection. Thus, membrane damage and ion leakage act as one of the marker elements of ROS in *SIRPT4*-mediated cell death. Interestingly, *SIRPT4* silenced samples showed non-significant difference in the level of both MDA and relative ion leakage in comparison to $H^{TRV:00}$ tissues (Supplementary Fig. 7C,D).

Discussion

Reports on the importance of 26SP subunits in independently targeting biological pathway regulators are increasingly apparent^{26–28}. Most phenotypes of 26SP subunit mutants are defective in proteolysis function. Such mutants may also show defect in the function of individual subunits which necessitates re-evaluation of the role of each subunit. Apart from functioning in protein degradation and turnover, proteasomes have RNase activity. This activity appears to be an integral part of plant defense against viruses as RNase activity of 26SP subunits were highlighted during *in vitro* interaction with viral RNAs^{29–31}. *Arabidopsis thaliana* proteasomal $\alpha 5$ subunit was identified as a factor to degrade Tobacco mosaic virus (TMV) and Lettuce mosaic virus (LMV)-derived RNAs *in vitro*³². Viral proteins may also interact and alter 20SP components catalytic activities. For example, HcPro

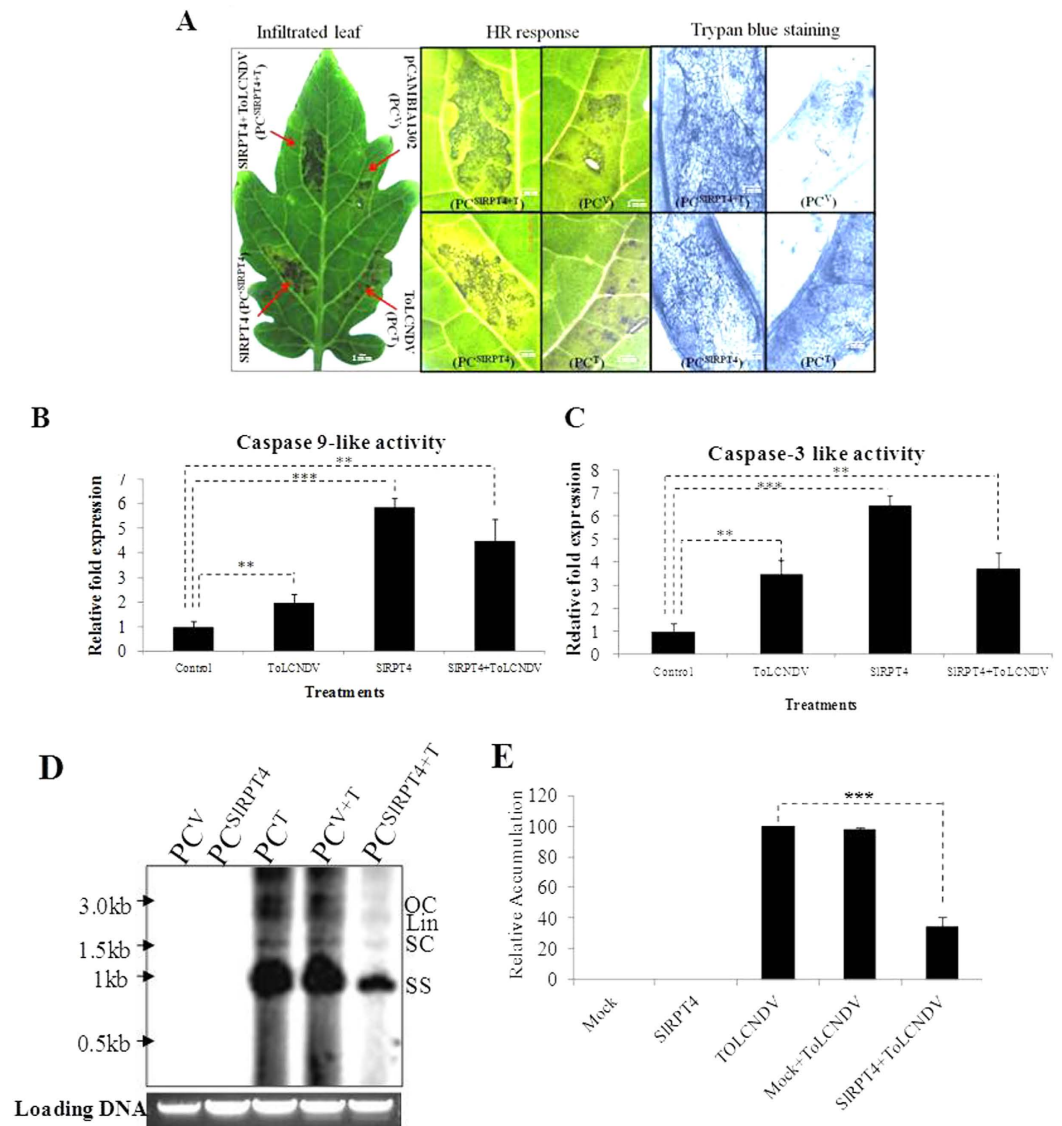


Figure 3. Agrobacterium-mediated transient overexpression of the *SIRPT4*. (A) Punjab Chhuhara leaves were agro-infiltrated with *SIRPT4* overexpression construct (PC^{SIRPT4}), pCambia1302 vector (PC^V), mixed treatment of *SIRPT4* overexpression construct and ToLCNDV construct (PC^{SIRPT4+T}), and ToLCNDV construct alone (PC^T). Leaves were stained with trypan blue to confirm the cell death. Estimation of caspase 9-like (B) and caspase 3-like activity (C). Extracts from Punjab Chhuhara leaves of different treatments (Control, PC^V, ToLCNDV, PC^T, *SIRPT4*, PC^{SIRPT4} and *SIRPT4*+ToLCNDV, PC^{SIRPT4+T}) were incubated with respective peptide substrates i.e., LEHD-AFC for caspase-9 like and DEVD-AFC for caspase-3 like activity, into caspase assay buffer. Their relative fluorescence was measured and enzymatic activities were normalized for protein concentration. (D) Accumulation of *Tomato leaf curl New Delhi virus* DNA in *SIRPT4* overexpressed tomato cultivar Punjab chhuhara. Southern blot of tomato genomic DNA from all experimental plants were hybridized with ToLCNDV-coat protein gene specific probe. (E) Relative accumulation of viral DNA in different treatments. Control, PC^V; ToLCNDV, PC^T; *SIRPT4*, PC^{SIRPT4} and *SIRPT4*+ToLCNDV, PC^{SIRPT4+T}. Data depicts means \pm SD of three independent experiments (n = 3); **P* < 0.05; ***P* < 0.01; ****P* < 0.001.

of *Potato virus Y* (PVY) interacted with the $\alpha 1$, $\beta 2$ and $\beta 5$ subunits of the *Arabidopsis thaliana* 20SP and modulated the RNase activity leading to compromised defense response against these viruses³³. It has also been suggested that the RNase activity of 26S proteasome subunits is differentially regulated through diverse extra-cellular signals³⁴. Thus, proteasome-dependent RNase activity may represent an example of battle between the plant and pathogens, especially viruses.

The present study highlights novel function of a tomato 26SP subunit RPT4 (*SIRPT4*) in defense against geminivirus infection. It was found to contain an active ATPase domain (Fig. 1A) which makes it a potential protein to regulate various cellular and molecular functions. Proteins containing such AAA domain have been shown to be involved in DNA replication, transcription control, degradation of protein, membrane fusion, microtubule regulation, signal transduction and the regulation of gene expression^{35,36}. Majority of reports highlighting the

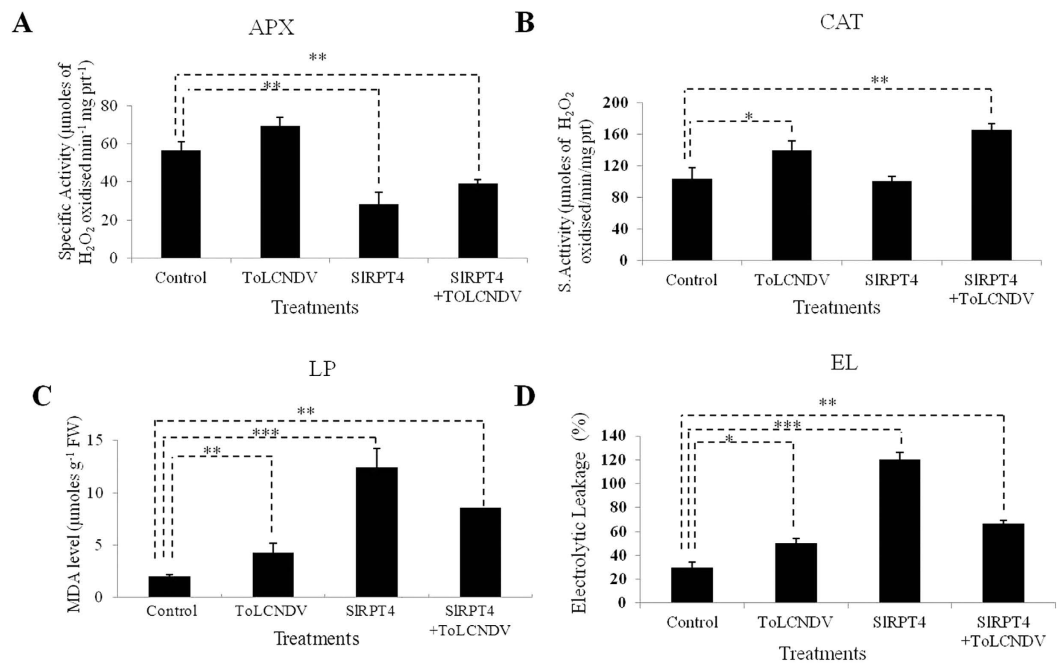


Figure 4. Estimation of antioxidant enzyme activity in cultivar Punjab Chhuhara. (A) Specific activity of APX was measured as $1 \mu\text{mol}$ of ascorbate oxidized min^{-1} . (B) Specific activity of CAT was measured as $1 \mu\text{mol}$ H_2O_2 oxidized min^{-1} . (C) Levels of lipid peroxidation expressed in terms of MDA concentration. (D) Percentage electrolytic leakage. Data depicts means \pm SD of three independent experiments ($n = 3$); * $P < 0.05$; ** $P < 0.01$; *** $P < 0.001$. Control, PC^V; ToLCNDV, PC^T; SIRPT4, PC^{SIRPT4} and SIRPT4+ ToLCNDV, PC^{SIRPT4+T}.

specific function RPTs are established in yeast. For example, proteasomal ATPase RPT4 helps in the dislocation of endoplasmic reticulum-associated degradation (ERAD) substrates³⁷. However very few reports are available, revealing the non-proteolytic functions of RPT4 in plants. A study showed that, rice RPT4 protein can interact with root architecture associated1 (RAA1) and facilitate the root growth and morphology³⁸. In this regard, we further explored the non-proteolytic function of *SIRPT4* leading to defense against ToLCNDV.

Geminivirus genome contains an IR from which viral genes are transcribed in both the viral and complementary sense³⁹. This bidirectional RNA polymerase II-type promoter is not only responsible for the transcription of viral genes but also contains specific sequence elements required for the viral DNA replication. *SIRPT4* was found to possess DNA binding characteristics, more specifically to ToLCNDV-IR (Fig. 1B,C). The *SIRPT4*-IR complexes were observed when corresponding region of DNA-A and DNA-B were incubated with the *SIRPT4*-GST fusion protein. Interestingly, IR of both these components have hairpin loop structure, which strengthen our assumption that the binding of *SIRPT4* with IR may be secondary structure specific. This structural specificity was also evaluated by *SIRPT4* binding with the DNA-A specific Rep region (which does not possess any stem loop structure; Fig. 1B). Absence of any stem loop structure in Rep region of ToLCNDV prevented the specific protein-DNA complex formation, confirming that the binding of *SIRPT4* with DNA is secondary structure specific for IR. Moreover, *SIRPT4* inhibited the binding of RNA-Pol II onto IR (Fig. 1E,F) which resulted in altered transcription of ToLCNDV (Fig. 1G,H, Supplementary Fig. 2). Transient expression of *SIRPT4* significantly inhibited accumulation of Rep (complementary sense strand) and coat protein (viral sense) gene specific transcripts (Fig. 1G,H, Supplementary Fig. 2) suggesting that *SIRPT4* can inhibit bidirectional transcription of viral genes.

Our results establish a strong correlation between decrease in the level of ToLCNDV specific transcripts due to binding of *SIRPT4* onto viral promoter. Thus, it can be posited that *SIRPT4* has a non-proteolytic role in alteration of viral gene transcription through specific affinity with geminivirus-IR. As transcription and replication of viral genome are nuclear bound events, our study also suggests a novel nucleus associated function of *SIRPT4* protein. Although, presence of 26SP complex in the nucleus has been reported in various studies, exact mechanism of transport is unclear^{40,41}. Component of 26SP subunits are highly conserved but only RPT2a has been shown to have nuclear localization signal (NLS)⁴². Lack of NLS in *SIRPT4* may denote that it has a NLS independent mechanism of transport into the nucleus.

This study also presents a direct evidence that inhibition of *SIRPT4* alters the tolerant characteristics of cultivar H-88-78-1 into susceptibility, both at phenotypic and molecular level (Fig. 2A–C, Supplementary Figs 5 and 6). VIGS of *SIRPT4* increases symptom severity in ToLCNDV inoculated tolerant cultivar H-88-78-1 (H^{TRV:SIRPT4+T}; Fig. 2A). Increased titer of both viral DNA-A and DNA-B in H^{TRV:SIRPT4+T} can be associated with their higher replication as a consequential effect of *SIRPT4* silencing. Therefore, loss of *SIRPT4* function (i.e. the IR binding activity) assists in viral genome replication which is essential for viral infection and multiplication.

Transient overexpression of *SIRPT4* revealed that affected cells exhibited characteristic features of apoptotic cell death thereby restricting the ToLCNDV spread and infection (Fig. 3A–C). This proteasome-mediated cell

death pathway is involved in caspase-9- and caspase-3-like activity (Fig. 3B,C). Several studies have reported that proteasomes are involved in conferring defense against pathogens^{43–45}. Suppression of proteasome activity has been correlated with PCD in plants^{23,46}. Contrastingly, diverse studies have revealed that activation of proteasome may also lead to PCD in plants^{47,48}. For example, proteasome function was found to be essential for activation of PCD in heat stressed tobacco Bright-Yellow 2 cells⁴⁸. During TMV infection in hot pepper, up-regulation of 26SP subunit RPN7 was associated with the activation of PCD⁴⁷. Similar findings were also reported from animal systems, in which cell type dependent apoptosis was regulated by proteasome and lead to both initiation and inhibition of PCD⁴⁹. Such evidences clearly suggest that the subunits of 26SP have complex function in PCD and precise role of each subunit needs to be investigated further. Our study highlights that upon transient expression of *SIRPT4*, transformed cells exhibited the characteristic cell death symptoms (Fig. 3A). We also showed that elevation of caspase-like enzymes possibly correlates with PCD. It is a localized response at the site of pathogen attack displaying PCD thereby limiting the spread of pathogens⁵⁰. Thus, upon *SIRPT4* overexpression in a plant cell, activation of HR leads to PCD which in turn restricts the virus spread from the infected tissues into the subsequent cells. This suggest that *SIRPT4a* may have generic response in regulation of ROS mediated PCD (Although ToLCNDV is a non-necrotic virus).

In most cases of plant-pathogen interaction, reactive oxygen species (ROS) act as positive regulators of the HR and activate plant defenses^{51,52}. Reduced ROS scavenging system (antioxidant) activities may also contribute to higher ROS accumulation leading to enhanced HR and defense against pathogens^{53–55}. Hence, we also examined the level of ROS scavenging systems in both transiently expressed and VIGS-mediated silencing of *SIRPT4* gene in susceptible and tolerant cultivar of tomato, respectively. Among the antioxidant enzymes, CAT and APX play important roles to cope-up excess ROS. Their down-regulation promotes increased ROS levels and cell death^{56,57}. Examination of their activity showed a significant decrease in *SIRPT4*-silenced susceptible cultivar, PC^{*SIRPT4*} (Fig. 4A,B). In contrast, *SIRPT4*-silenced tolerant cultivar of tomato showed relatively higher expression of APX in comparison to the mock treated plants (Table S1). It suggested that increased level of APX in *SIRPT4*-silenced cultivar H-88-78-1 helps in detoxification of ROS. However, there was no significant increase in the level of CAT. In our previous study, we had constructed a tomato suppression subtractive hybridization library in between mock and ToLCNDV infected cultivar H-88-78-1²¹. Interestingly, it was observed that the transcripts similar to the catalase and their isoforms showed down-regulation and basal pattern of gene expression²¹. This data also support our finding that in ToLCNDV tolerant cultivar H-88-78-1 activation of ROS system helps in the reduction of viral spread. ROS can also produce lipid derivatives like conjugated dienes, hydroperoxides and malondialdehyde (MDA) by non-enzymatic oxygenation that directs membrane damage thus affecting cell viability⁵⁸. Often, plant cell death is associated with high cellular electrolyte outflow⁵⁹, which can be measured by ion leakage. Reduced cellular viability at the site of attack limits the spread of pathogens and may act as a source of signals for establishment of further defenses^{50,60}. In this study, we found that MDA content was increased in *SIRPT4* transiently expressed plant along with the levels of relative ion leakage (Fig. 4C,D). Overall the above results suggest that ROS activation, altered response of antioxidant systems and reduced membrane stability may be related to the successful recognition of ToLCNDV infection and activation of defense signaling.

Collectively, these responses of *SIRPT4* check the viral spread and thereby inhibit pathogenesis. It has an active ATPase domain which suggests it may have additional function; however, functional importance of ATP hydrolysis against virus infection in tomato needs to be explored further. *SIRPT4* can interact with DNA, specifically at the stem loop structure, and can activate ROS and cell death process to regulate various defense related function against ToLCNDV. Up-regulation of *SIRPT4* in tomato may help spreading ToLCNDV infection in two ways; firstly restricting ToLCNDV multiplication by activation of PCD and HR; secondly by binding with viral promoter to inhibit ToLCNDV transcription. However, exact mechanism of cell death by the *SIRPT4* needs to be explored further. In this regard, protein-protein interaction study may also provide some evidence of *SIRPT4* based activation of HR. We are currently developing a stable transgenic line in tomato, to further investigate the role of *SIRPT4* in PCD. The emerging picture suggests that 26SP mediated defense occurs at different levels of plant-virus interaction. In addition, demonstrated novel antiviral role of *RPT4* will promote plant biologist and virologist to functionally characterize other components of the UPS for better understanding of plants and pathogens in incompatible interactions.

Materials and Methods

Plant material and growth conditions. *Solanum lycopersicum* (cultivar H-88-78-1 and cultivar Punjab Chhuhara) seeds were sown in composite soil (peat compost to vermiculite, 3:1 v/v), germinated and maintained in a growth chamber containing 2 cabinets (PGC-6L; Percival Scientific Inc., USA) under 14 h light/10 h dark cycle at 25 °C, 70% relative humidity, and a light intensity of approximately 250 $\mu\text{mol photons m}^{-2} \text{s}^{-1}$. For silencing experiment, the temperature was maintained at 22 °C throughout as higher temperature inhibits the T-DNA transfer.

Recombinant protein expression and purification. For bacterial expression, pGEX4T2:*SIRPT4* recombinant construct was prepared through specific primers listed in Table S1. GST-tagged-*SIRPT4*-protein was expressed in BL21 (DE3) strain. *SIRPT4*-GST fusion protein was induced by adding 1 mM isopropyl β -D-thiogalactopyranoside (IPTG) followed by re-suspension in lysis buffer [10 mM PBS, pH 7.0; 1 mM phenylmethylsulfonyl fluoride (PMSF), 2 $\mu\text{l/ml}$ protease inhibitors] and sonication. After centrifugation for 10 min at 12000 rpm, obtained pellet was dissolved in IBS buffer (G-biosciences) at 4 °C for 1 h. After centrifugation, supernatant was purified by affinity chromatography using Glutathione-Sepharose 4B. *SIRPT4*-GST fusion proteins were eluted through treatment with elution buffer (20 mM reduced Glutathione) and further dialyzed with dialysis buffer [50 mM 4-(2-hydroxyethyl)-1-piperazineethanesulfonic acid (HEPES), pH 7.5; 40 mM KCl].

ATPase assay. Thin-layer chromatography (TLC) method was used for ATPase assay. Briefly, different amounts of protein were incubated in ATPase buffer [10 mM Tris-HCl (pH 8.0), 5 mM MgCl₂, 50 mM KCl, 10 mM DTT, and 100 μg/ml BSA] containing 0.2 μCi of γ P³² labelled-ATP (Perkin Elmer Life Sciences, USA), at 37 °C for 30 minutes. TLC was performed. Reaction sample was spotted on a polyethyleneimine TLC plate. Air dried reaction mix was as resolved on a solvent consist of 0.5 M Lithium chloride and 1 M Formic acid. TLC paper was air dried and subsequently exposed to phosphor-screen and subjected to image scanning using phosphor-imager (Typhoon 9210).

Electrophoretic mobility shift assay (EMSA). EMSA was performed according to the protocol described⁶¹. PCR amplified product of DNA-A-IR, DNA-B-IR and Replication associated gene fragments were labeled with α P³²-dCTP at 5' end using Klenow fragment of DNA polymerase I. Further, binding reaction between purified SIRPT4-GST fusion protein and α P³²-dCTP labeled IR fragment was performed in 30 μL of binding buffer [75 mM HEPES, pH 7.5; 150 mM KCl, 0.1 mM DTT, 1 mM EDTA, pH 8; 5 mM MgCl₂, 30% (w/v) glycerol and 0.1 mg/ml BSA] containing poly (di-dC). Samples were incubated at 25 °C for 30 min. After incubation samples were resolved in 10% PAGE containing 2% glycerol in 1X-TAE (40 mM Tris base, 20 mM Acetic acid and 1 mM EDTA, pH-8.0) buffer at 10 mA. After running, the dried gel were exposed to phosphor-screen and subjected to image scanning using phosphor-imager (Typhoon 9210).

Chromatin immunoprecipitation assay (ChIP). To examine the DNA binding affinity of SIRPT4 with region corresponding IR of ToLCNDV DNA-A, ChIP assay was performed according to the protocol described⁶². Briefly, the process implicated were immune-precipitation, reverse cross-linking, digestion of protein followed by DNA precipitation. For this, leaves of cultivar Punjab Chhuhara were agro-infiltrated with pGWB17:SIRPT4-cmyc construct. Approximately, two gram of agroinfiltrated sample was subjected to cross-linking with the buffer containing (0.4 M Sucrose, 10 mM Tris-Cl (pH-8), 1 mM PMSF, 1 mM EDTA, and 1% Formaldehyde). Submerged leaves were vacuum-infiltrated for 20 minutes followed by 10 minutes vacuum infiltration of 2 M Glycine to stop cross-linking. Downstream processing including immune-precipitation, reverse cross-linking, digestion of protein followed by DNA precipitation was performed as described⁴⁹. Tissues were grounded to the fine powder using liquid Nitrogen and re-suspended and homogenized into Nuclei isolation buffer (0.25 M Sucrose, 10 mM Tris-HCl pH-8, 10 mM MgCl₂, 1% Triton X-100, 5 mM β -mercaptoethanol, 1 mM PMSF, Protease inhibitor). Homogenized mix was filtered through muslin cloth and centrifuged at 11,000 g for 20 min at 4 °C. Resultant pellet was dissolved in nuclei lysis buffer. This mix was sonicated by 8 times at 60% for 15 sec followed by centrifugation at 13000 g for 10 min at 4 °C. Sonicated chromatin was subjected to immuno-precipitation via anti-cmyc and anti-H₃K₉Me₃ antibodies to obtain the desired genomic DNA fragments of ToLCNDV-IR and *Actin7*, respectively. As the negative control anti-IgG-antibody immunoprecipitation was used, while input control was non-immunoprecipitated sample. Obtained DNA was used for PCR amplification of targeted region of IR and *Actin7* by region specific primers (Table S1). Amplified products were resolved in 1% agarose gel.

TRV-mediated VIGS and agroinfiltration. TRV mediated gene silencing was performed using the pTRV1 and pTRV2 vector (kindly provided by Dinesh-Kumar, Plant Biology Department, University of California, USA). The target gene silencing construct were prepared using pTRV1 and pTRV2 vectors according to the established protocol⁶³. Silencing efficiency of TRV-based VIGS system in cultivar H-88-78-1 was evaluated by silencing of an endogenous control *Phytoene desaturase* (SGN-U593894) along with *Nicotiana benthamiana* (to assess the degree of silencing). Tomato *26S proteasomal subunit RPT4a* (SGN-U566414) which was reported to differentially expressed in response to ToLCNDV infection in tolerant cultivar H-88-78-1, was selected for the silencing study. To minimize the effect of off target silencing, 231 bp fragment from 3'-UTR of *SIRPT4* was PCR amplified from tomato cDNA using primer (Table S1) and cloned into pTRV2 between *XhoI/BamHI* sites to form pTRV2:RPT4. The constructs were introduced into *Agrobacterium* strain EHA105 and cells harboring pTRV1 and pTRV2 or pTRV derivatives were cultured in liquid broth (containing 100 μM MES buffer; pH 5.5) supplemented with antibiotics (50 μg ml⁻¹ Kanamycin and 50 μg ml⁻¹ Rifampicin) and grown overnight at 28 °C. These cultures were centrifuged at 1,000 × g for 10 min and re-suspended in the same volume of re-suspension buffer (10 mM MgCl₂, 100 μM Acetosyringone and 1 mM MES buffer; pH 5.5). After adjusting OD₆₀₀ at 1, transformed cells were incubated at room temperature for 3 h. These cultures were mixed according to the experimental set up (i.e. control, mock and gene silencing constructs) in 1:1 ratio and infiltrated at two leaf stage into tomato leaves by pressing a 1 ml syringe against the lower surface. Subsequent to silencing experiment ToLCNDV agro-infection was done by piercing with a needle at stem node. Tomato cultivar H-88-78-1 was termed on the basis of various treatments, namely H^{TRV:00} (TRV:00 vector infiltrated H-88-78-1 as Mock), H^{TRV:SIRPT4} (*SIRPT4* silenced cultivar H-88-78-1), H^{TRV:SIRPT4+T} (*SIRPT4* silenced cultivar H-88-78-1 and ToLCNDV infected), H^{TRV:00+T} (Mock plants infected with ToLCNDV) and H^T (only ToLCNDV infected H-88-78-1). Each experiment was repeated three times.

Agrobacterium-Mediated Transient Overexpression of *SIRPT4*. For Agrobacterium-mediated transient overexpression, full length cDNA of *SIRPT4* gene was amplified using primer pairs (Table S1) and cloned into pCAMBIA1302 vector between *NcoI/SpeI* restriction sites. The resulting construct was transformed into *A. tumefaciens* strain GV3101. Transformed cells carrying pCAMBIA1302:SIRPT4 along with the empty vector were cultured and re-suspended as described above. The re-suspended culture's absorbance (OD₆₀₀) was adjusted to 0.8 and infiltrated into tomato leaves at two leaf stage. Tomato cultivar Punjab Chhuhara inoculated with different constructs were named as PC^V (pCAMBIA1302 vector inoculated cultivar Punjab Chhuhara), PC^{SIRPT4} (*SIRPT4* overexpressed cultivar Punjab Chhuhara), PC^{SIRPT4+T} (*SIRPT4* overexpressed cultivar Punjab Chhuhara).

and ToLCNDV infected) and PC^T (only ToLCNDV infected cultivar Punjab Chhuhara). After 2 to 3 days, the infiltrated leaves were used for molecular analysis analysis.

Southern hybridization. Total DNA was isolated from leaves of each infiltrated plant by the cetyl-trimethylammonium bromide (CTAB) method⁶⁴. For Southern hybridization, equal amount of total DNA (5 µg) from each experimental samples were electrophoresed on 1% agarose gel in TBE [Tris-borate EDTA; 45 mM Tris-borate, 1 mM EDTA (pH 8)] and transferred to positively charged nylon membrane (HYBOND-N⁺, Amersham Bioscience, USA). ToLCNDV-specific CP gene (DNA-A) and BC1 (DNA-B) probes were prepared as described²⁰ and DNA fragments were labeled with [α^{32} P]dCTP using NEBlot Kit according to the manufacturer's protocol (New England Biolabs).

RNA blot analysis. Total RNA was isolated using TRI reagent (Sigma-Aldrich, USA) from tomato leaves subjected to different treatments. For Northern blot analysis, 10 µg total RNA was electrophoresed on 1.2% denaturing formaldehyde agarose gel in 1X MOPS running buffer and transferred to positively charged nylon membrane (Hybond-N⁺, Amersham Bioscience, USA). For the viral replication specific transcript accumulation, Rep and CP gene of ToLCNDV were PCR amplified using specific primer pairs for probe preparation (Table-S1). Similarly probes specific to *Slpds*, *Nbps* and *SIRPT4* were amplified using gene specific primers listed in Table S1. Probes were labeled with [α^{32} P] dCTP using NEBlot Kit according to the manufacturer's protocol (New England Biolabs). Phosphor-imager (Typhoon-9210, GE Healthcare, USA) was used to scan the blots and further densitometry was done through available software (Quantity One; Bio-Rad, USA).

Trypan blue staining. Trypan blue staining was performed according to protocol⁶⁵. In brief, cell death in the tomato leaves was examined by staining with trypan blue reagent (10 ml Lactic acid, 10 ml Glycerol, 10 g phenol, and 10 mg Trypan blue). The treated leaves were boiled for 1 min in capped falcon tube and stained overnight in Chloral hydrate. Photographs were taken using a stereomicroscope (SMZ 1500, Nikon, USA).

Measurement of Caspase-like activity in SIRPT4 overexpressed tomato. Leaves from different treatments were ground and homogenized in caspase lysis buffer (G-biosciences, St Louis, MO, USA). Samples were incubated in ice for 15 min, further centrifuged, and supernatants collected. Resultant supernatants (50 µl) were mixed with 50 µl of 2X caspase assay buffer with 150 µM LEHD-AFC (G-biosciences, St Louis, MO, USA) for caspase 9-like activity and 150 µM DEVD-AFC (G-biosciences, St Louis, MO, USA) for caspase 3-like activity, as peptide substrates. Fluorescence generated through the AFC hydrolysis was quantified by spectrofluoro photometer (Varian, Victoria, Australia) at 400-nm excitation and 505-nm emission wavelengths after incubation at 37 °C for 60 min. To evaluate the protein concentration, enzymatic activity was normalized with the fold activity of control extracts. Three independent experiments were conducted for measurement of fold activity.

Measurement of catalase (CAT) and ascorbate peroxidase (APX) activity. CAT activity was assayed according to protocol⁶⁶. For this, 100 mg of leaves from each set of treatments were ground in liquid nitrogen, and suspended in 100 mM potassium phosphate buffer (pH 7.0) with 1 mM EDTA (pH 8.0). After centrifugation at 4 °C, supernatants were taken and measured for CAT activity with 60 mM H₂O₂ at 240 nm wave length using a UV-visible spectrophotometer (UV2550, Shimadzu, Japan). For APX, leaves were homogenized in the homogenization buffer (50 mM HEPES; pH 7.0, 0.1 mM EDTA; pH 8.0). After centrifugation at 4 °C, supernatants were measured for the APX activity with 0.03 mM Ascorbate and 0.1 mM H₂O₂ at 290 nm wavelength. Protein estimation was carried out using BSA as standard⁶⁷.

Lipid peroxidase (LP) activity and electrolytic leakage (EL). The lipid peroxidation levels in the experimental samples were evaluated through determining Malondialdehyde (MDA) content by 2-Thiobarbituric acid (TBA) reaction⁶⁸. For this 100 mg tissues were homogenized in 10 mM sodium phosphate buffer (pH 7.4) followed by centrifugation at 4,000 g for 5 min at room temperature. The supernatant (100 µl) was added to a reaction mixture containing 8.1% SDS (w/v), 20% Acetic acid (pH 3.5) (w/v) and 0.8% aqueous TBA (w/v). These mixtures were incubated at 98 °C for 1 h, cooled to room temperature and centrifuged at 4,000 g for 5 min. Incubated samples were subjected to the measurement of absorbance and non-specific absorbance at 535 nm and at 600 nm wavelength, respectively.

Electrolytic leakage (EL) was assessed according to protocol described elsewhere⁶⁹. After *Agrobacterium* infiltration, the infiltrated leaf from the different treatments were collected and analyzed. Fifteen leaf discs (7 mm in diameter) were floated on the 0.4 M sorbitol. The leaf discs were incubated in the dark for 12 h and the initial conductivity (E1) was recorded using a microprocessor based conductivity meter (Model 1601, ESICO, India). The pre-incubated leaves were boiled for 5 min, cooled to room temperature and further subjected to measure final conductivity (E2). Percentage EL was calculated using the formula i.e., (E1/E2) × 100.

Statistical analysis. Experimental data represent means of three independent tests. The significance (at * $P < 0.05$, ** $P < 0.01$, *** $P < 0.001$) differences between mean values of control and each treatment samples were statistically carried out via graphpad *t* test calculator software (<http://graphpad.com/quickcalcs/ttest1.cfm>).

References

- Dreher, K. & Callis, J. Ubiquitin, hormones and biotic Stress. *Ann Bot* **99**, 787–822 (2007).
- Citovsky, V., Zaltsman, A., Kozlovsky, S. V., Gafni, Y. & Krichevsky, A. Proteasomal degradation in plant-pathogen interactions. *Semin Cell Dev Biol* **20**, 1048–1054 (2009).

3. Dielen, A. S., Badaoui, S., Candresse, T. & German-Retana, S. The ubiquitin/26S proteasome system in plant–pathogen interactions: A never-ending hide-and-peek game. *Mol Plant Pathol* **11**, 293–308 (2010).
4. Trujillo, M. & Shirasu, K. Ubiquitination in plant immunity. *Curr Opin Plant Biol* **13**, 1–7 (2010).
5. Sahu, P. P., Sharma, N., Puranik, S., Muthamilarasan, M. & Prasad, M. Involvement of host regulatory pathways during geminivirus infection: a novel platform for generating durable resistance. *Funct Integr Genomics* **14**, 47–58 (2014).
6. Callis, J. & Vierstra, R. D. Protein degradation in signaling. *Curr Opin Plant Biol* **3**, 381–386 (2000).
7. Kim, H. S. & Delaney, T. P. Arabidopsis SON1 is an F-box protein that regulates a novel induced defense response independent of both salicylic acid and systemic acquired resistance. *Plant Cell* **14**, 1469–1482 (2002).
8. Peart, J. R. *et al.* Ubiquitin ligase-associated protein SGT1 is required for host and nonhost disease resistance in plants. *Proc Natl Acad Sci USA* **99**, 10865–10869 (2002).
9. Janjusevic, R., Abramovitch, R. B., Martin, G. B. & Stebbins, C. E. A bacterial inhibitor of host programmed cell death defenses is an E3 ubiquitin ligase. *Science* **311**, 222–226 (2006).
10. Trujillo, M., Ichimura, K., Casais, C. & Shirasu, K. Negative regulation of PAMP-triggered immunity by an E3 ubiquitin ligase triplet in Arabidopsis. *Curr Biol* **18**, 1396–1401 (2008).
11. Isaacson, M. K., Hidde, L. & Ploegh, H. L. Ubiquitination, ubiquitin-like modifiers, and deubiquitination in viral infection. *Cell Host Microbe* **5**, 559–570 (2009).
12. Spallek, T., Robatzek, S. & Gohre, V. How microbes utilize host ubiquitination. *Cellular Microbiol* **11**, 425–434 (2009).
13. Kurepa, J. & Smalle, J. A. Structure, function and regulation of plant proteasomes. *Biochimie* **90**, 324–335 (2008).
14. Smalle, J. & Vierstra, R. D. The ubiquitin 26S proteasome proteolytic pathway. *Annu Rev Plant Biol* **55**, 555–590 (2004).
15. Wolf, D. H. & Hilt, W. The proteasome: a proteolytic nanomachine of cell regulation and waste disposal. *Biochim Biophys Acta* **1695**, 19–31 (2004).
16. Chakraborty, S. Tomato leaf curl viruses from India In *Encyclopedia of Virology* (eds Mahy, B. W. J. *et al.*), 124–133 (Elsevier, 2008).
17. Chakraborty, S., Vanitharani, R., Chattopadhyay, B. & Fauquet, C. M. Supervirulent pseudorecombination and asymmetric synergism between genomic components of two distinct species of begomovirus associated with severe tomato leaf curl disease in India. *J Gen Virol* **89**, 818–828 (2008).
18. Muniyappa, V. *et al.* Tomato leaf curl virus resistant tomato lines TLB111, TLB130 and TLB182. *Hort science* **37**, 603–606 (2002).
19. Tripathi, S. & Varma, A. Identification of resistance in lycopersicon species to tomato leaf curl geminivirus (ToLCV) by agroinoculation. *Euphytica* **129**, 43–52 (2002).
20. Sankarappa, K. S. *et al.* Development of tomato hybrids resistant to tomato leaf curl virus disease in South India. *Euphytica* **164**, 531–539 (2008).
21. Sahu, P. P. *et al.* Tomato cultivar tolerant to *Tomato leaf curl New Delhi virus* infection induces virus-specific short interfering RNA accumulation and defense-associated host gene expression. *Mol Plant Pathol* **11**, 531–44 (2010).
22. Sahu, P. P., Puranik, S., Khan, M. & Prasad, M. Recent advances in tomato functional genomics: utilization of VIGS. *Protoplasma* **249**:1017–1027 (2012).
23. Kim M. *et al.* Activation of the programmed cell death pathway by inhibition of proteasome function in plants. *J Biol Chem* **278**, 19406–19415 (2003).
24. Mlejnek, P. & Prochazka, S. activation of caspase-like protease and induction of apoptosis by isopentenyladenosine tobacco BY-2 cells. *Planta* **215**, 158–166 (2002).
25. Xu, Q. & Zhang, L. Plant caspase-like proteases in plant programmed cell death. *Plant Signal Behav* **4**, 902–904 (2009).
26. Yao, C., Wu, Y., Nie, H. & Tang, D. RPN1a, a 26S proteasome subunit, is required for innate immunity in Arabidopsis. *Plant J* **71**, 1015–1128 (2012).
27. Üstün, S., König, P., Guttman, D. S. & Börnke, F. HopZ4 from *Pseudomonas syringae*, a member of the HopZ type III effector family from the YopJ superfamily, inhibits the proteasome in plants. *Mol Plant Microbe Interact* **27**, 611–623 (2014).
28. Yu, F., Wu, Y. & Xie, Q. Ubiquitin-Proteasome System in ABA Signaling: From Perception to Action. *Mol Plant* **9**, 21–33 (2016).
29. Pouch, M. N., Petit, F., Buri, J., Briand, Y. & Schmid, H. P. Identification and initial characterization of a specific proteasome (prosome) associated RNase activity. *J Biol Chem* **270**, 22023–22028 (1995).
30. Ballut, L. *et al.* Biochemical identification of proteasome-associated endonuclease activity in sunflower. *Biochim Biophys Acta* **1645**, 30–39 (2003).
31. Petit, F. *et al.* Involvement of proteasomal subunits zeta and iota in RNA degradation. *Biochem J* **326**, 93–98 (1997).
32. Dielen, A. S. *et al.* The 20S proteasome $\alpha 5$ subunit of Arabidopsis thaliana carries an RNase activity and interacts in planta with the lettuce mosaic potyvirus HcPro protein. *Mol Plant Pathol* **12**, 137–150 (2011).
33. Sahana, N. *et al.* Inhibition of the host proteasome facilitates Papaya ringspot virus accumulation and proteasomal catalytic activity is modulated by viral factor HcPro. *PLoS ONE* **7**, e52546 (2012).
34. Valentina, A. *et al.* 26S proteasome exhibits endoribonuclease activity controlled by extra-cellular stimuli. *Cell Cycle* **9**, 840–849 (2010).
35. Kedzierska, S. Structure, function and mechanisms of action of ATPases from the AAA superfamily of proteins. *Postepy Biochem* **2006**, **52**, 330–338 (2006).
36. George, B. *et al.* Mutational analysis of the helicase domain of a replication initiator protein reveals critical roles of Lys 272 of the B' motif and Lys 289 of the β -hairpin loop in geminivirus replication. *J Gen Virol* **95**, 1591–602 (2014).
37. Lipson, C. *et al.* A proteasomal ATPase contributes to dislocation of endoplasmic reticulum associated degradation (ERAD) substrates. *J Biol Chem* **283**, 7166–75 (2008).
38. Han, Y. *et al.* Rice ROOT ARCHITECTURE ASSOCIATED1 binds the proteasome subunit RPT4 and is degraded in a D-box and proteasome-dependent manner. *Plant Physiol* **148**, 843–855 (2008).
39. Bisaro, D. M. Geminivirus DNA replication In *DNA replication in eukaryotic cells* (ed. DePamphilis, M. L.) 833–854 (Cold Spring Harbor Laboratory Press, 1996).
40. Fu, H., Doelling, J. H., Rubin, D. M. & Vierstra R. D. Structural and functional analysis of the six regulatory particle triple-A ATPase subunits from the Arabidopsis 26S proteasome. *Plant J* **18**, 529–539 (1999).
41. Enenkel, C. Proteasome dynamics. *Biochimica et Biophysica Acta* **1843**, 39–46 (2014).
42. Enenkel, C. Nuclear Transport of Yeast Proteasomes. *Biomolecules* **4**, 940–955 (2014).
43. Becker, J., Kempf, R., Jeblick, W. & Kausch, H. Induction of competence for elicitation of defense responses in cucumber hypocotyls requires proteasome activity. *Plant J* **21**, 311–316 (2000).
44. Suty, L. *et al.* Preferential induction of 20S proteasome subunits during elicitation of plant defense reactions: towards the characterization of “plant defense proteasomes”. *Int J Biochem Cell Biol* **35**, 637–650 (2003).
45. Takizawa, M., Goto, A. & Watanabe, Y. The tobacco ubiquitin-activating enzymes NtE1A and NtE1B are induced by *Tobacco mosaic virus*, wounding and stress hormones. *Mol Cells* **19**, 228–231 (2005).
46. Jin, H., Li, S. & Villegas, A., Jr. Down-regulation of the 26S proteasome subunit RPN9 inhibits viral systemic transport and alters plant vascular development. *Plant Physiol* **142**, 651–661 (2006).
47. Lee, B.-J. *et al.* Functional study of hot pepper 26S proteasome subunit RPN7 induced by *Tobacco mosaic virus* from nuclear proteome analysis. *Biochem Biophys Res Commun* **351**, 405–411 (2006).
48. Vacca, R. A. *et al.* Proteasome function is required for activation of programmed cell death in heat shocked tobacco Bright-Yellow 2 cells. *FEBS Lett* **581**, 917–922 (2007).

49. Grimm, L. M. & Osborne, B. A. Apoptosis and the proteasome. *Results Probl Cell Differ* **23**, 209–228 (1999).
50. Mur, L. A. J., Kenton, P., Lloyd, A. J., Ougham, H. & Prats, E. The hypersensitive response; the centenary is upon us but how much do we know? *J Exp Bot* **59**, 501–520 (2008).
51. Bindschedler *et al.* Peroxidase-dependent apoplastic oxidative burst in Arabidopsis required for pathogen resistance. *Plant J* **47**, 851–863 (2006).
52. Choi, H. W., Kim Y. J., Lee, S. C., Hong, J. K. & Hwang, B. K. Hydrogen peroxide generation by the pepper extracellular peroxidase CaPO₂ activates local and systemic cell death and defense response to bacterial pathogens. *Plant Physiol* **145**, 890–904 (2007).
53. Dat, J. F. *et al.* Changes in hydrogen peroxide homeostasis trigger an active cell death process in tobacco. *Plant J* **33**, 621–632 (2003).
54. Mittler, R., Vanderauwera, S., Gollery, M. & Van Breusegem, F. Reactive oxygen gene network of plants. *Trends Plant Sci* **9**, 490–498 (2004).
55. Sahu, P. P. *et al.* Dynamics of defense-related components in two contrasting genotypes of tomato upon infection with Tomato Leaf Curl New Delhi Virus. *Mol Biotechnol.* **52**, 140–150 (2012).
56. Klessig, D. F. *et al.* Nitric oxide and salicylic acid signaling in plant defense. *Proc Natl Acad Sci USA* **97**, 8849–8855 (2000).
57. Yang, Y., Qi, M. & Mei, C. Endogenous salicylic acid protects rice plants from oxidative damage caused by aging as well as biotic and abiotic stress. *Plant J* **40**, 909–919 (2004).
58. Montillet, J.-L. *et al.* Fatty acid hydroperoxides and H₂O₂ in the execution of hypersensitive cell death in tobacco leaves. *Plant Physiol* **138**, 1516–1526 (2005).
59. Pontier, D., Tronchet, M., Rogowsky, P., Lam, E. & Roby, D. Activation of hsr203, a plant gene expressed during incompatible plant-pathogen interactions, is correlated with programmed cell death. *Mol Plant Microbe Interact* **11**, 544–554 (1998).
60. Torres, M. A. ROS in biotic interactions. *Physiol Plant* **138**, 414–429 (2010).
61. Hellman, L. M. & Fried, M. G. Electrophoretic mobility shift assay (EMSA) for detecting protein-nucleic acid interactions. *Nat Protoc.* **2**, 1849–1861 (2007).
62. Saleh, A., Alvarez-Venegas, R. & Avramova, Z. An efficient chromatin immunoprecipitation (ChIP) protocol for studying histone modifications in Arabidopsis plants. *Nat Protoc.* **3**, 1018–1025 (2008).
63. Liu, Y., Schiff, M. & Dinesh-Kumar, S. P. Virus induced gene silencing in tomato. *Plant J* **31**, 777–786 (2002).
64. Porebski, S., Bailey, L. G. & Baurin, B. R. Modification of a CTAB DNA extraction protocol for plants containing high polysaccharide and polyphenol components. *Plant Mol Biol Rep* **15**, 8–15 (1997).
65. Hwang, I. S. & Hwang, B. K. The Pepper 9-Lipoxygenase Gene CaLOX1 Functions in Defense and Cell Death Responses to Microbial Pathogens. *Plant Physio* **152**, 948–967 (2010).
66. Aebi, H. E. Catalase In *Methods of enzymatic analysis* (eds Bergmeyer, H. U. *et al.*) 273–286 (Verlag Chemie, 1983).
67. Bradford, M. M. A rapid and sensitive method for quantitation of microgram quantities of protein utilizing the principle of rotein dye binding. *Anal Biochem* **72**, 248–254 (1976).
68. Hodgson, R. A. J. & Raison, J. K. Lipid peroxidation and superoxide dismutase activity in relation to photo inhibition induced by chilling in moderate light. *Planta* **185**, 215–219 (1991).
69. Dionisio-Sese, M. L. & Tobita, S. Antioxidative responses of rice seedlings to salinity stress. *Plant Sci* **135**, 1–9 (1998).

Acknowledgements

We are grateful to the Director, National Institute of Plant Genome Research (NIPGR) and Dean, School of Life Sciences, Jawaharlal Nehru University for providing facilities. We gratefully acknowledge the financial support from Department of Biotechnology (Grant No. BT/PR8357/PBD/16/1033/2013), Govt. of India and core grant of NIPGR, New Delhi, India. Authors also acknowledge Prof. Savithamma Dinesh-Kumar, Plant Biology Department, University of California, Davis, for providing TRV-VIGS vectors.

Author Contributions

M.P. and S.C. conceived the idea, helped analysis and wrote the manuscript. P.P.S., N.S. and S.P. performed the wet lab experiments and wrote manuscript.

Additional Information

Supplementary information accompanies this paper at <http://www.nature.com/srep>

Competing financial interests: The authors declare no competing financial interests.

How to cite this article: Sahu, P. P. *et al.* Tomato 26S Proteasome subunit RPT4a regulates ToLCNDV transcription and activates hypersensitive response in tomato. *Sci. Rep.* **6**, 27078; doi: 10.1038/srep27078 (2016).



This work is licensed under a Creative Commons Attribution 4.0 International License. The images or other third party material in this article are included in the article's Creative Commons license, unless indicated otherwise in the credit line; if the material is not included under the Creative Commons license, users will need to obtain permission from the license holder to reproduce the material. To view a copy of this license, visit <http://creativecommons.org/licenses/by/4.0/>

Chilli leaf curl virus infection highlights the differential expression of genes involved in protein homeostasis and defense in resistant chilli plants

Nirbhay Kushwaha · Pranav Pankaj Sahu · Manoj Prasad · Supriya Chakraborty

Received: 8 September 2014 / Revised: 15 January 2015 / Accepted: 17 January 2015
© Springer-Verlag Berlin Heidelberg 2015

Abstract Geminiviruses have evolved with tremendous potential of recombination and possess the ability to manipulate several cellular processes of hosts. *Chilli leaf curl virus* (ChiLCV) is a monopartite *Begomovirus* (family *Geminiviridae*) which has emerged as a serious threat to chilli production worldwide. To date, development of resistant chilli varieties through conventional plant breeding techniques remains the major antiviral strategy. To explore the potential resistance factors in *Capsicum annuum* var. Punjab Lal, we performed a transcriptome analysis in ChiLCV-infected plants by exploiting the advantage of sensitivity and efficiency of suppression subtractive hybridization (SSH). Out of 480 clones screened, 231 unique expressed sequence tags (ESTs) involved in different cellular and physiological processes were identified. An interactome network of ChiLCV responsive differentially expressed genes revealed an array of proteins involved in key cellular processes including transcription, replication, photosynthesis, and defense. A comparative study of gene expression between resistant and susceptible chilli plants revealed upregulation of several defense-related genes such as nucleotide-binding site leucine-rich repeat (NBS-LRR) domain containing protein, lipid transfer protein, thionin, polyphenol oxidase, and other proteins like ATP/ADP transporter in the ChiLCV-resistant variety. Taken together, the present

study provides novel insights into the transcriptomics of ChiLCV-resistant chilli plants.

Keywords Geminivirus · Transcriptome analysis · Host gene expression · Resistance · Chilli · Suppression subtractive hybridization

Introduction

Plant viruses have evolved with enormous capabilities of exploiting and modulating host machineries for the establishment of successful infection. They modulate cellular processes of hosts to facilitate their replication, transcription, and movement (Wang and Maule 1995; Czosnek et al. 2013). During evolution, plants have also developed diverse defense machineries to counteract viral invasion (Soosaar et al. 2005; Kachroo et al. 2006; Zvereva and Kozlov 2012). Specific interactions between virus and host determine the fate of infection. Following recognition, a plant may initiate an incompatible interaction that is unfavorable for the virus (Flor 1971; Jones and Dangl 2006). As a consequence, a series of cascade of defense responses can be induced to limit virus multiplication within the infected areas, which may lead to resistance in plants (Kachroo et al. 2006). On the contrary, a compatible interaction between plant and virus takes place in a permissive host which favors virus multiplication and spread.

Chilli leaf curl virus (ChiLCV) is one of the devastating pathogens and poses a serious threat to chilli production in the tropical and subtropical countries (Kumar et al. 2006; Senanayake et al. 2007; Chattopadhyay et al. 2008). It is a member of the genus *Begomovirus* (family *Geminiviridae*) which contains a circular ssDNA of approximately 2.75 kb in size. ChiLCV infection in plants is often found to be associated with betasatellites (Chattopadhyay et al. 2008). The ChiLCV genome encodes six proteins, two from the virion sense strand

Electronic supplementary material The online version of this article (doi:10.1007/s00253-015-6415-6) contains supplementary material, which is available to authorized users.

N. Kushwaha · P. P. Sahu · S. Chakraborty (✉)
Molecular Virology Laboratory, School of Life Sciences,
Jawaharlal Nehru University, New Delhi 110067, India
e-mail: supriyachakrasls@yahoo.com

M. Prasad
National Institute of Plant Genome Research,
New Delhi 110067, India

(coat protein and pre-coat protein) and four from the complementary sense strand (replication initiator protein, transcription activator protein, replication enhancer protein, and pathogenicity determinant protein) (Chattopadhyay et al. 2008). Begomovirus-encoded proteins are involved in initiation of replication, activation of transcription, enhancement of replication, encapsidation of genome, nucleocytoplasmic trafficking, and cell-to-cell or long distance movement of virus (Lazarowitz et al. 1992; Hanley-Bowdoin et al. 2000; Fondong 2013). A betasatellite encodes a single protein β C1 which is known to be required for the movement and suppression of both transcriptional and post-transcriptional gene silencing (Briddon et al. 2003; Yang et al. 2011; Shukla et al. 2013).

Previous studies have highlighted the complexity of incompatible interaction between plants and viruses (Rowe and Kliebenstein 2008; Kang et al. 2005). Therefore, the mechanisms linked to the inhibition of viral accumulation inside host cells, prevention of virus movement within the plant, and activation of plant defense mechanisms have been partially elucidated (Ishibashi et al. 2007; Hofmann et al. 2009). Recently, the involvement of viral DNA methylation, activation of gene silencing machinery, and ubiquitination mediated defense against begomoviruses have been reported (Raja et al. 2008; Lozano-Duran et al. 2011; Marino et al. 2012; Sahu et al. 2014a, b). Nevertheless, identification of resistance factors and their mechanistic role in conferring ChiLCV resistance in chilli remains elusive.

In this study, we have generated for the first time a comprehensive and the largest transcriptome from ChiLCV-resistant chilli variety Punjab Lal. Our study signifies the differential expression of several genes involved in defense, transcription, DNA organization, replication, transport, signaling, stress, ribosome assembly, translation process, and resistance response against ChiLCV infection. Over-expression of defense-related genes in resistant chilli variety could be correlated with ChiLCV resistance.

Materials and methods

Plant growth

Seeds of chilli varieties (*Capsicum annuum*) resistant to ChiLCV (var. Punjab Lal) and ChiLCV susceptible (var. Kashi Anmol) were obtained from the Indian Institute of Vegetable Research, Varanasi, India. Plants were grown under controlled conditions of 16-h light and 8-h dark period at 25 ± 2 °C with relative humidity of 60 %.

Inoculation of test plants

Partial tandem repeat infectious clones of ChiLCV-DNA A (GenBank accession no EF190217) and betasatellite

(GenBank accession no EF190215) (Chattopadhyay et al. 2008) are available in our laboratory. These constructs were independently mobilized into *Agrobacterium tumefaciens* strain EHA105 (Chattopadhyay et al. 2008). *Agrobacterium* cultures were grown in Luria broth (pH 7.0) for 36 h at 28 °C. Cultures were centrifuged at 5000 rpm for 10 min, and pellets were dissolved in sterilized distilled water containing 10 mM $MgCl_2$. *Agrobacterium* cultures carrying DNA A and betasatellite were mixed in equimolar concentration. *Agrobacterium* harboring pCAMBIA2300 vector alone was used for mock treatments. Chilli plants at four-leaf stage were pierced around petiole and nodal regions and were inoculated with *Agrobacterium* suspension (0.8 OD). The inoculated plants were kept in a glass house under controlled conditions as stated above.

Isolation of total genomic DNA

Two uppermost leaves from both mock- and virus-inoculated plants were harvested at 7, 14, 21, and 28 days post-inoculation (dpi), and the total DNA was isolated following the method suggested by Dellaporta et al. (1983) with some modifications. Precisely, 100 mg of leaf tissues from each sample was homogenized in liquid nitrogen and suspended in 1 ml extraction buffer (100 mM TrisCl pH 8.0, 100 mM EDTA pH 8.0, 1.4 M NaCl). Sodium dodecyl sulfate (SDS; 10 %w/v) was added, and the samples were incubated at 65 °C for 15 min followed by addition of 5 M potassium acetate. Total genomic DNA was extracted by phenol/chloroform/isoamyl alcohol (25:24:1) followed by precipitation with 0.8 volume of isopropanol, and finally, the pellet was washed with 70 % ethanol. After air drying, the total DNA was dissolved in sterilized water. Concentration and quality of the total DNA were checked in a spectrophotometer (Nano Drop, Thermo Scientific, Waltham, USA). Three biological replicates and two technical replicates were maintained throughout the experiment.

Detection of viral genome by polymerase chain reaction

For detection of ChiLCV, 200 ng of total DNA was used for PCR reaction using AC1 (nt1521-2606) specific primers FP 5'-GGATCCTAATGCCTAGGGCTGGGAGA-3' and RP 5'-GAGCTCTCAACGCGTCGACGCTGGTCC-3'. The PCR was performed using the following profile: initial denaturation at 94 °C for 4 min, denaturation at 94 °C for 30 s, annealing at 60 °C for 30 s, and extension at 72 °C for 1 min and 20 s for 25 cycles. The PCR experiments were performed three times to ensure reliability, and PCR products were resolved in 0.8 % agarose gel.

Total RNA and mRNA isolation

Total RNA was isolated from two uppermost leaves of virus- and mock- inoculated plants using Tri-reagent (SIGMA, St. Louis, USA) following manufacturer's instructions. The quantity and integrity of total RNA were examined using a spectrophotometer (GE Amersham, Little Chalfont, UK). In addition, RNA integrity was also examined by resolving the samples on 1.2 % formaldehyde denaturing gel. Messenger RNA (mRNA) was purified from total RNA using the MagneSphere mRNA Purification Kit (Promega, Madison, USA) according to the manufacturer's protocol.

Construction of suppression subtractive hybridization cDNA library of chilli variety resistant to ChiLCV

The subtracted complementary DNA (cDNA) library of chilli variety Punjab Lal was constructed by suppression subtractive hybridization (SSH) approach, using the PCR-Select Subtractive Hybridization Kit (Clontech, CA, USA). For SSH library construction, 2 g of systemic leaves was harvested from mock- inoculated and ChiLCV-infected plants at 21 dpi. For library construction, 2 µg of the total mRNA from ChiLCV-inoculated plants at 21 dpi was used as the "tester." Similarly, for the "driver" sample, 2 µg of total mRNA from mock-inoculated plants at the same time point was used. The subtracted library was cloned into the pGEM-T easy vector (Promega, Madison, USA), and subsequently, clones were transformed into *Escherichia coli* strain DH5α (Invitrogen, CA, USA). A total of 480 colonies were screened and sequenced using M13 forward and reverse primers.

Data analysis

Annotation of the sequences was performed on using three databases such as Sol genomics Network (<http://solgenomics.net/>), NCBI, and TAIR. BlastX information was further used to perform second BlastX, and the most closely related sequence was used to carry out BLASTP on TAIR (www.arabidopsis.org). Accession numbers, E-value ($\leq 1e-5$), and organism names were recorded with their biological and molecular functions. A pie chart representing percentage of expressed sequence tags (ESTs) on the basis of their predicted function was drawn.

Reverse northern blotting

A total of 231 unique ESTs obtained through SSH were used for reverse northern blotting for further validation of subtracted library following the method described by Sahu et al. (2010). Actin gene was spotted as internal control to normalize the signals of two different blots corresponding to ChiLCV-infected and to mock-treated resistant variety. A

PCR product of the neomycin phosphotransferase II (NPTII) gene (Sahu et al. 2010) using primer sequences (5'-TTTCTCCCAATCAGGCTTG-3' and 5'-TCAGGCTCTTTCACCTCATC-3') was spotted as negative control. Total RNA from mock-inoculated and ChiLCV-infected plants (10 µg) was converted into radiolabeled cDNA probe using SuperScript III First-Strand Synthesis System (Invitrogen, CA, USA) following manufacturer's protocol. Hybridization was performed at 60 °C for 16 h. The first washing was carried out at room temperature for 15 min with 2× SSC and 0.2 % SDS followed by second washing with 1× SSC and 0.5 % SDS at 65 °C for 15 min. Images were developed and analyzed using a phosphor image system (Typhoon; GE Healthcare, Little Chalfont, UK).

Expression analysis by SOTA

The intensity of each spot generated from northern blot assays was quantified using the Quantity One software (Bio-Rad, CA, USA). The background value was subtracted followed by normalization using the intensity of internal control (actin). Expression profiles of the genes in ChiLCV-infected and mock-inoculated resistant variety Punjab Lal were analyzed with the hierarchical self-organization tree algorithm (SOTA) clustering. SOTA was constructed through the log-transformed fold expression values, across four time points using Multi Experiment Viewer software (The Institute for Genome Research; <http://www.tm4.org/mev.html>).

Protein interactome network

AGI codes of all the ESTs identified in SSH library were retrieved from Arabidopsis database (TAIR), and these codes were used to develop a protein interactome network on STRING (www.string-db.org) and PAIR (<http://www.cls.zju.edu.cn/pair/help/introduction.pair>).

qRT-PCR analysis of host gene expression and viral DNA accumulation

In order to reduce variation between sampling of leaves and plants, the uppermost two leaves were harvested. For evaluation of expression, three independent biological as well as technical replicates of samples (total RNA from biological replicate 1) were subjected to quantitative RT-PCR (qRT-PCR) analysis. For each biological replicate, total RNA was extracted from pooled virus-infected or mock-inoculated leaves at 7, 14, 21, and 28 dpi using Tri-reagent (SIGMA, St Louis, USA) following manufacturer's instructions. Primers for qRT-PCR were designed using PRIMER3 software (Supplementary Table S1). PCR reactions were carried out in 96-well plates using SYBR green master mix (Applied Biosystem, CA, USA)

at following PCR conditions: 94 °C for 10 min, 94 °C for 30 s, 55 °C for 20 s, and 72 °C for 20 s for 40 cycles. qRT-PCR was carried out for three biological samples, and each time three technical replicates were taken for expression analysis of each gene for the aforesaid time point for both mock-inoculated and virus infected plants.

For the comparative analysis of accumulation of viral genome in the resistant and susceptible plants, qRT-PCR was performed using 500 ng of total DNA isolated from the two uppermost leaves. The reaction mixture contained 1× SYBR Green master mix (Applied Biosystem, Foster City, CA, USA) with 100 nM of forward primer 5' GAATTCATGTGGGATCCATTAGTAAACGAG 3' and reverse primer 5' AAGCTTGGGAACATCTGGACTTCTGTAC 3'. The PCR program consisted of initial denaturation at 94 °C for 5 min, followed by 40 cycles of denaturation at 94 °C for 20 s, annealing at 55 °C for 30 s, and extension at 72 °C for 30 s. Actin was taken as internal control. The actin primer sequence is mentioned in Supplementary Table S1. Ct values of the genes or viral DNA were normalized with internal control, and for comparison of expression analysis, $\Delta\Delta C_t$ values were used to make relative expression graph using GraphPad PRISM software (www.graphpad.com).

Results

Infectivity analysis of ChiLCV in resistant chilli plant

Resistant (Punjab Lal) and susceptible (Kashi Anmol) chilli varieties were inoculated with infectious tandem repeats of ChiLCV by agro-inoculation, and levels of viral accumulation were compared by PCR analysis. The ChiLCV-resistant variety Punjab Lal showed accumulation of viral DNA at 7 and 14 dpi which drastically reduced to approximately one fourth at 21 dpi. ChiLCV DNA was barely detectable at 28 dpi. In contrast, the susceptible chilli

variety Kashi Anmol showed a detectable level of viral DNA until 28 dpi (Fig. 1a, b). To identify the resistant factors, Punjab Lal was selected for further experimentations.

Sequencing and annotation of differentially expressed ESTs by SSH

SSH was performed between mock- and ChiLCV-infected resistant chilli plants. A total of 480 EST clones were screened and sequenced. From the raw data, vector sequences were removed using VecScreen software (www.ncbi.nlm.nih.gov/VecScreen). The remaining 231 non-redundant sequences were searched for homology using the Sol Genomics Network (<http://solgenomics.net>; Supplementary Table S2). Further, nucleotide to nucleotide BLAST (BLASTN) and nucleotide 6-frame translation-protein BLAST (BLASTX) were carried out using NCBI (<http://blast.ncbi.nlm.nih.gov/Blast.cgi>) and TAIR (<https://www.arabidopsis.org/Blast/>) databases to retrieve sequence information including accession no, E-value, and putative biological and molecular function of each EST (Supplementary Table S3).

Identification and classification of ChiLCV responsive genes in resistant variety

The blast results of 231 non-redundant clones revealed that 17 % of the ESTs shared homology with genes involved in chromatin organization, transcription, and translation whereas 20 % ESTs showed homology with genes involved either directly or indirectly in metabolic processes (Fig. 2). Apart from these, other transcripts indicated considerable degree of homology with genes involved in different cellular and molecular processes of the host such as defense response (3 %), growth and development (7 %), transport (7 %), stress response (3 %), membrane protein

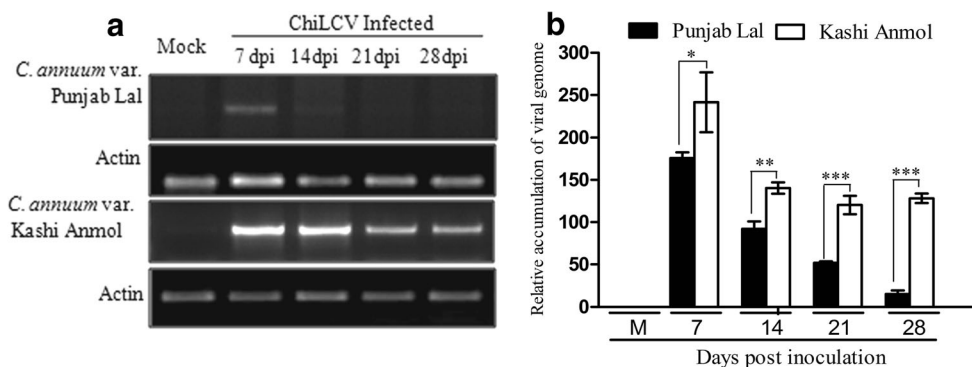


Fig. 1 Comparative accumulation of ChiLCV DNA in the resistant and the susceptible chilli variety. **a** PCR using primers for specific detection of the ChiLCV AC1 ORF (1086 nt). **b** Quantitative real-time PCR of relative accumulation of ChiLCV DNA in the resistant and susceptible chilli

varieties. Asterisk indicates significant difference in expression level of the viral genome in two varieties as analyzed by Student's *t* test (* $P=0.034$; ** $P=0.02$; *** $P<0.001$)

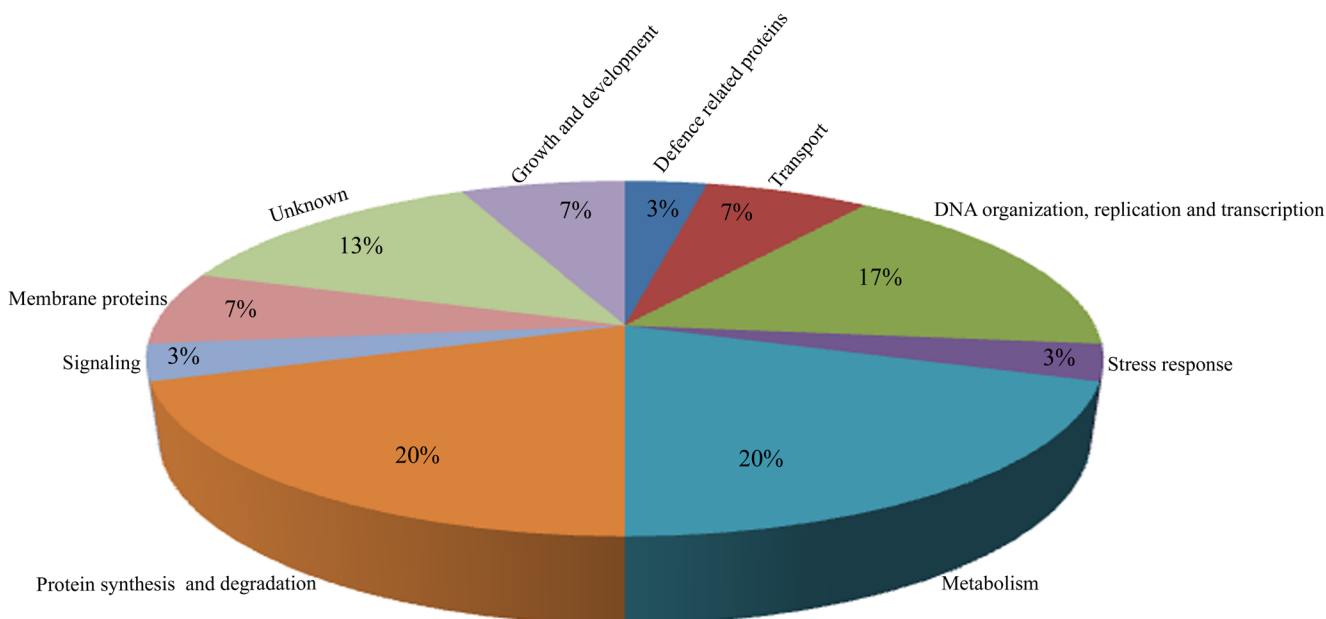


Fig. 2 Graphical representation of annotation of ChiLCV-responsive ESTs of *C. annuum* var. Punjab Lal. The sequences were checked for redundancy, and after sorting out, 231 unique EST sequences were searched for homology using BLASTN and BLASTX on the NCBI

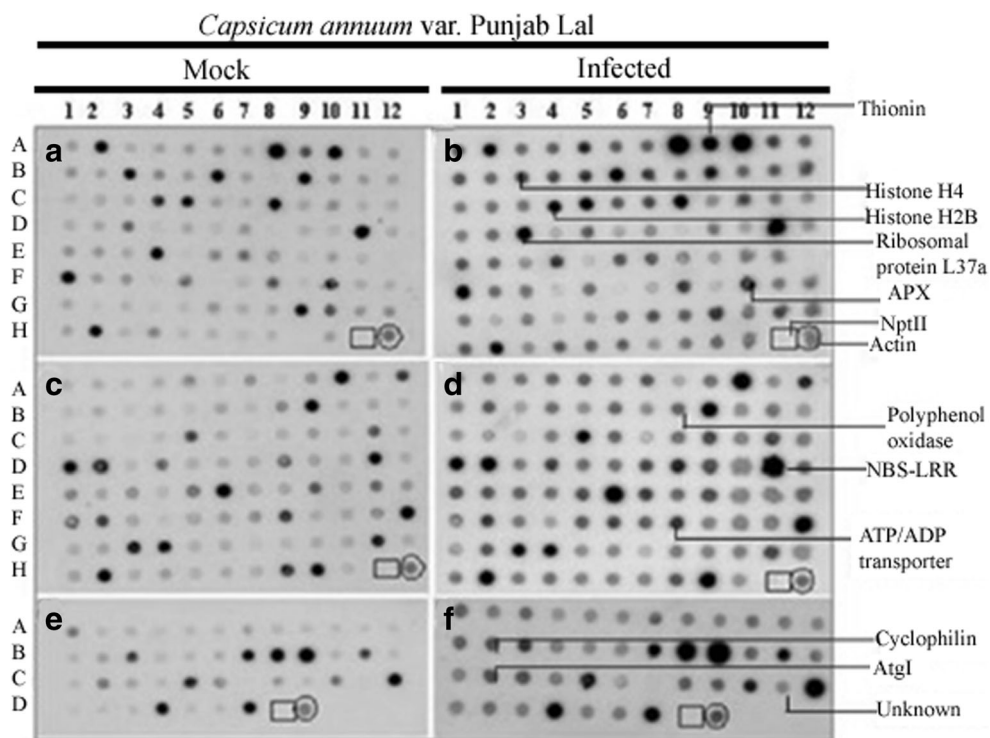
database. Genes were annotated and categorized on the basis of their putative biological functions. The pie charts illustrate the categorization and relative percentage of ESTs showing homology with known genes

(7 %), signaling (3 %), and protein degradation (20 %). Due to lack of complete annotation of plant genomes, functions could not be predicted for ~13 % of the ESTs (Fig. 2). The transcriptome analysis in resistant chilli plants provides the first evidence about the probable candidate gene(s) conferring natural resistance against ChiLCV.

Expression analysis of the non-redundant transcripts through reverse northern approach

Reverse northern was performed using radiolabeled cDNA prepared from mRNA of mock-inoculated and virus-infected plant samples (Fig. 3). Results indicated alteration in the

Fig. 3 Reverse northern blotting to validate subtractive hybridization results. PCR products were spotted onto a nylon membrane which was subsequently hybridized with radioactive cDNA prepared from mRNA of mock- and ChiLCV-infected plants. Intensity of the spots was quantified by Bio-Rad Quantity One software (BIORAD, CA, USA). Actin was used as internal control (in circle). *Npt* II was selected as negative control (in square). A few ESTs are marked at their respective DNA spots by the name of encoded proteins. For example, *D3* (blot B) indicates ribosomal protein L37a



expression of different genes belonging to various functional categories (Table 1). Basal defense-related genes such as thionin-like showed >5-fold upregulation, whereas a resistance gene for a nucleotide-binding site leucine-rich repeat (NBS-LRR) protein showed >8-fold enhanced expression in Punjab Lal upon ChiLCV infection in comparison to mock plants (Table 1). A few proteins involved in non-specific defense against this pathogen also showed enhanced level of expression in resistant chilli plants. For example, the genes

for polyphenol oxidase and ascorbate peroxidase were found to be upregulated (>7-fold), in the resistant variety as compared to mock-treated chilli plants (Table 1). Apart from these, genes for proteins involved in transport pathways such as precursor of lipid transfer proteins and ATP/ADP transporter proteins also showed elevated (>2-fold) expression in the resistant variety of chilli. ChiLCV also induced expression of genes involved in DNA organization, replication, and transcription. For example, histone H4 and histone H1E transcript

Table 1 Selected ESTs in the resistant chilli variety Punjab Lal upregulated upon ChiLCV infection

Annotation	Organism	E-value	Fold upregulation
<i>Defense-related proteins</i>			
Thionin-like protein	<i>Capsicum annuum</i>	3.00E-17	5.22
NBS-LRR-resistant protein	<i>Populus trichocarpa</i>	0	8.13
Polyphenol oxidase	<i>Nicotiana tabacum</i>	3.00E-24	7.44
Cytosolic ascorbate peroxidase	<i>C. annuum</i>	4.00E-86	7.36
Lipid transfer protein	<i>Nicotiana glauca</i>	6.00E-47	2.27
<i>Transport/signaling</i>			
ATP/ADP transporter	<i>Ricinus communis</i>	1.00E-69	2.76
Putative Ran/TC4 protein	<i>Capsicum chinense</i>	2.00E-10	3.13
N-Acetyltransferase mak3	<i>R. communis</i>	3.00E-29	1.73
<i>DNA organization/replication/transcription</i>			
Histone H4	<i>C. annuum</i>	0	6.634
Histone H1E	<i>Arabidopsis lyrata</i>	1.00E-47	5.26
DNA topoisomerase II	<i>N. tabacum</i>	1.00E-46	2.14
<i>Stress response</i>			
Stress-related protein 1 (SRP1)	<i>C. annuum</i>	6.00E-47	1.19
<i>Metabolism</i>			
Xyloglucan endotransglycosylase	<i>Solanum lycopersicum</i>	1.00E-32	2.77
Ribulosebiphosphate carboxylase activase	<i>N. tabacum</i>	7.00E-20	2.88
<i>Protein synthesis/degradation</i>			
60S ribosomal protein L37a	<i>C. chinense</i>	1.00E-24	5.45
Ubiquitin-conjugating protein	<i>C. annuum</i>	6.00E-04	2.5
Ribosomal protein L19	<i>C. annuum</i>	3.00E-23	9.79
Skp1	<i>C. annuum</i>	1.00E-114	2
Cyclophilin	<i>C. annuum</i>	1.00E-20	4.36
60S acidic ribosomal protein P0	<i>A. thaliana</i>	4.00E-50	4.02
Serine protease inhibitor-I	<i>Nicotiana sylvestris</i>	E-125	2.27
<i>Membrane proteins</i>			
TET9 (Tetraspanin 9)	<i>A. thaliana</i>	7.00E-05	1.67
Atg1 (<i>Arabidopsis</i> transmembrane protein G1p-related 1)	<i>A. thaliana</i>	1.00E-23	3.14
<i>Growth and development</i>			
Sp1L	<i>R. communis</i>	4.00E-28	3.81
Exostosin family protein	<i>A. thaliana</i>	2.00E-20	1.76
<i>Unknown</i>			
Conserved hypothetical protein	<i>R. communis</i>	3.00E-50	7.01
Unknown	–	–	5.01
JCVI-FLGm 20G6 unknown	–	–	2.13

levels were upregulated (up to 6- and 5-fold, respectively), whereas the gene for a topoisomerase, an enzyme actively involved in DNA replication, was ~2.1-fold upregulated. Moreover, ChiLCV infection also resulted in minor increase in the genes for expression of stress-related proteins (Table 1). Expression of an N-acetyltransferase gene was found to be altered (~1.7-fold) in virus-infected plants (Table 1). Metabolism-related genes also exhibited upregulation in Punjab Lal upon ChiLCV infection. Expression of genes for xyloglucan endo transglycosylase/hydrolase and ribulose biphosphate carboxylase activase were elevated by more than 2.5-fold. Protein metabolism plays crucial role during plant-virus interaction. This notion was supported by pronounced transcript accumulation of genes of ubiquitin conjugating protein (~2.5-fold), ribosomal protein L37 (~5-fold), ribosomal protein L19 (~9-fold), S-phase kinase-associated protein 1 (SKP1; ~2.0-fold), and cylophilin (~4-fold).

Several host proteins assist nucleocytoplasmic trafficking of viral genome. Altered level of these proteins is expected to occur during geminivirus pathogenesis. Ran is one of the karyophilic proteins involved in nucleocytoplasmic transport (Sacco et al. 2007). Interestingly, a >3-fold enhanced expression of Ran was observed in infected resistant chilli plants. The expression level of the gene for Atg1 (*Arabidopsis* transmembrane protein G1p-related 1), a membrane protein identified in SSH library, was upregulated by more than 3-fold. Reverse northern results suggested upregulation of several genes which did not share homology with any of the genes available on NCBI database and TAIR database. In addition, enhanced expression of genes for a hypothetical protein and proteins with unknown functions were also observed in this study (Table 1).

Expression analysis of ESTs by SOTA

SOTA is a system of hierarchical cluster analysis for global expression of data obtained from SSH. It is based on the standard statistical algorithms to analyze and arrange the genes according to the similarity in pattern of gene expression. The output is represented graphically which conveys the clustering (The Institute for Genome Research; <http://www.tm4.org/mev.html>). The expression values were selected for SOTA analysis which generated 11 groups on the basis of the hierarchical clustering method using the correlation coefficient of average linkage of the log-transformed ratio and according to the distance of correlation (Fig. 4a). The data sets were log-transformed to the base 2 in order to normalize the scale of expression and to reduce the noise (Jain and Chattopadhyay 2010). The color pattern of the ESTs in group no 2 indicated maximum alteration in gene expression. Further, 11 centroid images were also created using experimental viewer software (Fig. 4b). In centroid image group no 2, ESTs depicted similar expression pattern like SOTA, which was

higher (above mean line) in the virus-inoculated resistant variety and lower (below mean line) in the mock-inoculated resistant variety. The accession number of the genes and details of SOTA ID are provided in Supplementary Table S4.

Construction of a ChiLCV-responsive protein interactome network

ESTs identified in SSH library were annotated using Arabidopsis database (TAIR), and corresponding AGI codes were used to generate an interactome on STRING (Fig. 5) and PAIR (Supplementary Table S5). STRING generated a comprehensive protein interactome network. The maximum number of interactions was observed among proteins involved in ribosome assembly and translation, transcription, proteolysis, stress and chloroplast, and DNA organization/replication. On PAIR, a total of 158 proteins were identified out of 231 AGI codes which eventually generated a network exhibiting 1000 interactions. These interactions were predicted by a support vector machine (SVM) model that would integrate several indirect evidences for interaction such as domain interactions, gene co-expressions, GO annotations, phylogenetic profile similarities, co-localizations, and interologs (Lin et al. 2009). SVM scores were used to predict the level of confidence, the direct output of the SVM prediction function. Interactions showing a >1 SVM value were considered as equally confident (Supplementary Table S5). A higher SVM score indicated more confident prediction whereas a negative SVM score ruled out interaction between proteins. Out of 1000, some of the interactions showed a SVM score >2, an indication of higher confidence of computational interaction (Supplementary Table S5). Several interactions displayed either 1 or less than 1 SVM scores (Supplementary Table S5).

Comparative gene expression analysis in resistant and susceptible chilli varieties

Reverse northern and protein interactome mapping generated comprehensive information about the transcriptome changes occurring in a resistant chilli variety following ChiLCV infection. This information was further used to explore probable resistant factor(s) in the resistant chilli variety. On the basis of reverse northern and SOTA, genes showing significant alteration in expression were selected for comparative expression analysis between resistant (Punjab Lal) and susceptible (Kashi Anmol) chilli varieties.

ChiLCV infection resulted in upregulation of a NBS-LRR group of plant resistant gene (Fig. 6a). At early stage of infection, NBS-LRR transcript accumulation in the resistant variety was lower than in the susceptible variety. Later, a contrasting difference (>4-fold) in the expression of the NBS-LRR gene was observed in the resistant variety Punjab Lal at 21 dpi (Fig. 6a). The expression pattern of a polyphenol oxidase gene

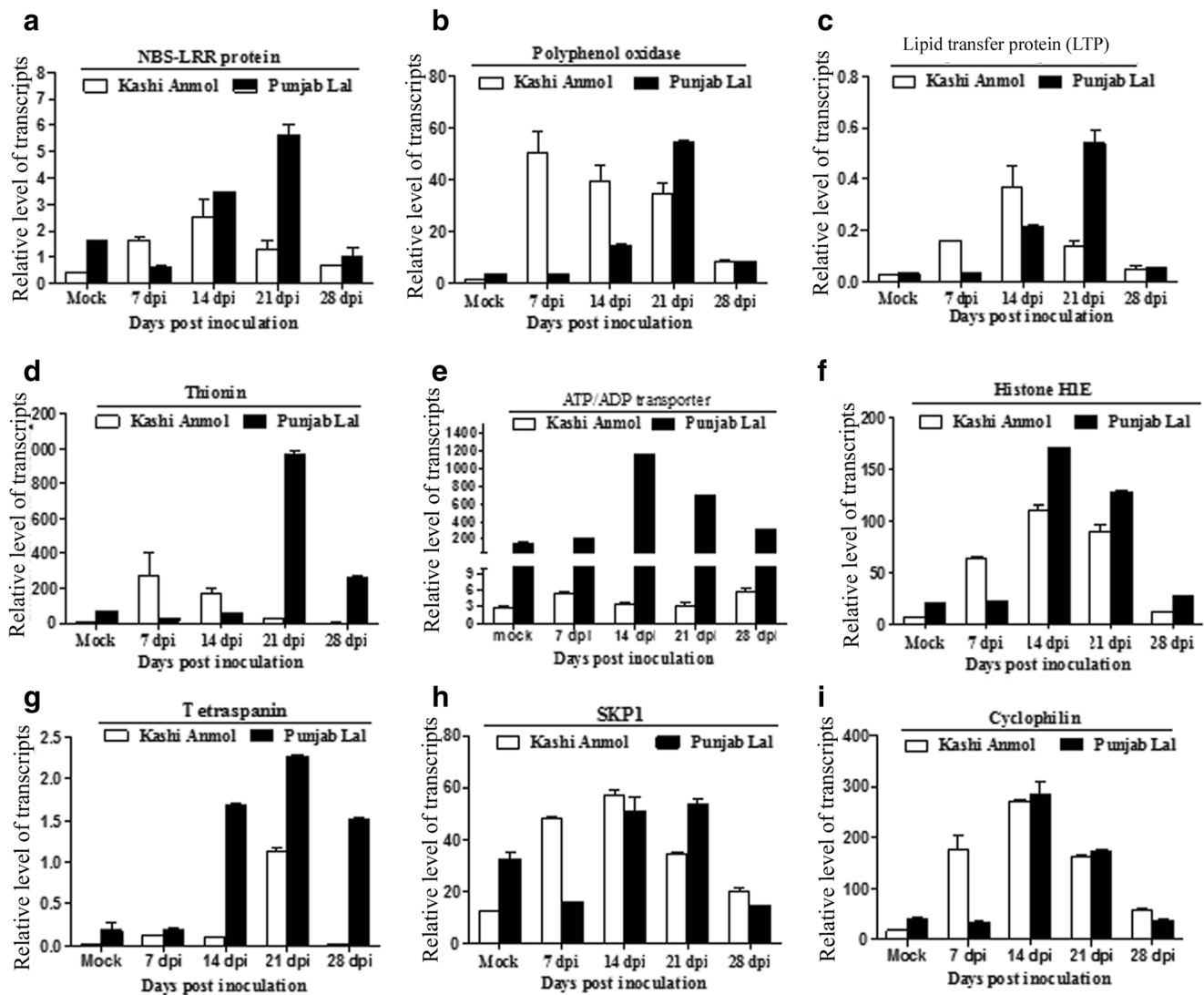


Fig. 6 Comparative expression analysis of host genes during ChiLCV infection. Relative levels of gene expression were studied in resistant (Punjab Lal) and susceptible (Kashi Anmol) chilli plants at 7, 14, 21,

and 28 dpi. **a** NBS-LRR. **b** Polyphenol oxidase. **c** Lipid transfer protein. **d** Thionin. **e** ATP/ADP transporter. **f** Histone H1E. **g** Tetraspanin. **h** SKP1. **i** Cyclophilin

(4-fold) of expression of the gene for LTP compared to the susceptible one. Analysis of thionin gene expression in chilli varieties revealed a 10-fold increase in the susceptible var. Kashi Anmol at 7 dpi which was further reduced to 2.3-fold at 14 dpi. Interestingly, at 21 dpi, the thionin gene expression was drastically increased (44-fold) in resistant chilli var. Punjab Lal. This elevated level of thionin gene expression was also steadily maintained at 28 dpi in the resistant plants (Fig. 6d). The thionin gene was reported to express at basal levels in plants, but transcripts are known to be accumulated in higher concentration following pathogen infection (Epple et al. 1997; Pelegrini and Franco 2005), and the protein product is considered as one of the PR (pathogenesis-related) proteins involved in maintaining innate plant defense.

The ATP/ADP transporter facilitates the transport of ATP into chloroplasts and mitochondria and is known to be preferentially expressed in stem and root rather than in mature leaves (Pebay-Peyroula et al. 2003; Reiser 2004). However, no direct or indirect evidence of involvement of the ATP/ADP transporter during any plant virus infection is currently available. Comparative expression analysis revealed that accumulation of its transcript was steadily higher in the resistant chilli variety compared to Kashi Anmol throughout the period of study (Fig. 6e). On the other hand, expression analysis of the genes for histone H1 (1.5-fold at 21 dpi) and tetraspanin (2-fold at 21 dpi) revealed elevated levels of expression in the resistant variety at 14 and 21 dpi (Fig. 6f, g). Interestingly, expression level of genes like for SKP1 and cyclophilin were comparatively similar in the leaves of both resistant and susceptible chilli varieties (Fig. 6h, i).

Discussion

Plants have evolved several specific and non-specific defense mechanisms, which are activated by the attack of diverse types of pathogens including viruses (Meyers et al. 2003). Resistant plants sense the pathogen with specific proteins (for example as encoded in *R* genes) and initiate defense response to limit pathogen infection. Viruses modulate the susceptible hosts and induce a permissive cellular environment to facilitate pathogenesis. ChiLCV, a monopartite begomovirus, is one of the devastating pathogens causing chilli leaf curl disease which has been reported to result in enormous economic losses worldwide especially in the Indian subcontinent (Chattopadhyay et al. 2008). Plant breeding techniques are the only available antiviral strategy for providing resistance to the plants, and the availability of a naturally resistant variety such as Punjab Lal has given a new dimension to decipher the mechanism of resistance in chilli against ChiLCV infection (Kumar et al. 2006).

During the plant-virus interaction, viruses affect several cellular and physiological machineries by altering the expression of the key genes (Sahu et al. 2010; Martin et al. 2013; Pierce and Rey 2013). In the present study, ChiLCV infection altered the expression of several host genes involved in different biological processes (Supplementary Table S2 and S3). It is hypothesized that upregulation in the expression of genes which are essential for ChiLCV replication, transcription, and movement at an early phase of infection may have some correlation with the resistance characteristics of chilli variety Punjab Lal. Subsequently, as the level of virus titer reached to threshold in the infected cells, a non-permissive host starts expressing defense-related genes. This may hamper the steps of viral pathogenesis (viz., replication, transcription, or movement of virus), as evidenced by drastic reduction of viral DNA at a later stage of infection (21 dpi) in resistant chilli plants.

Geminiviruses utilize host machineries for their transcription, translation, replication, and movement within permissive hosts. Resistant chilli plants express defense-related genes which are required for maintaining the fine tuning between other cellular pathways as evidenced by the ChiLCV-responsive protein interactome network. Both STRING and PAIR results revealed that all proteins identified in ChiLCV-infected resistant plants were involved in diverse cellular and physiological pathways. A maximum degree of interaction was observed among proteins involved in ribosome assembly and translation (P40, RPL17A, RPL37A, etc.). *Sweet potato feathery mottle virus* and *sweet potato chlorotic stunt virus* infection induced the expression of ribosomal protein genes in resistant sweet potato (McGregor et al. 2009). Alteration of ribosomal transcript levels was also observed in soybean plants infected with *soybean mosaic virus* (Babu et al. 2008). Indeed, upregulation of genes requires a highly active transcription machinery which in turn depends on an efficient

translation machinery. Presence of several ribosomal proteins and a high degree of interaction among them indicated that these proteins, probably, play a pivotal role during the host-virus interaction. Interaction among proteins involved in transcription, DNA organization/replication, and proteolysis, which are chloroplastic and stress-related, suggests a conserved role in virus-host interaction.

During the course of infection, both RNA and coat protein of *tobacco mosaic virus* (TMV) have been shown to be localized in the chloroplast. It was hypothesized that TMV coat protein was synthesized in the chloroplast by utilizing chloroplastic ribosomes and other proteins (Schoelz and Zaitlin 1989). Further, two host proteins ATP-synthase γ -subunit (AtpC) and rubisco activase (RCA) interacted with TMV-Rep protein (Bhat et al. 2013). Silencing of these genes resulted in enhanced susceptibility to TMV in *Nicotiana benthamiana*. These results indicated a role of both host-encoded proteins in a defense response against TMV. Another study revealed that the P3 protein encoded by *shallot yellow stripe virus* (onion isolate) physically interacted with the large subunit of the ribulose-1,5-bisphosphate carboxylase/oxygenase (RubisCO) protein in onion which affected normal functions of RubisCO leading to symptom development (Lin et al. 2011). Together, these results indicate that the interaction between chloroplastic proteins and viral proteins is a key feature of host-virus interaction process during viral pathogenesis or host defense response.

Microarray analysis of the *Arabidopsis* transcriptome in response to *cabbage leaf curl virus* (CaLCuV) infection uncovered 5365 genes differentially expressed in infected rosette leaves at 12 dpi. Data mining revealed that CaLCuV triggered a pathogen response via the salicylic acid pathway and induced expression of genes involved in programmed cell death, genotoxic stress, and DNA repair (Ascencio-Ibanez et al. 2008).

Further in this study, comparative gene expression analysis in resistant and susceptible chilli varieties indicated upregulation of defense-related genes upon ChiLCV infection. NBS-LRR is a conserved domain present in proteins involved in conferring resistance against viruses, bacteria, and insects (Meyers et al. 2003). During pathogen infection, elevated level of products of resistance genes has been shown to recognize the elicitors of the pathogen and initiate downstream defense signaling to block the pathogenesis (Whitham et al. 1996). To date, several *R* genes against bacteria and viruses have been isolated and characterized (Wan et al. 2012). The product of the *N* gene of tobacco is a member of the Toll-interleukin-1 receptor like nucleotide-binding site leucine-rich repeat (TIR-NBS-LRR) class of *R* genes which recognizes the replicase protein of TMV and induces a hypersensitive response to inhibit virus replication (Whitham et al. 1996). Several other genes for products with a conserved NBS-LRR domain have been identified from *Arabidopsis* (Gassmann et al. 1999;

Takahashi et al. 2002), tomato (Lauge et al. 1998), pepper (Wan et al. 2012), and potato (Bendahmane et al. 1999). In another study, a candidate resistance gene (for a protein CYR1) was found to be segregating with a resistant population of *Vigna mungo*. In silico analysis of the protein sequence of CYR1 reveals the presence of a conserved NBS-LRR domain which may assist in a potential interaction between CYR1 and coat protein of *mungbean yellow mosaic virus* (Maiti et al. 2012). However, in vivo and in vitro experimental evidences to support this hypothesis are presently lacking. The present study also highlights the active involvement of an NBS-LRR gene during ChiLCV infection in resistant chilli. Upon ChiLCV infection, expression of the NBS-LRR gene was upregulated >5-fold in the resistant variety of chilli, in comparison to the susceptible variety. At present, an NBS-LRR-mediated defense mechanism against ChiLCV is largely unknown and needs further experimental support to elucidate its role in conferring resistance.

Polyphenol oxidase (PPO) is a tetrameric copper containing 52–64-kDa protein (van Gelder et al. 1997), which possesses two sites for binding of oxygen containing aromatic compounds (Mayer 2006). PPO catalyzes the *o*-hydroxylation of phenols produced during an oxidative burst following a pathogen attack (Raj et al. 2006). Hence, it functions as a scavenger which protects the cell from damage due to reactive oxygen species and reactive phenolic molecules. Pathogen attack induces an activation of the defense machinery which also involves an oxidative burst to prevent the pathogen multiplication and spread (Fobert and Despres 2005; Torres and Dangl 2005). However, higher accumulation of reactive oxygen species may also cause cell damage and can interfere in several physiological and cellular processes (Jacobson 1996; Jones and Dangl 2006). As reported in various studies, PPO was shown to be involved in maintaining the basal defense against fungi, bacteria, and viruses (Constabel et al. 1995; Mayer 2006; Poiatti et al. 2009). Thus, an elevated level of PPO transcripts in the resistant chilli var. Punjab Lal may have a correlation with the activation of the basal defense following ChiLCV infection.

In the present study, upregulation of an ATP/ADP transporter in resistant chilli plants was initially observed by northern blotting and was further validated by qRT-PCR. Comparison of the expression of the ATP/ADP transporter gene revealed a persistent higher level in the resistant chilli variety. This ATP/ADP transporter catalyzes the highly specific transport of ATP across membranes (chloroplasts and mitochondria) in an exchange mode with ADP (Pebay-Peyroula et al. 2003; Reiser 2004). Little information is available indicating the role of the ATP/ADP transporter during plant-pathogen interaction. One of the studies indicated that the enhanced resistance of transgenic potato plants to *Erwinia carotovora* could be correlated with a reduced level of the ATP/ADP transporter 1 (AATP1) (Conrath et al. 2003). Further, it was

demonstrated that leaves of an AATP1 antisense transgenic plant produced an enhanced level of H₂O₂ and expressed defense-related genes which collectively delayed the appearance of disease symptoms (Conrath et al. 2003). In view of this, it could be hypothesized that during a plant-pathogen interaction, energy is required for both the partners. Activation of several defense and signaling machineries also requires efficient and incessant supply of energy.

Thionin, a small cysteine-rich highly basic protein having antimicrobial activity, is known to be involved in eliciting plant defense against several bacteria and fungi (Epple et al. 1997; Pelegrini and Franco 2005). Sequence analysis of ESTs sorted out in the SSH library of the resistant var. Punjab Lal showed similarity with γ -thionin of *Capsicum annuum* and defensin of *Solanum lycopersicum*. The role of γ -thionin has been elucidated in providing defense against a broad range of fungi (Terras et al. 1995). An elevated level of *PDF1.2* gene (which encodes for defensin) expression was observed in *N. benthamiana* plants infected with TMV (Mitter et al. 1998). Therefore, the enhanced expression of γ -thionin indicates a possible role of this protein in imparting basal defense responses in resistant chilli plants.

As obligate parasites, geminiviruses depend on host proteins for formation of minichromosomes, replication, transcription, and symptom development. An enhanced accumulation of histone H1 transcripts is probably a prerequisite for the viral minichromosome formation. Recent works have emphasized the role of histones in geminivirus pathogenesis. Studies on the movement of *bean dwarf mosaic virus* revealed an interaction of histone H3 with viral coat protein and movement protein. H3 was found to be localized in the cell cytoplasm and cell periphery along with movement protein (Zhou et al. 2011). Recently, deep transcriptome sequencing methods were employed for the analysis of transcriptomes in mock, symptomatic, and recovered pepper leaves upon *pepper golden mosaic virus* infection. Other studies also suggested differential expression of several genes encoding histones such as histone H4 (Gongora-Castillo et al. 2012).

S-phase kinase-associated protein 1 (SKP1) is a crucial subunit of the proteasome system and is required for the maintenance of protein homeostasis (Bai et al. 1996). Cyclophilin is a prolyl isomerase which catalyzes cis–trans isomerization of the peptidyl–prolyl bonds in proteins that determines the structure, function, and localization of candidate proteins (Romano et al. 2004). Results on expression in this study implicate a probable involvement of cyclophilin in proper folding and organization of host and viral proteins. Similar expression patterns of SKP1 and cyclophilin in resistant and susceptible plants suggest a conserved role in determining structure and function of proteins.

We have carried out a global transcriptome analysis of a ChiLCV-resistant chilli variety and have generated a comprehensive knowledge on ChiLCV-responsive genes. Results

indicate a cumulative and coordinated involvement of several cellular pathways during the defense response against ChiLCV. Thus, the present study will be useful to understand the molecular basis of host-virus infection and to develop durable resistant strategies against geminiviruses, particularly ChiLCV in the future.

Acknowledgments Nirbhay Kushwaha thanks the Council of Scientific and Industrial Research for providing a senior research fellowship. The authors gratefully acknowledge the financial support from the Department of Biotechnology, India (grant no. BT/PR/6504/AGII/106/878/2012). We thank Dr. V. K. Sharma and Ms. Mansi Bhardwaj for their suggestions and critical comments on the manuscript.

Conflict of interest The authors declare that they do not have any conflict of interest.

References

- Ascencio-Ibanez JT, Sozzani R, Lee TJ, Chu TM, Wolfinger RD, Cella R, Hanley-Bowdoin L (2008) Global analysis of *Arabidopsis* gene expression uncovers a complex array of changes impacting pathogen response and cell cycle during geminivirus infection. *Plant Physiol* 148:436–454
- Babu M, Gagariyova AG, Brandle JE, Wang A (2008) Association of the transcriptional response of soybean plants with *Soybean mosaic virus* systemic infection. *J Gen Virol* 89:1069–1080
- Bai C, Sen P, Hofmann K, Ma L, Goebel M, Harper JW, Elledge SJ (1996) SKP1 connects cell cycle regulators to the ubiquitin proteolysis machinery through a novel motif, the F-box. *Cell* 86:263–274
- Bendahmane A, Kanyuka K, Baulcombe DC (1999) The *Rx* gene from potato controls separate virus resistance and cell death responses. *Plant Cell* 11:781–792
- Bhat S, Folimonova SY, Cole AB, Ballard KD, Lei Z, Watson BS, Sumner LW, Nelson RS (2013) Influence of host chloroplast proteins on *Tobacco mosaic virus* accumulation and intercellular movement. *Plant Physiol* 161:134–147
- Bridson RW, Bull SE, Amin I, Idris AM, Mansoor S, Bedford ID, Dhawan P, Rishi N, Siwatch SS, Abdel-Salam AM, Brown JK, Zafar Y, Markham PG (2003) Diversity of DNA β , a satellite molecule associated with some monopartite begomoviruses. *Virology* 312:106–121
- Chattopadhyay B, Singh AK, Yadav T, Fauquet CM, Sarin NB, Chakraborty S (2008) Infectivity of the cloned components of a begomovirus: DNA β complex causing chilli leaf curl disease in India. *Arch Virol* 153:533–539
- Conrath U, Linke C, Jeblick W, Geigenberger P, Quick WP, Neuhaus HE (2003) Enhanced resistance to *Phytophthora infestans* and *Alternaria solani* in leaves and tubers, respectively, of potato plants with decreased activity of the plastidic ATP/ADP transporter. *Planta* 217:75–83
- Constabel CP, Bergey DR, Ryan CA (1995) Systemin activates synthesis of wound-inducible tomato leaf polyphenol oxidase via the octadecanoid defense signaling pathway. *Proc Natl Acad Sci U S A* 92:407–411
- Czosnek H, Eybishtz A, Sade D, Gorovits R, Sobol I, Bejarano E, Rosas-Diaz T, Lozano-Duran R (2013) Discovering host genes involved in the infection by the *Tomato yellow leaf curl virus* complex and in the establishment of resistance to the virus using Tobacco Rattle Virus-based post transcriptional gene silencing. *Viruses* 5:998–1022
- Dellaporta SL, Wood J, Hicks JB (1983) A plant DNA miniprep: Version II. *Plant Mol Biol Rep* 1:19–21
- Epple P, Apel K, Bohlmann H (1997) Overexpression of an endogenous thionin enhances resistance of *Arabidopsis* against *Fusarium oxysporum*. *Plant Cell* 9:509–520
- Flor HH (1971) Current status of the gene-for-gene concept. *Ann Rev Phytopathol* 9:275–296
- Fobert PR, Despres C (2005) Redox control of systemic acquired resistance. *Curr Opin Plant Biol* 8:378–382
- Fondong VN (2013) Geminivirus protein structure and function. *Mol Plant Pathol* 14:635–649
- Gassmann W, Hinsch ME, Staskawicz BJ (1999) The *Arabidopsis RPS4* bacterial-resistance gene is a member of the TIR-NBS-LRR family of disease-resistance genes. *Plant J* 20:265–277
- Gongora-Castillo E, Ibarra-Laclette E, Trejo-Saavedra DL, Rivera-Bustamante RF (2012) Transcriptome analysis of symptomatic and recovered leaves of geminivirus-infected pepper (*Capsicum annuum*). *Virol J* 9:295
- Hanley-Bowdoin L, Settledge SB, Orozco BM, Nagar S, Robertson D (2000) Geminiviruses: models for plant DNA replication, transcription, and cell cycle regulation. *Crit Rev Biochem Mol Biol* 35:105–140
- Hofmann C, Niehl A, Sambade A, Steinmetz A, Heinlein M (2009) Inhibition of *Tobacco mosaic virus* movement by expression of an actin-binding protein. *Plant Physiol* 149:1810–1823
- Ishibashi K, Masuda K, Naito S, Meshi T, Ishikawa M (2007) An inhibitor of viral RNA replication is encoded by a plant resistance gene. *Proc Natl Acad Sci U S A* 104:13833–13838
- Jacobson MD (1996) Reactive oxygen species and programmed cell death. *Trends Biochem Sci* 21:83–86
- Jain D, Chattopadhyay D (2010) Analysis of gene expression in response to water deficit of chickpea (*Cicer arietinum*L.) varieties differing in drought tolerance. *BMC Plant Biol* 10:24
- Jones JD, Dangl JL (2006) The plant immune system. *Nature* 444:323–329
- Kachroo P, Chandra-Shekhara AC, Klessig DF (2006) Plant signal transduction and defense against viral pathogens. *Adv Virus Res* 66:161–191
- Kang BC, Yeom I, Jahn MM (2005) Genetics of plant virus resistance. *Annu Rev Phytopathol* 43:581–621
- Kumar S, Kumar S, Singh M, Singh AK, Rai M (2006) Identification of host plant resistance to *Pepper leaf curl virus* in chilli (*Capsicum species*). *Sci Horticult* 110:359–361
- Lauge R, Joosten MH, Haanstra JP, Goodwin PH, Lindhout P, de Wit PJ (1998) Successful search for a resistance gene in tomato targeted against a virulence factor of a fungal pathogen. *Proc Natl Acad Sci U S A* 95:9014–9018
- Lazarowitz SG, Wu LC, Rogers SG, Elmer JS (1992) Sequence-specific interaction with the viral AL1 protein identifies a geminivirus DNA replication origin. *Plant Cell* 4:799–809
- Lin M, Hu B, Chen L, Sun P, Fan Y, Wu P, Chen X (2009) Computational identification of potential molecular interactions in *Arabidopsis*. *Plant Physiol* 151:34–46
- Lin L, Luo Z, Yan F, Lu Y, Zheng H, Chen J (2011) Interaction between potyvirus P3 and ribulose-1,5-bisphosphate carboxylase/oxygenase (RubisCO) of host plants. *Virus Genes* 43:90–92
- Lozano-Duran R, Rosas-Diaz T, Gusmaroli G, Luna AP, Taconnat L, Deng XW, Bejarano ER (2011) Geminiviruses subvert ubiquitination by altering CSN-mediated derubylation of SCF E3 ligase complexes and inhibit jasmonate signaling in *Arabidopsis thaliana*. *Plant Cell* 23:1014–1032
- Maiti S, Pal S, Pal A (2012) Isolation, characterization, and structure analysis of a non-TIR-NBS-LRR encoding candidate gene from MYMIV-resistant *Vigna mungo*. *Mol Biotechnol* 52:217–233
- Marino D, Peeters N, Rivas S (2012) Ubiquitination during plant immune signaling. *Plant Physiol* 160:15–27

- Martin DP, Chen T, Lv Y, Zhao T, Li N, Yang Y, Yu W, He X, Liu T, Zhang B (2013) comparative transcriptome profiling of a resistant vs. susceptible tomato (*Solanum lycopersicum*) cultivar in response to infection by *Tomato yellow leaf curl virus*. PLoS ONE 8:e80816
- Mayer AM (2006) Polyphenol oxidases in plants and fungi: going places? A review. Phytochem 67:2318–2331
- Mc Gregor CE, Miano DW, LaBonte DR (2009) Differential gene expression of resistant and susceptible sweet potato plants after infection with the causal agents of sweet potato virus disease. J Amer Soc Hort Sci 134:658–666
- Meyers BC, Kozik A, Griego A, Kuang H, Michelmore RW (2003) Genome-wide analysis of NBS-LRR-encoding genes in *Arabidopsis*. Plant Cell 15:809–834
- Mitter N, Kazan K, Way HM, Broekaert WF, Manners JM (1998) Systemic induction of an *Arabidopsis* plant defensin gene promoter by *Tobacco mosaic virus* and jasmonic acid in transgenic tobacco. Plant Sci 136:169–180
- Pebay-Peyroula E, Dahout-Gonzalez C, Kahn R, Trezeguet V, Lauquin GJ, Brandolin G (2003) Structure of mitochondrial ADP/ATP carrier in complex with carboxyatractyloside. Nature 426:39–44
- Pelegriani PB, Franco OL (2005) Plant γ -thionins: novel insights on the mechanism of action of a multi-functional class of defense proteins. Int J Biochem Cell Biol 37:2239–2253
- Pierce EJ, Rey MEC (2013) Assessing global transcriptome changes in response to *South African cassava mosaic virus* [ZA-99] infection in susceptible *Arabidopsis thaliana*. PLoS ONE 8(6):e67534
- Poiatti VA, Dalmas FR, Astarita LV (2009) Defense mechanisms of *Solanum tuberosum* L. in response to attack by plant-pathogenic bacteria. Biol Res 42:205–215
- Raj SN, Sarosh BR, Shetty HS (2006) Induction and accumulation of polyphenol oxidase activities as implicated in development of resistance against pearl millet downy mildew disease. Funct Plant Biol 33:563
- Raja P, Sanville BC, Buchmann RC, Bisaro DM (2008) Viral genome methylation as an epigenetic defense against geminiviruses. J Virol 82:8997–9007
- Reiser J (2004) Molecular physiological analysis of the two plastidic ATP/ADP transporters from *Arabidopsis*. Plant Physiol 136:3524–3536
- Romano PGN, Horton P, Gray JE (2004) The *Arabidopsis* cyclophilin gene family. Plant Physiol 134:1268–1282
- Rowe HC, Kliebenstein DJ (2008) Complex genetics control natural variation in *Arabidopsis thaliana* resistance to *Botrytis cinerea*. Genetics 180:2237–2250
- Sacco MA, Mansoor S, Moffett P (2007) A RanGAP protein physically interacts with the NB-LRR protein Rx, and is required for Rx-mediated viral resistance. Plant J 52:82–93
- Sahu PP, Rai NK, Chakraborty S, Singh M, Chandrappa PH, Ramesh B, Chattopadhyay D, Prasad M (2010) Tomato cultivar tolerant to *Tomato leaf curl New Delhi virus* infection induces virus-specific short interfering RNA accumulation and defence-associated host gene expression. Mol Plant Pathol 11:531–544
- Sahu PP, Sharma N, Puranik S, Muthamilarasan M, Prasad M (2014a) Involvement of host regulatory pathways during geminivirus infection: a novel platform for generating durable resistance. Funct Integr Genomics 14:47–58
- Sahu PP, Sharma N, Puranik S, Prasad M (2014b) Post-transcriptional and epigenetic arms of RNA silencing: a defense machinery of naturally tolerant tomato plant against *Tomato leaf curl New Delhi virus*. Plant Mol Biol Rep 32:1015–1029
- Schoelz JE, Zaitlin M (1989) *Tobacco mosaic virus* RNA enters chloroplasts in vivo. Proc Natl Acad Sci U S A 86:4496–4500
- Senanayake DMJB, Mandal B, Lodha S, Varma A (2007) First report of *Chilli leaf curl virus* affecting chilli in India. Plant Pathol 56:343–343
- Shukla R, Dalal S, Malathi VG (2013) Suppressors of RNA silencing encoded by tomato leaf curl betasatellites. J Biosci 38:45–51
- Soosaar JL, Burch-Smith TM, Dinesh-Kumar SP (2005) Mechanisms of plant resistance to viruses. Nat Rev Microbiol 3:789–798
- Takahashi H, Miller J, Nozaki Y, Takeda M, Shah J, Hase S, Ikegami M, Ehara Y, Dinesh-Kumar SP (2002) RCY1, an *Arabidopsis thaliana* RPP8/HRT family resistance gene, conferring resistance to cucumber mosaic virus requires salicylic acid, ethylene and a novel signal transduction mechanism. Plant J 32:655–667
- Terras FR, Eggermont K, Kovaleva V, Raikhel NV, Osborn RW, Kester A, Rees SB, Torrekens S, Van Leuven F, Vanderleyden J (1995) Small cysteine-rich antifungal proteins from radish: their role in host defense. Plant Cell 7:573–588
- Torres MA, Dangl JL (2005) Functions of the respiratory burst oxidase in biotic interactions, abiotic stress and development. Curr Opin Plant Biol 8:397–403
- van Gelder CW, Flurkey WH, Wichers HJ (1997) Sequence and structural features of plant and fungal tyrosinases. Phytochemistry 45:1309–1323
- Wan H, Yuan W, Ye Q, Wang R, Ruan M, Li Z, Zhou G, Yao Z, Zhao J, Liu S, Yang Y (2012) Analysis of TIR- and non-TIR-NBS-LRR disease resistance gene analogous in pepper: characterization, genetic variation, functional divergence and expression patterns. BMC Genom 13:502
- Wang D, Maule AJ (1995) Inhibition of host gene expression associated with plant virus replication. Science 267:229–231
- Whitham S, McCormick S, Baker B (1996) The *N* gene of tobacco confers resistance to *Tobacco mosaic virus* in transgenic tomato. Proc Natl Acad Sci U S A 93:8776–8781
- Yang X, Xie Y, Raja P, Li S, Wolf JN, Shen Q, Bisaro DM, Zhou X (2011) Suppression of methylation-mediated transcriptional gene silencing by β C1-SAHH protein interaction during geminivirus-betasatellite infection. PLoS Pathog 7:e1002329
- Zhou Y, Rojas MR, Park MR, Seo YS, Lucas WJ, Gilbertson RL (2011) Histone H3 interacts and colocalizes with the nuclear shuttle protein and the movement protein of a geminivirus. J Virol 85:11821–11832
- Zvereva EL, Kozlov MV (2012) Sources of variation in plant responses to belowground insect herbivory: a meta-analysis. Oecologia 169:441–452